UNIVERSITAT POLITÈCNICA
DE CATALUNYA
BARCELONATECH

# *Singularities and symmetries on the crossroads of geometry and physics*

**Pau Mir Garcia**


DOCTORAL THESIS

# Singularities and symmetries on the crossroads of geometry and physics

*Author:*
Pau MIR GARCIA

*Supervisor:*
Prof. Dr. Eva MIRANDA GALCERÁN

*A thesis submitted in fulfillment of the requirements for the PhD program in Computational and Applied Physics by the Universitat Politècnica de Catalunya*

November 7, 2023

# *Abstract*

In this thesis we study several mathematical objects that are essential to formulate and model physical systems. Applying the tools provided by differential geometry, we develop and analyze different mathematical structures that are used in three physical contexts: dissipative dynamics, integrable systems and geometric quantization. To do it, we mainly employ the setting of $b$-symplectic geometry, a natural extension of symplectic geometry which is specifically designed to address manifolds with boundary. It is based on the concept of $b$-forms introduced by Melrose and was initiated by Guillemin, Miranda and Pires.

Firstly, in the context of dissipative dynamics, we introduce and discuss a variety of twisted $b$-cotangent models. In these models, defined on the cotangent bundle of a smooth manifold, the fundamental structure is a $b$-symplectic form that is singular within the fibers of the bundle. Our models give rise to dynamical systems governed by the standard Hamiltonian of a free particle, accompanied by a position-dependent potential. After examining different types of potentials and finding that all of them induce dissipation of energy in the system, we prove that these twisted $b$-cotangent models offer a suitable Hamiltonian formulation for dissipative systems. Consequently, they expand the scope of Hamiltonian dynamics and bring a new approach to the study of non-conservative systems.

Secondly, in the context of integrable systems, we introduce and investigate $b$-semitoric systems, a family of systems that generalizes simultaneously semitoric systems and $b$-toric systems, and which is tailored for $b$-symplectic manifolds. We provide a comprehensive definition of $b$-semitoric systems, that adapts the characteristics of semitoric systems to the framework of $b$-symplectic manifolds, and we construct three examples of this type of system. The three examples are based on modifications of the coupled angular momenta system, a classical semitoric system that represents the coupling of two rigid rotors. Our examination of the examples, which includes the classification of the singular points and the study of the global dynamics, allows us to highlight the unique characteristics of $b$-semitoric systems.

Thirdly, in the context of geometric quantization, we introduce a Bohr-Sommerfeld quantization method for $b$-symplectic toric manifolds. We establish that the dimension of this quantization method depends on a signed count of the integer points in the image of the moment map of the toric action. Additionally, we demonstrate its equivalence with the formal geometric quantization of such manifolds. Furthermore, we present a geometric quantization model based on sheaf cohomology, suitable for integrable systems with non-degenerate singularities, that also relies on the count of the integer points in the image of the moment map.

# *Resum*

En aquesta tesi estudiem diversos objectes matemàtics que són essencials per a formular i modelar sistemes físics. Aplicant les eines proporcionades per la geometria diferencial, desenvolupem i analitzem diferents estructures matemàtiques que s'utilitzen en tres contextos físics: la dinàmica dissipativa, els sistemes integrables i la quantització geomètrica. Per a fer-ho, utilitzem principalment el marc de la geometria $b$-simplèctica, una extensió natural de la geometria simplèctica dissenyada específicament per a varietats amb vora, basada en el concepte de $b$-formes introduït per Melrose, i iniciada per Guillemin, Miranda i Pires.

En primer lloc, en el context de la dinàmica dissipativa, introduïm i estudiem un conjunt de models $b$-cotangents. En aquests models, definits al fibrat cotangent d'una varietat suau, l'estructura fonamental és una forma $b$-simplèctica que és singular a les fibres. Aquests models generen sistemes dinàmics governats pel Hamiltonià estàndard d'una partícula lliure, acompanyat d'un potencial que depèn de la posició de la partícula. Després d'analitzar diferents tipus de potencials i de trobar que en tots ells s'observa dissipació de l'energia del sistema, demostrem que els models $b$-cotangents permeten una formulació Hamiltoniana adequada per a sistemes dissipatius. D'aquesta manera, aquests models amplien l'abast de la dinàmica Hamiltoniana i aporten una nova aproximació a l'estudi de sistemes no conservatius.

En segon lloc, en el context dels sistemes integrables, introduïm i investiguem els sistemes $b$-semitòrics, una família de sistemes que generalitza simultàniament els sistemes semitòrics i els sistemes $b$-tòrics i que està adaptada per a les varietats $b$-simplèctiques. Proporcionem una definició completa dels sistemes $b$-semitòrics, que fa encaixar les característiques dels sistemes semitòrics en el marc de les varietats $b$-simplèctiques, i construïm tres exemples d'aquest tipus de sistema. Els tres exemples es basen en modificacions del sistema de moments angulars acoblats, un sistema semitòric clàssic que representa l'acoblament de dos rotors rígids. La nostra anàlisi dels exemples, que inclou la classificació dels punts singulars i l'estudi de la dinàmica global, ens permet ressaltar les característiques úniques dels sistemes $b$-semitòrics.

En tercer lloc, en el context de la quantització geomètrica, introduïm un mètode de quantització de Bohr-Sommerfeld per a les varietats $b$-simplèctiques tòriques. Establim que la dimensió d'aquest mètode de quantització depèn del recompte amb signe dels punts enters a la imatge de l'aplicació moment de l'acció tòrica. A més, demostrem la seva equivalència amb la quantització geomètrica formal d'aquestes varietats. També presentem un model de quantització geomètrica basat en la cohomologia de feixos, adequat per a sistemes integrables amb singularitats no degenerades, que també depèn del recompte dels punts enters a la imatge de l'aplicació moment.

# *Acknowledgements*

I would like to express my gratitude to all the amazing people who have been by my side during this doctoral journey. Your support has been invaluable in many different ways, each of you has played a unique and special impact on my academic and personal growth, and I appreciate it more than words can tell.

I am so thankful for your support that I have chosen to write and send a personal acknowledgment to each of you. These acknowledgments will be a way of showing how much your accompaniment has meant to me and I will be reaching out to you directly to express my thanks and share my thoughts.

Once again, thank you all for being part of this important chapter in my life, your support has made all the difference. I am eager to convey my gratitude in a more personal manner and I look forward to expressing it to you.

# *Funding statement*

During this thesis I have been funded and supported by:

- The grant 100010434LCF/BQ/DR21/11880025 Inphinit - Retainig of “la Caixa” Foundation.
- The grant PID2019-103849GB-I00 of MCIN/AEI/10.13039/501100011033 of the Spanish State Research Agency.
- The grant 2021 SGR 00603 of the Agència de Gestió d’Ajuts Universitaris i de Recerca of the Generalitat de Catalunya.
- The grant 2020 FPI-UPC-112 of the Universitat Politècnica de Catalunya.

# Contents

# List of Figures

# Chapter 1

# Introduction

In the field of mathematical physics, one of the main goals is understanding the behavior of dynamical systems. These systems, which evolve under the influence of forces and interactions, often give rise to complex equations that require sophisticated mathematical tools for their analysis. One such tool is *symplectic geometry*, the geometry of symplectic manifolds, which is the fundamental mathematical language for Hamiltonian mechanics and geometric quantization.

A *symplectic manifold* consists of an even-dimensional smooth manifold equipped with a non-degenerate closed 2-form, called *symplectic form*, which endows the manifold with a notion of volume. It is the natural geometric setting for modeling and studying *Hamilton's equations*, a set of first-order differential equations that describes the evolution of a dynamical system in classical mechanics, and it is the proper framework for understanding the dynamics of systems in which there are conserved physical quantities.

In classical mechanics, the *phase space* of a mechanical system is a manifold that represents all the possible states of the system, which are described by the positions and momenta of its particles. When the phase space is equipped with a symplectic form, Hamilton's equations can be formulated in a natural way. These equations connect the time derivatives of position and momentum variables to the partial derivatives of a function called *Hamiltonian* which is related to the energy of the system. Their solution generates a flow that governs the time evolution of the mechanical system and preserves the symplectic form. This guarantees the preservation of the phase space's main features during the system's evolution, which ensures that fundamental physical laws, such as the conservation of energy and momentum, are systematically encoded in the geometric structure of the symplectic manifold.

Symplectic manifolds arise naturally in various physical systems, like the motion of planets in celestial mechanics and the behavior of charged particles in electromagnetic fields, and their study has applications in diverse areas of mathematics and theoretical physics. The main example of a symplectic manifold is the *cotangent bundle* of a smooth manifold, which can be endowed with a symplectic form and which is the standard model for the phase space of a mechanical system.

Symplectic geometry, although it provides a powerful framework for understanding the dynamics of Hamiltonian systems, can fall short of fully capturing the complexity of the underlying physical processes in certain scenarios, for instance in

systems with boundaries or singularities. In these cases, it may be not possible to define a global symplectic form and, therefore, the traditional symplectic framework fails to adequately describe the dynamics. This limitation has led to the development of other geometric settings such as *Poisson geometry* and *b-symplectic geometry*.

Poisson geometry is the geometry of Poisson manifolds, smooth manifolds equipped with a bi-linear operator, the *Poisson bracket*, which endows the space of smooth functions on a smooth manifold with a Lie algebra structure. The Poisson bracket is characterized by its skew-symmetry, the Leibniz rule and the Jacobi identity, properties that encompass the fundamental structure governing the evolution of observables in classical mechanical systems. The Poisson bracket plays a similar role to the symplectic form in symplectic geometry but allows for modeling more general mathematical and physical systems, including integrable systems and quantum systems.

*b*-Symplectic geometry is a geometric setting that emerges as a natural extension of symplectic geometry. In *b*-symplectic geometry, the language of *b-forms* introduced by Melrose in [Mel93] is used to adapt the symplectic setting to manifolds with boundary. A *b*-symplectic manifold is a smooth manifold in which a *b-form* which is singular along a hypersurface that may represent a boundary plays the role of a symplectic form. This approach was brought in by Nest and Tsygan in [TN96] and is based on the fact that there is a class of *b*-forms called *b-symplectic forms* that can effectively endow a manifold with boundary with a notion of volume in the same way that a symplectic form does in a symplectic manifold. A *b*-symplectic manifold can also be seen as a special class of a Poisson manifold in which the dual of the Poisson bracket is a *b*-form that is singular on a critical hypersurface.

In this thesis, we make intensive use of the tools of *b*-symplectic geometry introduced by Guillemin, Miranda and Pires in [GMP11] and [GMP14]. We apply these tools in three different contexts: fluids with dissipation, integrable systems of semitoric type and geometric quantization.

Firstly, we introduce and study several *twisted b-cotangent models*. They are mathematical setups defined on cotangent bundles that admit a *b*-symplectic structure that exhibits a singularity within the fibers. In these models, the evolution of a dynamical system is governed by the standard Hamiltonian of a free particle along with a potential that depends on its position. We study different types of potentials, which give rise to distinct physical interpretations that have dissipation of energy as their common feature and, overall, we prove that twisted *b*-cotangent models provide a Hamiltonian formulation that is suitable for dissipative systems. Thereby, these models expand the scope of Hamiltonian dynamics and offer a new approach to investigating non-conservative systems.

Secondly, we introduce *b-semitoric systems*, objects that generalize *semitoric systems* and that are tailored specifically for *b*-symplectic manifolds. A semitoric system is a 4-dimensional integrable system that satisfies specific conditions: one of its first integrals is proper and induces a global $S^1$ action and all its singular points are non-degenerate and devoid of hyperbolic components. We provide a comprehensive definition of *b*-semitoric systems that essentially adapts the features of semitoric systems to the setting of *b*-symplectic manifolds. We then construct three examples

of such systems, which we use to explore their unique characteristics. These examples are built by modifying a classical semitoric system, the *coupled angular momenta system*, and, through them, we examine the classification of singular points and the global dynamics of $b$-semitoric systems.

Thirdly, we define a *Bohr-Sommerfeld quantization* method for *b-symplectic toric manifolds* using $\mathbb{T}$-modules. We establish that the dimension of this quantization is determined by a signed count of the integer points found within the moment polytope of the toric action and we demonstrate its equivalence with the *formal geometric quantization* of such manifolds. Additionally, we present a geometric quantization model based on sheaf cohomology which is suitable for integrable systems with non-degenerate singularities and which is also based on the count of the integer points in the moment polytope.

## b-Cotangent models for fluids with dissipation

The study of fluid mechanics has a rich and long history, revealing complex structures both on the physical and on the mathematical level. In fluid mechanics, one deals with the motion of a continuous medium, the fluid, and studies how it behaves under diverse conditions such as turbulence or changes in pressure and temperature.

Traditionally, fluid mechanics is described using partial differential equations like the Navier-Stokes equations, which govern the evolution of various fluid variables such as velocity and pressure. While this approach is still essential for many fluid problems, the application of symplectic techniques and, in particular, the Hamiltonian formalism offers an alternative perspective and a powerful toolbox for understanding certain aspects of fluid mechanics.

In [Mor86], Morrison extended the Hamiltonian formalism to include dissipation while preserving a conserved energy-like quantity, in what he called the *metriplectic* formalism. This formalism combines the Poisson brackets from the Hamiltonian symplectic formalism with the metric brackets from the out-of-equilibrium thermodynamics. It describes systems with both Hamiltonian and dissipative components, making it suitable for modeling friction, electric resistivity, collisions and other phenomena in contexts that include biophysics, geophysics and plasma physics.

In this thesis, we present a different approach to dissipation which also makes use of the Hamiltonian formalism. We use the setting of $b$-symplectic geometry and we formulate dissipation using the *b-cotangent models* introduced by Kiesenhofer and Miranda in [KM17]. These models are constructed endowing the cotangent bundle of a smooth manifold with a $b$-symplectic form and are divided into *canonical b-cotangent models*, in which the $b$-symplectic form is singular along the base manifold, and *twisted b-cotangent models*, in which the $b$-symplectic form is singular along the fibers.

We show that the twisted $b$-cotangent models are especially well-suited to formulate dissipation because we observe that trajectories in these systems stabilize asymptotically, revealing dissipation of energy. In particular, we recover relevant

dissipative models using Hamiltonian functions with different potential terms and we exhibit that any twisted $b$-cotangent model can serve as a model for a dissipative system.

One of the twisted $b$-cotangent models we present is equivalent to Stokes' Law, a basic result in fluid mechanics that describes the motion of free-falling particles in flows with viscosity. We prove that a one-dimensional system with a deceleration that is proportional to the velocity of the particle can be effectively modeled using a twisted $b$-cotangent model. For this case, we take a standard free particle Hamiltonian and a potential depending linearly on the position.

With other potentials, such as a quadratic potential and a periodic potential, and in higher dimensions, we produce models which are also dissipative. After their exploration, we discuss how the dissipation in our models essentially emerges from the singularity of the $b$-symplectic form in a natural way.

## Constructions of b-semitoric systems

Hamiltonian systems play a crucial role in modeling many physical phenomena and find applications in fields such as differential geometry, calculus of variations, celestial mechanics, physics, biology and engineering. In particular, questions concerning conservation laws are closely connected to Hamiltonian systems.

An *integrable Hamiltonian system* possesses the maximum possible number of independent conserved quantities or *first integrals*, smooth functions on the underlying symplectic manifold that make up the *moment map* of the system. It has a natural semi-local toric action associated with a special set of coordinates, the *action-angle coordinates*, its solutions can be determined in an explicit functional form and its motion is confined to a submanifold of its phase space. Although there exist powerful results that completely characterize integrable Hamiltonian systems under some hypotheses, such as the *Arnold-Liouville theorem*, their global dynamics can be intricate and complex and they are still objects of active research.

In recent decades, many classification schemes of integrable systems have been constructed based on several invariants. These invariants capture different aspects of these systems and are used to classify them following various notions of equivalence. These classification procedures provide an overview of all possible systems within a certain class and enable the distinction between non-equivalent systems. A notable classification of integrable Hamiltonian systems from the symplectic point of view is the classification of *toric systems* started by Atiyah in [Ati82] and by Guillemin and Sternberg in [GS82a] and completed by Delzant in [Del88].

A special class of four-dimensional completely integrable systems is the class of *semitoric systems*. In these systems, one of the first integrals is proper and generates a global $S^1$ action, and the singular points are assumed to be non-degenerate and devoid of hyperbolic components.

In a general integrable Hamiltonian system, the first integrals induce $\mathbb{R}$ actions on the manifold and their flows can exhibit extremely complex behaviors. In the particular case of a toric system, all the first integrals give rise to $S^1$ actions on the

manifold, which leads to numerous constraints on the system such as the impossibility of having singular points of a type other than elliptic. Then, semitoric systems can be seen as a first generalization of toric systems in four dimensions, with the significant difference between them being that, in a semitoric system, only one first integral is required to give rise to an $\mathbb{S}^1$ action. This allows for the presence of singular points of focus-focus type, which, in turn, obstruct the global existence of action-angle coordinates, as shown by Duistermaat in [Dui80].

The study of semitoric systems and their closely related counterparts, almost-toric systems, started with the works of Symington and Leung in [Sym03] and [LS10] and of Pelayo and Vũ Ngọc in [Vũ 07] and [PV09]. The term "semitoric" has been used in algebraic geometry since the 1980s to describe a related concept, and it has also appeared in various contexts in equivariant symplectic geometry, such as in embedding problems or group actions.

From the topological point of view, semitoric systems can be characterized using the theory of singular Lagrangian fibrations developed by Bolsinov and Fomenko in [BF04] and by Zung in [Zun03]. From the symplectic point of view, semitoric systems with at most one focus-focus point per fiber were classified in terms of five symplectic invariants by Pelayo and Vũ Ngọc in [PV09] and [PV11] and a general classification of semitoric systems was achieved by Palmer, Pelayo and Tang in [PPT19].

Semitoric systems appear naturally in physics, for example in the Jaynes-Cummings model (see the work of Babelon and Cantini and Douçot in [BCD09]) and in the coupled angular momenta system (see the work of Sadovskii and Zhilinskii in [SZ99]). The classification invariants of both semitoric systems were computed by Alonso, Dullin and Hohloch in [ADH19] and [ADH20].

Semitoric systems are an active field of research and, in the last five years, many advances have been made in its global understanding and towards a complete theory. Alonso and Hohloch surveyed the state of the art in [AH19] and several recent papers extend their survey such as the works by Pelayo in [Pel21], by Hohloch and Palmer in [HP21], by Gullentops and Hohloch in [GH22] and [GH23] and by Le Floch and Palmer in [LP23].

In this thesis we introduce and study *b-semitoric systems*, a particular type of *b-integrable systems*. *b*-Integrable systems are the analog of completely integrable systems for the class of *b*-symplectic manifolds and were introduced by Guillemin, Miranda and Pires in [GMP14]. A *b*-integrable system is given by a set of *b-functions* on a *b*-symplectic manifold that play the role of first integrals, that is, they are in involution with respect to the bracket induced by the *b*-symplectic form and are independent almost everywhere.

The most well-known family of *b*-integrable systems is the family of *b-toric systems*, in which all the *b*-functions give rise to $\mathbb{S}^1$ actions on the manifold. They are the analog of toric systems in the setting of *b*-symplectic manifolds and were described by Guillemin, Miranda, Pires and Scott in [Gui+15] and by Gualtieri, Li, Pelayo and Ratiu in [Gua+17]. Their classification is based on the same combinatorial invariant that classifies toric systems, the *Delzant polytope*.

In this thesis we introduce and examine *b-semitoric systems*, a generalization of *b*-toric systems. *b*-Semitoric systems are defined as 4-dimensional *b*-integrable systems in which one of the *b*-functions generates a global $\mathbb{S}^1$ action and whose singular points are non-degenerate and contain no hyperbolic components. They generalize 4-dimensional *b*-toric systems because the induced action is not an action of $\mathbb{T}^2$ but is only required to have one $\mathbb{S}^1$ component. This allows the study of 4-dimensional *b*-integrable systems which have not only singular points of elliptic type but also singular points of focus-focus type.

*b*-Semitoric systems are, at the same time, the generalization of semitoric systems to the setting of *b*-symplectic manifolds. In this class of manifolds, in which the symplectic structure is singular along a hypersurface, *b*-semitoric systems exhibit the same dynamical features that one can encounter in semitoric systems.

Given this, there are two natural ways to construct, from a pre-existing system, a *b*-semitoric system that is not just a semitoric system or a *b*-toric system. One way is to take a semitoric system, introduce a singularity on the symplectic form along a hypersurface, which turns it into a *b*-symplectic form, and modify the first integrals to turn them into *b*-functions. If this is done appropriately, a *b*-semitoric system is produced from the semitoric system. The other way is to take a 4-dimensional *b*-toric system and perturb its *b*-functions in a way that the system is still a *b*-integrable system, its singular points are non-degenerate and contain no hyperbolic components and only one *b*-function generates a global $\mathbb{S}^1$ action.

In this thesis, we take as a starting point a pre-existing family of semitoric systems to construct three different families of *b*-semitoric systems. We begin with the *coupled angular momenta* system, a 1-parameter family of systems that models the classical version of the addition of two quantum angular momenta. It is defined on the product of two copies of $\mathbb{S}^2$ and represents, for example, the reduced hydrogen-like atom in the presence of parallel electric and magnetic fields (see the work of Sadovskii, Zhilinskii and Michel in [SZM96]).

We modify the coupled angular momenta system in three different ways, each of which produces a 1-parameter family of *b*-integrable systems. To identify and classify the singular points of the three of them we combine their local analyses with the previous studies on the original coupled angular momenta system by Sadovskii and Zhilinskii in [SZ99], by Le Floch and Pelayo in [LP19] and by Alonso, Dullin and Hohloch in [ADH20]. We describe their moment maps, we characterize their dynamics and we conclude that they are indeed *b*-semitoric systems.

In one of the *b*-semitoric systems, we explicitly compute the trajectories of a particular point under the flow of the system with numerical methods. The point we take is a regular one in the fiber of a fixed point of focus-focus type. In a semitoric system, the orbit of this point would be a pinched torus and we show that this is also the case in our *b*-semitoric system.

Our analyses of the different examples of *b*-semitoric systems open the door to finding a global classification of *b*-semitoric systems. We expect that it will depend on several invariants similar to that of the semitoric classification and that it will also take into account the constraints imposed by the underlying *b*-symplectic structure.

## Bohr-Sommerfeld quantization of b-symplectic toric manifolds

As a general principle, quantization consists of associating a Hilbert space with a symplectic manifold. In geometric quantization, this Hilbert space is constructed endowing the manifold with a line bundle with a connection and identifying which of its sections are *covariantly constant* or *polarized* with respect to the direction given by the leaves of a selected polarization. The space of smooth square-integrable polarized sections makes up for the quantization Hilbert space and one can define the quantum operators there.

Polarized sections are not always defined globally along all the leaves of a polarization but only at a special set of leaves, the set of *Bohr-Sommerfeld leaves*. This set is discrete and, under some hypotheses, finite, and gives rise to the definition of a particular type of geometric quantization called *Bohr-Sommerfeld quantization*.

Kostant introduced the main ideas of geometric quantization in [Kos70] and they remain useful and have applications in representation theory and a wide variety of physical problems. Kostant's model goes through the cohomology associated with the sheaf of polarized sections and is well-adapted for real polarizations given by the level sets of integrable systems.

Souriau's research endeavors in [Sou66] were directed towards the quantization of physical systems and involved a comprehensive examination of a circle bundle situated over the phase space. Within Souriau's body of work, the prequantization condition prominently incorporated the fundamental Planck's constant $h$. Subsequently, Blattner integrated the methodologies of Kostant and Souriau in [Bla73] by employing the complex line bundle while maintaining the prequantization condition that encompassed Planck's $h$.

Using the formal geometric quantization of Weitsman in [Wei01] and Paradan in [Par09], Guillemin, Miranda and Weitsman proved in [GMW18b] that the *formal geometric quantization* of a $b$-symplectic toric manifold is a finite-dimensional vector space. This raised the natural question of whether there is a true geometric quantization of such a space. An answer was given in the affirmative by Braverman, Lin, Loizides, Sjamaar and Song in [BLS21] and in [Lin+22], where virtual modules agreeing with the formal geometric quantization were constructed analytically using index theory. In this thesis, we revisit the question in the context of Bohr-Sommerfeld quantization, following the work by Guillemin and Sternberg in [GS83] but restricting ourselves to the case of $b$-toric systems.

It was proved by Guillemin, Miranda, Pires and Scott in [Gui+15] that $b$-symplectic toric manifolds are in one-to-one correspondence with *b-Delzant polytopes*, the analog of Delzant polytopes for toric systems introduced by Delzant in [Del88]. Then, in the same way in which Guillemin and Sternberg proved in [GS83] that the Bohr-Sommerfeld quantization of a toric system can be read from the integer points in its Delzant polytope, in this thesis we define the Bohr-Sommerfeld quantization of a $b$-toric system in such a way that it can be read from the integer points in its $b$-Delzant polytope.

The result of Guillemin and Sternberg in [GS83] identifies each Bohr-Sommerfeld leaf of a toric system with an integer point in the image of its moment map. Since their amount in the case of a compact manifold is finite, the Bohr-Sommerfeld quantization of a compact toric system produces a finite-dimensional Hilbert space. However, if one tries to apply the same idea to $b$-toric systems on compact manifolds, the Bohr-Sommerfeld quantization produces an infinite-dimensional Hilbert space because the amount of integer points in the image of its moment map is infinite.

For this reason, our definition of a Bohr-Sommerfeld quantization for $b$-toric systems is a *Bohr-Sommerfeld quantization with sign*, which we prove gives a finite-dimensional Hilbert space in the case of a compact manifold. We show that this definition coincides with the formal geometric quantization and, in particular, we prove that its dimension is given by a signed count of the integral points in the $b$-Delzant polytope.

Finally, we also provide a new quantization model that allows the quantization of integrable systems with non-degenerate singular points with elliptic and hyperbolic components. This quantization uses the real polarization given by the integrable system and is constructed using sheaf cohomology. We consider two different sheaves: the sheaf of smooth polarized sections and the sheaf of analytic polarized sections. We obtain that the contribution of the hyperbolic components of the singularities to the geometric quantization is zero, making it coincide with the quantization obtained by Hamilton in [Ham10] and making it different from the one obtained by Hamilton and Miranda in [HM10].

## Guide to content

The content of this thesis is derived from various articles produced over the last three years in collaboration with my co-authors. The central ideas and results of each article are included in the thesis with some modifications in the presentation. I have restructured the exposition, consolidated the common preliminary information from each chapter into a single preliminaries section and expanded on certain discussions.

Chapter 2 contains the essential background to all the results of this thesis, including the basic definitions and an introduction to each of the objects of study in the remaining chapters.

Chapter 3 is based on the article

- *Singular cotangent models and complexity in fluids with dissipation*. Physica D: Nonlinear Phenomena 446 (2023). B. Coquinot, P. Mir and E. Miranda. [CMM23]

Chapter 4 is based on the article

- *Constructions of b-semitoric systems*. Journal of Mathematical Physics Special Collection: Learning from Insulators: New Trends in the Study of Conduction Properties of Metal (2023). J. Brugués, S. Hohloch, P. Mir and E. Miranda. [Bru+23]

Chapter 5 is based on the articles

- *Bohr-Sommerfeld quantization of b-symplectic toric manifolds*. Pure and Applied Mathematics Quarterly (2023). P. Mir, E. Miranda and J. Weitsman. [MMW22]
- *Geometric quantization via cotangent models*. Analysis and Mathematical Physics 11 (2021). P. Mir, E. Miranda. [MM21]

Appendices A and B contain extra material to complement Chapter 4.

# Chapter 2

# Preliminaries

In this chapter we introduce the basic terminology, definitions and results used in this thesis. We first introduce symplectic forms, the main geometric structures in the formulation of classical and quantum physics. Then, we present the concept of an integrable system and describe the classification of singular points of such a system. Next, we present $b$-symplectic forms, which generalize symplectic forms and are well-suited to study systems defined in manifolds with boundary. Then, we give a brief introduction of cotangent models on both symplectic and $b$-symplectic manifolds. Finally, we introduce geometric quantization and its main ingredients.

## 2.1 Symplectic manifolds

Symplectic forms are the fundamental geometric tool in the formulation of classical mechanics. They provide a unique manner to turn a smooth function into a vector field in such a way that the function is constant along the flow lines of the vector field.

**Definition 2.1.** *Let $M^{2n}$ be a smooth manifold. A smooth 2-form $\omega$ on $M$ is a* symplectic form *if it is:*

- *closed: $d\omega = 0$, and*
- *non-degenerate: for any smooth 1-form $\alpha$ on $M$, there exists a unique vector field $X$ on $M$ that solves $\iota_X \omega = \alpha$.*

*If a manifold $M$ admits a symplectic form $\omega$ we call the pair $(M, \omega)$ a* symplectic manifold.

The condition of non-degeneracy of a symplectic form $\omega$ on a manifold $M^{2n}$ is equivalent to the condition that $\omega^n$ is a volume form on $M^{2n}$. In particular, it implies that, if a manifold $M$ admits a symplectic form, it has to be orientable. And, besides orientability, other obstructions may prevent a manifold from being symplectic. However, the majority of manifolds modeling physical systems turn out to be symplectic, as the next three examples of well-known manifolds show.

**Example 2.2.** *Consider the Euclidean space $\mathbb{R}^{2n}$ and consider the standard coordinates $x_1, \ldots, x_n, y_1, \ldots, y_n$. The 2-form*

$$\omega = \sum_{i=1}^{n} dx_i \wedge dy_i$$

*is a symplectic form on* $\mathbb{R}^{2n}$.

**Example 2.3.** *The torus* $\mathbb{T}^{2n}$ *with coordinates* $\theta_1, \dots, \theta_{2n}$ *can be equipped with the symplectic form*

$$\omega = \sum_{i=1}^{n} d\theta_{2i-1} \wedge d\theta_{2i}.$$

**Example 2.4.** *The unit sphere* $\mathbb{S}^2 \subset \mathbb{R}^3$ *can be endowed with a symplectic form* $\omega$ *in the following way. For every unit vector* $p \in \mathbb{S}^2$ *and any pair of tangent vectors* $u, v \in T_p\mathbb{S}^2$, *define* $\omega$ *using the scalar product* $\langle\ ,\ \rangle$ *and the vector product* $\times$ *as*

$$\omega|_p := \langle p, u \times v \rangle.$$

*In cylindrical coordinates* $\theta, z$ *of* $\mathbb{S}^2$ *and away from the poles,* $\omega$ *writes as* $d\theta \wedge dz$.

The symplectic forms in the examples of the $2n$-dimensional Euclidean space, the $2n$-torus and the 2-sphere are called *standard symplectic forms* since they are the most natural in these manifolds and, therefore, the most used. Their coordinate expression is similar in the three examples, which is no coincidence that because a symplectic manifold is locally equivalent to any other symplectic manifold of the same dimension.

On a symplectic manifold, any smooth function defines a vector field, called *Hamiltonian vector field*, in the following way.

**Definition 2.5.** *Let* $H$ *be a smooth function on a symplectic manifold* $(M, \omega)$. *The* Hamiltonian vector field associated to $H$, *and denoted by* $X_H$, *is defined as the only solution of*

$$\iota_{X_H}\omega = -dH.$$

*The flow of* $X_H$ *is called the* Hamiltonian flow of $H$.

A vector field can be identified with a dynamical system understanding its flow as the evolution of the system with time. Then, on a symplectic manifold $(M, \omega)$, any smooth function $H$ induces a dynamical system, which is given by the flow of $X_H$, the associated Hamiltonian vector field. The triple $(M, \omega, H)$ is known as the *Hamiltonian system given by* $H$.

One of the properties of the Hamiltonian vector field is that its flow always preserves the value of the function that induces it, which we call the *Hamiltonian function* or just the *Hamiltonian*. In other words, the value of the Hamiltonian is conserved along the integral curves of its Hamiltonian vector field.

In physics and, especially, in mechanics, it is usual to encounter functions that depend on the variables of a dynamical system and that at the same time remain constant throughout the evolution of the system. Mechanical energy, linear momentum and angular momentum are examples of quantities that are found to be constant over time for many physical systems. For this reason, Hamiltonian vector fields and Hamiltonian functions on symplectic manifolds are the natural setting to formulate and study physical systems and what makes symplectic geometry an essential environment for the development of mathematical physics.

Another important property of the Hamiltonian vector field of a function is that the symplectic form is preserved by its flow. This is necessary because if the symplectic form was not preserved, after running time forward using the flow, the vector field would not be the Hamiltonian vector field of the original function anymore.

A particular kind of manifold that always admits a canonical symplectic form is the *cotangent bundle* of a smooth manifold, as the next example shows.

**Example 2.6.** *Let $T^*M$ be the cotangent bundle of a smooth manifold $M$ of dimension $n$. There is an intrinsic canonical linear 1-form $\lambda$ on $T^*M$ defined pointwise in the following way: for all $p \in T^*M$ and $v \in T_p(T^*M)$, $\lambda$ is the form such that*

$$\langle \lambda_p, v \rangle = \langle p, d\pi_p v \rangle,$$

*where $\pi : T^*M \longrightarrow M$ is the canonical projection. Its differential $\omega = d\lambda$ is a symplectic form on $T^*M$.*

*In local coordinates $q_1, \ldots, q_n, p_1, \ldots, p_n$ of $T^*M$, the canonical 1-form has the expression $\lambda = \sum_{i=1}^n p_i \, dq_i$ and the symplectic form writes as $\omega = \sum_{i=1}^n dp_i \wedge dq_i$.*

When a manifold represents the set of possible positions of a particle system, called *configuration space*, its cotangent bundle can be thought of as the set of possible pairs of position and momentum, called *phase space*. This, together with the fact that cotangent bundles are symplectic manifolds and any smooth function on them can be taken as Hamiltonian function, makes them especially well-suited to model mechanical systems. Indeed, as the following example shows, Hamilton's equations from classical mechanics are naturally obtained from the definition of the Hamiltonian vector field associated with the energy function of a system.

**Example 2.7.** *Let an $n$-dimensional smooth manifold $M$ be the configuration space of a particle in a mechanical system and let its cotangent bundle $T^*M$ be the phase space. Take local position-momentum coordinates $q_1, \ldots, q_n, p_1, \ldots, p_n$ on $T^*M$ and equip it with the symplectic form $\omega = \sum_{i=1}^n dp_i \wedge dq_i$. Let $H(q_1, \ldots, q_n, p_1, \ldots, p_n)$ be the function representing the mechanical energy of the system, which may depend on position and momentum coordinates. The Hamiltonian vector field $X_H$ associated to $H$ is defined as the only vector field satisfying $\iota_{X_H}\omega = -dH$. The left-hand side of this equality can be rewritten as*

$$\iota_{X_H}\omega = \iota_{\sum_{i=1}^n X_H^{q_i} \frac{\partial}{\partial q_i} + \sum_{i=1}^n X_H^{p_i} \frac{\partial}{\partial p_i}} \left( \sum_{i=1}^n dp_i \wedge dq_i \right) = \sum_{i=1}^n X_H^{p_i} dq_i - \sum_{i=1}^n X_H^{q_i} dp_i,$$

*while its right-hand side can be expanded as:*

$$-dH = -\sum_{i=1}^n \frac{\partial H}{\partial q_i} dq_i - \sum_{i=1}^n \frac{\partial H}{\partial p_i} dp_i.$$

*By identifying terms, one obtains* Hamilton's equations*:*

$$\begin{cases} X_H^{q_i} = \frac{\partial H}{\partial p_i} \\ X_H^{p_i} = -\frac{\partial H}{\partial q_i} \end{cases}.$$

*The flow of the vector field $X_H$ solving Hamilton's equations, which are equivalent to Newton's second law, determines the dynamics of the mechanical system. Because of this association between the flow of $X_H$ and the evolution of the system with time, in physics it is common to formulate the Hamilton's equations as the following system of ODEs:*

$$\begin{cases} \dot{q} := \frac{dq_i}{dt} = \frac{\partial H}{\partial p_i} \\ \dot{p} := \frac{dp_i}{dt} = -\frac{\partial H}{\partial q_i} \end{cases} .$$

The fact that a manifold admits a symplectic form or not is independent of its connectedness. However, since the configuration space of a physical system is, in the the vast majority of the cases, a connected manifold, from now on and unless we specify the opposite, we will assume that all the manifolds that we talk about are connected.

On a smooth manifold, the symplectic form induces an operator called *Poisson bracket* which provides the space of smooth functions on the manifold with the structure of a Lie algebra and gives an elegant way to state definitions and results.

**Definition 2.8.** *Let $(M, \omega)$ be a symplectic manifold. The operator defined by*

$$\begin{array}{rccc} \{\cdot,\cdot\}: & \mathcal{C}^\infty(M) \times \mathcal{C}^\infty(M) & \longrightarrow & \mathcal{C}^\infty(M) \\ & (f,g) & \longmapsto & \{f,g\} := \omega(X_f, X_g) \end{array} ,$$

*where $X_f$ and $X_g$ are the Hamiltonian vector fields of $f$ and $g$, respectively, is called the* Poisson bracket.

If $f$ and $g$ are smooth functions on a symplectic manifold, by definition, $\{f,g\} = \omega(X_f, X_g) = X_g(f) = df(X_g)$, which is equivalent to the rate of change of $f$ along the flow of $X_g$. The Poisson bracket is, then, the essential tool to analyze how functions change along flows of Hamiltonian vector fields. In particular, $\{f,g\} = 0$ and we say that *$f$ and $g$ Poisson commute* or simply *commute* if and only if the Hamiltonian flow of $g$ preserves $f$.

For all $f, g, h \in \mathcal{C}^\infty(M)$ and $a, b \in \mathbb{R}$, the Poisson bracket satisfies:

1. Bi-linearity: $\{af + bg, h\} = a\{f,h\} + b\{g,h\}, \{h, af + bg\} = a\{h,f\} + b\{h,g\}$.
2. Skew-symmetry:$\{f,g\} = -\{g,f\}$.
3. Jacobi's identity: $\{f,\{g,h\}\} + \{g,\{h,f\}\} + \{h,\{f,g\}\} = 0$.
4. Leibniz rule: $\{f,gh\} = \{f,g\}h + g\{f,h\}$.

In general, any operator $\{\cdot,\cdot\}$ satisfying these four properties is called a *Poisson bracket operator* and a manifold $M$ admitting such an operator is a *Poisson manifold*.

Skew-symmetry of the Poisson bracket implies that it measures both how $f$ changes when flowing along $X_g$ and how $g$ changes when flowing along $X_f$, and that the Hamiltonian flow of $g$ preserves $f$ if and only if the Hamiltonian flow of $f$ preserves $g$.

If we assume that the way a certain physical system evolves in time is by following the Hamiltonian flow of a distinguished function $H$ which is preserved along the trajectories, then the function $H$ should be physically interpreted as the total energy of the system. In this case, the value of another function $f$ evolves through time according to the solutions of the differential equation $\frac{df}{dt} = \{f, H\}$.

The case where $\{f, H\} = 0$ happens exactly when the Hamiltonian flow of $H$ preserves $f$, which means that $f$ is a quantity which is conserved by the laws of physics and we call it an *integral of motion* of the Hamiltonian system given by $H$ or a *first integral* of the system. At the same time, the Hamiltonian flow of an integral of motion $f$ preserves the total energy $H$. This implies that there is a one-to-one correspondence between Hamiltonian vector fields that preserve the total energy of the system and scalar functions which are conserved by the laws of physics.

## 2.2 Integrable systems

In a Hamiltonian system $(M, \omega, H)$, the level sets of the Hamiltonian $H$ define a foliation of $M$ which is left invariant by the flow of the Hamiltonian vector field $X_H$. If, a part from $H$, there is another quantity $f$ functionally independent of $H$ which commutes with $H$ and therefore is also constant along the flow of $X_H$, then $f$ a first integral of the system and its level sets define another invariant foliation of $M$. The intersections of the leaves of the two foliations, which are generically of co-dimension 1, define a new foliation of $M$ which is generically of co-dimension 2 and is invariant by the flows of $X_H$ and $X_f$. In general, each independent first integral of a Hamiltonian system $(M, \omega, H)$ reduces in one the dimension of the invariant submanifolds of $M$ containing the Hamiltonian flows of all of them.

The number of independent first integrals in a Hamiltonian system, including the Hamiltonian function itself, is limited to half the dimension of the symplectic manifold. Having the maximum possible number of independent first integrals is, however, a very strong assumption that characterizes completely the dynamics of the system and the topology of the underlying manifold.

Specifically, if in a $2n$-dimensional Hamiltonian system there exist $n$ first integrals which are functionally independent everywhere and commute pairwise, then their joint level sets are invariant under the Hamiltonian flow, each of their connected components is diffeomorphic to the $n$-dimensional tori and the dynamics on them are rigid rotations (see the work of Arnold in [Arn78]). And in such a dynamical system there are no fixed points, which is not a physically reasonable assumption.

However, if the independence of $n$ pairwise commuting first integrals in a $2n$-dimensional Hamiltonian system is weakened to happen only *almost everywhere* on the manifold, then the Hamiltonian system does admit fixed points. This situation is more realistic in physics and most of the models in classical mechanics fit in this class of Hamiltonian systems, called *integrable systems*.

**Definition 2.9.** *Let $(M, \omega)$ be a symplectic manifold of dimension $2n$. Let $H$ be a Hamiltonian defined on $M$. The Hamiltonian system $(M, \omega, H)$ is* completely integrable *or* integrable *if there exists a smooth function $F = (f_1, \ldots, f_n) : M \to \mathbb{R}^n$ such that:*

1. $df_1, \ldots, df_n$ *are linearly independent almost everywhere in* $M$.

2. $f_1, \ldots, f_n, H$ *commute pairwise.*

*The Hamiltonian* $H$ *may be one of the* $f_i$*'s and the function* $F$ *is called the* moment map *of the integrable system. The triple* $(M, \omega, F = (f_1, \ldots, f_n))$ *and, sometimes, just the moment map* $F = (f_1, \ldots, f_n)$*, are directly referred to as the* integrable system.

On a symplectic manifold $(M, \omega)$, the space $\mathcal{C}^\infty(M)$ of smooth functions on $M$ is a Lie algebra when we equip it with the Poisson bracket induced by $\omega$. It turns out that another way to define an integrable system on $(M, \omega)$ is as a Lie subalgebra of $\mathcal{C}^\infty(M)$. In particular, an integrable system $F$ is a commutative Lie subalgebra of $\mathcal{C}^\infty(M)$ such that the space $dF(p) := \{df(p) \mid f \in F\} \subset T_p^*M$ has dimension $n$ for almost every $p \in M$. This more algebraic definition is useful to talk about the nature of the points of an integrable Hamiltonian system in which the independence of the first integrals fails.

If the Hamiltonian vector fields of each first integral $f_i$ of an integrable system $(M^{2n}, \omega, F = (f_1, \ldots, f_n))$ are complete, then their commuting flows $\phi^1_{t_1}, \ldots, \phi^n_{t_n}$ induce an $\mathbb{R}^n$ action on $M$ which preserves the joint level sets of $F$. It is called the *joint flow of the integrable system* and is defined by

$$\begin{array}{rccc} \rho: & \mathbb{R}^n \times M & \longrightarrow & M \\ & (t_1, \ldots, t_n, p) & \longmapsto & \phi^1_{t_1} \circ \cdots \circ \phi^n_{t_n}(p) \end{array}.$$

In an integrable system $(M, \omega, F = (f_1, \ldots, f_n))$, for any $a \in \mathbb{R}^n$ in the image of the moment map $F : M \to \mathbb{R}^n$, the joint level set $F^{-1}(a) \subset M$ is called a *fiber* and each connected component of a fiber is called a *leaf*.

In the theory of integrable systems, the *Arnold-Liouville theorem* is the cornerstone which gives the complete description of these systems around regular points. Although it is attributed to Liouville, who was the first one to study it at a local level, and to Arnold, who rediscovered and proved it in [Arn78], this theorem is also due to Mineur (see the work by Mineur in [Min36]).

**Theorem 2.10** (Arnold-Liouville [Arn78])**.** *Let* $(M^{2n}, \omega, F = (f_1, \ldots, f_n))$ *be an integrable system. Suppose that* $p \in M$ *satisfies* $df_1 \wedge \cdots \wedge df_n(p) \neq 0$ *and that* $F(p) = a \in \mathbb{R}^n$*. Assuming that the fiber* $\Lambda_a = F^{-1}(a)$ *is compact and connected, then:*

1. $\Lambda_a$ *is diffeomorphic to the torus* $\mathbb{T}^n$ *and it is called a* Liouville torus.

2. *A neighborhood of* $\Lambda_a$ *is diffeomorphic to the direct product of the torus* $\mathbb{T}^n$ *and the disc* $\mathbb{D}^n$.

3. *In this neighborhood there exist coordinates* $\theta_1, \ldots, \theta_n, p_1, \ldots, p_n$ *such that* $\omega = \sum_{i=1}^n d\theta_i \wedge dp_i$ *and* $F$ *only depends on* $p_1, \ldots, p_n$.

*The* $p_i'$*s are called* action coordinates *and the* $\theta_i'$*s are called* angle coordinates.

A point $p \in M$ such that $df_1 \wedge \cdots \wedge df_n(p) \neq 0$ is called a *regular point of* $F$ and a fiber of $F$ containing only regular points is a *regular fiber of* $F$. The Arnold-Liouville theorem characterizes the neighborhood of any regular compact connected

fiber of the moment map but, in order to obtain the topology and dynamics of the fibers containing non-regular points, it is necessary to further explore the integrable system.

**Definition 2.11.** *Let $(M^{2n}, \omega, F = (f_1, \dots, f_n))$ be an integrable system. A point $p \in M$ is called* singular *or* a singularity of $F$ *if $df_1 \wedge \cdots \wedge df_n(p) = 0$ or, equivalently, if the rank of $dF = (df_1, \dots, df_n)$ at $p$ is less than $n$. A fiber of $F$ containing a singular point is a* singular fiber of $F$. *The* rank of a point $p$ *is defined to be the rank of $dF$ at $p$.*

The fixed points of an integrable system $(M^{2n}, \omega, F = (f_1, \dots, f_n))$ are the points where all the Hamiltonian vector fields $X_{f_i}$ vanish or, equivalently, where all the differentials $df_i$ are 0. Therefore, the fixed points are the singular points of rank 0. On the opposite, regular points correspond to the points where none of the differentials and, therefore, none of the vector fields vanishes. Then, regular points are the points of maximal rank $n$.

Typically, the degeneracy of $dF = (df_1, \dots, df_n)$ at the singular fibers of an integrable system makes it difficult to obtain results about the topology and the dynamics there. Nevertheless, in the case of *non-degenerate singularities*, which are the most elementary singular points, several classification results and, in particular, semi-global normal forms have been obtained. To define this class of simple singularities properly, we need to recover the algebraic description of an integrable system.

Let $F$ be an integrable system on a symplectic manifold $(M, \omega)$, thought of as a commutative Lie subalgebra of $\mathcal{C}^\infty(M)$ such that $dF(p) = \{df(p) \mid f \in F\} \subset T_p^*M$ has dimension $n$ almost everywhere in $M$. Suppose that $p \in M$ is a singular point of $F$ and let $f \in F$ be such that $df(p) = 0$ and, hence, $X_f = 0$ at $p$. Consider the linearization of $X_f$ at $p$, which is a linear operator $DX_f : T_pM \to T_pM$ that belongs to the symplectic Lie algebra $\mathfrak{sp}(T_pM, \omega)$. Since, for any $f_1, f_2 \in F$ we have $\{f_1, f_2\} = 0$ and their Hamiltonian vector fields $X_{f_1}$ and $X_{f_2}$ commute, the linear operators $DX_{f_1}$ and $DX_{f_2}$ also commute and $\{DX_f \mid f \in F, df(x) = 0\}$ is a commutative subalgebra of $\mathfrak{sp}(T_pM, \omega)$.

Now, consider the space $\mathcal{X}_F := \{X_f(p) \mid f \in F\} \subset T_pM$ and let $\mathcal{X}_F^\perp \subset T_pM$ be its symplectic orthogonal complement. Since $F$ is commutative, $\mathcal{X}_F \subset \mathcal{X}_F^\perp$ and the form $\omega$ descends to the quotient $\mathcal{X}_F^\perp / \mathcal{X}_F$, which is turned into a symplectic space. Now, for any $f \in F$ such that $df(p) = 0$, the operator $DX_f$ also descends to $\mathcal{X}_F^\perp / \mathcal{X}_F$. The collection of these descended operators, which we denote by $\mathcal{D}_F$, forms, by construction, a commutative subalgebra of $\mathfrak{sp}(\mathcal{X}_F^\perp / \mathcal{X}_F, \omega)$, which is used to define non-degenerate singularities.

**Definition 2.12.** *Let $(M, \omega, F)$ be an integrable system. A singular point $p \in M$ is called* non-degenerate *if the commutative associated subalgebra $\mathcal{D}_F \subset \mathfrak{sp}(\mathcal{X}_F^\perp / \mathcal{X}_F, \omega)$ is a Cartan subalgebra.*

In view of this definition, the classification of non-degenerate singular points of integrable systems is equivalent to the classification of Cartan subalgebras in the symplectic Lie algebra up to conjugation. This classification was obtained by Williamson in [Wil36] and normal forms for this type of singular points were determined in the works of Rüssmann in [Rüs64], Vey in [Vey78], Colin de Verdière

and Vey in [CV79], Eliasson in [Eli90a] and [Eli90b], Dufour and Molino in [DM88], Zung in [Zun96], Miranda in [Mir03] and [Mir14], Miranda and Zung in [MZ04], Miranda and Vũ Ngọc in [MV05], Vũ Ngọc and Wacheux in [VW13] and Chaperon in [Cha13].

**Theorem 2.13** (Local normal forms for non-degenerate singular points)**.** *Consider a $2n$-dimensional integrable system $(M, \omega, F = (f_1, \dots, f_n))$ and let $p \in M$ be a non-degenerate singular point. Then:*

1. *There exists an open neighborhood $U \subset M$ of $p$, coordinates $x_1, \dots, x_n, y_1, \dots, y_n$ locally defined on $U$ and smooth functions $q_1, \dots, q_n : U \to \mathbb{R}$ or* components of the non-degenerate singular point *such that $\omega = \sum_{i=1}^{n} dx_i \wedge dy_i$, $p$ is mapped to the origin in these coordinates, $\{q_i, f_j\} = 0$ for all $i, j \in \{1, \dots, n\}$ and each $q_i$ is of one of the following forms:*
   - $q_i = y_i$ (regular component),
   - $q_i = (x_i^2 + y_i^2)/2$ (elliptic component),
   - $q_i = x_i y_i$ (hyperbolic component),
   - $q_i = x_i y_{i+1} - x_{i+1} y_i$ *and* $q_{i+1} = x_i y_i + x_{i+1} y_{i+1}$ (focus-focus component).
2. *If there are no hyperbolic components, then the system of equations $\{q_i, f_j\} = 0$ for $i, j \in \{1, \dots, n\}$ is equivalent to the existence of a local diffeomorphism near the origin $g : \mathbb{R}^n \to \mathbb{R}^n$ such that*

$$g \circ f = (q_1, \dots, q_n) \circ (x_1, \dots, x_n, y_1, \dots, y_n).$$

The focus-focus component is a "double" component, it always appears in pairs and therefore can only exist in integrable systems of dimension at least 4. The number of elliptic, hyperbolic, and focus-focus components, denoted respectively by $k_e$, $k_h$ and $k_f$, locally classifies a non-degenerate singular point and is referred to as its *Williamson type*. The number of regular components of a non-degenerate singular point coincides with its rank and, hence, a fixed point has none of them. In general, in a non-degenerate singular point of rank $k$ of an integrable system $(M^{2n}, \omega, F = (f_1, \dots, f_n))$, one always has $k + k_e + k_h + 2k_f = n$.

### 2.2.1 Toric systems and symplectic toric manifolds

Theorem 2.13 establishes the local classification of integrable systems whose singular points are all non-degenerate in terms of their Williamson types. However, a global classification of such systems is still lacking and it is only for very specific sub-classes of integrable systems that it has been achieved. The most remarkable class of systems for which there exists a global classification is the class of *toric integrable systems* or just *toric systems* on compact symplectic manifolds.

**Definition 2.14.** *An integrable system $(M^{2n}, \omega, F = (f_1, \dots, f_n))$ is called* toric *if the flow of each $X_{f_i}$ is $2\pi$-periodic almost everywhere.*

In a toric system $(M^{2n}, \omega, F = (f_1, \dots, f_n))$, the flow of each Hamiltonian vector field $X_{f_i}$ induces an $\mathbb{S}^1$ action on $M$. The condition that each flow is $2\pi$-periodic means that the minimal common period of all the $\mathbb{S}^1$ actions is $2\pi$ and, therefore, the joint flow of a toric system induces an effective action of $\mathbb{T}^n$ on $M$. This property can be used to give an alternative definition of a toric system as a $2n$-dimensional integrable system $(M^{2n}, \omega, F = (f_1, \dots, f_n))$ such that the joint flow of $F$ generates an effective action of $\mathbb{T}^n$ on $M$ (see the work of Cannas Da Silva in [Can01]).

One of the main properties of toric systems is that the orbit of any point by the joint flow is an embedded torus of dimension equal to the rank of the point. This torus coincides with the entire fiber of the point and all the points in the same fiber have, therefore, the same rank, making it natural to talk about the *rank of a fiber*, which is the rank of any of its points. Besides, the singular points of a toric system are all non-degenerate and have only regular and elliptic components, what makes toric systems a relatively small class of systems. Still, it turns out that many integrable systems coming from physics are "almost" toric systems in a sense that we will explain later.

Symplectic manifolds which are compact and admit a toric system are called *symplectic toric manifolds*. Usually, we identify a toric system $(M, \omega, F)$ defined on a compact symplectic manifold $(M, \omega)$ with the symplectic toric manifold itself, and we use the expression *symplectic toric manifold* both to talk about the system and the manifold.

Before symplectic toric manifolds were classified, it was proved by Atiyah in [Ati82] and by Guillemin and Sternberg in [GS82a] that the image of the moment map of a symplectic toric manifold is a convex polytope.

**Theorem 2.15** (Atiyah [Ati82], Guillemin-Sternberg [GS82a])**.** *Let $(M^{2n}, \omega, F)$ be a symplectic toric manifold. Then:*

1. *The fibers of F are connected.*
2. *The image $F(M)$ of the moment map $F : M \to \mathbb{R}^n$ is a convex polytope called* moment polytope*. In particular, it is the convex hull of the images of the fixed points of F.*

Later, it was proved by Delzant in [Del88] that the moment polytope captures all the intrinsic information of the toric integrable system and, hence, it provides a way to completely classify symplectic toric manifolds. In particular, there is a correspondence between symplectic toric manifolds and *Delzant polytopes*, a special family of convex polytopes.

**Definition 2.16.** *A convex polytope $\Delta \subset \mathbb{R}^n$ is a* Delzant polytope *if it is:*

1. Simple*: exactly n edges meet at each vertex.*
2. Rational*: all edges have rational slope, meaning, they are of the form $p + vt$, where $p \in \mathbb{R}^n$ is the vertex, $v \in \mathbb{Z}^n$ is the directional vector of the given edge and $t \in \mathbb{R}$.*
3. Smooth*: at each vertex, the directional vectors of the meeting edges form a basis of $\mathbb{Z}^n$.*

Delzant polytopes are combinatorial objects much simpler than symplectic manifolds or integrable systems, but they encode the essential geometric information of a symplectic toric manifold, as it is stated in Delzant theorem.

**Theorem 2.17** (Delzant [Del88])**.** *For any symplectic toric manifold $(M^{2n}, \omega, F)$, the moment polytope $F(M)$ is a Delzant polytope in $\mathbb{R}^n$.*

*Conversely, for any Delzant polytope $\Delta \subset \mathbb{R}^n$, there exists a symplectic toric manifold $(M^{2n}, \omega, F)$ such that its moment polytope $F(M)$ is exactly $\Delta$.*

*Finally, if there exists a diffeomorphism $\varphi : M_1 \to M_2$ between two symplectic toric manifolds $(M_1^{2n}, \omega_1, F_1)$ and $(M_2^{2n}, \omega_2, F_2)$ which satisfies $\varphi^* \omega_2 = \omega_1$ and $F_2 \circ \varphi = F_1$, then their Delzant polytopes $F_1(M_1)$ and $F_2(M_2)$ coincide up to a translation.*

Delzant theorem provides a classification of symplectic toric manifolds in terms of the combinatorial data of their moment polytope. Moreover, given a Delzant polytope, one can explicitly construct the associated symplectic toric manifold. This allows for practical computations and explicit examples, and makes it possible to deduce geometric and topological properties of a toric system by studying its moment polytope.

All the substantial information of the singular points of a symplectic toric manifold $(M^{2n}, \omega, F)$ is enclosed in the moment polytope $F(M)$. In fact, the image of the singular fibers of the system corresponds to the boundary of Delzant polytope, while the interior corresponds to the image of the regular fibers. In particular, the vertices of the moment map are the images of the fixed points of $F$, the edges are the images of the singular fibers of rank 1 and, in general, for $l = 1, \dots, n$, the intersections of $l$ facets of the moment polytope are the images of the singular fibers of rank $n - l$, which are made of singular points with $l$ elliptic components.

### 2.2.2 Semitoric systems

Toric systems do not possess non-degenerate singular points with hyperbolic or focus-focus components, since they can only exhibit components of regular and elliptic type. In dimension 4, a natural generalization of toric systems is the wider class of *semitoric systems*, which does allow for the existence of singular points of focus-focus type.

Semitoric systems were first introduced by Vũ Ngọc in [Vũ 07], and they hold significant interest because their definition possesses enough flexibility to accommodate singularities of focus-focus type and, at the same time, it maintains sufficient restrictiveness to avoid other intricate behaviors, thus rendering them a compelling candidate for expanding the symplectic classification of toric systems.

**Definition 2.18.** *A 4-dimensional completely integrable system $(M, \omega, F = (f_1, f_2))$ is called* semitoric *if*

1. *The first integral $f_1$ is a proper function and the flow of the Hamiltonian vector field $X_{f_1}$ is $2\pi$-periodic almost everywhere.*
2. *All singular points of $F = (f_1, f_2)$ are non-degenerate and do not include components of hyperbolic type.*

The condition that one first integrals is a proper function that appears in the definition of a semitoric system is automatically satisfied if the manifold $M$ is compact. The component of $F$ which generates the $2\pi$-periodic flow in the semitoric system is typically denoted by $L$ or by $J$, while the other component is denoted by $H$.

In a semitoric system, all singular points are non-degenerate and their non-regular components can be of elliptic or focus-focus type. Therefore, the only possibilities for a singular point in these systems are:

- to be a fixed point with two elliptic components, or
- to be a fixed point with one focus-focus component, or
- to be a rank 1 singular point with one regular and one elliptic component.

These three types of singular points are called, respectively, *elliptic-elliptic*, *focus-focus* and *elliptic-regular*, and it is the presence of focus-focus singularities what makes semitoric systems more general and dynamically more intricate than toric systems.

A semitoric system $(M, \omega, F = (L, H))$ is *simple* if there is at most one focus-focus point in each fiber of $L$, which is the case of all semitoric systems appearing in this thesis. The fiber $\Lambda_p$ of a focus-focus singular point $p$ in a simple semitoric system $(M, \omega, F = (L, H))$ is topologically not a torus $\mathbb{T}^2$ but a *pinched torus*, with the focus-focus singularity being the pinch point. There are two orbits of the system in $\Lambda$: one is made by a single point, the focus-focus point $p$, which is fixed by $X_L$ and $X_H$, and the other is made by the rest of the pinched torus. This second orbit is a 2-dimensional submanifold of $M$ diffeomorphic to the infinite cylinder $\mathbb{S}^1 \times \mathbb{R}$, with $X_L$ and $X_H$ generating, respectively, its circle component and its axial component.

In a simple semitoric system, the fiber of a point is of one of the following four types, depicted in Figure 2.1:

- If the point is regular, its fiber is a *regular fiber*, which is topologically a two dimensional torus.
- If the point is singular of elliptic-regular type, its fiber is a singular *elliptic-regular fiber*, which is topologically a circle.
- If the point is singular of focus-focus type, its fiber is a singular *focus-focus fiber*, which is topologically a pinched torus.
- If the point is singular of elliptic-elliptic type, its fiber is a singular *elliptic-elliptic fiber*, which is a point.

Simple semitoric systems can be completely classified in terms of five *semitoric invariants*: the number of focus-focus points, the semitoric polygon, the height invariant, the Taylor series invariant, and the twisting index invariant. The semitoric polygon and the Taylor series were defined by Vũ Ngọc in [Vũ 03; Vũ 07] and the other three invariants were defined and stated to be invariants by Pelayo and Vũ Ngọc in [PV09]. This classification was extended to non-simple semitoric systems by Palmer, Pelayo and Tang in [PPT19].

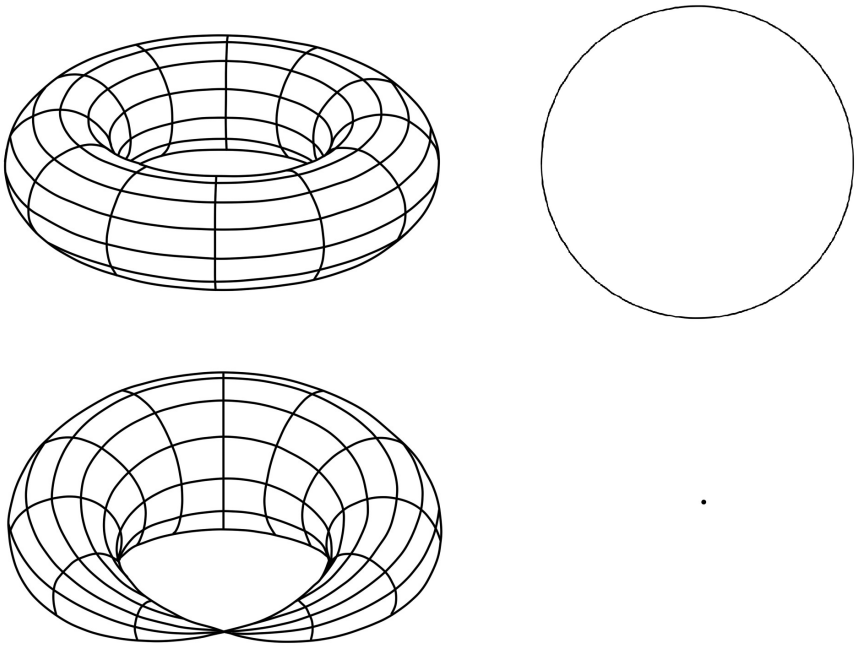

FIGURE 2.1: Representation of the four possible fibers of a point in a simple semitoric system. From left to right and from top to bottom: regular fiber, elliptic-regular fiber, focus-focus fiber, elliptic-elliptic fiber.

In [LP18], Le Floch and Palmer introduced *semitoric families*, which are one-parameter families of integrable systems with a fixed $S^1$ action that are semitoric for all but finitely many values of the parameter.

**Definition 2.19.** *A* semitoric family *is a family of integrable systems* $(M^4, \omega, F_t = (L, H_t))$, *with* $0 \leq t \leq 1$ *and* $H_t = H(t, \cdot)$ *such that:*

- $H : [0,1] \times M \to \mathbb{R}$ *is smooth.*
- *There exist* $k \in \mathbb{Z}_{\geq 0}$ *and* $t_1, \ldots, t_k \in [0,1]$ *such that* $(M, \omega, F_t)$ *is semitoric if and only if* $t \notin \{t_1, \ldots, t_k\}$.

*The values* $t_1, \ldots, t_k$ *are called* degenerate times.

A particular class of semitoric families is the class of *semitoric transition families*, studied by Le Floch and Palmer in [LP18] and [LP23], in which a single non-degenerate fixed point of elliptic-elliptic type becomes focus-focus after a degenerate time.

**Definition 2.20.** *A* semitoric transition family *with* transition point $p \in M$ *and* transition times $t^-, t^+ \in (0,1)$, $t^- < t^+$, *is a semitoric family* $(M, \omega, (L, H_t))$, *with* $0 \leq t \leq 1$, *with degenerate times* $t^-$ *and* $t^+$, *such that*

- *For* $t < t^-$ *and* $t > t^+$ *the point* $p$ *is singular of elliptic-elliptic type.*
- *For* $t^- < t < t^+$, *the point* $p$ *is singular of focus-focus type.*

- *For $t = t^-$ and $t = t^+$ there are no degenerate singular points in $M \setminus \{p\}$.*
- *If $p$ is a maximum (respectively a minimum) of $(H_0)_{|L^{-1}(L(p))}$ then $p$ is a minimum (respectively a maximum) of $(H_1)_{|L^{-1}(L(p))}$.*

One of the most accessible physical examples of semitoric systems is the *coupled angular momenta* system, which has been classified and for which the five semitoric invariants have been computed by Le Floch and Pelayo in [LP19] and by Alonso, Dullin and Hohloch in [ADH20]. The coupled angular momenta is, in fact, a semitoric transition family.

**The coupled angular momenta**

The coupling of two classical angular momenta was introduced by Sadovksii and Zhilinskii in [SZ99] and it is a well-known semitoric system. It is called the *coupled angular momenta* and is defined as the coupling of two rigid rotors, each of them modeled in a sphere $\mathbb{S}^2$. The strength of the coupling is measured by a *coupling parameter* $t$ and the amplitudes of the angular momenta are settled by fixing the radius of both spheres. Noticeably, in contrast with other semitoric systems such as the coupled spin-oscillator (see the works of Jaynes and Cummings in [JC63] and of Pelayo and Vũ Ngọc in [PV12]), this semitoric system is defined on a compact manifold.

The symplectic study of the coupled angular momenta was carried out by Le Floch and Pelayo in [LP19] and by Alonso, Dullin and Hohloch in [ADH20]. We adopt their notation to describe it.

**Definition 2.21.** *Consider $M = \mathbb{S}^2_1 \times \mathbb{S}^2_2$ and endow it with the symplectic form $\omega = -(R_1\omega_{\mathbb{S}^2_1} + R_2\omega_{\mathbb{S}^2_2})$, where, for $i \in \{1,2\}$, $\omega_{\mathbb{S}^2_i}$ is the standard symplectic form on $\mathbb{S}^2_i$ and $0 < R_1 < R_2$ are constants. For $i \in \{1,2\}$, let $x_i, y_i, z_i$ be the Cartesian coordinates on the unit sphere $\mathbb{S}^2_i$ and consider the parameter $t \in [0,1]$.*

*The* coupled angular momenta *is the family of 4-dimensional integrable systems $(M, \omega, F_t = (L, H_t))$ parameterized by $t$ and defined by*

$$\begin{cases} L(x_1, y_1, z_1, x_2, y_2, z_2) &:= R_1 z_1 + R_2 z_2, \\ H_t(x_1, y_1, z_1, x_2, y_2, z_2) &:= (1-t)z_1 + t(x_1x_2 + y_1y_2 + z_1z_2). \end{cases} \tag{2.1}$$

The coupled angular momenta is a semitoric transition family in which, for any value of $t$, the $L$ component of the moment map $F_t$ generates a simultaneous rotation of the two spheres around their vertical axes. Also, for any value of $t$, the coupled angular momenta has 4 fixed points at $p_{\pm,\pm} := (0,0,\pm 1,0,0,\pm 1)$. All of them are of elliptic-elliptic type except for the point $p_{+,-} = (0,0,1,0,0,-1)$, which is non-degenerate and of elliptic-elliptic type if $t < t^-$ or $t > t^+$, non-degenerate and of focus-focus type for $t^- < t < t^+$ and degenerate for $t \in \{t^-, t^+\}$, where

$$t^\pm = \frac{R_2}{2R_2 + R_1 \mp 2\sqrt{R_1R_2}}.$$

For any possible choice of $R_1$ and $R_2$, the critical values $t^-$ and $t^+$ satisfy $0 < t^- < \frac{1}{2} < t^+ \leq 1$. Hence, for $t = \frac{1}{2}$, the coupled angular momenta has always a focus-focus singular point. The image of the moment map of different systems in the semitoric transition family of the coupled angular momenta is depicted in Figure 2.2.

#### Classification of non-degenerate singular points in dimension 4

In Chapter 4 we work with integrable systems in 4-dimensional manifolds. In view of Theorem 2.13, a 4-dimensional integrable system $(M^4, \omega, F = (f_1, f_2))$ admits exactly six possible types of non-degenerate singular points, depending on its rank, which is 0 or 1, and on the type of their components.

A non-degenerate singular point of rank 0 is a fixed point and has no regular components. It can be:

- of *elliptic-elliptic* type, if it has two elliptic components,
- of *hyperbolic-hyperbolic* type, if it has two hyperbolic components,
- of *elliptic-hyperbolic* type, if it has one elliptic and one hyperbolic component,
- of *focus-focus* type, if it has one focus-focus component.

A non-degenerate singular point of rank 1 has a regular component. Depending on the other component, it can be:

- of *elliptic-regular* type, if the other component is elliptic,
- of *hyperbolic-regular* type, if the other component is hyperbolic.

Recall that in a 4-dimensional toric system the non-degenerate singular points can only be of elliptic-elliptic or elliptic-regular type, while in a semitoric system there can also exist non-degenerate singular points of focus-focus type.

For the classification of non-degenerate singular points of rank 0 of 4-dimensional integrable systems that we carry out in Chapter 4, we follow the recipe given by Bolsinov and Fomenko in [BF04]. This procedure is based in a handy adaptation of the general definition of non-degenerate singular points (see Definition 2.12) to the case of non-degenerate fixed points in 4-dimensional integrable systems.

**Definition 2.22.** *[BF04, Bolsinov and Fomenko, Definition 1.22] A fixed point $p$ of a completely integrable system $(M, \omega, F = (f_1, f_2))$ is non-degenerate if the Lie algebra $K(f_1, f_2)$ generated by the linear parts of the Hamiltonian vector fields $X_{f_1}$ and $X_{f_2}$ at $p$ is a Cartan subalgebra in $\mathfrak{sp}(4, \mathbb{R})$.*

The Lie algebra $K(f_1, f_2)$ can be described in terms of $f_1$ and $f_2$ and, in particular, in terms of the value at the fixed point $p$ of their quadratic parts, the Hessians $d^2 f_1$ and $d^2 f_2$: the Hessians, together with the matrix representation $\Omega$ of the symplectic form at $p$, induce the linear symplectic operators $A_{f_1} := \Omega^{-1} d^2 f_1$ and

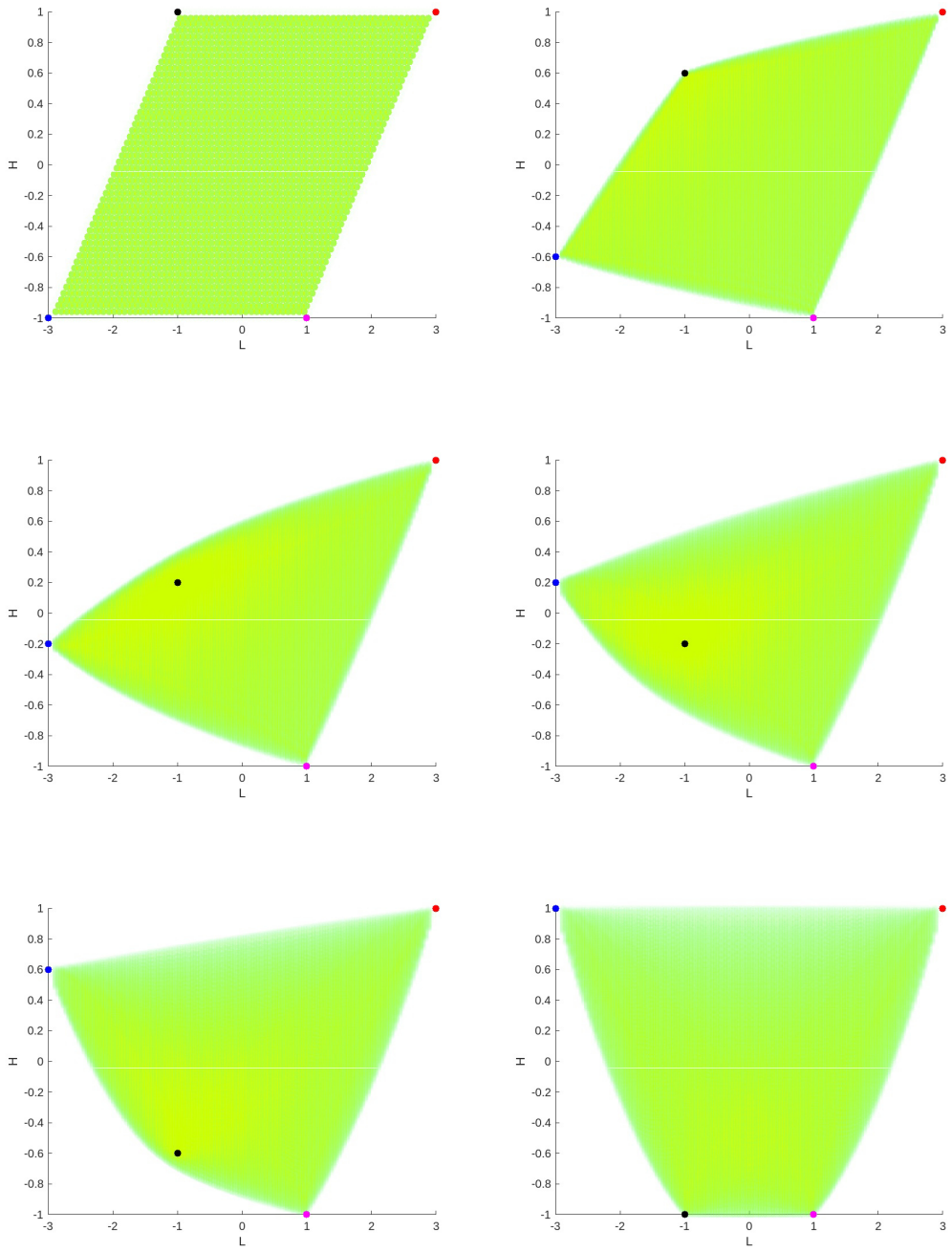


FIGURE 2.2: Image of the moment map of the classical coupled angular momenta for $R_1 = 1, R_2 = 2$ and values of $t$ between 0 (top left) and 1 (bottom right) by intervals of 0.2. The image of the focus-focus singularity is depicted in red, while the image of the other fixed points is depicted in black, magenta and blue. The pictures have been obtained numerically, see the code in Section B.1.1 in Appendix A.

$A_{f_2} := \Omega^{-1} d^2 f_2$, which coincide with the linear parts of $X_{f_1}$ and $X_{f_2}$ at $p$. Then, the Lie algebra $K(f_1, f_2)$ is the algebra generated by $A_{f_1}$ and $A_{f_2}$.

To check if $K(f_1, f_2)$ is a Cartan subalgebra in $\mathfrak{sp}(4, \mathbb{R})$, one has to see that it is 2-dimensional and that contains an element whose 4 eigenvalues are all different. If

this is the case, then the fixed point is proved to be non-degenerate.

After identifying a non-degenerate fixed point, one can determine its type using a classification result of Williamson (see the work of Williamson in [Wil36]), who proved that there are four Cartan subalgebras of $\mathfrak{sp}(4,\mathbb{R})$ up to conjugation. Each of them is generated by one of the following operators:

$$\begin{pmatrix} 0 & 0 & -\alpha & 0 \\ 0 & 0 & 0 & -\beta \\ \alpha & 0 & 0 & 0 \\ 0 & \beta & 0 & 0 \end{pmatrix} \begin{pmatrix} -\alpha & 0 & 0 & 0 \\ 0 & 0 & 0 & -\beta \\ 0 & 0 & \alpha & 0 \\ 0 & \beta & 0 & 0 \end{pmatrix} \begin{pmatrix} -\alpha & 0 & 0 & 0 \\ 0 & -\beta & 0 & 0 \\ 0 & 0 & \alpha & 0 \\ 0 & 0 & 0 & \beta \end{pmatrix} \begin{pmatrix} -\alpha & -\beta & 0 & 0 \\ \beta & -\alpha & 0 & 0 \\ 0 & 0 & \alpha & -\beta \\ 0 & 0 & \beta & \alpha \end{pmatrix}, \quad (2.2)$$

where $\alpha, \beta \in \mathbb{R}$.

The Lie algebra $K(f_1, f_2)$ of a non-degenerate fixed point $p$ has to be conjugate to one of the four above and one can find which of them by picking one element $A$ of $K(f_1, f_2)$ which has four different eigenvalues $\lambda_1, \lambda_2, \lambda_3, \lambda_4$. Then, according to Rüssmann (see the work of Rüssmann in [Rüs64]), the type of $p$ is:

- elliptic-elliptic, if $A$ four imaginary eigenvalues of the form $\{\lambda_1, \lambda_2\} = \{\pm i\alpha\}$ and $\{\lambda_3, \lambda_4\} = \{\pm i\beta\}$,
- elliptic-hyperbolic, if $A$ has two real and two imaginary eigenvalues of the form $\{\lambda_1, \lambda_2\} = \{\pm i\alpha\}$ and $\{\lambda_3, \lambda_4\} = \{\pm\beta\}$,
- hyperbolic-hyperbolic, if $A$ has four real eigenvalues of the form $\{\lambda_1, \lambda_2\} = \{\pm\alpha\}$ and $\{\lambda_3, \lambda_4\} = \{\pm\beta\}$,
- focus-focus, if $A$ has four complex eigenvalues of the form $\{\lambda_1, \lambda_2, \lambda_3, \lambda_4\} = \{\pm\alpha \pm i\beta\}$,

in all cases with $\alpha, \beta \in \mathbb{R}^{\neq 0}$, and for the elliptic-elliptic and hyperbolic-hyperbolic cases with $\alpha \neq \beta$.

Summarizing, the non-degeneracy and the type of a fixed point can be determined through the eigenvalues of any operator $A$ given by a linear combination of $A_{f_1} = \Omega^{-1} d^2 f_1$ and $A_{f_2} = \Omega^{-1} d^2 f_2$ whose eigenvalues are all different. The matrix form of the operator $A$ will be conjugate to one of the above matrices and its spectrum will be of one of the above types.

## 2.3 b-Symplectic manifolds

The formulation of classical mechanics that we have introduced in the previous sections is based on the geometric features of symplectic manifolds, which are just manifolds admitting a symplectic form. Symplectic forms are used to define Hamiltonian vector fields and integrable systems but, if one looks closely, the object on which the definition of these concepts truly relay is not the symplectic form but th Poisson bracket operator induced from it. In modern physics, the usual and more general setting to study dynamics is Poisson manifolds, which are generalizations of symplectic manifolds in which the main structure, instead of a symplectic form, is directly a Poisson bracket operator (see the work of Marsden and Ratiu in [MR99]).

Inside the large class of Poisson manifolds we encounter *b-symplectic manifolds*, a family of manifolds which is wider than the one of symplectic manifolds and contains it.

The motivation for the definition and study of *b*-symplectic manifolds is to have a way to equip systems with boundaries with symplectic forms, as inaugurated by Nest and Tsygan in [TN96]. This can be performed using a kind of differential forms called *b-symplectic forms* that extend the capabilities of symplectic forms. These forms give raise to *b-symplectic geometry* and with them one can formulate classical dynamics in systems with boundaries.

To work with systems with boundaries, one option is to directly consider manifolds with boundary and then use on them the language of *b*-forms and *b*-calculus introduced by Melrose in [Mel93]. Another option is to use the same language but replacing the manifolds with boundary by manifolds without boundary in which a distinguished hypersurface is selected to represent the boundary. The formulation of *b*-symplectic geometry is based on the second approach, which we summarize next while referring to the works of Guillemin, Miranda, Pires and Scott in [GMP11], [GMP14] and [Gui+15] for further details.

A *b-manifold* is a pair $(M, Z)$ where $M$ is a connected manifold and $Z \subset M$ is an embedded submanifold of co-dimension 1 which we usually call *critical hypersurface*. A *b-map* is a map $f : (M_1, Z_1) \longrightarrow (M_2, Z_2)$ between *b*-manifolds such that $f$ is transverse to $Z_2$ and $Z_1 = f^{-1}(Z_2)$.

**Definition 2.23** (*b*-vector field)**.** *A vector field on a b-manifold $(M, Z)$ is called a* b-vector field *if it is tangent to $Z$ at every point in $Z$.*

Let $(M^n, Z)$ be a *b*-manifold. If $f$ is a local defining function of $Z$ on an open set $U \subset M$ and $(f, x_2, \ldots, x_n)$ is a chart on $U$, then the set of *b*-vector fields on $U$ is a free $C^\infty(M)$-module with basis

$$(f\frac{\partial}{\partial f}, \frac{\partial}{\partial x_2}, \ldots, \frac{\partial}{\partial x_n}).$$

There exists a vector bundle associated to this module called the *b-tangent bundle* and denoted by ${}^bTM$. The *b-cotangent bundle* ${}^bT^*M$ of $M$ is defined to be the vector bundle dual to ${}^bTM$.

For each $k > 0$, ${}^b\Omega^k(M)$ denotes the space of *differential b-forms of degree k* or sections of $\bigwedge^k({}^bT^*M)$. Fixing a local defining function $f$ of $Z$, every *b*-form $\omega$ of degree $k$ can be written as

$$\omega = \alpha \wedge \frac{df}{f} + \beta, \text{ with } \alpha \in \Omega^{k-1}(M) \text{ and } \beta \in \Omega^k(M). \tag{2.3}$$

This decomposition enables us to extend the exterior differential operator $d$ to ${}^b\Omega(M)$ by setting

$$d\omega = d\alpha \wedge \frac{df}{f} + d\beta.$$

The right hand side agrees with the usual exterior differential operator $d$ on $M \setminus Z$

and extends smoothly over $M$ as a section of $\bigwedge^{k+1}({}^bT^*M)$. The fact that $d^2 = 0$ allows us to define the *complex of b-forms* ${}^b\Omega(M)$ on the *b*-cotangent bundle. The cohomology associated to this complex is the *b-cohomology* and it is denoted by ${}^bH^*(M)$. The elements of ${}^b\Omega^0(M)$ are also called *b-functions* and the following definition characterizes them.

**Definition 2.24** (*b*-function)**.** *A* *b*-function *on a b-manifold $(M, Z)$ is a function which takes values in $\mathbb{R} \cup \{\infty\}$, which is smooth away from $Z$ and which near $Z$ has the form*

$$c \log |f| + g,$$

*where $c \in \mathbb{R}$, $f$ is a local defining function of $Z$ and $g$ is a smooth function on $M$. The set of b-functions on a b-manifold $(M, Z)$ is denoted by ${}^bC^\infty(M, Z)$.*

The differential operator $d$ acts on *b*-functions as:

$$d(c \log |f| + g) := c \frac{df}{f} + dg \in {}^b\Omega^1(M),$$

where $dg$ and $df$ are the standard de Rham derivatives.

A special class of differential *b*-forms of degree 2 is the class of *b-symplectic forms*, which are, on *b*-manifolds, the analogue of symplectic forms.

**Definition 2.25** (*b*-symplectic manifold)**.** *Let $(M^{2n}, Z)$ be a b-manifold and let $\omega$ be a b-form of degree 2 on $(M, Z)$. We say that $\omega$ is a* *b*-symplectic form *if:*

- *closed: $d\omega = 0$, and*
- *non-degenerate: for all $p \in M$, $\omega_p$ is of maximal rank as an element of $\bigwedge^2({}^bT^*_pM)$.*

*If $(M, Z)$ admits a b-symplectic form, the triple $(M, Z, \omega)$ is called a* *b*-symplectic manifold.

The simplest examples of *b*-symplectic manifolds are analogue of the basic examples of symplectic manifolds.

**Example 2.26.** *Consider the Euclidean space $\mathbb{R}^{2n}$ with coordinates $x_1, \ldots, x_n, y_1, \ldots, y_n$. Define $Z \subset \mathbb{R}^{2n}$ as $Z := \{(x_1, \ldots, x_n, y_1, \ldots, y_n) \in \mathbb{R}^{2n} \mid x_1 = 0\}$. Then, $(\mathbb{R}^{2n}, Z)$ is a b-manifold and the b-form of degree 2*

$$\omega = \frac{dx_1}{x_1} \wedge dy_1 + \sum_{i=2}^{n} dx_i \wedge dy_i$$

*is a b-symplectic form on $(\mathbb{R}^{2n}, Z)$.*

**Example 2.27.** *The torus $\mathbb{T}^{2n}$ with coordinates $\theta_1, \ldots, \theta_{2n}$ can be turned into a b-manifold by defining the critical hypersurface $Z$ as $Z := \{(\theta_1, \ldots, \theta_{2n}) \in \mathbb{T}^{2n} \mid \theta_1 \in \{0, \pi\}\}$. Then, $(\mathbb{T}^{2n}, Z)$ can be equipped with the b-symplectic form*

$$\omega = \frac{d\theta_1}{\sin \theta_1} \wedge d\theta_2 + \sum_{i=2}^{n} d\theta_{2i-1} \wedge d\theta_{2i}.$$

**Example 2.28.** *Consider the unit sphere $\mathbb{S}^2 \subset \mathbb{R}^3$. Define the critical hypersurface $Z$ as $Z := \{(x, y, z) \in \mathbb{S}^2 \mid z = 0\}$. The b-manifold $(\mathbb{S}^2, Z)$ can be endowed with a b-symplectic form $\omega$ that coincides with the standard symplectic form of $\mathbb{S}^2$ in the North and South poles and has the expression*

$$\omega = d\theta \wedge \frac{dz}{z}$$

*in the rest of $(\mathbb{S}^2, Z)$ in cylindrical coordinates.*

These examples of *b*-symplectic manifolds are called, respectively, the *b-2n-dimensional Euclidean space*, the *b-2n-torus* and the *b-2-sphere*. The *b*-symplectic forms which we equipped them with are called *standard b-symplectic forms*.

Some properties of *b*-symplectic forms are directly deduced from the decomposition of Equation (2.3). Suppose that $(M^{2n}, Z, \omega)$ is a compact *b*-symplectic manifold and that $f : M \to \mathbb{R}$ is a defining function of $Z$. Then, $\omega$ decomposes as

$$\omega = \alpha \wedge \frac{df}{f} + \beta, \text{ with } \alpha \in \Omega^1(M) \text{ and } \beta \in \Omega^2(M)$$

and is symplectic in $M \setminus Z$. The form $\omega$ is also symplectic at any $p \in Z$ as an element of $\bigwedge^2(\text{span}\{T_p^*Z, \left(\frac{df}{f}\right)_p\})$. If $\iota_Z : Z \to M$ is the inclusion map, then $\iota_Z^*\alpha$ is an intrinsically defined 1-form on $Z$ which defines a foliation of $Z$ by symplectic leaves of dimension $2n-2$ called the *symplectic foliation of $Z$*. The symplectic form at each leaf $L$ of the symplectic foliation of $Z$ is exactly $\iota_L^*\beta$ where $\iota_L$ is the inclusion map $\iota_L : L \to M$.

In the same way that a smooth function on a symplectic manifold induces a vector field, a *b*-function on a a *b*-symplectic manifold induces a *b*-vector field called *Hamiltonian b-vector field*. It preserves the value of the *b*-function that induces it, which is called the *Hamiltonian b-function* or the *b-Hamiltonian*.

**Definition 2.29.** *Let $H$ be a b-function on a b-symplectic manifold $(M, Z, \omega)$. The* b-Hamiltonian vector field associated to *$H$, and denoted by $X_H$, is defined as the only b-vector field satisfying $\iota_{X_H}\omega = -dH$.*

Then, on a *b*-symplectic manifold $(M, Z, \omega)$, any *b*-function $H$ induces a dynamical system whose evolution in time is given by the flow of $X_H$. The tuple $(M, Z, \omega, H)$ is known as the *b-Hamiltonian system given by $H$*.

On a *b*-symplectic manifold, the *b*-symplectic form also induces a *Poisson bracket* operator.

**Definition 2.30.** *Let $(M, Z, \omega)$ be a b-symplectic manifold. The operator defined by*

$$\begin{array}{rccc} \{\cdot,\cdot\}: & {}^b\mathcal{C}^\infty(M,Z) \times {}^b\mathcal{C}^\infty(M,Z) & \longrightarrow & {}^b\mathcal{C}^\infty(M,Z) \\ & (f,g) & \longmapsto & \{f,g\} := \omega(X_f, X_g) \end{array},$$

*where $X_f$ and $X_g$ are the Hamiltonian b-vector fields of $f$ and $g$, respectively, is called the* Poisson bracket.

The Poisson bracket induced by a *b*-symplectic form satisfies the same properties as the Poisson bracket induced by a symplectic form does. Therefore, it can also be

used to define first integrals of $b$-Hamiltonian systems in a smart way. Similarly to the case of Hamiltonian systems, a first integral of a $b$-Hamiltonian system given by a $b$-function $H$ is any $b$-function $f$ such that $\{f, H\} = 0$.

### 2.3.1 b-Integrable systems and b-symplectic toric manifolds

The notion of integrability of Hamiltonian systems based on the existence of a maximal number of first integrals can be naturally extended to $b$-Hamiltonian systems.

**Definition 2.31.** *Let $(M, Z, \omega)$ be a $b$-symplectic manifold of dimension $2n$. Let $H$ be a $b$-Hamiltonian defined on $M$. The $b$-Hamiltonian system given by $H$ is* completely $b$-integrable *or* $b$-integrable *if there exists a tuple of $n$ $b$-functions $f_1, \dots, f_n$ such that:*

1. *$df_1, \dots, df_n$, as sections of ${}^bT^*M$, are linearly independent almost everywhere in $M$ and in $Z$, and*
2. *$f_1, \dots, f_n, H$ commute pairwise.*

*The $b$-Hamiltonian $H$ may be one of the $f_i$'s and the tuple $F = (f_1, ..., f_n)$ is called the* $b$-moment map *of the $b$-integrable system. Sometimes, the $b$-moment map $F$ is directly referred to as the* $b$-integrable system.

The *joint flow* of a $b$-integrable system $(M, Z, \omega, F = (f_1, ..., f_n))$ is the $\mathbb{R}^n$ action on $M$ induced by the commuting flows of the Hamiltonian $b$-vector fields of the first integrals $f_1, ..., f_n$. It preserves the joint level sets of $F = (f_1, \dots, f_n)$ and it also preserves the critical hypersurface $Z$.

Note that, in general, the image of the $b$-moment map $F : M \to \mathbb{R}^n$ of a $b$-integrable system $(M^{2n}, Z, \omega, F = (f_1, \dots, f_n))$ is not bounded even if $M$ is compact (see Figure 2.3). Because each $f_i : M \to \mathbb{R}$ is a $b$-function (see Definition 2.24), they may contain a logarithm term that makes them unbounded. This is a main issue when one tries to obtain a finite Bohr-Sommerfeld quantization of a $b$-symplectic manifold and the reason why we introduce *Bohr-Sommerfeld quantization with sign* in Chapter 5.

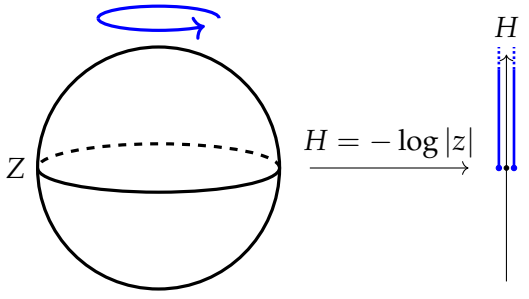


FIGURE 2.3: On the standard $b$-2-sphere $(\mathbb{S}^2, Z, \omega)$, the $b$-Hamiltonian $H = -\log|z|$ defines a $b$-integrable system. The flow of the associated Hamiltonian $b$-vector field $X_H$ induces a rotation action around the $z$ axis of $(\mathbb{S}^2, Z)$.

Normal forms of $b$-integrable systems were obtained by Guillemin, Miranda and Pires in [GMP14] and by Kiesenhofer, Miranda and Scott in [KMS16]. In particular,

they showed that there exists a semi-local invariant associated to each connected component of the critical hypersurface $Z \subset M$, the *modular weight* or the *modular period* (see the work of Radko in [Rad02]).

**Theorem 2.32** (Kiesenhofer-Miranda-Scott [KMS16]). *Let $(M^{2n}, Z, \omega, F)$ be a b-integrable system and let $p \in Z$ be a regular point of $F$ such that the fiber $\Lambda$ of $F$ containing $p$ is compact. Then, $\Lambda$ is diffeomorphic to $\mathbb{T}^n$ and there exists an open neighborhood $U$ of $\Lambda$ and a coordinate chart $(\theta_1, \dots, \theta_n, p_1, \dots, p_n) : U \to \mathbb{T}^n \times \mathbb{R}^n$ such that*

$$\omega|_U = \sum_{i=1}^{n-1} dp_i \wedge d\theta_i + c\frac{dp_n}{p_n} \wedge d\theta_n, \tag{2.4}$$

*and such that $F$ only depends on the coordinates $p_1, \dots, p_n$. The constant $c \in \mathbb{R}$ in Equation (2.4) does not depend on the particular coordinate chart and it is an invariant associated to the connected component $Z_i$ of $Z$ containing $p$. It is called the* modular weight of the connected component $Z_i$ *or just the* modular weight.

A particular class of $b$-integrable systems are *b-symplectic toric manifolds*, the $b$-symplectic analogues of toric manifolds. These systems were studied by Guillemin, Miranda, Pires and Scott in [Gui+15] and also by Gualtieri, Li, Pelayo and Ratiu in [Gua+17] in the case that the critical hypersurface admits a normal self-crossing.

**Definition 2.33.** *A b-integrable system $(M^{2n}, Z, \omega, F = (f_1, \dots, f_n))$ is called* $b$-toric *if the flow of each $X_{f_i}$ is $2\pi$-periodic almost everywhere.*

As in the case of toric systems, the joint flow of a $b$-toric system $(M^{2n}, Z, \omega, F = (f_1, \dots, f_n))$ always induces an effective action of $\mathbb{T}^n$ on $M$ and this property can be used as its definition. If a $b$-symplectic manifold is compact and admits a $b$-toric integrable system, we call it a *b-symplectic toric manifold*. We typically identify a $b$-toric system $(M, Z, \omega, F)$ defined on a compact $b$-symplectic manifold $(M, Z, \omega)$ with the $b$-symplectic toric manifold itself, and we use the expression *b-symplectic toric manifold* both to talk about the system and the manifold.

In general, the image of the $b$-moment map $F : M \to \mathbb{R}^n$ of a $b$-symplectic toric manifold $(M^{2n}, Z, \omega, F = (f_1, \dots, f_n))$ is unbounded and, hence, it is not a convex polytope as it is in the case of symplectic toric manifolds. In [Gui+15], Guillemin, Miranda, Pires and Scott define the notion of *b-moment map codomain*, which is essentially a $b$-manifold $(\mathcal{R}^n, \mathcal{Z})$ in which a modification $\tilde{F} : M \to \mathcal{R}^n$ of the $b$-moment map $F : M \to \mathbb{R}^n$ takes values.

In the $b$-moment map codomain there exists the concept of *b-polytope*, a combinatorial object analogous to a convex polytope, and it turns out that the image of $\tilde{F}$, called *b-moment polytope*, is always a $b$-polytope. Moreover, there is a special class of $b$-polytopes called *Delzant b-polytopes* that can be used to classify $b$-symplectic toric manifolds in the same way that Delzant polytopes classify symplectic toric manifolds. See the work of Guillemin, Miranda, Pires and Scott in [Gui+15] for the details of the definition of $b$-moment map codomain, $b$-polytope and Delzant $b$-polytope.

**Theorem 2.34** (Guillemin-Miranda-Pires-Scott [Gui+15]). *For any b-symplectic toric manifold $(M^{2n}, Z, \omega, F)$, the b-moment polytope $\widetilde{F}(M)$ is a Delzant b-polytope.*

*Conversely, for any Delzant b-polytope $\Delta \subset \mathcal{R}^n$, there exists a b-symplectic toric manifold $(M^{2n}, Z, \omega, F)$ such that its b-moment polytope $\widetilde{F}(M)$ is exactly $\Delta$.*

*Finally, if there exists a diffeomorphism $\varphi : M_1 \to M_2$ between two b-symplectic toric manifolds $(M_1^{2n}, Z_1, \omega_1, F_1)$ and $(M_2^{2n}, Z_2, \omega_2, F_2)$ which satisfies $\varphi^{-1}(Z_2) = Z_1$, $\varphi^*\omega_2 = \omega_1$ and $F_2 \circ \varphi = F_1$, then their Delzant b-polytopes $\widetilde{F}_1(M_1)$ and $\widetilde{F}_2(M_2)$ coincide up to a translation.*

A consequence of Theorem 2.34 is that every *b*-symplectic toric manifold is either a product of a *b*-2-torus with a symplectic toric manifold, or a manifold obtained from a product of a *b*-2-sphere with a smooth symplectic toric manifold by a sequence of symplectic cuts performed at the north and south "polar caps", away from the critical hypersurface $Z$ (see the work of Lerman in [Ler95] for details on symplectic cuts).

In [Gui+15], Guillemin, Miranda, Pires and Scott proved the following result about the semi-local expression of the moment map of a *b*-symplectic toric manifold.

**Proposition 2.35** (Guillemin-Miranda-Pires-Scott [Gui+15])**.** *Let $(M^{2n}, Z, \omega, F)$ be a b-symplectic toric manifold, $L$ a leaf of the symplectic foliation of a connected component $Z_i$ of $Z$ and $c$ the modular weight of $Z_i$. Then, there is a neighborhood $L \times \mathbb{S}^1 \times (-\varepsilon, \varepsilon) \cong U \subseteq M$ of $Z_i$ such that the moment map on $U \setminus Z_i$ is:*

$$\begin{array}{rccc} F_{U\setminus Z_i}: & L \times \mathbb{S}^1 \times ((-\varepsilon,\varepsilon)\setminus\{0\}) & \longrightarrow & \mathbb{R}^{n-1}\times\mathbb{R} \\ & (\ell,\theta,t) & \longmapsto & (F_L(\ell), c\log|t|) \end{array},$$

*where $F_L : L \to \mathbb{R}^{n-1}$ is a moment map for the b-toric integrable system restricted to $L$.*

The singular points of a *b*-symplectic toric manifold are all non-degenerate and have only elliptic components. The easiest examples of *b*-integrable systems with more complicated singular points were developed by Kiesenhofer and Miranda in [KM17] in 6-dimensional *b*-symplectic manifolds. In their examples, the singular points admit focus-focus type components and are located at the critical hypersurface $Z$.

## 2.4 Cotangent models

The cotangent bundle of a smooth manifold is the type of symplectic manifold which is best suited to model physical systems, as Examples 2.6 and 2.7 show. The features of cotangent bundles that make them optimal for the study of physics problems, especially in mechanics, are the following:

- If a smooth manifold $M^n$ models the set of possible positions or the *configuration space* of a particle system, its cotangent bundle $T^*M$ represents the set of possible pairs of position and momentum or the *phase space* of the system.
- In the cotangent bundle $T^*M$ of a smooth manifold $M^n$ there is an intrinsic canonical linear 1-form $\lambda$, called *Liouville form*, which, in local coordinates

$q_1, \ldots, q_n, p_1, \ldots, p_n$ of $T^*M$ has the expression

$$\lambda = \sum_{i=1}^{n} p_i \, dq_i,$$

and whose differential is a symplectic form $\omega$, which writes as

$$\omega = \sum_{i=1}^{n} dp_i \wedge dq_i.$$

- If $H(q_1, \ldots, q_n, p_1, \ldots, p_n)$ is a function on the cotangent bundle $(T^*M, \omega)$ that represents the energy of a particle system, Hamilton's equations from classical mechanics, which write as

$$\begin{cases} X_H^{q_i} = \frac{\partial H}{\partial p_i} \\ X_H^{p_i} = -\frac{\partial H}{\partial q_i} \end{cases},$$

are obtained from the definition of the Hamiltonian vector field $X_H$ corresponding to $H$. That is, the evolution of the system is given by the flow of the only vector field $X_H$ that satisfies

$$\iota_{X_H}\omega = -dH.$$

Physical systems modeled on cotangent bundles, which provide the mathematical framework for analyzing their dynamics, are called *cotangent models*. A tool which complements cotangent models is the *cotangent lift*, a procedure which establishes a correspondence between the dynamics in the configuration space of a system and the dynamics in the phase space of the same system.

**Definition 2.36.** *Let $\rho : G \times M \longrightarrow M$ be a group action of a Lie group $G$ on a smooth manifold $M$. For each $g \in G$, there is an induced diffeomorphism $\rho_g : M \longrightarrow M$. The* cotangent lift *of $\rho_g$, denoted by $\hat{\rho}_g$, is the diffeomorphism on $T^*M$ defined in the following way: for all $(q, p) \in T^*M$,*

$$\hat{\rho}_g(q, p) := (\rho_g(q), ((d\rho_g)_q^*)^{-1}(p)).$$

Figure 2.4 depicts the construction of the cotangent lift. From its definition, one can check that the following diagram commutes:

$$\begin{array}{ccc} T^*M & \xrightarrow{\hat{\rho}_g} & T^*M \\ \downarrow{\scriptstyle \pi} & & \downarrow{\scriptstyle \pi} \\ M & \xrightarrow{\rho_g} & M \end{array}$$

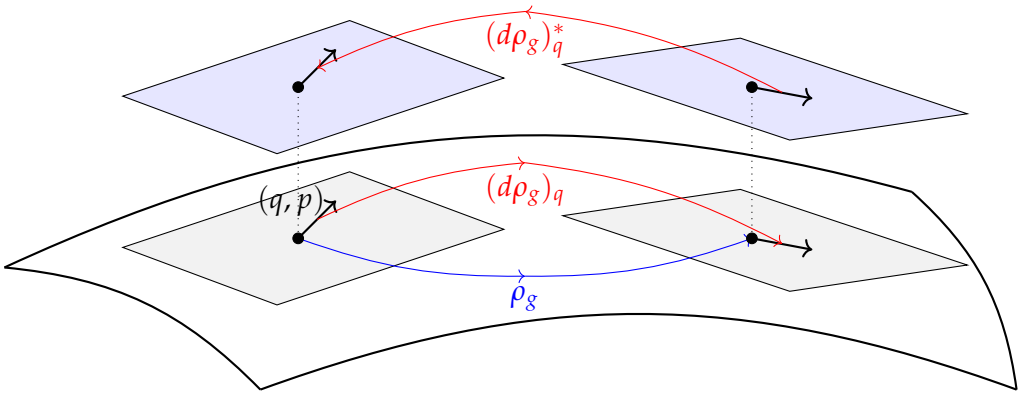


FIGURE 2.4: The cotangent lift of a map $\rho_g$ on $M$ is a map $\hat{\rho}_g$ on the cotangent bundle $T^*M$.

The cotangent lift gives a systematic way to lift the dynamics from the space of positions $M$ to the space of positions and momenta $T^*M$, which has a canonical symplectic form. One of its properties is that it preserves the Liouville form $\lambda$ of $T^*M$ and, hence, it also preserves the symplectic form $\omega = d\lambda$ of $T^*M$. Another of its properties is that, for any vector field $X$ on $M$, there exists a Hamiltonian vector field $\hat{X}$ on $T^*M$ whose flow is the cotangent lift of the flow of $X$ and whose Hamiltonian function is $\lambda(X)$ (for more details, see the work of Guillemin and Sternberg in [GS84]). These properties are essential to use the cotangent lift to obtain physical conclusions about integrable systems, specially in the context of mechanics, as the following basic examples show.

**Example 2.37.** *Consider the cotangent bundle $T^*\mathbb{R}^3$, which corresponds to the phase space of a free particle moving in a 3-dimensional space. In coordinates $q_1, q_2, q_3, p_1, p_2, p_3$ of $T^*\mathbb{R}^3$, the canonical symplectic form writes as $\omega = \sum_{i=1}^{n} dp_i \wedge dq_i$ and the energy of a particle of mass $m$ is $H = \frac{p^2}{2}$. Now let $\rho : (\mathbb{R}^3, +) \times \mathbb{R}^3 \to \mathbb{R}^3$ be the Lie group action corresponding to a spatial translation of the particle, which is defined by $\rho_x(q) = q + x$.*

*By definition, $\hat{\rho}_x$, the cotangent lift of $\rho_x$, is the following map in $T^*\mathbb{R}^3$*

$$\hat{\rho}_x(q,p) = (\rho_x(q), ((d\rho_x)^*_q)^{-1}(p)) = (q+x, ((Id^*)^{-1}(p)) = (q+x, p). \tag{2.5}$$

*Besides preserving the symplectic form, the cotangent lift preserves $H = \frac{p^2}{2}$, the energy of the particle.*

**Example 2.38.** *Consider again the cotangent bundle $T^*\mathbb{R}^3$, which represents the phase space of a free particle in a 3-dimensional space. Let $\rho : SO(3,\mathbb{R}) \times \mathbb{R}^3 \to \mathbb{R}^3$ be the Lie group action corresponding to a rotation of the particle, which is defined by $\rho_A(q) = A \cdot q$.*

*By definition, $\hat{\rho}_A$, the cotangent lift of $\rho_A$, is the following map in $T^*\mathbb{R}^3$*

$$\hat{\rho}_A(q,p) = (\rho_A(q), ((d\rho_A)^*_q)^{-1}(p)) = (A\cdot q, ((A^*)^{-1}(p)) = (A\cdot q, A\cdot p). \tag{2.6}$$

*Again, the cotangent lift preserves, a part of the symplectic form $\omega = \sum_{i=1}^{n} dp_i \wedge dq_i$, the energy $H = \frac{p^2}{2}$ of the particle.*

The cotangent lift can also be used to generate two of the three types of non-regular components of a non-degenerate singular point of an integrable system $(M, \omega, F = (f_1, \dots, f_n))$, the hyperbolic and the focus-focus types. This is because there exist Lie group actions whose cotangent lifts coincide with the group actions induced by a hyperbolic and by a focus-focus component of the moment map, as the next examples show.

**Example 2.39.** *Consider $\mathbb{R}^2$, take coordinates $x, y$ and equip it with the standard symplectic form $\omega = dx \wedge dy$. Consider the integrable system $(\mathbb{R}^2, \omega, F = (f_1) = xy)$, which has a non-degenerate fixed point at the origin. The only component $f_1$ of the moment map $F$ is already in normal form at the fixed point and it corresponds to that of a hyperbolic component.*

*The Hamiltonian vector field associated to $f_1$ is*

$$X_{f_1} = -x\frac{\partial}{\partial x} + y\frac{\partial}{\partial y},$$

*its Hamiltonian flow is*

$$\phi_t^{f_1}(x, y) = (xe^{-t}, ye^t)$$

*and it induces an action of $\mathbb{R}$ on $\mathbb{R}^2$.*

*Now, consider the action of $\mathbb{R}$ on $\mathbb{R}$ given by:*

$$\begin{array}{rccccc} \rho^h : & \mathbb{R} & \times & \mathbb{R} & \longrightarrow & \mathbb{R} \\ & t & , & x & \longmapsto & e^{-t}x \end{array}.$$

*The cotangent lift $\hat{\rho}_t^h$ of $\rho_t^h$, in coordinates $x, y$ of $T^*\mathbb{R} \cong \mathbb{R}^2$, is*

$$\begin{array}{rccccc} \hat{\rho}^h : & \mathbb{R} & \times & T^*\mathbb{R} & \longrightarrow & T^*\mathbb{R} \\ & t & , & \begin{pmatrix} x \\ y \end{pmatrix} & \longmapsto & \begin{pmatrix} e^{-t}x \\ e^t y \end{pmatrix} \end{array},$$

*and it coincides with the Hamiltonian flow of $f_1$.*

**Example 2.40.** *Consider $\mathbb{R}^4$, take coordinates $x_1, x_2, y_1, y_2$ and equip it with the standard symplectic form $\omega = dx_1 \wedge dy_1 + dx_2 \wedge dy_2$. Consider the integrable system $(\mathbb{R}^2, \omega, F = (f_1, f_2) = (x_1y_2 - x_2y_1, x_1y_1 + x_2y_2))$, which has a non-degenerate fixed point at the origin. The components $f_1$ and $f_2$ of the moment map $F$ are already in normal form at the fixed point and it corresponds to that of a focus-focus double component.*

*The Hamiltonian vector field associated to $f_1$ is*

$$X_{f_1} = x_2\frac{\partial}{\partial x_1} - x_1\frac{\partial}{\partial x_2} + y_2\frac{\partial}{\partial y_1} - y_1\frac{\partial}{\partial y_2}$$

*and the Hamiltonian vector field associated to $f_2$ is*

$$X_{f_2} = -x_1\frac{\partial}{\partial x_1} - x_2\frac{\partial}{\partial x_2} + y_1\frac{\partial}{\partial y_1} + y_2\frac{\partial}{\partial y_2}.$$

*Their respective Hamiltonian flows are*

$$\phi_s^{f_1}(x_1, x_2, y_1, y_2) = (x_1 \cos s + x_2 \sin s, -x_1 \sin s + x_2 \cos s, \\ y_1 \cos s + y_2 \sin s, -y_1 \sin s + y_2 \cos s)$$

*and*

$$\phi_t^{f_2}(x_1, x_2, y_1, y_2) = (x_1 e^{-t}, x_2 e^{-t}, y_1 e^{t}, y_2 e^{t}).$$

*Then, the joint flow of $f_1$ and $f_2$ induces an action of $\mathbb{S}^1 \times \mathbb{R}$ on $\mathbb{R}^4$.*

*Now, consider the action of $S^1 \times \mathbb{R}$ on $\mathbb{R}^2$ given by*

$$\begin{array}{rccccc} \rho^f : & (S^1 \times \mathbb{R}) & \times & \mathbb{R}^2 & \longrightarrow & \mathbb{R}^2 \\ & (s,t) & , & \begin{pmatrix} x_1 \\ x_2 \end{pmatrix} & \longmapsto & \begin{pmatrix} e^{-t} & 0 \\ 0 & e^{-t} \end{pmatrix} \begin{pmatrix} \cos s & \sin s \\ -\sin s & \cos s \end{pmatrix} \begin{pmatrix} x_1 \\ x_2 \end{pmatrix} \end{array} .$$

*The cotangent lift $\hat{\rho}_{s,t}^f$ of $\rho_{s,t}^f$, in coordinates $x_1, x_2, y_1, y_2$ of $T^*\mathbb{R}^2 \cong \mathbb{R}^4$, is:*

$$\begin{array}{rccccc} \hat{\rho}^f : & (S^1 \times \mathbb{R}) & \times & T^*\mathbb{R}^2 & \longrightarrow & T^*\mathbb{R}^2 \\ & (s,t) & , & \begin{pmatrix} x_1 \\ x_2 \\ y_1 \\ y_2 \end{pmatrix} & \longmapsto & \begin{pmatrix} e^{-t}(x_1 \cos s + x_2 \sin s) \\ e^{-t}(-x_1 \sin s + x_2 \cos s) \\ e^{t}(y_1 \cos s + y_2 \sin s) \\ e^{t}(-y_1 \sin s + y_2 \cos s) \end{pmatrix} \end{array} ,$$

*and it coincides with the joint flow of $f_1$ and $f_2$.*

### 2.4.1 Cotangent models for b-symplectic manifolds

Cotangent models and the procedure of the cotangent lift can also be considered in the setting of *b*-symplectic forms and *b*-symplectic manifolds. In [KM17], Kiesenhofer and Miranda introduced the *b-cotangent models*, the *b*-symplectic versions of the cotangent models of Examples 2.6 and 2.7, which are defined in the *b*-cotangent bundle of a *b*-manifold. It turns out that the *b*-cotangent bundle of a *b*-manifold can realized as a *b*-symplectic manifold because there is an intrinsic *b*-symplectic form which it can be endowed with: the so-called *canonical b-symplectic form*.

**Definition 2.41.** *Let $(M^n, Z)$ be a b-manifold and let ${}^bT^*M$ be its b-cotangent bundle. Defining a critical hypersurface on ${}^bT^*M$ by $\pi^{-1}(Z)$, where $\pi :^b T^*M \longrightarrow M$ is the canonical projection, $({}^bT^*M, \pi^{-1}(Z))$ is a b-manifold. There is an intrinsic canonical linear b-form of degree 1 on $({}^bT^*M, \pi^{-1}(Z))$ denoted by $\lambda$ and defined pointwise in the following way: for all $p \in^b T^*M$ and $v \in^b T({}^bT^*M)$, $\lambda$ is the b-form such that*

$$\langle \lambda_p, v \rangle = \langle p, d\pi_p v \rangle. \tag{2.7}$$

*Its differential $\omega = d\lambda$ is a b-symplectic form on $({}^bT^*M, \pi^{-1}(Z))$ called* canonical *b*-symplectic form.

*In local coordinates $q_1, \ldots, q_n, p_1, \ldots, p_n$ of ${}^bT^*M$, where $q_1$ is a local defining function of $Z$, the canonical b-form of degree 1 has the expression $\lambda = p_1 \frac{dq_1}{q_1} + \sum_{i=2}^n p_i\, dq_i$ and the*

*canonical b-symplectic form writes as* $\omega = dp_i \wedge \frac{dq_1}{q_1} + \sum_{i=2}^{n} dp_i \wedge dq_i$.

On any $b$-manifold, a *canonical b-cotangent lift* can be defined.

**Definition 2.42.** *Let* $\rho : G \times M \longrightarrow M$ *be a Lie group action on a b-manifold* $(M, Z)$ *that preserves the critical hypersurface* $Z \subset M$. *For each* $g \in G$, *there is an induced diffeomorphism* $\rho_g : M \longrightarrow M$. *The* canonical $b$-cotangent lift *of* $\rho_g$, *denoted by* $\hat{\rho}_g$, *is the diffeomorphism on* ${}^bT^*M$ *defined in the following way: for all* $(q, p) \in {}^bT^*M$,

$$\hat{\rho}_g(q, p) := (\rho_g(q), ((d\rho_g)_q^*)^{-1}(p)).$$

The condition that a Lie group action $\rho : G \times M \longrightarrow M$ on a $b$-manifold $(M, Z)$ preserves the critical hypersurface $Z \subset M$ is equivalent to the condition that for all $g \in G$ the diffeomorphism $\rho_g$ is a $b$-map. If the $b$-cotangent bundle ${}^bT^*M$ of $(M, Z)$ is endowed with the canonical $b$-symplectic form $\omega$, the canonical $b$-cotangent lift preserves $\omega$. Moreover, for any $b$-vector field $X$ on $(M, Z)$, there exists a Hamiltonian $b$-vector field $\hat{X}$ on ${}^bT^*M$ whose flow is the $b$-cotangent lift of the flow of $X$ and whose Hamiltonian $b$-function is $\lambda(X)$ (for more details, see the work of Kiesenhofer and Miranda in [KM17]).

There are manifolds whose cotangent bundles can be realized as $b$-manifolds by endowing them with a $b$-symplectic form called *twisted b-symplectic form* which is essentially different from the *canonical b-symplectic form*. These manifolds were investigated by Kiesenhofer and Miranda in [KM17] and we adapt their definition to the class of parallelizable manifolds $M^n$, whose cotangent bundle is the trivial bundle $M \times \mathbb{R}^n$.

**Definition 2.43.** *Let* $M^n$ *be a parallelizable manifold and let* $T^*M = M \times \mathbb{R}^n$ *be its cotangent bundle. Define a critical hypersurface on* $T^*M$ *by selecting a co-dimension* 1 *submanifold* $Z \subset T^*M$ *of the form* $M \times N$. *Take local coordinates* $q_1, \ldots, q_n, p_1, \ldots, p_n$ *on* $T^*M$ *in such a way that* $p_1$ *is a local defining function of* $Z$. *There is a linear b-form of degree* 1 *on* $(T^*M, Z)$ *denoted by* $\lambda$ *which has the expression* $\lambda = \log|p_1|\, dq_1 + \sum_{i=2}^{n} p_i\, dq_i$. *Its differential* $\omega = d\lambda$ *is a b-symplectic form on* $(T^*M, Z)$, *called* twisted $b$-symplectic form, *which writes as* $\omega = \frac{dp_1}{p_1} \wedge dq_i + \sum_{i=2}^{n} dp_i \wedge dq_i$.

In view of the previous definitions, there are two $b$-cotangent models of $\mathbb{R}^n$, that is, there are two ways to turn the cotangent bundle $T^*\mathbb{R}^n$ of $\mathbb{R}^n$ into a $b$-symplectic manifold:

- To consider a critical hypersurface $Z$ on $\mathbb{R}^n$ and endow the $b$-cotangent bundle $(T^*\mathbb{R}^n, \pi^{-1}(Z))$ with the canonical $b$-symplectic form. If $q_1, \ldots, q_n, p_1, \ldots, p_n$ are local coordinates on $T^*\mathbb{R}^n$ in such a way that $q_1$ is a local defining function of $Z$, the canonical $b$-symplectic form writes as

$$\omega = dp_1 \wedge \frac{dq_1}{q_1} + \sum_{i=2}^{n} dp_i \wedge dq_i.$$

  This is called the *canonical b-cotangent model*.

- To consider a critical hypersurface on $T^*\mathbb{R}^n$ by selecting a co-dimension 1 submanifold $Z \subset T^*\mathbb{R}^n$ of the form $\mathbb{R}^n \times N$ and endow $(T^*\mathbb{R}^n, Z)$ with the twisted $b$-symplectic form. If $q_1, \ldots, q_n, p_1, \ldots, p_n$ are local coordinates on $T^*\mathbb{R}^n$ in such a way that $p_1$ is a local defining function of $Z$, the twisted $b$-symplectic form writes as
$$\omega = \frac{dp_1}{p_1} \wedge dq_i + \sum_{i=2}^{n} dp_i \wedge dq_i.$$
This is called the *twisted b-cotangent model*.

The essential difference between the canonical $b$-cotangent model and the twisted $b$-cotangent model is that, in the first one, the canonical $b$-symplectic form carries the singularity at the base of the cotangent bundle, while, in the second one, the twisted $b$-symplectic form carries the singularity at the fibers of the cotangent bundle.

## 2.5 Geometric quantization

In classical mechanics, a physical system is modeled on a symplectic manifold $(M, \omega)$, its state is described by using the points in $M$ and its observables are given by smooth functions on $M$. On the other hand, in quantum mechanics, a physical system is modeled on a Hilbert space $\mathcal{H}$, its state is described using complex valued functions in $\mathcal{H}$ and its observables are operators on $\mathcal{H}$. Any procedure that associates a quantum system with a given classical system and satisfies certain conditions is called a *quantization* and one of the most effective quantization methods is *geometric quantization*, which provides a prescription for constructing, from a symplectic manifold $(M, \omega)$, a quantum Hilbert space $\mathcal{H}$ and quantum operators that correspond to classical observables in $M$.

We introduce here the basics on geometric quantization using the definitions of Kostant in [Kos70] and Guillemin-Sternberg in [GS82b], and we refer to the books of Woodhouse [Woo92] and Hall [Hal13] for further details.

The first step in the geometric quantization of a symplectic manifold $(M^{2n}, \omega)$ is called *prequantization* and consists in constructing a Hermitian line bundle $\pi : \mathbb{L} \to M$ with Hermitian connection $\nabla$ for which the curvature 2-form is equal to $\omega/\hbar$, where $\hbar$ is the Planck's constant. Such a pair $(\mathbb{L}, \nabla)$ exists if $(M, \omega)$ is *quantizable* or *integral*, that is, if it satisfies the following integrability condition: the integral of $\omega$ over any closed orientable 2-dimensional submanifold of $M$ is an integer multiple of $2\pi\hbar$. This is equivalent to the condition that $\omega$ is *integral*, that is, that $\frac{1}{2\pi\hbar}[\omega]$ represents an integral cohomology class. This integrality condition is satisfied in the case of $\mathbb{R}^{2n}$ with the standard symplectic form and in the case of the cotangent bundle $T^*M$ of any smooth manifold $M$ with the canonical symplectic form, since in both cases the symplectic form is exact and so its cohomology class is zero.

Then, one defines the *prequantum Hilbert space* as the space $\mathcal{H}_{\text{pre}}$ of square integrable sections $s : M \to \mathbb{L}$ endowed with the global inner product

$$\langle s_1, s_2 \rangle = \frac{1}{n!} \int_{p \in M} (s_1(p), s_2(p)) \omega^n(p),$$

where $(\cdot, \cdot)$ is the pointwise inner product on each fiber $\pi^{-1}(p)$ given by the Hermitian structure on the line bundle $\mathbb{L}$. In the prequantum Hilbert space $\mathcal{H}_{\text{pre}}$, the *prequantum operator* associated to a $f \in \mathcal{C}^\infty(M)$ is the operator $\hat{f}$ which acts on a section $s : M \to \mathbb{L}$ as

$$\hat{f}(s) = -i\hbar \nabla_{X_f}(s) + f \cdot s.$$

The next step in the procedure of geometric quantization is to choose a *polarization* $P$ of the symplectic manifold $(M, \omega)$, that is, a subbundle $P$ of $TM^{\mathbb{C}}$, the complexified tangent bundle of $M$, such that it is:

- *involutive*: if two complex vector fields $X$ and $Y$ lie in $P$, then so does $[X, Y]$,
- *Lagrangian*: the restriction of the symplectic form $\omega$ vanishes on $P$ and $P$ is of maximal dimension, and
- *of constant rank*: at each point $p \in M$, the dimension of the intersection of fibers $P_p \cap \bar{P}_p \cap T_pM$ is constant.

A polarization $P$ that satisfies $P = \bar{P}$ is called a *real polarization*, while a polarization that satisfies $P \cap \bar{P} = \{0\}$ is called a *purely complex polarization* or a *Kähler polarization*. The maximal connected integral submanifolds of a polarization are called the *leaves of the polarization*. Note that an integrable system $(M^{2n}, \omega, F = (f_1, \ldots, f_n))$ whose Hamiltonian vector fields $X_{f_1}, \ldots, X_{f_n}$ are all complete defines a real polarization, since the integral submanifolds of the distribution spanned by $X_{f_1}, \ldots, X_{f_n}$ are involutive, Lagrangian and of constant rank.

The choice of a polarization $P$ on $M$ defines a special subset of the square integrable sections of the prequantum Hilbert space $\mathcal{H}_{\text{pre}}$, the set of *polarized sections*, which is used to construct the quantum Hilbert space $\mathcal{H}$ on which the quantum observables act as operators.

**Definition 2.44.** *Let $(M, \omega)$ be a quantizable symplectic manifold, $\pi : \mathbb{L} \to M$ a Hermitian line bundle with connection $\nabla$ of curvature $\omega/\hbar$ and $P$ a polarization of $(M, \omega)$. A smooth section $s$ of $\mathbb{L}$ is* polarized with respect to $P$ *if*

$$\nabla_X(s) = 0, \tag{2.8}$$

*for every vector field $X$ lying in $P$.*

The polarized sections are precisely the sections of $\mathbb{L}$ which are constant along the leaves of the polarization. They are also called *covariant constant sections*, *leaf-wise flat sections* or just *flat sections* and are the basis to construct the quantum Hilbert space $\mathcal{H}$.

**Definition 2.45.** *Let $(M, \omega)$ be a quantizable symplectic manifold, $\pi : \mathbb{L} \to M$ a Hermitian line bundle with connection $\nabla$ of curvature $\omega/\hbar$ and $P$ a polarization of $(M, \omega)$. The quantum Hilbert space $\mathcal{H}$ associated with $P$ is the closure in the prequantum Hilbert space $\mathcal{H}_{\text{pre}}$ of the space of smooth square-integrable polarized sections of $\mathbb{L}$.*

If $(M^{2n}, \omega, F = (f_1, \dots, f_n))$ is an integrable system defined on a quantizable symplectic manifold, which therefore admits a Hermitian line bundle $\pi : \mathbb{L} \to M$ with connection $\nabla$ of curvature $\omega/\hbar$, the quantum Hilbert space $\mathcal{H}$ is given by the smooth square-integrable sections $s$ of $\mathbb{L}$ that satisfy $\nabla_X(s) = 0$ for any vector field $X$ tangent to the fibers of the moment map $F$, which induces a real polarization of $M$.

When $M$ is compact, there are no smooth global sections $s$ of $\mathbb{L}$ satisfying $\nabla_X(s) = 0$. Instead, such polarized sections are concentrated on the fibers $F^{-1}(b)$ of $F$ such that $b \in \text{Im}(F) \subset \mathbb{R}^n$ and $\mathbb{L}|_{F^{-1}(b)}$ is a trivial bundle. These fibers are called *Bohr-Sommerfeld fibers* or *Bohr-Sommerfeld leaves*, and the set of all Bohr-Sommerfeld leaves of $F$ is called the *Bohr-Sommerfeld set*. The set of points in $\mathbb{R}^n$ that correspond to the images by $F$ of the Bohr-Sommerfeld set, namely,

$$\{b \in \text{Im}(F) \subset B \colon \mathbb{L}|_{F^{-1}(b)} \text{ is trivial}\},$$

is also referred to as the *Bohr-Sommerfeld set*.

The quantum Hilbert space $\mathcal{H}$ can be directly defined via the Bohr-Sommerfeld leaves as

$$\mathcal{H} = \bigoplus_{b \in B_{BS}} \mathbb{C}\langle s_b \rangle, \tag{2.9}$$

where $B_{BS}$ is the Bohr-Sommerfeld set and $s_b$ is the corresponding polarized section of $\mathbb{L}|_{F^{-1}(b)}$. This definition of geometric quantization is called *Bohr-Sommerfeld quantization*.

### 2.5.1 Formal geometric quantization

Another definition of geometric quantization, which is based on the index of a Dirac operator, is *formal geometric quantization* (see the works of Sjamaar in [Sja96], Weitsman in [Wei01], Hochs and Mathai in [HM16] and Paradan in [Par09].

Let $(M, \omega)$ be a compact quantizable symplectic manifold and let $(\mathbb{L}, \nabla)$ be a Hermitian line bundle with connection of curvature $\omega/\hbar$. By twisting the spin-$\mathbb{C}$ Dirac operator on $M$ by $\mathbb{L}$, one obtains an elliptic operator $\bar{\partial}_{\mathbb{L}}$. The *formal geometric quantization* of $M$, which we denote by $Q(M)$, is defined by

$$Q(M) = \text{ind}(\bar{\partial}_{\mathbb{L}}),$$

and it is a virtual vector space.

If $\rho : \mathbb{T} \times M \to M$ is a Hamiltonian action of a torus $\mathbb{T}$ on $(M, \omega)$ with moment map $\mu$ which is equivariant with respect to $\rho$, we call $(M, \omega, \rho, \mu)$ a *Hamiltonian $\mathbb{T}$-space*. In a Hamiltonian $\mathbb{T}$-space $(M, \omega, \rho, \mu)$, the action $\rho : \mathbb{T} \times M \to M$ can be lifted

to $\mathbb{L}$ and the almost complex structure of $\mathbb{L}$ can be chosen to be invariant with respect to $\mathbb{T}$. In this case, the formal geometric quantization $Q(M)$ is a finite-dimensional virtual $\mathbb{T}$-module.

For $\xi \in \mathfrak{t}^*$, denote by $M/\!/_\xi T$ the reduced space of $M$ at $\xi$. For $\alpha$ a weight of $\mathbb{T}$ and $V$ a virtual $\mathbb{T}$-module, denote by $V^\alpha$ the sub-module of $V$ of weight $\alpha$. The following result states that the component of weight $\alpha$ of the formal geometric quantization of $M$ equals the formal geometric quantization of the reduced space of $M$ at $\alpha$.

**Theorem 2.46** (Quantization commutes with reduction [Mei96])**.** *Let $(M, \omega)$ be a compact quantizable symplectic manifold. Suppose $M$ is also Hamiltonian $\mathbb{T}$-space $(M, \omega, \rho, \mu)$ and let $\alpha$ be a weight of $\mathbb{T}$. Then*

$$Q(M)^\alpha = Q(M/\!/_\alpha \mathbb{T}). \tag{2.10}$$

*In other words,*

$$Q(M) = \bigoplus_\alpha Q(M/\!/_\alpha \mathbb{T})\alpha. \tag{2.11}$$

Theorem 2.46 and Equation (2.11) are valid only for regular values of the moment map $\mu$ of the Hamiltonian action $\rho$ of $\mathbb{T}$. In the case of singular values of the moment map, the singular quotient must be replaced by a slightly different construction using the *shifting trick* of $\alpha$ (for details on this construction see the work of Meinrenken in [Mei96]). A similar caution applies in the case of Hamiltonian $\mathbb{T}$-spaces which are non-compact and in the case of $b$-symplectic manifolds.

In the case where the Hamiltonian $\mathbb{T}$-space $(M, \omega, \rho, \mu)$ is non-compact, Equation (2.10) may be used to *define* the formal geometric quantization of such Hamiltonian $\mathbb{T}$-spaces.

**Definition 2.47** (Weitsman [Wei01])**.** *Let $(M, \omega, \rho, \mu)$ be a Hamiltonian $\mathbb{T}$-space with $\omega$ an integral symplectic form. Suppose the moment map $\mu$ for the action of $\mathbb{T}$ is proper. Let $V$ be an infinite-dimensional virtual $\mathbb{T}$-module with finite multiplicities. We say*

$$V = Q(M)$$

*if for any compact Hamiltonian $\mathbb{T}$-space $N$ with integral symplectic form, we have*

$$(V \otimes Q(N))^{\mathbb{T}} = Q((M \times N)/\!/_0 \mathbb{T}). \tag{2.12}$$

*In other words, as in Equation (2.11),*

$$Q(M) = \bigoplus_\alpha Q(M/\!/_\alpha \mathbb{T})\alpha,$$

*where the sum is taken over all weights $\alpha$ of $\mathbb{T}$.*

The fact that the moment map is proper implies that the reduced space $(M \times N)/\!/_0 \mathbb{T}$ is compact for any compact Hamiltonian $\mathbb{T}$-space $N$, so that the right hand side of Equation (2.12) is well-defined.

Suppose now that $(M, \omega, Z)$ is a compact $b$-symplectic manifold. We say that it is *quantizable* or *integral* if, in the following decomposition of $\omega$:

$$\omega = \alpha \wedge \frac{df}{f} + \beta, \text{ with } \alpha \in \Omega^1(M) \text{ and } \beta \in \Omega^2(M),$$

where $f : M \to \mathbb{R}$ is a defining function of $Z$, the forms $\alpha$ and $\beta$ are *integral*, that is, if $\frac{1}{2\pi\hbar}[\iota_Z^* \alpha]$ represents an integral cohomology class in $H^1(Z)$ and $\frac{1}{2\pi\hbar}[\beta]$ represents an integral cohomology class in $H^2(M)$.

Suppose that a quantizable $b$-symplectic manifold $(M, \omega, Z)$ is equipped with a Hamiltonian action of a torus $\mathbb{T}$, with nonzero modular weight. Let $\mathbb{L}$ be a complex line bundle on $M$ with connection $\nabla$ on $\mathbb{L}|_{M \setminus Z}$ whose curvature is $\omega|_{M \setminus Z}/\hbar$. The formal geometric quantization $Q(M)$ is defined as follows by Guillemin, Miranda and Weitsman in [GMW18b] and [GMW21].

**Definition 2.48.** *Let $V$ be a virtual $\mathbb{T}$-module with finite multiplicities. We say*

$$V = Q(M)$$

*if for any compact Hamiltonian $\mathbb{T}$-space $N$ with integral symplectic form, we have*

$$(V \otimes Q(N))^{\mathbb{T}} = \varepsilon Q((M \times N)/\!/_0 \mathbb{T}), \tag{2.13}$$

*where $Q(N)$ denotes the standard geometric quantization of $N$, $Q((M \times N)/\!/_0 \mathbb{T})$ is the geometric quantization of the compact integral symplectic manifold $(M \times N)/\!/_0 \mathbb{T}$, and $\varepsilon$ is $+1$ if the symplectic orientation on the symplectic quotient $(M \times N)/\!/_0 \mathbb{T}$ agrees with the orientation inherited from $M \times N$ and $-1$ otherwise.*

This means that $Q(M) = Q(M \setminus Z) = \oplus_i \varepsilon_i Q((M \setminus Z)_i)$, where the $(M \setminus Z)_i$ are the connected components of $M \setminus Z$, $Q(M \setminus Z)$ is the formal geometric quantization of the non-compact Hamiltonian $\mathbb{T}$-space $M \setminus Z$, and the $\varepsilon_i \in \{\pm 1\}$ are determined by the relative orientations of the symplectic forms on the components of $M \setminus Z$ and the overall orientation of $M$. Alternatively,

$$Q(M) = \bigoplus_{\alpha} \varepsilon(\alpha) Q(M/\!/_\alpha \mathbb{T})\alpha, \tag{2.14}$$

where $Q(M/\!/_\alpha \mathbb{T})$ must be defined using the shifting trick of $\alpha$ if $\alpha$ is not a regular value of the moment map, and each $\varepsilon(\alpha) \in \{\pm 1\}$ is determined by the relative orientations of $M$ and $M/\!/_\alpha \mathbb{T}$.

In the $b$-symplectic case, the condition that the modular weight is non-zero guarantees that the reduced space $(M \times N)/\!/_0 \mathbb{T}$ is compact and symplectic for any compact Hamiltonian $\mathbb{T}$-space $N$, so that $Q((M \times N)/\!/_0 \mathbb{T})$ is well-defined.

### 2.5.2 Bohr-Sommerfeld quantization via sheaves

Bohr-Sommerfeld quantization can also be formulated using sheaf theory, an approach which is more convenient to deal with cotangent models (see the works of

Śniatycki in [Śni77] and Hamilton in [Ham10]). Let $(M, \omega)$ be a quantizable symplectic manifold endowed with a Hermitian line bundle $\pi : \mathbb{L} \to M$ with connection $\nabla$ of curvature $\omega/\hbar$. For the Bohr-Sommerfeld quantization of a completely integrable system $(M, \omega, F)$, it is natural to choose the real polarization given by the foliation of $M$ by the fibers of the moment map $F$. The set of polarized sections $s$ of $\mathbb{L}$, the ones satisfying $\nabla_X(s) = 0$ for any vector field $X$ tangent to fibers of $F$, forms a sheaf. We denote it by $\mathcal{J}$ and call it the *sheaf of polarized sections*. The Bohr-Sommerfeld quantization is then defined through the cohomology groups of the sheaf cohomology of $\mathcal{J}$.

We recall the construction of the cohomology of sheaves or the *sheaf cohomology*, which is used to define the geometric quantization. We start defining presehaves and sheaves.

**Definition 2.49.** *Let $X$ be a topological space. A* presheaf $\mathcal{F}$ *on $X$ assigns to every open set $U$ of $X$ an abelian group $\mathcal{F}(U)$, usually called the* set of sections of $\mathcal{F}$ over $U$. *It also assigns, to any $V \subset U$, a* restriction map $\mathcal{F}(U) \to \mathcal{F}(V)$, *such that if $W \subset V \subset U$ and $\sigma \in \mathcal{F}(U)$, then*

$$\sigma|_W = (\sigma|_V)|_W,$$

*and if $V = U$ then the restriction is just the identity map.*

**Definition 2.50.** *A presheaf $\mathcal{J}$ is a* sheaf *if the following properties hold:*

1. *For any pair of open sets $U$, $V$, and sections $\sigma \in \mathcal{J}(U)$ and $\tau \in \mathcal{J}(V)$ which agree on the intersection $U \cap V$, there exists a section $\rho \in \mathcal{J}(U \cup V)$ which restricts to $\sigma$ on $U$ and $\tau$ on $V$.*
2. *If $\sigma$ and $\tau$ in $\mathcal{J}(U \cup V)$ have equal restrictions to $U$ and $V$, then they are equal on $U \cup V$.*

To construct the cochains and the coboundary operator of the cohomology, one starts fixing an open cover $\mathcal{A} = \{A_\alpha\}$ of the manifold $M$. A *k-cochain* assigns, to each $(k+1)$-fold intersection of elements from the cover $\mathcal{A}$, a section of the sheaf $\mathcal{J}$. We denote an intersection of the form $A_{\alpha_0} \cap \cdots \cap A_{\alpha_k}$, where the $\alpha_j$ are distinct, by $A_{\alpha_0 \cdots \alpha_k}$. Then, a $k$-cochain is an assignment $f_{\alpha_0 \cdots \alpha_k} \in \mathcal{J}(A_{\alpha_0 \cdots \alpha_k})$ for each $(k+1)$-fold intersection in the cover $\mathcal{A}$. The set of $k$-cochains is denoted by $C^k_{\mathcal{A}}(M; \mathcal{J})$, or just by $C^k_{\mathcal{A}}$.

The coboundary operator $\delta$ that makes $C^*_{\mathcal{A}}$ into a cochain complex is defined in the following way:

$$(\delta f)_{\alpha_0 \cdots \alpha_k} = \sum_{j=0}^{k} (-1)^j f_{\alpha_0 \cdots \hat{\alpha}_j \cdots \alpha_k}|_{A_{\alpha_0 \cdots \cdots \alpha_k}}, \tag{2.15}$$

where the $\hat{}$ denotes that the index is omitted. Then, if $f = \{f_{\alpha_0 \cdots \alpha_{k-1}}\}$ is a $(k-1)$-cochain, $\delta f$ is a $k$-cochain. With this definition, for instance, $(\delta f)_{123} = f_{23} - f_{13} + f_{12}$ and $(\delta \circ \delta f)_{123} = \delta(f_{23} - f_{13} + f_{12}) = f_3 - f_2 - f_3 + f_1 + f_2 - f_1 = 0$. In general, $\delta \circ \delta = 0$ and $C^*_{\mathcal{A}}$ is a well-defined cochain complex. Hence, we can define

**Definition 2.51.** *With the above definitions, the* sheaf cohomology of $M$ with respect to the cover $\mathcal{A}$ *is the cohomology of this complex:*

$$H^k_{\mathcal{A}}(M;\mathcal{J}) = \frac{\ker \delta^k}{im\, \delta^{k-1}},$$

*where by $\delta^k$ denotes the map $\delta$ on $C^k_{\mathcal{A}}$.*

The sheaf cohomology of a manifold can be defined independently of the cover by taking a limit over cover refinements. A cover $\mathcal{B}$ is a *refinement* of a cover $\mathcal{A}$ if every element of $\mathcal{B}$ is a subset of some element of $\mathcal{A}$. A refinement provides a map $\rho\colon \mathcal{B} \to \mathcal{A}$, where $B \subset \rho(B)$ for all $B \in \mathcal{B}$, and gives a map $\phi\colon C^k_{\mathcal{A}}(U,\mathcal{J}) \to C^k_{\mathcal{B}}(U,\mathcal{J})$ induced by the restriction maps in the sheaf. Then, if $\eta \in C^k_{\mathcal{A}}$ is a cochain, $\phi\eta$ is defined by

$$(\phi\eta)_{B_0B_1\cdots B_k} = (\eta)_{(\rho B_0)(\rho B_1)\cdots(\rho B_k)}\big|_{B_0B_1\cdots B_k}.$$

This map commutes with $\delta$ and induces a map on cohomology $H^*_{\mathcal{A}} \to H^*_{\mathcal{B}}$. All the possible choices of maps $\rho$ turn the collection of $H^*_{\mathcal{A}}$ for all open covers of $M$ into a directed system and the sheaf cohomology can be defined as the limit of this system, which can be proved to exist.

**Definition 2.52.** *The* sheaf cohomology of $M$ *is defined as the limit of the directed system:*

$$H^*(M;\mathcal{J}) = \varinjlim H^*_{\mathcal{A}}(M;\mathcal{J}).$$

Then, since the set of polarized sections forms a sheaf, one can define the Bohr-Sommerfeld quantization of a completely integrable system using the sheaf cohomology of polarized sections.

**Definition 2.53.** *Let $(M,\omega,F)$ be a completely integrable system defined on a quantizable symplectic manifold $(M,\omega)$ endowed with a Hermitian line bundle $\pi : \mathbb{L} \to M$ with connection $\nabla$ of curvature $\omega/\hbar$. Choose the polarization of $M$ given by $F$ and let $\mathcal{J}$ be the sheaf of polarized sections. The* Bohr-Sommerfeld quantization *of $M$, which we denote by $\mathcal{Q}(M)$, is*

$$\mathcal{Q}(M) = \bigoplus_{k\geq 0} H^k(M;\mathcal{J}),$$

*where $H^k(M;\mathcal{J})$ is the k-th sheaf cohomology group.*

In general, there is no direct way to compute the sheaf cohomology groups $H^k(M;\mathcal{J})$ in the definition of the Bohr-Sommerfeld quantization $\mathcal{Q}(M)$. Nevertheless, they can be characterized in terms of the *Bohr-Sommerfeld leaves*, a special type of leaves of the polarization the definition of which we recall here.

**Definition 2.54.** *Let $(M,\omega)$ be a quantizable symplectic manifold endowed with a Hermitian line bundle $\pi : \mathbb{L} \to M$ with connection $\nabla$ of curvature $\omega/\hbar$. Suppose $P$ is a polarization of $M$. A leaf $\ell$ of $P$ is a* Bohr-Sommerfeld leaf *if there exists a non-zero polarized section $s$ of $\mathbb{L}$ defined over all of $\ell$.*

A leaf is Bohr-Sommerfeld if and only if its holonomy is trivial around all the loops contained in the leaf and it turns out that the *Bohr-Sommerfeld set*, the set of all the Bohr-Sommerfeld leaves of a polarization, is discrete in the leaf space. Then, the amount of Bohr-Sommerfeld leaves is countable, it may be finite, and it is the basis of the following result on Bohr-Sommerfeld quantization using real polarizations.

**Theorem 2.55** (Śniatycki [Śni77])**.** *Let $(M^{2n}, \omega)$ be a quantizable symplectic manifold with Hermitian line bundle $\pi : \mathbb{L} \to M$ with connection $\nabla$ of curvature $\omega/\hbar$. Take a real polarization $P$ such that its fibers are compact. Then, for all $k \neq n$, $H^k(M; \mathcal{J}) = 0$. Therefore,*

$$\mathcal{Q}(M) = H^n(M; \mathcal{J}).$$

*Furthermore, $H^n(M; \mathcal{J})$ can be expressed in terms of the Bohr-Sommerfeld leaves and its dimension is exactly the number of Bohr-Sommerfeld leaves of $P$.*

For the particular case of symplectic toric manifolds, the number of Bohr-Sommerfeld leaves of a Kähler polarization, which correspond to the leaves admitting holomorphic sections of $\mathbb{L}$, can be easily obtained from the moment map. Then, it is straightforward to obtain the dimension of the Bohr-Sommerfeld quantization of a symplectic toric manifold using a Kähler polarization (see the work by Guillemin, Ginzburg and Karshon in [GGK02]).

**Theorem 2.56.** *Let $(M^{2n}, \omega, F = (f_1, \ldots, f_n))$ be a quantizable symplectic toric manifold and let $\Delta$ its moment polytope. Then, there is a one-to-one correspondence between integer lattice points in $\Delta$ and Bohr-Sommerfeld leaves of a Kähler polarization of $M$. Hence, the dimension of the Bohr-Sommerfeld quantization using a Kähler polarization is equal to the number of integer lattice points in $\Delta$, that is,*

$$\dim \mathcal{Q}(M) = \#(\Delta \cap \mathbb{Z}^n).$$

As a vector space, $\mathcal{Q}(M)$ is isomorphic to the direct sum of copies of $\mathbb{C}$, with one copy for each Bohr-Sommerfeld leaf. Then,

$$\mathcal{Q}(M) \cong \mathbb{C}^{n_{BS}},$$

where $n_{BS}$ is the number of Bohr-Sommerfeld leaves.

In [Ham10], Hamilton calculated explicitly the sheaf cohomology groups of a quantizable symplectic toric manifold using a real polarization instead of a Kähler polarization. From them, he obtained a Bohr-Sommerfeld quantization that differs from the one in Theorem 2.56 in the fact that its dimension is not equal to the number of integer lattice points in the moment polytope but to the number of integer lattice points in the *interior* of the moment polytope, that is, excluding the ones in the boundary. Remarkably, the points in the boundary of the moment polytope correspond to singular leaves of the foliation induced by $F$, that is, to *singular Bohr-Sommerfeld leaves*. Then, Hamilton's Bohr-Sommerfeld quantization differs from Theorem 2.56 because it does not take into account any contribution from the singular Bohr-Sommerfeld leaves.

**Theorem 2.57** (Hamilton [Ham10]). *Let $(M, \omega, F = (f_1, \dots, f_n))$ be a quantizable symplectic toric manifold with Hermitian line bundle $\pi : \mathbb{L} \to M$ with connection $\nabla$ of curvature $\omega/\hbar$. Let $\mathcal{J}$ be the sheaf of polarized sections of $\mathbb{L}$ with respect to the real polarization induced by $F$. Then, the cohomology groups $H^k(M; \mathcal{J})$ are zero for all $k \neq n$, and, on the other hand,*

$$H^n(M; \mathcal{J}) \cong \mathbb{C}^{\hat{n}_{BS}},$$

*where $\hat{n}_{BS}$ is the number of regular Bohr-Sommerfeld leaves. Hence,*

$$\dim \mathcal{Q}(M) = \dim H^n(M; \mathcal{J}) = \#(\mathrm{Int}\Delta \cap \mathbb{Z}^n).$$

In [HM10], Hamilton and Miranda produced a quantization result for systems with hyperbolic singularities and, in [MPS20], Miranda, Presas and Solha produced a quantization result for systems with focus-focus singularities.

**Theorem 2.58** (Hamilton-Miranda [HM10]). *Let $(M, \omega, F)$ be a 2-dimensional, compact, completely integrable system, whose moment map has only non-degenerate singularities. Suppose $M$ has a prequantum line bundle $\mathbb{L}$, and let $\mathcal{J}$ be the sheaf of sections of $\mathbb{L}$ which are polarized with respect to the leaves of $F$. The cohomology $H^1(M, \mathcal{J})$ has two contributions of the form $\mathbb{C}^{\mathbb{N}}$ for each hyperbolic singularity, each one corresponding to a space of Taylor series in one complex variable. It also has one $\mathbb{C}$ term for each non-singular Bohr-Sommerfeld leaf. That is,*

$$H^1(M; \mathcal{J}) \cong \bigoplus_{p \in \mathcal{H}} (\mathbb{C}^{\mathbb{N}} \oplus \mathbb{C}^{\mathbb{N}}) \oplus \bigoplus_{b \in BS} \mathbb{C}_b, \tag{2.16}$$

*where $\mathcal{H}$ is the set of hyperbolic singularities. The cohomology in other degrees is zero. Thus, the quantization of $M$ is given by Equation (2.16).*

**Theorem 2.59** (Miranda-Presas-Solha [MPS20]). *For a 4-dimensional semitoric system $M$, with $n_r$ regular Bohr-Sommerfeld fibers and $n_f$ focus-focus Bohr-Sommerfeld fibers, the quantization $\mathcal{Q}(M)$ of $M$ is:*

$$\mathcal{Q}(M) \cong \mathbb{C}^{n_r} \oplus \left( \bigoplus_{j \in \{1, \dots, n_f\}} (\mathcal{C}^\infty(\mathbb{R}; \mathbb{C}))^{n(j)} \right), \tag{2.17}$$

*with $n(j)$ the number of nodes on the $j$-th focus-focus Bohr-Sommerfeld fiber.*

Theorems 2.58 and 2.59 show that non-degenerate singularities of both hyperbolic and focus-focus type give rise to infinite-dimensional quantization spaces. In the first case, the infinities arise from the infinite-dimensional space $\mathbb{C}^{\mathbb{N}} \oplus \mathbb{C}^{\mathbb{N}}$ in $H^1(M; \mathcal{J})$ and, in the second case, they arise from the infinite-dimensional space $\mathcal{C}^\infty(\mathbb{R}; \mathbb{C})$ in $\mathcal{Q}(M)$. In Theorem 2.59, the computations that yield the infinite-dimensional spaces $\mathcal{C}^\infty(\mathbb{R}; \mathbb{C})$ in Equation (2.17) arise attached to the Taylor series used in the resolution of the differential equation that polarized sections have to satisfy.

# Chapter 3

# b-Cotangent models for fluids with dissipation

In this chapter we employ Hamilton's equations to model a system that exhibits dissipative behavior in the classical sense. The novel approach we take is to leave the conservative Hamilton's equations unchanged. Instead, we introduce a singularity at the level of the symplectic structure of the manifold by equipping it with a twisted $b$-symplectic form.

With respect to the published paper [CMM23], this chapter is organized in the same way and contains essentially the same results.

This chapter is organized as follows: In Section 3.1 we introduce the new model for fluids with dissipation based on a twisted $b$-symplectic structure. We start with the 1-dimensional case and the linear potential, which provides an analogue of the Stokes' Law, we extend it to higher dimensions and more general potentials and we observe the existence of escape orbits in the twisted model. In Section 3.2 we consider time-dependent singular models in which friction arises from a re-scaling of time.

## 3.1 The twisted b-symplectic model for dissipation

In this section, we describe how $b$-symplectic geometry offers a way to model, in a Hamiltonian fashion, a particle moving in a dissipative fluid with viscosity. In particular, we construct an example that uses the twisted $b$-symplectic form in the cotangent bundle of $\mathbb{R}$. This example gives precisely the equation of the friction drag force exerted on a small spherical particle moving through a viscous laminar fluid in one dimension, the so-called Stokes' Law. Then, we generalize this model to higher dimensions and to other configuration spaces different from $\mathbb{R}^n$.

Consider the 1-dimensional space $\mathbb{R}$ and its cotangent bundle $T^*\mathbb{R} \cong \mathbb{R}^2$ with coordinates $(q, p)$. It represents the phase space of a particle moving in a line whose position and momentum are parametrized by $q$ and $p$, respectively. Consider the Hamiltonian

$$H(q, p) = \frac{p^2}{2} + f(q), \tag{3.1}$$

which corresponds to the energy of a particle subject to a potential $f(q)$ that only depends on the position $q$. The Hamilton's equations derived from $\iota_{X_H}\omega = -dH$

with the standard symplectic form $\omega = dp \wedge dq$ have the following expression:

$$\begin{cases} \dot{q} = p \\ \dot{p} = -\frac{\partial f}{\partial q} \end{cases}, \tag{3.2}$$

where $\dot{q}$ and $\dot{p}$ are equal to the $q$ and $p$ components of $X_H$, respectively. This ODE system governs the main toy models in classical mechanics in which the energy $H$ is supposed to be conserved along the trajectory of the particles.

If, in the Hamilton's equations $\iota_{X_H}\omega = -dH$, the standard symplectic form $\omega$ is replaced by the twisted $b$-symplectic form

$$\omega = \frac{dp}{p} \wedge dq$$

on $T^*\mathbb{R}$, with the critical hypersurface $Z$ defined as the line $p = 0$ in $T^*\mathbb{R}$, one obtains another version of the Hamilton's equations which we call the *twisted Hamilton's equations*. Explicitly, the ODE system derived from the twisted Hamilton's equations together with the Hamiltonian $H(q, p) = \frac{p^2}{2} + f(q)$ writes as:

$$\begin{cases} \dot{q} = p^2 \\ \dot{p} = -p\frac{\partial f}{\partial q} \end{cases}, \tag{3.3}$$

This system can be studied separately in three regions of the plane $T^*\mathbb{R} = \mathbb{R}^2$: the axis $p = 0$, the half-plane $p > 0$ and the half-plane $p < 0$. On the line $p = 0$, there are just fixed points and the twisted Hamilton's equations give no dynamics. On the two half-planes, the Hamiltonian vector field $X_H = \dot{q}\frac{\partial}{\partial q} + \dot{p}\frac{\partial}{\partial p}$ is symmetric with respect to the axis $p = 0$. Hence, the dynamical study of the system can be reduced to the region $p > 0$, because for $p < 0$ the results will be the same as in the region $p > 0$ except for a change of sign in the $\frac{\partial}{\partial p}$ component of $X_H$.

Note that, although we have associated $q$ to the position coordinate, $\dot{q}$ is not equal to the standard physical momentum $p$ but to $p^2$. However, we can still think of $p = \sqrt{\dot{q}}$ as a modified physical momentum, since it is an increasing function of $\dot{q}$. Taking into account this point of view, we proceed to obtain various models of dynamics for different families of potentials $f(q)$.

Also note that, differentiating the first equation of System (3.3) and substituting it into the second one, we find

$$\ddot{q} = -2\dot{q}\frac{\partial f}{\partial q}, \tag{3.4}$$

which is a second order ODE depending only on $q$. During the study of the models that we present, we are also going to use this standard approach that turns the first order ODE System (3.3) into the equivalent second order ODE (3.4).

### 3.1.1 The linear case: the Stokes' Law as a twisted b-cotangent model

A natural choice for the potential $f(q)$ in the Hamiltonian $H(q,p) = \frac{p^2}{2} + f(q)$ is a function of linear type. This simple model already gives an original way of formulating dissipation as a Hamiltonian model in the $b$-symplectic setting, as the following result proves.

**Theorem 3.1** (Dissipation as a twisted $b$-cotangent model, Coquinot-Mir-Miranda [CMM23])**.** *Consider the Hamiltonian $H(q,p) = \frac{p^2}{2} + f(q)$ in $T^*\mathbb{R}$ and consider the associated twisted Hamilton's equations, which write as:*

$$\begin{cases} \dot{q} = p^2 \\ \dot{p} = -p\frac{\partial f}{\partial q} \end{cases}. \tag{3.5}$$

*The particular case $f(q) = \frac{\lambda}{2}q$, with $\lambda > 0$, corresponds to the model of a spherical particle moving in a fluid with viscosity and suffering a friction proportional to its velocity, that is, to a motion governed by the Stokes' Law.*

*Proof.* If one takes $f(q) = \frac{\lambda}{2}q$, with $\lambda > 0$, in the Hamiltonian $H(q,p) = \frac{p^2}{2} + f(q)$, the associated twisted Hamilton's equations write as:

$$\begin{cases} \dot{q} = p^2 \\ \dot{p} = -\frac{\lambda}{2}p \end{cases}. \tag{3.6}$$

The second order ODE which is equivalent to this system is

$$\ddot{q} = -\lambda\dot{q}, \tag{3.7}$$

which corresponds exactly to the equation of a free massive particle moving in one dimension and affected by viscous friction. In fact, the Stokes' Law (3.8) describes precisely the same case, which appears in the study of non-ideal fluids. It states that the frictional force $F$ is:

$$F = 6\pi\mu R v, \tag{3.8}$$

where $\mu$ is the dynamic viscosity, $R$ is the radius of the particle and $v$ is the flow velocity relative to the object (or minus the object velocity relative to the flow). The Stokes' Law computes the magnitude of the drag force that is acting against the particle motion and slowing it. This force is proportional to the velocity of the particle with respect to the fluid and of opposite direction.

Denoting the velocity $v$ by $\dot{q}$, assuming that the force $F$ is proportional to the acceleration $\ddot{q}$ and combining physical constants, we deduce that Equation (3.7) is equivalent to the Stokes' Law. □

Observe that, in the classical symplectic setting, in which the motion is governed by the standard Hamilton's Equations (3.2), the particular case of a linear potential

of the form $f(q) = \frac{\lambda}{2}q$, with $\lambda > 0$, gives rise to the dynamics of a rectilinear motion with a constant acceleration. It is, for instance, the model for the free fall of a particle subject to a 1-dimensional constant gravity field, a system in which there is no loss of energy.

### Description of the dynamics

From the point of view of dynamical systems, the phase portrait in the $(q, p)$-plane of the trajectories that solve the twisted Hamilton's Equations (3.3) for a potential $f(q) = \frac{\lambda}{2}q$ is highly similar to the phase portrait of the standard Hamilton's Equations (3.2) for the same potential, since the components $\dot{q}$ and $\dot{p}$ of the vector fields associated to both systems are proportional by the same factor $p$. The main difference between both systems is found at the axis $p = 0$. There, the orbits that cross the axis transversally in the classical model given by System (3.2) are "broken" and new punctual orbits appear in the twisted $b$-cotangent model given by System (3.3). Besides, in the twisted $b$-cotangent model the orbits in the half-plane $p < 0$ change direction with respect to the same orbits in the classical model. See in Figure 3.1 the phase space representation of both systems.

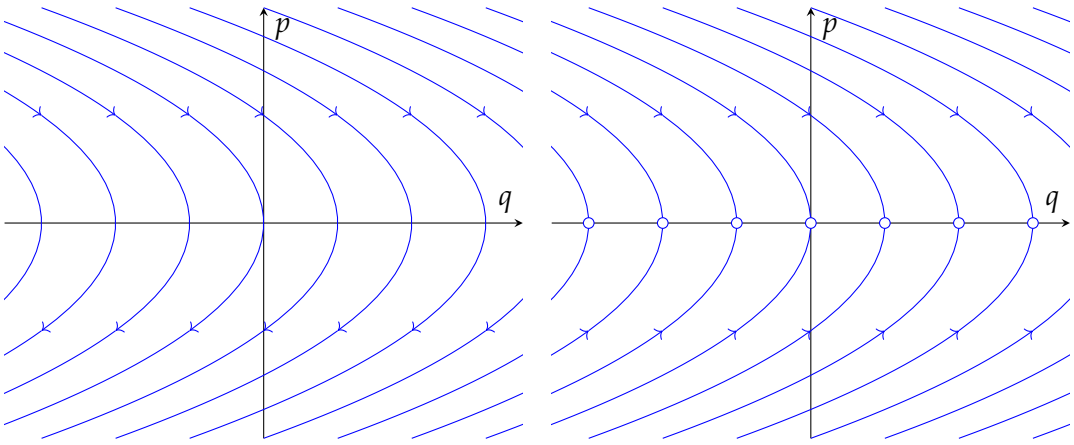


FIGURE 3.1: Some orbits in the phase spaces of the standard Hamilton's Equations (3.2) on the left and of the twisted Hamilton's Equations (3.3) on the right, in both cases choosing the linear potential $f(q) = \frac{\lambda}{2}q$.

Although the phase portraits of Figure 3.1 are similar, the dynamical evolution of a physical system driven by the Hamiltonian $H(q, p) = \frac{1}{2}p^2 + \frac{\lambda}{2}q$ and the standard symplectic form $\omega = dp \wedge dq$ is really different from the dynamical evolution of a physical system governed by the same Hamiltonian but taking the twisted $b$-symplectic form $\omega = \frac{dp}{p} \wedge dq$.

In the standard case, the orbits of the system are parabolas of the form $q = -p^2 + c$, with $c$ a constant, everywhere (see the phase portrait on the left of Figure 3.1). The trajectory of a particle in this system is unbounded and, for any initial conditions, $q, p \underset{t\to\infty}{\longrightarrow} -\infty$. This is the model of a massive particle moving in an infinite 1-dimensional well, subject to a constant force field and with no friction.

In the twisted $b$-cotangent case the orbits are of two types. On the one hand, in the line $p = 0$ there are only fixed points. On the other hand, there are half-parabolas of the same form $q = -p^2 + c$, with $c$ a constant, at each side of the axis $p = 0$ (see the phase portrait on the right of Figure 3.1). The evolution of a particle starting at a point $(q_0, p_0)$ either in the upper or in the lower plane is similar: in both cases it will approach asymptotically the fixed point $(q_0 + p_0^2, 0)$ in the axis $p = 0$ following the parabola $q = -p^2 + q_0 + p_0^2$. Then, at a finite time, a particle will be found at $p = 0$ if and only if it already started there. This has physical sense since the Stokes' Law states that the drag force acts proportionally to the speed of the particle and in the opposite direction. Then, a particle with non-zero initial velocity slows down continuously, but it never completely stops because the acting force also decreases in correspondence.

The nature of the trajectories $q(t)$ in both systems is also very different. In Figure 3.2 we can see some trajectories corresponding to the standard Hamilton's Equations (3.2) and some trajectories corresponding to the twisted Hamilton's Equations (3.3), in both cases taking the same linear potential in the Hamiltonian $H(q, p) = \frac{1}{2}p^2 + \frac{\lambda}{2}q$.

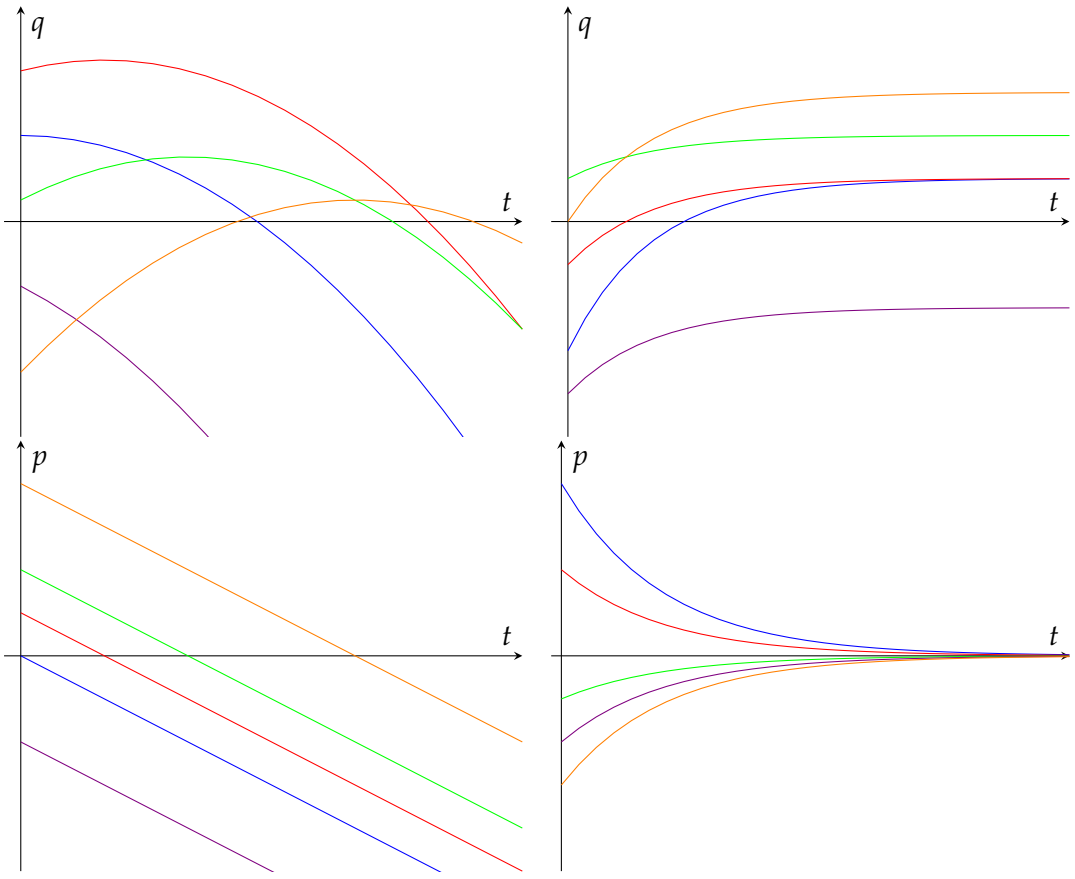


FIGURE 3.2: On the left, some trajectories $q(t)$ and $p(t)$ given by the standard Hamilton's Equations (3.2). On the right, some trajectories $q(t)$ and $p(t)$ given by the twisted Hamilton's Equations (3.3). In both cases it has been taken a linear potential in the Hamiltonian $H(q, p) = \frac{1}{2}p^2 + \frac{\lambda}{2}q$.

The trajectory $q(t)$ of a particle under the classical System (3.2) is of the form

$q(t) = -\frac{\lambda}{4}t^2 + c_1 t + c_0$. It depends on the constants $c_0, c_1$ (equivalently, on the starting $q$ and $p$) but, for any initial conditions, $q(t), p(t) \underset{t\to\infty}{\longrightarrow} -\infty$. This corresponds to the aforementioned 1-dimensional "free fall" of a particle in a constant force field.

On the other hand, the trajectory $q(t)$ of a particle under the twisted System (3.3) is of the form $q(t) = d_0 - \frac{d_1^2}{\lambda}e^{-\lambda t}$. Hence, the particle's trajectory is bounded and has a limit at a fixed $q = d_0$ greater or equal than the initial $q_0$, no matter which initial conditions are chosen.

The orbits that "break" at the axis $p = 0$ can be identified with "escape orbits" of a $b$-symplectic manifold, objects introduced in [MO21] and studied in [MOP22] by Miranda, Oms and Peralta-Salas.

What we have observed is exceptional because friction is a non-conservative force and, while it cannot be described by the usual basic Hamiltonian setup, it can be described using the twisted $b$-cotangent setting. The critical hypersurface of our example is the line $p = 0$, which corresponds to the zero momentum set, which is physically consistent with the fact that viscous friction alone cannot bring a particle to zero velocity in finite time.

### 3.1.2 The higher-dimensional linear case

We have formulated a 1-dimensional model that is equivalent to the Stokes' Law using the twisted $b$-cotangent setting and now it is natural to consider higher-dimensional models. The most direct generalization is to extend the particle's Hamiltonian to $T^*\mathbb{R}^n$ in the following way: consider the phase space $T^*\mathbb{R}^n$ of a particle moving in an $n$-dimensional space, take coordinates $(q_1, \dots, q_n, p_1, \dots, p_n)$, and consider the general Hamiltonian

$$H(q_1, \dots, q_n, p_1, \dots, p_n) = \frac{1}{2}\sum_{i=1}^{n} p_i^2 + \frac{\lambda}{2}q_1,$$

where the potential is a linear function of the position coordinate $q_1$.

In the $b$-manifold $(T^*\mathbb{R}, Z = \{p_1 = 0\})$, consider the same Hamiltonian and the twisted $b$-symplectic form

$$\omega = c\frac{dp_1}{p_1} \wedge dq_1 + \sum_{i=2}^{n} dp_i \wedge dq_i, \tag{3.9}$$

where $c \in \mathbb{R}$ is a constant parameter that we call the *dissipation weight* and accounts for the relative weight of the component in which there is dissipation with respect

to the other components. The associated twisted Hamilton's equations are:

$$\begin{cases} \dot{q_1} = \frac{1}{c} p_1^2 \\ \dot{q_2} = p_2 \\ \quad \vdots \\ \dot{q_n} = p_n \\ \dot{p_1} = -\frac{\lambda}{2c} p_1 \\ \dot{p_2} = 0 \\ \quad \vdots \\ \dot{p_n} = 0 \end{cases} . \tag{3.10}$$

The dynamics associated to this system is the following. In the direction of $q_1$, the particle behaves by the Stokes' Law: it suffers dissipation and the corresponding velocity component tends to zero. In the other directions, the motion corresponds to that of a free particle. As a consequence, the evolution of the trajectory is a curve in $\mathbb{R}^n$ that starts with an initial direction given by the value of $(p_1, \ldots, p_n)$ at time 0 and tends to be parallel to the hyperplane $q_1 = 0$, because the momentum in the $q_1$ direction tends to 0 while the other momenta keep being constant.

This is a generalization of the linear 1-dimensional model to a higher-dimensional model in which the friction is still affecting just one dimension and does not allow to consider friction simultaneously in all directions. We shall see in Section 3.2 how to tackle this problem.

The dissipation weight $c$ appearing in the twisted $b$-symplectic form in Equation (3.9) is giving a measure of the predominance of the singular term over the regular terms. In a way, the dissipation weight is a measure of the relative importance of the direction in which there is dissipative friction with respect to the other directions.

**Definition 3.2** (Reynolds number)**.** *In the fluid context, the Reynolds number is the ratio of the inertial force to the viscous force. It is defined as*

$$Re = \frac{\rho v d}{\mu},$$

*where $\rho$ is the density of the fluid, $v$ the velocity of the fluid, $d$ the diameter or characteristic length of the system and $\mu$ the dynamic viscosity of the fluid.*

The Reynolds number quantifies the relative importance of viscosity in the system, in the sense that a lower Reynolds number means that viscous forces are dominant. In practice, it is used to determine whether a fluid exhibits laminar or turbulent flow. On the other hand, the Stokes' Law (3.8) is obtained by solving the axisymmetric and stationary incompressible Navier–Stokes equations disregarding the nonlinear term. Accordingly, the Stokes' Law describes a fluid flow with an spherical object in the laminar regime, that is, when the Reynolds number is 0, although it is a good approximation when the Reynolds number is small enough.

As a consequence, we obtain the following relationship between the Reynolds number and the dissipation weight. The dissipation weight $c$ gives a measure of the

importance of the dissipative direction compared to the other directions in which there is free motion. Then, it can be associated with an analogue of the Reynolds number $Re$ when $Re \approx 0$. A high dissipation weight $c$ implies that there is a big influence of the dissipation by viscosity in the overall system, which is equivalent to a low $Re$.

### 3.1.3 The quadratic potential

Consider again the phase space $T^*\mathbb{R} \cong \mathbb{R}^2$ of a particle moving in a line. Take coordinates $(q, p)$ and now consider a quadratic potential of the type $f(q) = \frac{\lambda}{4}q^2$. The dynamics of a physical system driven by the Hamiltonian $H(q, p) = \frac{1}{2}p^2 + \frac{\lambda}{4}q^2$ and the standard symplectic form $\omega = dp \wedge dq$ corresponds to a simple harmonic oscillator. Explicitly, the standard Hamilton's equations in this case are:

$$\begin{cases} \dot{q} = p \\ \dot{p} = -\frac{\lambda}{2}q \end{cases} . \tag{3.11}$$

Orbits in the phase space of System (3.11) are circles of the form $p^2 + \frac{\lambda}{2}q^2 = c$, with $c$ a constant, everywhere except from the fixed point at the origin (see the phase portrait on the left of Figure 3.3). The position of a particle in this system is bounded and so is its momentum for any initial conditions, since $q(t)$ and $p(t)$ are sine waves (see the trajectories $q(t)$ and $p(t)$ on the left of Figure 3.4). This behavior, which can always be modeled by a quadratic potential, is called in classical mechanics the *simple harmonic oscillator*.

However, and more interestingly, the same Hamiltonian together with the twisted $b$-symplectic form $\omega = \frac{dp}{p} \wedge dq$ gives another very different dynamics. The twisted Hamilton's equations corresponding to $H(q, p) = \frac{1}{2}p^2 + \frac{\lambda}{4}q^2$ are:

$$\begin{cases} \dot{q} = p^2 \\ \dot{p} = -\frac{\lambda}{2}pq \end{cases} . \tag{3.12}$$

On the right of Figure 3.3 we can see the phase space representation of the orbits of System (3.12), and on the right of Figure 3.4 we can see some trajectories $q(t)$ and $p(t)$ of the system.

The second order ODE equivalent to System (3.12) is:

$$\ddot{q} = -\lambda \dot{q} q, \tag{3.13}$$

which is a highly non-linear equation with the following solution for the trajectory $q(t)$:

$$q(t) = \frac{c_1}{\sqrt{\lambda}} \tanh\left(\frac{c_1\sqrt{\lambda}}{2}t + c_2\right),$$

where $c_1$ and $c_2$ are constants that depend on the initial conditions.

On the right of Figure 3.4, we can see some trajectories $q(t)$ and $p(t)$ for different

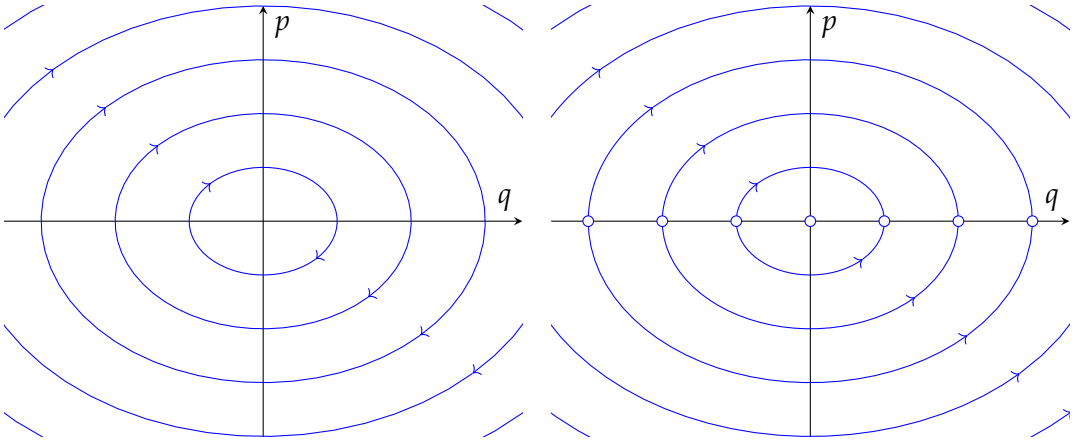


FIGURE 3.3: Some orbits in the phase spaces of the standard Hamilton's Equations (3.11) on the left and of the twisted Hamilton's Equations (3.12) on the right, in both cases choosing the quadratic potential $f(q) = \frac{\lambda}{4}q^2$.

values of $c_1$ and $c_2$. We observe that the position $q(t)$ of a particle under this potential is bounded in the range $(-c_1, c_1)$ and, in accordance, $p(t) \underset{t\to\pm\infty}{\longrightarrow} 0$. We can think that this is the model for a particle which is enclosed in a 1-dimensional container and goes from one of its ends to the other. It does so by starting to separate slowly from one end, then accelerating fast to pass over the mid space of the container, and then slowing again when arriving to the other end.

The twisted $b$-cotangent model corresponding to a quadratic potential, then, models a particle crossing the interior of a box at a slow speed when it is near each edge and at a high speed in the middle. Observe that the orbits in the twisted model "break" again like in the linear twisted case, allowing an infinite number of "escape orbits". In this model, the escape orbits here correspond exactly to genuine *singular periodic orbits* as the ones described in [MO21]. These singular periodic orbits are indeed the union of 4 different trajectories: two symmetric hetero-clinic half-circles and the two fixed points on the $p = 0$ axis at their ends.

A natural next step is to consider a combination of the pure quadratic potential with the linear potential studied previously. Consider again a particle moving in a viscous fluid and obeying the Stokes' Law. Suppose that the fluid has a non-uniform viscosity $\eta$, which is, for instance, the case whenever there is a gradient of temperature, as the viscosity usually depends on the temperature. For small perturbations, the viscosity can be written as a function of the position as $\eta = \frac{\lambda}{2}(1 + \frac{\alpha}{2}q)$, where $\lambda, \alpha > 0$ are constant parameters. Then, the potential $f(q)$ accounting for the drag coefficient becomes $f(q) = \frac{\lambda}{2}q(1 + \frac{\alpha}{2}q)$ and the associated Hamiltonian of the particle is

$$H(p,q) = \frac{p^2}{2} + \frac{\lambda}{2}q\left(1 + \frac{\alpha}{2}q\right).$$

This Hamiltonian gives raise to the following twisted Hamilton's equations:

$$\begin{cases} \dot{q} = p^2 \\ \dot{p} = -\frac{\lambda}{2}p(1 + \alpha q) \end{cases}, \tag{3.14}$$

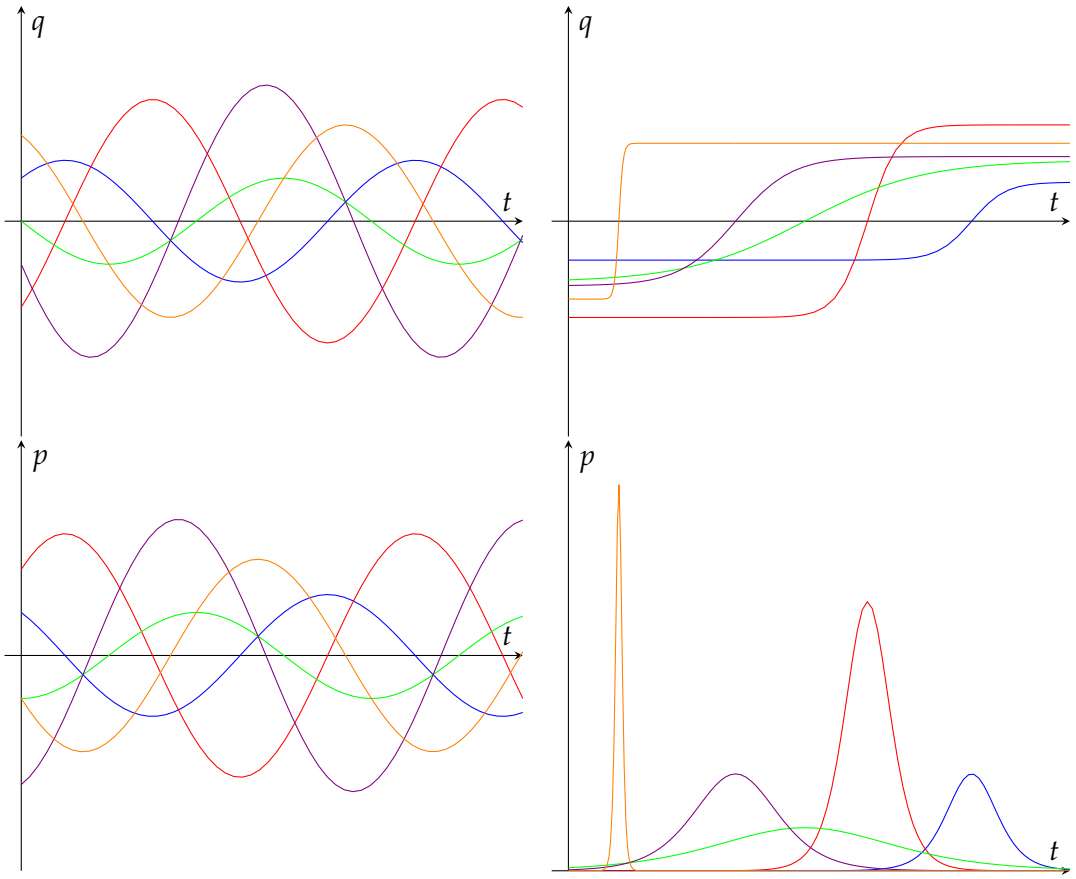


FIGURE 3.4: On the left, some trajectories $q(t)$ and $p(t)$ given by the standard Hamilton's Equations (3.11). On the right, some trajectories $q(t)$ and $p(t)$ given by the twisted Hamilton's Equations (3.12). In both cases it has been taken a quadratic potential in the Hamiltonian $H(q,p) = \frac{1}{2}p^2 + \frac{\lambda}{4}q^2$.

and the corresponding second order ODE is

$$\ddot{q} = -\lambda(1+\alpha q)\dot{q},$$

and includes both the linear regime and the quadratic regime as a perturbation. If the linear term is expected to be dominant, one can assume that $\alpha$ is close to 0. From the physical point of view, this model is the most natural generalization of the 1-dimensional viscous linear regime.

### 3.1.4 The periodic potential

Another option is to consider dissipation in space configurations which are not $\mathbb{R}^n$. An immediate generalization of the 1-dimensional twisted $b$-cotangent model in spaces that are not $\mathbb{R}^n$ is to consider a particle moving over a cylinder $\mathbb{S}^1 \times \mathbb{R}$. In this case, and in coordinates $(\theta, q, p_\theta, p_q)$ on $T^*(\mathbb{S}^1 \times \mathbb{R})$, one can take the twisted $b$-symplectic form $\omega = c\frac{dp_q}{p_q} \wedge dq + dp_\theta \wedge d\theta$, where $c$ is the dissipation weight, and the Hamiltonian

$$H(\theta, q, p_\theta, p_q) = \frac{p_\theta^2 + p_q^2}{2} + \frac{\lambda}{2}q,$$

in which it has been taken a potential depending linearly on the axial coordinate. The corresponding twisted Hamilton's equations are:

$$\begin{cases} \dot{\theta} = p_\theta \\ \dot{q_1} = \frac{1}{c} p_q^2 \\ \dot{p_\theta} = 0 \\ \dot{p_q} = -\frac{\lambda}{2c} p_q \end{cases} . \tag{3.15}$$

and give raise to an spiraling trajectory that tends to a circular periodic orbit around the cylinder (see Figure 3.5). In this twisted $b$-cotangent model the $b$-symplectic form is singular at $p_q = 0$, that is, the singularity appears at the fiber component conjugate to the axial direction of the cylinder. Together with the choice of a linear potential depending on the axial position, this system is able to model dissipation occurring only in the axial direction of the cylinder.

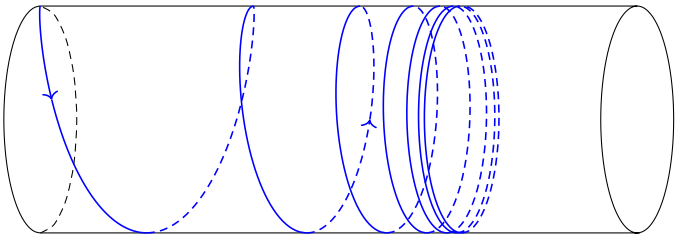

FIGURE 3.5: A dissipating trajectory in the cylinder corresponding to a solution of the twisted Hamilton's Equations (3.15).

If the cylinder $\mathbb{S}^1 \times \mathbb{R}$ is itself assumed to be directly the phase space of a particle moving in the circle $\mathbb{S}^1$, it makes sense to consider a potential which is not function of the axial coordinate but of the angular coordinate and which is, therefore, periodic.

Take coordinates $(\theta, p_\theta)$ on the phase space $T^*\mathbb{S}^1 \cong \mathbb{S}^1 \times \mathbb{R}$ and consider the periodic potential $f(\theta) = \frac{\lambda}{2}\cos\theta$. The dynamical evolution of a physical system driven by the standard Hamilton's equations obtained from the Hamiltonian $H(\theta, p_\theta) = \frac{1}{2}p_\theta^2 + \frac{\lambda}{2}\cos\theta$ and the standard symplectic form $\omega = dp_\theta \wedge d\theta$ corresponds to the model of the simple pendulum. Explicitly, the standard Hamilton's equations of this model are:

$$\begin{cases} \dot{\theta} = p_\theta \\ \dot{p_\theta} = \frac{\lambda}{2}\sin\theta \end{cases} . \tag{3.16}$$

There are many different types of orbits in this system: there is a stable fixed point at $(0,0)$, where the Hamiltonian has a singularity of elliptic type, there is a saddle fixed point at $(\pi, 0)$, where the Hamiltonian has a singularity of hyperbolic type, there are two homoclinic orbits emanating from the saddle fixed point $(\pi, 0)$, there is a 1-parameter family of periodic orbits encircling the stable point and between the two homoclinic orbits, and there is a 1-parameter family of periodic orbits around the cylinder filling the rest of the space away from the homoclinic orbits (see the phase portrait on the left of Figure 3.6). The position of a particle in this system

is bounded and so is its velocity, but it depends on the initial conditions whether it keeps moving periodically or, on the opposite, it stabilizes, which only happens at the fixed points or at the homoclinic orbits.

The same Hamiltonian gives another kind of dynamics in the twisted $b$-cotangent setting. If we consider the twisted $b$-symplectic form $\omega = \frac{dp_\theta}{p_\theta} \wedge d\theta$, the twisted Hamilton's equations corresponding to the Hamiltonian $H(\theta, p_\theta) = \frac{1}{2}p_\theta^2 + \frac{\lambda}{2}\cos\theta$ are:

$$\begin{cases} \dot{\theta} = p_\theta^2 \\ \dot{p_\theta} = \frac{\lambda}{2} p_\theta \sin\theta \end{cases}, \tag{3.17}$$

and the equivalent second order ODE is:

$$\ddot{\theta} = \lambda\dot{\theta}\sin\theta. \tag{3.18}$$

On the right of Figure 3.6 we can see the phase space representation of the orbits of this system.

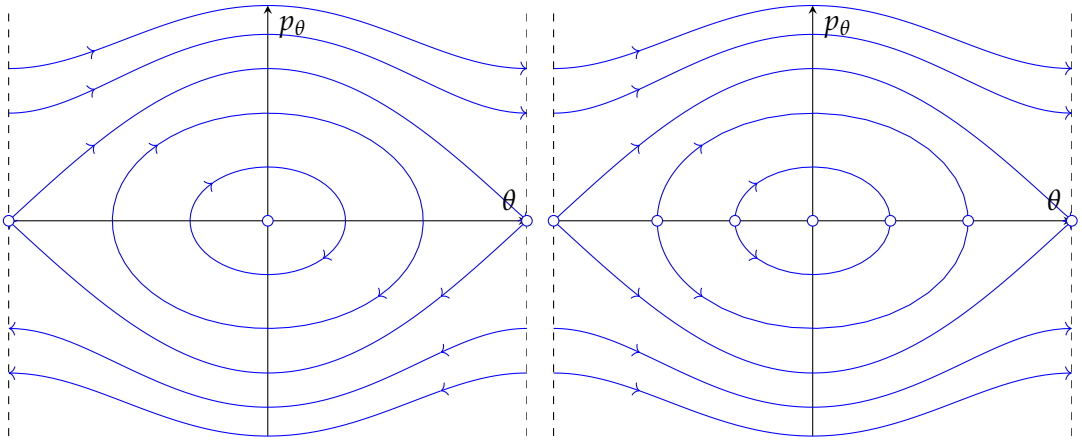


FIGURE 3.6: Some orbits in the phase spaces of the standard Hamilton's Equations (3.16) on the left and of the twisted Hamilton's Equations (3.17) on the right, in both cases choosing the periodic potential $f(q) = \frac{\lambda}{2}\cos\theta$.

We observe that, outside the region enclosed by the homoclinic orbits, the dynamics is the same for both the standard Hamiltonian system and the twisted Hamiltonian system. In this region there is a 1-parameter family of periodic orbits that fill the two half-spaces away from the two homoclinic orbits, something which makes this twisted $b$-cotangent model different from the twisted $b$-cotangent models studied before, in which there were no periodic orbits. On the other hand, the dynamics inside the region enclosed by the homoclinic orbits is the same dynamics that we obtained for the quadratic potential: the circular periodic orbits encircling the origin in the standard Hamiltonian setting are "broken" in the twisted Hamiltonian setting. Each of them is turned into four different orbits: two fixed points on the line $p_\theta = 0$ and two heteroclinic orbits going from one fixed point to the other, one at each side of the line $p_\theta = 0$.

### 3.1.5 General dynamics of the twisted b-symplectic model

With the previous illustrative examples in mind, the interpretation of the general twisted $b$-cotangent model is straightforward. In the most general 1-dimensional setting, we work with a parallelizable 1-dimensional manifold $M$ and we consider its cotangent bundle $T^*M \cong M \times \mathbb{R}$, which represents the phase space of the system. We then select a critical hypersurface $Z \subset T^*M$ of the form $M \times \{p\}$ and, in local coordinates $q, p$ such that $p$ is a defining function of $Z$, the twisted $b$-symplectic form on $T^*M$ writes as

$$\omega = \frac{dp}{p} \wedge dq.$$

Then, a general Hamiltonian $H$ on $T^*M$ gives raise to the Hamiltonian vector field $X_H = p\frac{\partial H}{\partial p}\frac{\partial}{\partial q} - p\frac{\partial H}{\partial q}\frac{\partial}{\partial p}$. And the corresponding twisted Hamilton's equations are:

$$\begin{cases} \dot{q} = p\frac{\partial H}{\partial p} \\ \dot{p} = -p\frac{\partial H}{\partial q} \end{cases} . \tag{3.19}$$

If the Hamiltonian corresponds to the energy of a free particle, that is, it has the form $H = \frac{p^2}{2} + f(q)$, the twisted Hamilton's equations reduce to:

$$\begin{cases} \dot{q} = p^2 \\ \dot{p} = -p\frac{\partial f}{\partial q} \end{cases} .$$

The behavior of a particle under $H$ is clearly conditioned by the singularity of the system at $p = 0$. If it starts zero momentum, it will remain at the same position as time passes, while if it starts with non-zero momentum and it follows a trajectory that tends to $p = 0$, it will decelerate. The most direct physical interpretation of the model is, then, that of a decelerating motion, for instance the one encountered in a dissipative system. If the particle follows a trajectory that goes away from $p = 0$, it can be interpreted just in the same way but with time reversed.

Notice that, for a Hamiltonian of the type $H = \frac{p^2}{2} + f(q)$, the relation between the Hamiltonian vector field $\tilde{X}_H$ given by the twisted Hamilton's Equations (3.3)) and the Hamiltonian vector field $X_H$ given by the classical Hamilton's Equations (3.2)) is $\tilde{X}_H = pX_H$. Accordingly, the orbits of $\tilde{X}_H$ coincide with those of $X_H$ away from the critical line $p = 0$, which is filled by a set of stagnation points of $\tilde{X}_H$, and up to a reversed time parametrization for $p < 0$. As a consequence, any point $(q, 0)$ which is not a critical point of the potential $f(q)$ yields an escape orbit of $\tilde{X}_H$ because the corresponding orbit of $X_H$ is regular and transverse to the line $p = 0$.

The implications of having the singularity at the fibers of the cotangent bundle $T^*M$ extend further than it seems at first glance. The singularity determines an unreachable location in the fiber, that is, that zero momentum is unreachable. But the momentum of the particle will tend there (or escape from there) for many different initial conditions. As a consequence, the position of the particle is also indirectly conditioned by the singularity, since tending to zero momentum will cause the position to stabilize.

The twisted $b$-symplectic model with the singular fiber at zero is, then, a physical model that can explain systems in which velocity decays and so does the change in position of the particle as a consequence.

What we have seen is that dissipation emerges naturally in the direction transversal to the hypersurface where a $b$-symplectic form is singular. In particular, the model we give for 1-dimensional friction uses the techniques $b$-symplectic geometry to provide a finite-dimensional analogy of fluid mechanics that contemplates dissipation in conditions of no turbulence.

The twisted $b$-cotangent model presented here is suited for the case of laminar viscous flows in which the Reynolds number is small enough. In general, the model is good for flows of low complexity and no turbulence, and for which the Stokes' Law is a valid approximation. The model can be generalized to multiple dimensions and to an arbitrary external potential by including an additional dimension to describe the physical time and energy. Therefore, any $n$-dimensional system with an external potential and a global dissipation given by a fixed dissipation factor can be naturally described using the language of Hamiltonian dynamics on a $b$-symplectic manifold.

The use of the twisted $b$-cotangent model, in which the singularity of the $b$-symplectic form is located at the fibers of the cotangent bundle, reveals that there is essential information about the dynamics of the system contained in the fibers of the configuration space $T^*M$. Indeed, the core of the 1-dimensional linear model is that the fixed singularity at the 0 fiber of the cotangent bundle $T^*M$ makes any trajectory tend to a fixed point on the base. And in the non-linear models, the effect is analogous for any orbit that would intersect the 0 fiber in the classical standard symplectic setting.

The key features of the model are perfectly illustrated in the phase portraits of Figures 3.1, 3.3 and 3.6. There, the orbits that intersect transversally the 0 fiber in the classical symplectic setting are transformed into *escape orbits* when replacing the standard symplectic form by the twisted $b$-symplectic form. This type of orbits, which can be seen as union of trajectories, also arises in other contexts such as celestial mechanics, and has been recently investigated by Miranda, Oms and Peralta-Salas in [MO21] and [MOP22]. Our twisted $b$-cotangent models detect an infinite number of this type of orbits and this situation aligns with the conjecture of *"2 or infinity"* in the number of periodic orbits [HWZ98; CHP19].

## 3.2 Time-dependent singular models

In order to generalize the model of 1-dimensional friction to a model in which the friction happens in multiple dimensions, the idea is to extend the $n$-dimensional configuration space $M$ to $M \times \mathbb{R}$. In $M \times \mathbb{R}$, we let the $\mathbb{R}$ component describe the real time $t$ while the dynamics inside the configuration space is computed according to a *curvilinear time* $s$, a procedure which is known as the *method of characteristics* in the context of PDEs and which requires $\frac{dt}{ds} = \dot{t} > 0$ to be consistent.

In accordance with the extension of the configuration space, the original $2n$-dimensional phase space $T^*M$ is extended to $T^*M \times T^*\mathbb{R}$. Since the energy is the natural conjugate of time in physics, we denote by $E$ the conjugate variable associated with $t$. Following the line of Section 3.1, where we introduced a 1-dimensional model of dissipation using a twisted $b$-cotangent model, our goal now is to formulate the dissipation in $T^*M \times T^*\mathbb{R}$ using this new energy variable $E$. After computing the solution of the system in $T^*M \times T^*\mathbb{R}$, to recover the solution in real time one only needs to project the trajectory on the original phase space $T^*M$.

We start from a base model in the extended phase space $T^*M \times T^*\mathbb{R}$ in which there is no friction. Take position coordinates $q = (q_1, \dots, q_n)$ and momentum coordinates $p = (p_1, \dots, p_n)$ in $T^*M$, and $(t, E)$ coordinates in $T^*\mathbb{R}$. Consider the Hamiltonian

$$H(p, q, t, E) = \frac{p^2}{2} + V(q, t) - E \tag{3.20}$$

and the symplectic form

$$\omega = \sum_i dp_i \wedge dq_i - dE \wedge dt. \tag{3.21}$$

The corresponding Hamilton's equations write as:

$$\frac{dq_i}{ds} = \dot{q}_i = p_i \qquad \frac{dp_i}{ds} = \dot{p}_i = -\frac{\partial V(q,t)}{\partial q_i} \tag{3.22}$$

$$\frac{dt}{ds} = \dot{t} = 1 \qquad \frac{dE}{ds} = \dot{E} = \frac{\partial V(q,t)}{\partial t} \tag{3.23}$$

In this model, in the curvilinear coordinate coincides with the real time: $s = t$, and the particle follows the standard dynamics under a potential $V$ that we allow to depend on time.

Now, to model friction, it is natural to consider adding to the Hamiltonian a factor depending on a friction coefficient $\lambda$. The friction will slow down the dynamics and thus it will slow the real time $t$ with respect to the curvilinear time $s$. To deduce the suitable time re-scaling, we first re-scale the Hamiltonian $H$ by an exponential factor $\frac{e^{\lambda t}}{\lambda}$, since when considering dissipative dynamics it is natural to expect exponential decays. Indeed, a close-to-the-equilibrium relaxation mode provides a Lyapunov coefficient to control the decay of the perturbation [GM13; GP71]. Such re-scaling ideas have already been suggested in different contexts, see for instance [FL85]. Note that the potential $V$ will remain associated with the real time $t$ and thus it will appear accelerated with respect to the curvilinear time $s$.

For our purpose, we consider the Hamiltonian

$$H(p, q, t, E) = \frac{p^2}{2} + \frac{e^{2\lambda t}}{\lambda^2} V(q, t) - \frac{e^{\lambda t}}{\lambda} E, \tag{3.24}$$

with the same symplectic form $\omega = \sum_i dp_i \wedge dq_i - dE \wedge dt$. The associated Hamilton's equations write as:

$$\frac{dq_i}{ds} = \dot{q}_i = p_i \qquad \frac{dp_i}{ds} = \dot{p}_i = -\frac{e^{2\lambda t}}{\lambda^2}\frac{\partial V(q,t)}{\partial q_i} \tag{3.25}$$

$$\frac{dt}{ds} = \dot{t} = \frac{e^{\lambda t}}{\lambda} \qquad \frac{dE}{ds} = \dot{E} = \frac{e^{2\lambda t}}{\lambda^2}\frac{\partial V(q,t)}{\partial t} + \frac{2e^{2\lambda t}}{\lambda}V(q,t) - e^{\lambda t}E \tag{3.26}$$

The first two terms describe the energy of the system linked with the time-dependence of the potential. The last term describes the loss of energy caused by the viscous dissipation. The equation for $t$ can be solved exactly: $t(s) = -\frac{\ln(-s)}{\lambda}$. In particular, $ds = \lambda e^{-\lambda t}dt$. Applying this change of variables, we obtain the following equations, which give us the reconstructed particle dynamics in function of the real time $t$:

$$\frac{dq_i}{dt} = \lambda e^{-\lambda t}\dot{q}_i = \lambda e^{-\lambda t}p_i \qquad \frac{dp_i}{dt} = \lambda e^{-\lambda t}\dot{p}_i \quad = -\tfrac{e^{\lambda t}}{\lambda}\tfrac{\partial}{\partial q_i}V(q,t). \tag{3.27}$$

The equivalent second order ODE is:

$$\frac{d^2q_i}{dt^2} = -\lambda\frac{dq_i}{dt} - \frac{\partial}{\partial q_i}V(q,t), \tag{3.28}$$

which is the equation of a particle in an $n$-dimensional space with a viscous friction $\lambda$ and under a time-dependent potential $V(q,t)$.

In this model, the friction arises from an exponential re-scaling of time and such a re-scaling is actually the source of a singularity. In particular, a $b$-symplectic form arises naturally after the change of variables from $t$ to $s$ in the symplectic form $\omega$. Using $s(t) = e^{-\lambda t}$, $dt = -\frac{ds}{\lambda s}$ and, for convenience, redefining $E_s = E/\lambda$, we obtain

$$\omega = \sum_i dq_i \wedge dp_i + \frac{ds}{s} \wedge dE_s, \tag{3.29}$$

which is the canonical $b$-symplectic form in the $b$-cotangent bundle of $(M \times \mathbb{R}, Z = M \times \{0\})$. The Hamiltonian becomes

$$H(p,q,s,E_s) = \frac{p^2}{2} + \frac{V(q,t(s))}{(\lambda s)^2} - \frac{E_s}{s}, \tag{3.30}$$

and has a simpler expression in these coordinates. But the main advantage is that the intrinsic time (the curvilinear coordinate) now corresponds to the coordinate $s$. Indeed, the equations of motion now read as follows:

$$\dot{q}_i = p_i \qquad \dot{p}_i = -\frac{1}{(\lambda s)^2}\frac{\partial V(q,t(s))}{\partial q_i} \tag{3.31}$$

$$\dot{s} = 1 \qquad \dot{E} = \frac{\partial}{\partial s}\left(\frac{1}{(\lambda s)^2}V(q,t(s))\right) + \frac{E_s}{s^2} \tag{3.32}$$

The coordinate $s$ is now trivial and we may omit this dimension, leaving a standard Hamiltonian dynamics with a modified time-dependent potential. The dynamics

then writes as:

$$\ddot{q}_i(s) = -\frac{1}{(\lambda s)^2}\frac{\partial V(q,s)}{\partial q_i} \tag{3.33}$$

and the real-time solution is obtained by undoing the change of variables $s(t) = e^{-\lambda t}$.

One could think about extending the singular models considered in this section to include the effects of an electromagnetic field acting on a charged particle. In this case, the configuration space is $\mathbb{R}^3$, with an electric potential function $\phi$ and a magnetic vector potential $\vec{A}$. The corresponding electric and magnetic fields are $\vec{E} = \nabla\phi$ and $\vec{B} = \nabla \times \vec{A}$, respectively, both depending on the position $q \in \mathbb{R}^3$ of the particle. The force $\vec{F}$ acting on the particle is the Lorentz force $\vec{F} = e(\vec{E} + \vec{v} \times \vec{B})$, a function of both position and velocity.

The problem can be studied in the Hamiltonian setting by identifying the tangent and the cotangent vectors via a fixed Riemannian metric. The magnetic field $\vec{B}$ is associated with a 2-form $B = \iota_{\vec{B}}\Omega$, where $\Omega$ is the volume form associated with the fixed Riemannian metric. The Maxwell equation $\nabla \cdot \vec{B} = 0$, which allows for the existence of the vector potential, becomes the condition $dB = 0$. By means of the Poincaré Lemma, there exists a 1-form $A$ such that $B = dA$ and such that $A = \langle \vec{A}, \cdot \rangle$. The electrodynamics naturally appears in the phase space $(T^*M, \omega_B)$, where $\omega_B$ is the sum of the canonical symplectic form $\omega_M$ on $T^*M$ and the pull-back of the 2-form $B$ by the natural projection $\pi : T^*M \to M$, i.e., $\omega_B = \omega_M + \pi^*B$.

The discussion on the multidimensional case is still valid under the presence of a time-dependent magnetic potential $B = B_{ij}(q,t)dq_i \wedge dq_j$, and the subtlety in the case of dissipation is to adjust the speed of the magnetic field. Similarly to what has been done in this section, the recipe in this case would be given by the change $B \to \frac{e^{\lambda t}}{\lambda}B$. Nevertheless, since the magnetic field would no longer be closed, the method presented here would need further development to be convenient for magnetic dynamics.

# Chapter 4

# Constructions of b-semitoric systems

In this chapter we introduce $b$-semitoric systems as a generalization of semitoric systems for $b$-symplectic manifolds. The primary objective is to present examples of these systems and explore their unique characteristics. A $b$-semitoric system is a 4-dimensional $b$-integrable system that satisfies these conditions: one of its moment map components is proper and generates an effective global $\mathbb{S}^1$ action, and all singular points are non-degenerate and lack hyperbolic components. We illustrate this concept through three examples of families of $b$-semitoric systems, all of them built by modifying the coupled angular momenta, which is a family of semitoric systems. Additionally, we classify the singular points and describe the dynamics using the respective moment maps.

To construct examples of 4-dimensional $b$-integrable systems with focus-focus singularities we first analyze the properties of these singular points. We find that focus-focus singularities cannot occur at the critical set $Z$, where the $b$-symplectic form becomes singular. Instead, these singularities are limited to the open symplectic manifold $M \setminus Z$, where we can apply the results obtained from semitoric systems.

To illustrate our conclusions we also compute and plot numerically the flow of the two Hamiltonian $b$-vector fields of a $b$-semitoric system in the fiber of a focus-focus fixed point, which turns out to be a pinched torus like in the semitoric case.

With respect to the published paper [Bru+23], we added in this thesis a good amount of details of the computations of the different systems and rearranged them between Section 4.2 in this chapter and Sections A.1, A.2, A.3 and A.4 in Appendix A. We also introduced the entire numerical analysis of Section 4.3, which we thought that would be appreciated by anyone who wants to study further the dynamical properties of $b$-semitoric systems.

This chapter is organized as follows: In Section 4.1 we define the notion of $b$-semitoric system and we prove that it contains no fixed points in $Z$. In Section 4.2 we modify the semitoric transition family of the coupled angular momenta system to construct three families of $b$-semitoric systems. We identify and classify their fixed points and compute the image of their moment maps. In Section 4.3 we discuss the type of fibers that are admitted in a $b$-semitoric system and we compute numerically the flow in the fiber of a fixed point of focus-focus type of one of the $b$-semitoric systems introduced.

## 4.1 b-Semitoric systems and b-semitoric families

In Chapter 2 we introduced *semitoric systems* as 4-dimensional integrable systems $(M, \omega, F = (L, H))$ such that $L$ is a proper function and its Hamiltonian flow is $2\pi$-periodic almost everywhere, and whose singular points are non-degenerate and only admit non-regular components of elliptic and focus-focus type (see Definition 2.18). On the other hand, we introduced *b-toric systems* as $b$-integrable systems $(M^{2n}, Z, \omega, F = (f_1, \dots, f_n))$ such that the flow of each $X_{f_i}$ is $2\pi$-periodic almost everywhere (see Definition 2.33).

In this chapter we explore a broader class of systems, which we call *b-semitoric systems*, that includes both semitoric systems and $b$-toric systems.

**Definition 4.1.** *A 4-dimensional b-integrable system $(M, Z, \omega, (L, H))$ is called* $b$-semitoric *if*

1. *$L$ is a proper function and the flow of $X_L$ is $2\pi$-periodic almost everywhere.*
2. *All singular points of $F = (L, H)$ are non-degenerate and do not include components of hyperbolic type.*

The class of $b$-semitoric systems generalizes the class of semitoric systems because it admits systems with the same dynamics of semitoric type but in which the manifold has a critical hypersurface in which the $b$-symplectic form is singular. At the same time, the class of $b$-semitoric systems generalizes the class of $b$-toric systems in 4 dimensions because it just requires one of the components of the moment map to be $2\pi$-periodic, not both of them.

The singularities of a $b$-semitoric system are all non-degenerate and can only be of one of the following three types, depending on their components:

- a fixed point with two elliptic components, or
- a fixed point with one focus-focus component, or
- a rank 1 singular point with one regular and one elliptic component.

These three of singular points are called, respectively, *elliptic-elliptic*, *focus-focus* and *elliptic-regular*. They coincide with the types of singular points admitted by a standard semitoric system but, unlike the latter, they cannot occur everywhere on the manifold $M$.

In [KMS16] it was proved that, in $b$-integrable systems which only have non-degenerate singularities in the sense of Definition 2.12, the minimal rank of the $b$-moment map is 1 along $Z$. In particular, the critical hypersurface $Z$ cannot contain fixed points of the system and this is the reason why the fixed points of a $b$-semitoric system can only occur on $M \setminus Z$. Then, in the $b$-semitoric systems that we introduce and study next, elliptic-elliptic and focus-focus singularities will be found away from the critical hypersurface $Z$.

In an analogous way to the definition of *semitoric families* of integrable systems (see Definition 2.19), one can also define *b-semitoric families* of $b$-integrable systems.

**Definition 4.2.** *A* $b$-semitoric family *is a family of* $b$*-integrable systems* $(M^4, \omega, Z, F_t = (L, H_t))$*, with* $0 \leq t \leq 1$ *and* $H_t = H(t, \cdot)$ *such that:*

- *for any* $t \in [0,1]$*,* $H_t$ *is a* $b$*-function, and*
- *there exist* $k \in \mathbb{Z}_{\geq 0}$ *and* $t_1, \ldots, t_k \in [0,1]$ *such that* $(M, \omega, F_t)$ *is* $b$*-semitoric if and only if* $t \notin \{t_1, \ldots, t_k\}$*.*

*The values* $t_1, \ldots, t_k$ *are called* degenerate times*.*

## 4.2 The b-coupled angular momenta

Throughout this section we study three new families of $b$-integrable systems that we build as modifications of semitoric family of the *coupled angular momenta* or *classical coupled angular momenta* described in Section 2.2.2.

**Definition 4.3.** *Consider* $M = \mathbb{S}^2_1 \times \mathbb{S}^2_2$ *and endow it with the symplectic form* $\omega = -(R_1 \omega_{\mathbb{S}^2_1} + R_2 \omega_{\mathbb{S}^2_2})$*, where, for* $i \in \{1,2\}$*,* $\omega_{\mathbb{S}^2_i}$ *is the standard symplectic form on* $\mathbb{S}^2_i$ *and* $0 < R_1 < R_2$ *are constants. For* $i \in \{1,2\}$*, let* $x_i, y_i, z_i$ *be the Cartesian coordinates on the unit sphere* $\mathbb{S}^2_i$ *and consider the parameter* $t \in [0,1]$*.*

*The* coupled angular momenta *is the semitoric transition family of* 4*-dimensional integrable systems* $(M, \omega, F_t = (L, H_t))$ *parameterized by* $t$ *and defined by*

$$\begin{cases} L(x_1, y_1, z_1, x_2, y_2, z_2) := R_1 z_1 + R_2 z_2, \\ H_t(x_1, y_1, z_1, x_2, y_2, z_2) := (1-t) z_1 + t(x_1 x_2 + y_1 y_2 + z_1 z_2). \end{cases} \tag{4.1}$$

There are three natural ways to create a family of $b$-integrable systems as a modification of the coupled angular momenta family $(L, H_t)$ defined on $(M = \mathbb{S}^2_1 \times \mathbb{S}^2_2, \omega = -(R_1 \omega_{\mathbb{S}^2_1} + R_2 \omega_{\mathbb{S}^2_2}))$. All of them are obtained by selecting a hypersurface $Z \subset M$ and a $b$-symplectic structure on $M$ which is singular at $Z$, and by modifying the functions $L$ and $H_t$ into $b$-functions compatible with the $b$-symplectic structure:

- *System 1*: We take $Z = \{z_1 = 0\} \subset M$, endow $M$ with the $b$-symplectic form $\omega = -(R_1 \frac{1}{z_1} \omega_{\mathbb{S}^2_1} + R_2 \omega_{\mathbb{S}^2_2})$ and modify $L$ to: $L(\theta_1, z_1, \theta_2, z_2) = R_1 \log |z_1| + R_2 z_2$.
- *System 2*: In the same setting as in the previous case, we also modify $H_t$ to: $H_t(\theta_1, z_1, \theta_2, z_2) = (1-t) \log |z_1| + t \left( \sqrt{(1-z_1^2)(1-z_2^2)} \cos(\theta_1 - \theta_2) + z_1 z_2 \right)$.
- *System 3*: We take $Z = \{z_2 = 0\} \subset M$, endow $M$ with the $b$-symplectic form $\omega = -(R_1 \omega_{\mathbb{S}^2_1} + R_2 \frac{1}{z_2} \omega_{\mathbb{S}^2_2})$ and modify $L$ to: $L(\theta_1, z_1, \theta_2, z_2) = R_1 z_1 + R_2 \log |z_2|$.

Note that there is apparently another fourth equally natural option to turn the classical coupled angular momenta into a family of $b$-integrable systems. It consists of taking $Z$ as in Systems 1 and 2 and only modify $H_t$ like in System 2. However, this option does not really produce a $b$-integrable system. Indeed, if we

take $Z = \{z_1 = 0\}$, $L(\theta_1, z_1, \theta_2, z_2) = R_1 z_1 + R_2 z_2$ and $H_t(x_1, y_1, z_1, x_2, y_2, z_2) = (1-t)\log|z_1| + t(x_1x_2 + y_1y_2 + z_1z_2)$ then the system is not integrable. This can bee realized by taking into account that the vector field $X_L$ will no longer represent a rotation in this system or, in a more explicitly way, computing $\{L, H_t\}$ in $M^{0,0}$:

$$\{L, H_t\} = t(z_1 - 1)\sqrt{\left(1 - z_1^2\right)\left(1 - z_2^2\right)}\sin\left(\theta_1 - \theta_2\right),$$

which is generically different from 0.

In Systems 1 and 2 the hypersurface $Z$ where the $b$-symplectic structure is singular is $Z = \{z_1 = 0\} \subset \mathbb{S}_1^2 \times \mathbb{S}_2^2$. It is the 3-dimensional submanifold of $\mathbb{S}_1^2 \times \mathbb{S}_2^2$ obtained as a product of the equator of $\mathbb{S}_1^2$ and $\mathbb{S}_2^2$ (see Figure 4.1).

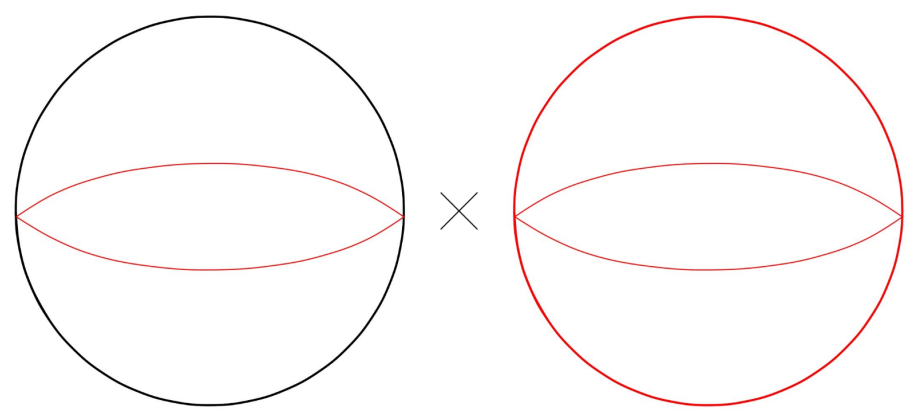

FIGURE 4.1: In red, the 3-dimensional submanifold $Z = \{z_1 = 0\} \subset \mathbb{S}_1^2 \times \mathbb{S}_2^2$ where the $b$-symplectic structure in Systems 1 and 2 is singular.

In System 3, the hypersurface $Z$ where the $b$-symplectic structure is singular is $Z = \{z_2 = 0\} \subset \mathbb{S}_1^2 \times \mathbb{S}_2^2$. It is the 3-dimensional submanifold of $\mathbb{S}_1^2 \times \mathbb{S}_2^2$ obtained as a product of $\mathbb{S}_1^2$ and the equator of $\mathbb{S}_2^2$ (see Figure 4.2).

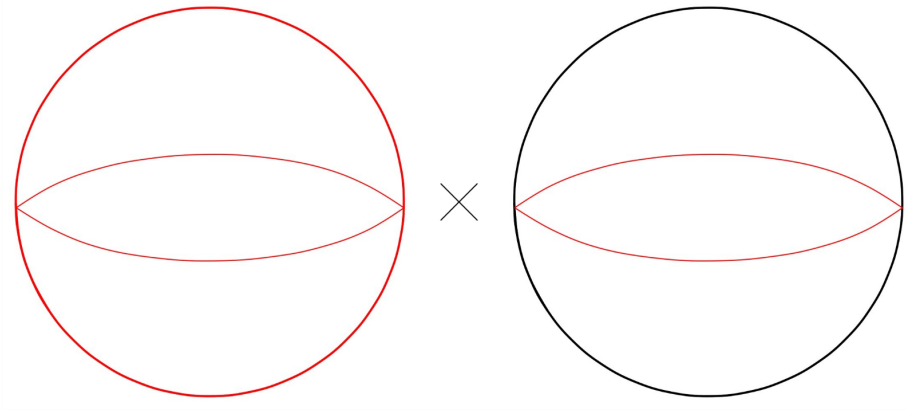

FIGURE 4.2: In red, the 3-dimensional submanifold $Z = \{z_2 = 0\} \subset \mathbb{S}_1^2 \times \mathbb{S}_2^2$ where the $b$-symplectic structure in System 3 is singular.

Our goal in this chapter is to study the three families of $b$-integrable systems (Systems 1, 2 and 3), classify their singularities and prove that they are families of

$b$-semitoric systems or $b$-semitoric families (see Definition 4.2). Since they are constructed straight out of the classical coupled angular momenta by introducing the $b$-symplectic setting in it, one can think of them as *$b$-coupled angular momenta systems*.

For the complete study of each of the three families of $b$-integrable systems we follow the same scheme. First, we prove that any system in the family is indeed a $b$-integrable system because it satisfies the requirements of Definition 2.31). Then, we identify its fixed points and classify them following Theorem 2.13. Next, we find its singular points of rank 1 and classify them. Finally, we conclude that it is a $b$-semitoric family as introduced in Definition 4.2.

However, before starting the study of Systems 1, 2 and 3, it will be useful to go back and take a look at the local analysis of the fixed points of the classical coupled angular momenta, which were already identified, studied and classified in [SZ99; LP19; ADH20]. We will use the local analysis techniques for 4-dimensional integrable systems introduced in Section 2.2.2 and we will take advantage of the similarities between the local behavior of Systems 1, 2 and 3 and the local behavior of the classical coupled angular momenta at the critical points.

To carry out this study we need to work with different coordinate charts on $M = \mathbb{S}^2_1 \times \mathbb{S}^2_2$. We will think of it as the product of two spheres of radius 1 embedded in $\mathbb{R}^3 \times \mathbb{R}^3$. To prove global properties of the systems, the double cylindrical chart in $M$ is well suited, while to study local behaviors around the fixed points at the double poles, the double Cartesian chart in $M$ is more convenient. We will see that, for completeness, we still need other coordinate charts that combine cylindrical coordinates in one sphere component and Cartesian coordinates in the other sphere component.

### 4.2.1 The coordinate charts

We use the classical coupled angular momenta system to introduce the different coordinate charts that we need later for the study of the three $b$-coupled angular momenta systems.

On the one hand, to study the coupled angular momenta away from the double poles $p_{\pm,\pm} := ((0,0,\pm 1),(0,0,\pm 1))$ we use the double cylindrical coordinates $\theta_1, z_1, \theta_2, z_2$ of the *double cylindrical chart* of $\mathbb{S}^2_1 \times \mathbb{S}^2_2$.

**Definition 4.4.** *The* double cylindrical chart *is the chart* $(\phi_1, U_1^0) \times (\phi_2, U_2^0)$ *of* $\mathbb{S}^2_1 \times \mathbb{S}^2_2$ *in which, for* $i \in \{1,2\}$,

$$U_i^0 = \{(x_i, y_i, z_i) \in \mathbb{S}^2_i \mid |z| < 1\} \subset \mathbb{S}^2_i,$$

$$\begin{array}{rccc} \phi_i : & \mathbb{S}^2_i \subset \mathbb{R}^3 & \longrightarrow & \mathbb{S}^1 \times \mathbb{R}^1 \\ & (x_i, y_i, z_i) & \longmapsto & (\theta_i, z_i) \end{array}$$

*and*

$$\begin{cases} \theta_i = \arg(x_i + i y_i) \\ z_i = \pm\sqrt{1 - x_i^2 - y_i^2}. \end{cases}$$

The double cylindrical chart $(\phi_1, U_1^0) \times (\phi_2, U_2^0)$ covers

$$M^{0,0} := U_1^0 \times U_2^0 \subset \mathbb{S}_1^2 \times \mathbb{S}_2^2,$$

that is, it covers the entire $M = \mathbb{S}_1^2 \times \mathbb{S}_2^2$ except for the 2-dimensional submanifolds $\{(0,0,\pm 1)\} \times \mathbb{S}_2^2$ and $\mathbb{S}_1^2 \times \{(0,0,\pm 1)\}$, which include the four fixed points at the double poles (see Figure 4.3).

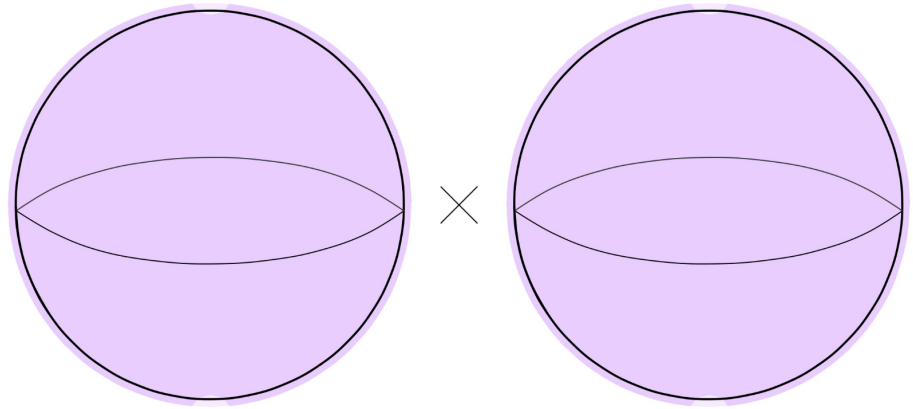

FIGURE 4.3: The double cylindrical chart $(\phi_1, U_1^0) \times (\phi_2, U_2^0)$ covers $M^{0,0} = U_1^0 \times U_2^0 \subset \mathbb{S}_1^2 \times \mathbb{S}_2^2$, a submanifold of $M$ which does not include the double poles.

On $M^{0,0}$, the symplectic form $\omega = -(R_1 \omega_{\mathbb{S}_1^2} + R_2 \omega_{\mathbb{S}_2^2})$ writes as

$$\omega = -R_1 \, d\theta_1 \wedge dz_1 - R_2 \, d\theta_2 \wedge dz_2.$$

And the functions $L$ and $H_t$ can be rewritten on $M^{0,0}$ as

$$\begin{cases} L(\theta_1, z_1, \theta_2, z_2) = R_1 z_1 + R_2 z_2, \\ H_t(\theta_1, z_1, \theta_2, z_2) = (1-t) z_1 + t \left( \sqrt{(1-z_1^2)(1-z_2^2)} \cos(\theta_1 - \theta_2) + z_1 z_2 \right) \end{cases}.$$

On the other hand, to study the coupled angular momenta around the fixed points at the double poles $p_{\pm,\pm}$, we use the double Cartesian coordinates $x_1, y_1, x_2, y_2$ of the *double Cartesian charts* of $\mathbb{S}_1^2 \times \mathbb{S}_2^2$.

**Definition 4.5.** *The* double Cartesian charts *are the charts* $(\varphi_1, U_1^{\varepsilon_1}) \times (\varphi_2, U_2^{\varepsilon_2})$ *of* $\mathbb{S}_1^2 \times \mathbb{S}_2^2$ *in which, for* $i, j \in \{1,2\}$ *and* $\varepsilon_1, \varepsilon_2 \in \{+,-\}$,

$$U_i^{\varepsilon_j} = \{(x_i, y_i, z_i) \in \mathbb{S}_i^2 \mid \varepsilon_j z_i > 0\} \subset \mathbb{S}_i^2,$$

$$\begin{array}{rccc} \varphi_i : & \mathbb{S}_i^2 \subset \mathbb{R}^3 & \longrightarrow & \mathbb{R}^2 \\ & (x_i, y_i, z_i) & \longmapsto & (x_i, y_i) \end{array}.$$

A double Cartesian chart $(\varphi_1, U_1^{\varepsilon_1}) \times (\varphi_2, U_2^{\varepsilon_2})$ covers

$$M^{\varepsilon_1, \varepsilon_2} := U_1^{\varepsilon_1} \times U_2^{\varepsilon_2} \subset \mathbb{S}_1^2 \times \mathbb{S}_2^2,$$

that is, it covers the product of two hemispheres, one of each sphere component of $M = \mathbb{S}_1^2 \times \mathbb{S}_2^2$, without including the equators.

The collection of the four double Cartesian charts

$$(\varphi_1, U_1^+) \times (\varphi_2, U_2^+), (\varphi_1, U_1^+) \times (\varphi_2, U_2^-), (\varphi_1, U_1^-) \times (\varphi_2, U_2^+), (\varphi_1, U_1^-) \times (\varphi_2, U_2^-)$$

covers all $M = \mathbb{S}_1^2 \times \mathbb{S}_2^2$ except for the points which belong to the 3-dimensional submanifolds $\{z_1 = 0\} \times \mathbb{S}_2^2$ and $\mathbb{S}_1^2 \times \{z_2 = 0\}$ (see Figure 4.4).

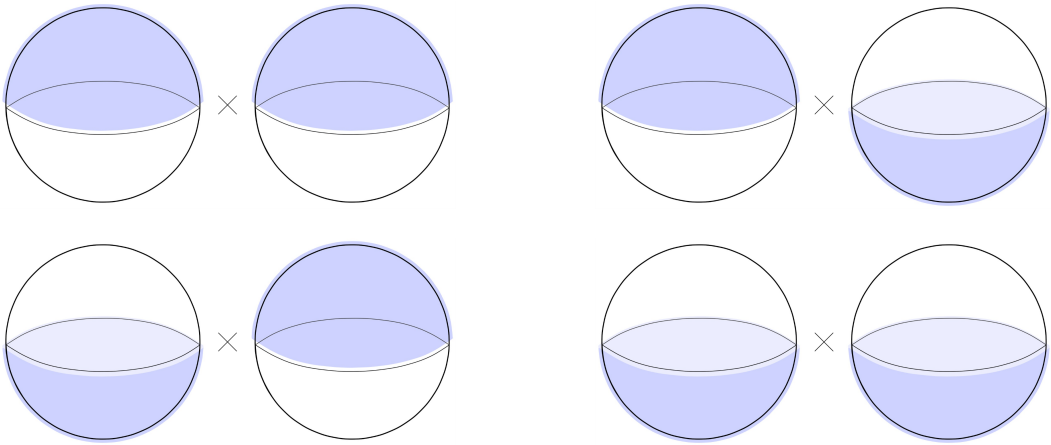

FIGURE 4.4: From left to right and from top to bottom, illustrations of the four double Cartesian charts $(\varphi_1, U_1^+) \times (\varphi_2, U_2^+)$, $(\varphi_1, U_1^+) \times (\varphi_2, U_2^-)$, $(\varphi_1, U_1^-) \times (\varphi_2, U_2^+)$, $(\varphi_1, U_1^-) \times (\varphi_2, U_2^-)$. They cover, respectively, the submanifolds $M^{+,+}$, $M^{+,-}$, $M^{-,+}$ and $M^{-,-}$.

On $M^{\varepsilon_1,\varepsilon_2}$, the symplectic form $\omega = -(R_1\omega_{\mathbb{S}_1^2} + R_2\omega_{\mathbb{S}_2^2})$ writes as

$$\omega = -\varepsilon_1 R_1 \frac{1}{\sqrt{1 - x_1^2 - y_1^2}} dx_1 \wedge dy_1 - \varepsilon_2 R_2 \frac{1}{\sqrt{1 - x_2^2 - y_2^2}} dx_2 \wedge dy_2.$$

And the functions $L$ and $H_t$ can be rewritten on $M^{\varepsilon_1,\varepsilon_2}$ as

$$\begin{cases} L(x_1, y_1, x_2, y_2) = & \varepsilon_1 R_1 \sqrt{1 - x_1^2 - y_1^2} + \varepsilon_2 R_2 \sqrt{1 - x_2^2 - y_2^2} \\ H_t(x_1, y_1, x_2, y_2) = & \varepsilon_1 (1 - t) \sqrt{1 - x_1^2 - y_1^2} + \\ & t \left( x_1 x_2 + y_1 y_2 + \varepsilon_1 \varepsilon_2 \sqrt{(1 - x_1^2 - y_1^2)(1 - x_2^2 - y_2^2)} \right) \end{cases}.$$

The union of $M^{0,0}$ and $M^{\varepsilon_1,\varepsilon_2}$ still does not cover the entire $M$, since

$$M \setminus \left( M^{0,0} \cup M^{\varepsilon_1,\varepsilon_2} \right) = \left( \{z_1 = 0\} \times \{(0, 0, \pm 1)\} \right) \cup \left( \{(0, 0, \pm 1)\} \times \{z_2 = 0\} \right).$$

Then, for completeness, we need a last set of charts to cover the whole $M = \mathbb{S}_1^2 \times \mathbb{S}_2^2$. The combination of a cylindrical chart $(\phi_i, U_i^0)$ in one $\mathbb{S}^2$ component and a Cartesian chart $(\varphi_i, U_i^{\varepsilon_j})$ in the other $\mathbb{S}^2$ component of $M$ will do the job.

**Definition 4.6.** *For $\varepsilon_2 \in \{+,-\}$, the* cylindrical-Cartesian chart *is the chart of $\mathbb{S}^2_1 \times \mathbb{S}^2_2$ of the form $(\phi_1, U^0_1) \times (\varphi_2, U^{\varepsilon_2}_2)$ in*

$$M^{0,\varepsilon_2} := U^0_1 \times U^{\varepsilon_2}_2 \subset \mathbb{S}^2_1 \times \mathbb{S}^2_2.$$

*The coordinates in this chart are $\theta_1, z_1, x_2, y_2$. For $\varepsilon_1 \in \{+,-\}$, the* Cartesian-cylindrical chart *is the chart of $\mathbb{S}^2_1 \times \mathbb{S}^2_2$ of the form $(\varphi_1, U^{\varepsilon_1}_1) \times (\phi_2, U^0_2)$ in*

$$M^{\varepsilon_1,0} := U^{\varepsilon_1}_1 \times U^0_2 \subset \mathbb{S}^2_1 \times \mathbb{S}^2_2.$$

*The coordinates in this chart are $x_1, y_1, \theta_2, z_2$.*

We illustrate the two cylindrical-Cartesian charts and the two Cartesian-cylindrical charts in Figure 4.5.

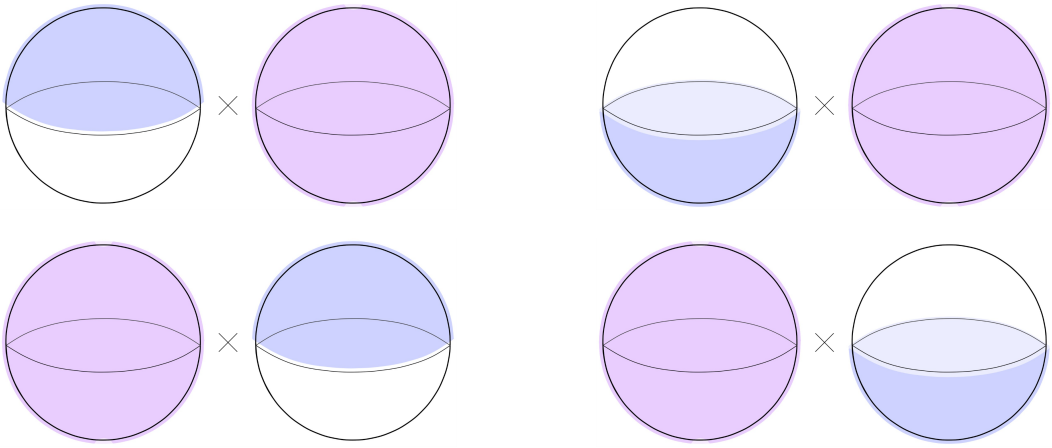

FIGURE 4.5: From left to right and from top to bottom, illustrations of the four charts $(\varphi_1, U^+_1) \times (\phi_2, U^0_2)$, $(\varphi_1, U^-_1) \times (\phi_2, U^0_2)$, $(\phi_1, U^0_1) \times (\varphi_2, U^+_2)$, $(\phi_1, U^0_1) \times (\varphi_2, U^-_2)\}$. They cover, respectively, the submanifolds $M^{+,0}$, $M^{-,0}$, $M^{0,+}$ and $M^{0,-}$.

On $M^{\varepsilon_1,0}$, in Cartesian-cylindrical coordinates $x_1, y_1, \theta_2, z_2$, the symplectic form $\omega = -(R_1\omega_{\mathbb{S}^2_1} + R_2\omega_{\mathbb{S}^2_2})$ writes as

$$\omega = -\varepsilon_1 R_1 \frac{1}{\sqrt{1 - x_1^2 - y_1^2}} dx_1 \wedge dy_1 - R_2\, d\theta_2 \wedge dz_2.$$

The functions $L$ and $H_t$ can be rewritten on $M^{\varepsilon_1,0}$ as

$$\begin{cases} L(x_1, y_1, \theta_2, z_2) = & \varepsilon_1 R_1 \sqrt{1 - x_1^2 - y_1^2} + R_2 z_2, \\ H_t(x_1, y_1, \theta_2, z_2) = & \varepsilon_1 (1-t)\sqrt{1 - x_1^2 - y_1^2} + \\ & t\left((x_1 \cos\theta_2 + y_1 \sin\theta_2)\sqrt{1 - z_2^2} + \varepsilon_1 \sqrt{1 - x_1^2 - y_1^2} z_2\right) \end{cases}.$$

On $M^{0,\varepsilon_2}$, in cylindrical-Cartesian coordinates $\theta_1, z_1, x_2, y_2$, the symplectic form $\omega = -(R_1\omega_{S_1^2} + R_2\omega_{S_2^2})$ writes as

$$\omega = -R_1\, d\theta_1 \wedge dz_1 - \varepsilon_2 R_2 \frac{1}{\sqrt{1-x_2^2-y_2^2}} dx_2 \wedge dy_2.$$

The functions $L$ and $H_t$ can be rewritten on $M^{0,\varepsilon_2}$ as

$$\begin{cases} L(\theta_1, z_1, x_2, y_2) = & R_1 z_1 + \varepsilon_2 R_2 \sqrt{1-x_2^2-y_2^2}, \\ H_t(\theta_1, z_1, x_2, y_2) = & (1-t)z_1 + \\ & t\left((x_2\cos\theta_1 + y_2\sin\theta_1)\sqrt{1-z_1^2} + \varepsilon_2\sqrt{1-x_2^2-y_2^2}\, z_1\right) \end{cases}.$$

Now, the collection of nine charts

$$\begin{gathered}(\phi_1, U_1^0)\times(\phi_2, U_2^0), (\varphi_1, U_1^+)\times(\varphi_2, U_2^+), (\varphi_1, U_1^+)\times(\varphi_2, U_2^-), \\ (\varphi_1, U_1^-)\times(\varphi_2, U_2^+), (\varphi_1, U_1^-)\times(\varphi_2, U_2^-), (\varphi_1, U_1^+)\times(\phi_2, U_2^0), \\ (\varphi_1, U_1^-)\times(\phi_2, U_2^0), (\phi_1, U_1^0)\times(\varphi_2, U_2^+), (\phi_1, U_1^0)\times(\varphi_2, U_2^-)\end{gathered}$$

covers $M = S_1^2 \times S_2^2$ and we can fully develop the study of Systems 1, 2 and 3.

### 4.2.2 Local analysis of the fixed points of the classical coupled angular momenta

One of our main objectives is to determine the nature of the singular points of the $b$-integrable systems 1, 2 and 3. To do so, we will take advantage of the fact that the non-degeneracy and the type of a singular point of an integrable system depend only on the local properties of the moment map components up to second order. Equivalently, at a fixed point of an integrable system $(M, \omega, (H, L))$, the operators $\omega$, $d^2L$ and $d^2H_t$ determine its type (see the classification of non-degenerate singular points in dimension 4 in Section 2.2.2 for details).

More precisely, we will use that there exist similarities between the local forms of $\omega$, $d^2L$ and $d^2H_t$ at the fixed points of the $b$-integrable systems 1, 2 and 3 and the local forms of the same operators at the fixed points of the classical coupled angular momenta. Since the latter ones are already classified in function of the parameters $t, R_1, R_2$ (see [LP19; ADH20]), using these similarities we will be able to characterize the former ones and to conclude about its type.

In the classical coupled angular momenta (see Definition 4.3), for any $t$, there are 4 fixed points at $p_{\pm,\pm} = (0, 0, \pm 1, 0, 0, \pm 1) \in S_1^2 \times S_2^2$. All of them are of elliptic-elliptic type for all values of $t$ except for the point $p_{+,-} = (0, 0, 1, 0, 0, -1)$, which is non-degenerate and of elliptic-elliptic type if $t < t^-$ or $t > t^+$, non-degenerate and of focus-focus type for $t^- < t < t^+$ and degenerate for $t \in \{t^-, t^+\}$, where

$$t^{\pm} = \frac{R_2}{2R_2 + R_1 \mp 2\sqrt{R_1 R_2}}.$$

Our purpose is to analyze the local expressions of the operators $\Omega$ (the matrix local form of $\omega$), $d^2L$, $d^2H_t$, $\Omega^{-1}d^2L$ and $\Omega^{-1}d^2H_t$ at the fixed points of the classical coupled angular momenta system, which are just the four double poles $p_{\pm,\pm}$.

For $\varepsilon_1\varepsilon_2 \in \{+,-\}$, the double pole $p_{\varepsilon_1,\varepsilon_2} = (0,0,\varepsilon_1 1),(0,0,\varepsilon_2 1)$ corresponds to the point $(0,0,0,0)$ in coordinates $x_1, y_1, x_2, y_2$ in the double Cartesian chart $(\varphi_1, U_1^{\varepsilon_1}) \times (\varphi_2, U_2^{\varepsilon_2})$ of $M^{\varepsilon_1,\varepsilon_2}$ (see Definition 4.5). Then, we will use the double Cartesian charts and take the combination of signs $\varepsilon_1, \varepsilon_2 \in \{+,-\}$ corresponding to each fixed point to compute the local expressions of the operators on $M^{\varepsilon_1,\varepsilon_2}$ at the fixed points.

Later in this section we will compute the local expressions of the same operators at the fixed points of System 1, 2 and 3 using the same coordinate charts. We will find out that they are similar, meaning that the nature of the corresponding fixed points in these systems is the same.

For $\varepsilon_1\varepsilon_2 \in \{+,-\}$, the symplectic form $\omega$ on $M^{\varepsilon_1,\varepsilon_2}$ writes as

$$\omega = -\varepsilon_1 R_1 \frac{1}{\sqrt{1-x_1^2-y_1^2}} dx_1 \wedge dy_1 - \varepsilon_2 R_2 \frac{1}{\sqrt{1-x_2^2-y_2^2}} dx_2 \wedge dy_2.$$

Then, the operator $\Omega$ at the double pole $p_{\varepsilon_1,\varepsilon_2}$ writes as

$$\Omega = \begin{pmatrix} 0 & -\varepsilon_1 R_1 & 0 & 0 \\ \varepsilon_1 R_1 & 0 & 0 & 0 \\ 0 & 0 & 0 & -\varepsilon_2 R_2 \\ 0 & 0 & \varepsilon_2 R_2 & 0 \end{pmatrix}$$

The expression of $L$ on $M^{\varepsilon_1,\varepsilon_2}$ is

$$L(x_1, y_1, x_2, y_2) = \varepsilon_1 R_1 \sqrt{1-x_1^2-y_1^2} + \varepsilon_2 R_2 \sqrt{1-x_2^2-y_2^2}$$

and the expression of $d^2L$ at $p_{\varepsilon_1,\varepsilon_2}$ is

$$d^2L = \begin{pmatrix} -\varepsilon_1 R_1 & 0 & 0 & 0 \\ 0 & -\varepsilon_1 R_1 & 0 & 0 \\ 0 & 0 & -\varepsilon_2 R_2 & 0 \\ 0 & 0 & 0 & -\varepsilon_2 R_2 \end{pmatrix}.$$

The expression of $H_t$ on $M^{\varepsilon_1,\varepsilon_2}$ is

$$\begin{aligned} H_t(x_1, y_1, x_2, y_2) =& \varepsilon_1(1-t)\sqrt{1-x_1^2-y_1^2} + \\ & t\left(x_1x_2 + y_1y_2 + \varepsilon_1\varepsilon_2\sqrt{(1-x_1^2-y_1^2)(1-x_2^2-y_2^2)}\right) \end{aligned}$$

and the expression of $d^2H_t$ at $p_{\varepsilon_1,\varepsilon_2}$ is

$$d^2H_t = \begin{pmatrix} \varepsilon_1(-1+t-\varepsilon_2 t) & 0 & t & 0 \\ 0 & \varepsilon_1(-1+t-\varepsilon_2 t) & 0 & t \\ t & 0 & -\varepsilon_1\varepsilon_2 t & 0 \\ 0 & t & 0 & -\varepsilon_1\varepsilon_2 t \end{pmatrix}.$$

For the details of the computations of the expressions of $d^2L$ and $d^2H_t$ at the four critical points $p_{\varepsilon_1,\varepsilon_2}$ see Section A.1 in Appendix A.

For any values of $t, \varepsilon_1, \varepsilon_2$ the matrices $d^2L$ and $d^2H_t$ are independent and give raise to the operators $A^0_L := \Omega^{-1}d^2L$ and $A^0_{H_t} := \Omega^{-1}d^2H_t$, which have the expressions:

$$A^0_L = \begin{pmatrix} 0 & -1 & 0 & 0 \\ 1 & 0 & 0 & 0 \\ 0 & 0 & 0 & -1 \\ 0 & 0 & 1 & 0 \end{pmatrix}, \qquad A^0_{H_t} = \begin{pmatrix} 0 & \frac{-\varepsilon_2 t+t-1}{R_1} & 0 & \frac{t}{\varepsilon_1 R_1} \\ -\frac{-\varepsilon_2 t+t-1}{R_1} & 0 & -\frac{t}{\varepsilon_1 R_1} & 0 \\ 0 & \frac{t}{\varepsilon_2 R_2} & 0 & -\frac{\varepsilon_1 t}{R_2} \\ -\frac{t}{\varepsilon_2 R_2} & 0 & \frac{\varepsilon_1 t}{R_2} & 0 \end{pmatrix},$$

where the superscript 0 just indicates that they correspond to the classical coupled angular momenta.

Now, following the procedure detailed in Section 2.2.2 to classify fixed points, we construct a new operator $A^0$ that, at any double pole $p_{\varepsilon_1,\varepsilon_2}$, will be conjugated to one of the four Cartan subalgebras of $\mathfrak{sp}(4,\mathbb{R})$ and will allow us to obtain its type (see Equation (2.2)). We define $A^0$ as the linear combination $A^0 := A^0_L + A^0_{H_t}$, which has the form

$$A^0 = \begin{pmatrix} 0 & \frac{-\varepsilon_2 t+t-1}{R_1} - 1 & 0 & \frac{t}{\varepsilon_1 R_1} \\ -\frac{-\varepsilon_2 t+t-1}{R_1} + 1 & 0 & -\frac{t}{\varepsilon_1 R_1} & 0 \\ 0 & \frac{t}{\varepsilon_2 R_2} & 0 & -\frac{\varepsilon_1 t}{R_2} - 1 \\ -\frac{t}{\varepsilon_2 R_2} & 0 & \frac{\varepsilon_1 t}{R_2} + 1 & 0 \end{pmatrix}.$$

At each one of the four double poles $p_{\varepsilon_1,\varepsilon_2}$, the expression of $A^0$ a is:

$$A^0_{p_{+,+}} = \begin{pmatrix} 0 & -\frac{1}{R_1} - 1 & 0 & \frac{t}{R_1} \\ \frac{1}{R_1} + 1 & 0 & -\frac{t}{R_1} & 0 \\ 0 & \frac{t}{R_2} & 0 & -\frac{t}{R_2} - 1 \\ -\frac{t}{R_2} & 0 & \frac{t}{R_2} + 1 & 0 \end{pmatrix}$$

$$A^0_{p_{+,-}} = \begin{pmatrix} 0 & \frac{2t-1}{R_1} - 1 & 0 & \frac{t}{R_1} \\ -\frac{2t-1}{R_1} + 1 & 0 & -\frac{t}{R_1} & 0 \\ 0 & -\frac{t}{R_2} & 0 & -\frac{t}{R_2} - 1 \\ \frac{t}{R_2} & 0 & \frac{t}{R_2} + 1 & 0 \end{pmatrix}$$

$$A^0_{p_{-,+}} = \begin{pmatrix} 0 & -\frac{1}{R_1} - 1 & 0 & -\frac{t}{R_1} \\ \frac{1}{R_1} + 1 & 0 & \frac{t}{R_1} & 0 \\ 0 & \frac{t}{R_2} & 0 & \frac{t}{R_2} - 1 \\ -\frac{t}{R_2} & 0 & -\frac{t}{R_2} + 1 & 0 \end{pmatrix}$$

$$A^0_{p_{-,-}} = \begin{pmatrix} 0 & \frac{2t-1}{R_1} - 1 & 0 & -\frac{t}{R_1} \\ -\frac{2t-1}{R_1} + 1 & 0 & \frac{t}{R_1} & 0 \\ 0 & -\frac{t}{R_2} & 0 & \frac{t}{R_2} - 1 \\ \frac{t}{R_2} & 0 & -\frac{t}{R_2} + 1 & 0 \end{pmatrix}$$

And their characteristic polynomials are, respectively:

$$\begin{aligned} P^0_{+,+}(\lambda) =& \lambda^4 + \left( \frac{1}{R_1^2} + \frac{2(t^2+R_2)}{R_1R_2} + \frac{t(t+2R_2)}{R_2^2} + 2 \right) \lambda^2 + \\ & \frac{(-t^2+tR_1+t+R_1R_2+R_2)^2}{R_1^2R_2^2} \\ P^0_{+,-}(\lambda) =& \lambda^4 + \left( \frac{(1-2t)^2}{R_1^2} + \frac{2(R_2-t^2-2tR_2)}{R_1R_2} + \frac{t(t+2R_2)}{R_2^2} + 2 \right) \lambda^2 + \\ & \frac{(-t^2+tR_1-2tR_2+t+R_1R_2+R_2)^2}{R_1^2R_2^2} \\ P^0_{-,+}(\lambda) =& \lambda^4 + \left( \frac{1}{R_1^2} + \frac{2(R_2-t^2)}{R_1R_2} + \frac{t(t-2R_2)}{R_2^2} + 2 \right) \lambda^2 + \\ & \frac{(t^2-tR_1-t+R_1R_2+R_2)^2}{R_1^2R_2^2} \\ P^0_{-,-}(\lambda) =& \lambda^4 + \left( \frac{(1-2t)^2}{R_1^2} + \frac{2(R_2+t^2-2tR_2)}{R_1R_2} + \frac{t(t-2R_2)}{R_2^2} + 2 \right) \lambda^2 + \\ & \frac{(-t^2+tR_1+2tR_2+t-R_1R_2-R_2)^2}{R_1^2R_2^2} \end{aligned}$$

By the works on the classification of the singular points of the coupled angular momenta by Le Floch and Pelayo [LP19], for any value of $t$ the matrices $A^0_{p_{+,+}}, A^0_{p_{-,+}}, A^0_{p_{-,-}}$ have two pairs of imaginary eigenvalues and this shows that the non-degenerate fixed points $p_{+,+}, p_{-,+}, p_{-,-}$ are of elliptic-elliptic type. However, the matrix $A^0_{p_{+,-}}$ has two pairs of imaginary eigenvalues for $0 \leq t < t^-$ or $1 \geq t > t^+$ or four paired complex conjugate eigenvalues for $t^- < t < t^+$, which shows that $p_{+,-}$ is non-degenerate of elliptic-elliptic type or of focus-focus type, respectively. Also, for $t \in \{t^-, t^+\}$, where

$$t^\pm = \frac{R_2}{2R_2 + R_1 \mp 2\sqrt{R_1R_2}},$$

the fixed point $p_{+,-}$ is degenerate.

### 4.2.3 Study of System 1

In this section we study System 1, prove that, for any value of $t$ it is a $b$-integrable system, classify its singular points and conclude that it is a $b$-semitoric family. We start giving its complete definition.

**Definition 4.7.** *Consider $M = \mathbb{S}^2_1 \times \mathbb{S}^2_2$ and take $Z = \{z_1 = 0\} \subset M$. Endow $(M, Z)$ with the b-symplectic form $\omega = -(R_1 \frac{1}{z_1} \omega_{\mathbb{S}^2_1} + R_2 \omega_{\mathbb{S}^2_2})$, where, for $i \in \{1, 2\}$, $\omega_{\mathbb{S}^2_i}$ is the*

*standard symplectic form on* $\mathbb{S}^2_i$ *and* $0 < R_1 < R_2$ *are constants. For* $i \in \{1,2\}$*, let* $x_i, y_i, z_i$ *be the Cartesian coordinates on the unit sphere* $\mathbb{S}^2_i$ *and introduce the parameter* $t \in [0,1]$*.*

System 1 *is the family of* 4*-dimensional systems* $(M, Z, \omega, F_t = (L, H_t))$ *parameterized by* $t$ *and defined by*

$$\begin{cases} L(x_1,y_1,z_1,x_2,y_2,z_2) := R_1 \log|z_1| + R_2 z_2 \\ H_t(x_1,y_1,z_1,x_2,y_2,z_2) := (1-t)z_1 + t(x_1x_2 + y_1y_2 + z_1z_2) \end{cases} . \tag{4.2}$$

With respect to the original coupled angular momenta system (see Definition 4.3), the changes introduced in System 1 are:

1. The choice of the hypersurface $Z = \{z_1 = 0\} \subset M$ where the $b$-symplectic form is singular.
2. The replacement of the $R_1 z_1$ term by the $R_1 \log|z_1|$ term in the $L$ component of the moment map.

We start proving that System 1 is a $b$-integrable system and then we analyze its singularities.

**Lemma 4.8.** *System 1 is a b-integrable system.*

*Proof.* We check that System 1, as introduced in Definition 4.7, satisfies the conditions of a $b$-integrable system (see Definition 2.31). That is, first, that the moment map differentials $dL$ and $dH_t$ are independent almost everywhere and, second, that $\{L, H_t\} = 0$ everywhere.

In the double cylindrical chart in $M^{0,0}$, $dL$ and $dH_t$ are expressed as:

$$\begin{cases} dL(\theta_1,z_1,\theta_2,z_2) & = R_1\frac{dz_1}{z_1} + R_2 dz_2 \\ dH_t(\theta_1,z_1,\theta_2,z_2) & = \left(z_1 - tz_1 + tz_1z_2 - t\frac{z_1^2}{\sqrt{1-z_1^2}}\sqrt{1-z_2^2}\cos(\theta_1-\theta_2)\right)\frac{dz_1}{z_1} \\ & \quad -t\sqrt{(1-z_1^2)(1-z_2^2)}\sin(\theta_1-\theta_2)d\theta_1 \\ & \quad +t\left(z_1 - \frac{z_2}{\sqrt{1-z_2^2}}\sqrt{1-z_1^2}\cos(\theta_1-\theta_2)\right)dz_2 \\ & \quad +t\sqrt{(1-z_1^2)(1-z_2^2)}\sin(\theta_1-\theta_2)d\theta_2 \end{cases} . \tag{4.3}$$

First, we prove that, for any value of $t$, the subset of points where $dL$ and $dH_t$ are not independent belongs to the union of two submanifolds of measure zero in $M$.

First, from Equation (4.3), we see that $dL$ does not vanish on $M^{0,0}$ and that the solution of $\mu dL + dH = 0$ in $M^{0,0}$ is a submanifold of $\{\theta_1 = \theta_2\} \cup \{\theta_1 = \theta_2 + \pi\} \subset M^{0,0}$, which is 3-dimensional and, hence, a zero-measure submanifold of $M$.

Second, the submanifold $M \setminus M^{0,0}$ of points which are not covered by the double cylindrical chart is the 2-dimensional submanifold $\left(\{(0,0,\pm 1)\} \times \mathbb{S}^2_2\right) \cup \left(\mathbb{S}^2_1 \times \{(0,0,\pm 1)\}\right)$, which is again of measure 0 in $M$.

Hence, $dL$ and $dH_t$ are independent almost everywhere in $M$.

Now we prove that $\{L, H_t\} = 0$ everywhere. The computation of $\{L, H_t\} = 0$ on $M^{0,0}$ yields:

$$\{L, H_t\} = X_L(H_t) =$$
$$\left(-\frac{\partial}{\partial\theta_1} - \frac{\partial}{\partial\theta_2}\right)\left((1-t)z_1 + t\left(\sqrt{(1-z_1^2)(1-z_2^2)}\cos(\theta_1-\theta_2) + z_1z_2\right)\right) =$$
$$t\sqrt{(1-z_1^2)(1-z_2^2)}\sin(\theta_1-\theta_2) - t\sqrt{(1-z_1^2)(1-z_2^2)}\sin(\theta_1-\theta_2) = 0.$$

Since $M \setminus M^{0,0}$ is of measure 0 in $M$, $\{L, H_t\}$ is equal to 0 almost everywhere in $M$. Then, by continuity of $\{L, H_t\}$ in $M$, for every value of $t$ it is constantly 0 on the entire manifold $M$. □

With the next lemma we prove that System 1 has a global symmetry that we can exploit later during the classification of singular points.

**Lemma 4.9.** *Let $\sigma : \mathbb{S}^2_1 \times \mathbb{S}^2_2 \to \mathbb{S}^2_1 \times \mathbb{S}^2_2$ act as the antipodal reflection in $\mathbb{S}^2_1$ and the identity in $\mathbb{S}^2_2$. Then System 1 has the global symmetry $(L, H_t) = (L, -H_t) \circ \sigma$.*

*Proof.* The map $\sigma$ satisfies the following relationship in double cylindrical coordinates

$$(L, H_t)(\theta_1, z_1, \theta_2, z_2) = (L, -H_t)(-\theta_1, z_1 + \pi, \theta_2, z_2).$$

Direct computation shows that

$$L(-\theta_1, z_1+\pi, \theta_2, z_2) = R_1 \log|-z_1| + R_2 z_2 = R_1 \log|z_1| + R_2 z_2 = L(\theta_1, z_1, \theta_2, z_2)$$

and that

$$\begin{aligned} H_t(-\theta_1, z_1+\pi, \theta_2, z_2) =& (1-t)(-z_1) + \\ & t\left(\sqrt{(1-(-z_1)^2)(1-z_2^2)}\cos(\theta_1+\pi-\theta_2) + (-z_1)z_2\right) \\ =& -(1-t)z_1 - t\left(\sqrt{(1-z_1^2)(1-z_2^2)}\cos(\theta_1-\theta_2) + z_1z_2\right) \\ =& -H_t(\theta_1, z_1, \theta_2, z_2) \end{aligned}$$

on $M^{0,0}$. By continuity of $L$ and $H_t$, this equality extends to $M$. □

Observe that the global symmetry of Lemma 4.9 can be written in Cartesian coordinates as $(L, H_t)(x_1, y_1, x_2, y_2) = (L, -H_t)(-x_1, -y_1, x_2, y_2)$. In this case, one has to take into account that if $(-x_1, -y_1, x_2, y_2)$ is covered by the double Cartesian chart $(\varphi_1, U_1^{\varepsilon_1}) \times (\varphi_2, U_2^{\varepsilon_2})$, then $(x_1, y_1, x_2, y_2)$ is covered by the double Cartesian chart $(\varphi_1, U_1^{-\varepsilon_1}) \times (\varphi_2, U_2^{\varepsilon_2})$.

**Corollary 4.10.** *Two points of the system $(L, H_t)$ in $M = \mathbb{S}^2_1 \times \mathbb{S}^2_2$ which are antipodal in $\mathbb{S}^2_1$ and have the same coordinates in $\mathbb{S}^2_2$ have the same rank, non-degeneracy and type.*

*Proof.* The local normal form of an integrable system $(f_1, \ldots, f_n)$ at a neighbourhood of a point is invariant under regular linear changes of the functions $f_1, \ldots, f_n$ (see

Bolsinov and Fomenko [BF04]). Since the rank, the non-degeneracy and the type of a point are determined by its local normal form, these features corresponding to a point $p \in \mathbb{S}^2_1 \times \mathbb{S}^2_2$ coincide with these same features of the point $\sigma(p) \in \mathbb{S}^2_1 \times \mathbb{S}^2_2$. □

We now identify and classify the fixed points of System 1.

**Proposition 4.11.** *System 1 has 4 fixed points. They are located at the double poles $p_{\pm,\pm} = ((0,0,\pm 1),(0,0,\pm 1)) \in \mathbb{S}^2_1 \times \mathbb{S}^2_2$. The fixed points $p_{+,+}$ and $p_{-,+}$ are non-degenerate of elliptic-elliptic type for all values of $t$. The fixed points $p_{+,-}$ and $p_{-,-}$ are non-degenerate and of elliptic-elliptic type if $t < t^-$ or $t > t^+$, non-degenerate and of focus-focus type if $t^- < t < t^+$, and degenerate if $t \in \{t^-, t^+\}$, where*

$$t^{\pm} = \frac{R_2}{2R_2 + R_1 \mp 2\sqrt{R_1 R_2}}.$$

*Proof.* The fixed points of the system correspond to the points in $M$ where the rank of $dF_t = (dL, dH_t)$ is 0, which coincide with the points where the Hamiltonian $b$-vector fields $X_L$ and $X_{H_t}$ vanish.

The expressions of the Hamiltonian $b$-vector field $X_L$ in the different charts reveal that, for any value of $t$, it does not vanish in $M^{0,0}$, $M^{\varepsilon_1,0}$ or $M^{0,\varepsilon_2}$. It only vanishes in $M^{\varepsilon_1,\varepsilon_2}$ at the four double poles $p_{\pm,\pm} = ((0,0,\pm 1),(0,0,\pm 1))$. On the other hand, the expression of the Hamiltonian $b$-vector field $X_{H_t}$ in $M^{0,0}$ shows that it vanishes on the submanifold $\{(\theta_1, z_1, \theta_2, z_2) \in M^{0,0} | z_1 = 0, z_2 = 0, \theta_1 = \theta_2 + k\pi\}$, where $k \in \{0,1\}$. In $M^{\varepsilon_1,0}$ and $M^{0,\varepsilon_2}$ it does not vanish and in $M^{\varepsilon_1,\varepsilon_2}$ it vanishes only at the four double poles $p_{\pm,\pm}$. For the complete expressions of $X_L$ and $X_{H_t}$ see Equations (A.5), (A.7), (A.11), (A.13) in Section A.2 in Appendix A.

Then, the Hamiltonian $b$-vector fields $X_L$ and $X_{H_t}$ vanish simultaneously only at the four double poles $p_{\pm,\pm} = ((0,0,\pm 1),(0,0,\pm 1)) \in \mathbb{S}^2_1 \times \mathbb{S}^2_2$, meaning that they are the only fixed points of the system.

To see that the four fixed points $p_{\pm,\pm}$ are non-degenerate and to determine its type, we find the local expression of the operators $\Omega$, $d^2L$ and $d^2H_t$ there. Each point $p_{\varepsilon_1,\varepsilon_2}$ corresponds to the point $(0,0,0,0)$ in coordinates $x_1, y_1, x_2, y_2$ in the double Cartesian chart $(\varphi_1, U_1^{\varepsilon_1}) \times (\varphi_2, U_2^{\varepsilon_2})$ of $M^{\varepsilon_1,\varepsilon_2}$. Then, we find the expressions of $\Omega$, $d^2L$ and $d^2H_t$ for the four critical points simultaneously by using the combination of signs $\varepsilon_1, \varepsilon_2 \in \{+,-\}$ corresponding to each of them, as in Section 4.2.2.

For $\varepsilon_1\varepsilon_2 \in \{+,-\}$, the $b$-symplectic form $\omega$ on $M^{\varepsilon_1,\varepsilon_2}$ writes as

$$\omega = -\frac{R_1}{1 - x_1^2 - y_1^2} dx_1 \wedge dy_1 - \varepsilon_2 \frac{R_2}{\sqrt{1 - x_2^2 - y_2^2}} dx_2 \wedge dy_2.$$

Then, the operator $\Omega$ at the double pole $p_{\varepsilon_1,\varepsilon_2}$ writes as

$$\Omega = \begin{pmatrix} 0 & -R_1 & 0 & 0 \\ R_1 & 0 & 0 & 0 \\ 0 & 0 & 0 & -\varepsilon_2 R_2 \\ 0 & 0 & \varepsilon_2 R_2 & 0 \end{pmatrix}$$

At a fixed double pole $p_{\varepsilon_1,\varepsilon_2}$ we obtain the following expression for $d^2L$:

$$d^2L = \begin{pmatrix} -R_1 & 0 & 0 & 0 \\ 0 & -R_1 & 0 & 0 \\ 0 & 0 & -\varepsilon_2 R_2 & 0 \\ 0 & 0 & 0 & -\varepsilon_2 R_2 \end{pmatrix}$$

and the following expression for $d^2H_t$:

$$d^2H_t = \begin{pmatrix} \varepsilon_1(-1+t-\varepsilon_2 t) & 0 & t & 0 \\ 0 & \varepsilon_1(-1+t-\varepsilon_2 t) & 0 & t \\ t & 0 & -\varepsilon_1\varepsilon_2 t & 0 \\ 0 & t & 0 & -\varepsilon_1\varepsilon_2 t \end{pmatrix}$$

For details on the computations of $d^2L$ and $d^2H_t$ see Equations (A.8) and (A.9) in Section A.2 in Appendix A.

For any values of $t, \varepsilon_1, \varepsilon_2$, the matrices $d^2L$ and $d^2H_t$ are independent and give raise to the operators $A^1_L := \Omega^{-1} d^2L$ and $A^1_{H_t} := \Omega^{-1} d^2H_t$, which have the expression:

$$A^1_L = \begin{pmatrix} 0 & -1 & 0 & 0 \\ 1 & 0 & 0 & 0 \\ 0 & 0 & 0 & -1 \\ 0 & 0 & 1 & 0 \end{pmatrix}, \qquad A^1_{H_t} = \begin{pmatrix} 0 & \frac{\varepsilon_1(-\varepsilon_2 t+t-1)}{R_1} & 0 & \frac{t}{R_1} \\ -\frac{\varepsilon_1(-\varepsilon_2 t+t-1)}{R_1} & 0 & -\frac{t}{R_1} & 0 \\ 0 & \frac{t}{\varepsilon_2 R_2} & 0 & -\frac{\varepsilon_1 t}{R_2} \\ -\frac{t}{\varepsilon_2 R_2} & 0 & \frac{\varepsilon_1 t}{R_2} & 0 \end{pmatrix}.$$

At a double pole $p_{\varepsilon_1,\varepsilon_2}$, the linear combination $A^1 := A^1_L + A^1_{H_t}$ has the form

$$A^1 = \begin{pmatrix} 0 & \frac{\varepsilon_1(-\varepsilon_2 t+t-1)}{R_1} - 1 & 0 & \frac{t}{R_1} \\ -\frac{\varepsilon_1(-\varepsilon_2 t+t-1)}{R_1} + 1 & 0 & -\frac{t}{R_1} & 0 \\ 0 & \frac{t}{\varepsilon_2 R_2} & 0 & -\frac{\varepsilon_1 t}{R_2} - 1 \\ -\frac{t}{\varepsilon_2 R_2} & 0 & \frac{\varepsilon_1 t}{R_2} + 1 & 0 \end{pmatrix}.$$

And, at each of the four poles $\{p_{+,+}, p_{+,-}, p_{-,+}, p_{-,-}\}$, $A^1$ has the following expression:

$$A^1_{p_{+,+}} = \begin{pmatrix} 0 & -\frac{1}{R_1} - 1 & 0 & \frac{t}{R_1} \\ \frac{1}{R_1} + 1 & 0 & -\frac{t}{R_1} & 0 \\ 0 & \frac{t}{R_2} & 0 & -\frac{t}{R_2} - 1 \\ -\frac{t}{R_2} & 0 & \frac{t}{R_2} + 1 & 0 \end{pmatrix}$$

$$A^1_{p_{+,-}} = \begin{pmatrix} 0 & \frac{2t-1}{R_1} - 1 & 0 & \frac{t}{R_1} \\ -\frac{2t-1}{R_1} + 1 & 0 & -\frac{t}{R_1} & 0 \\ 0 & -\frac{t}{R_2} & 0 & -\frac{t}{R_2} - 1 \\ \frac{t}{R_2} & 0 & \frac{t}{R_2} + 1 & 0 \end{pmatrix}$$

$$A^1_{p_{-,+}} = \begin{pmatrix} 0 & \frac{1}{R_1} - 1 & 0 & \frac{t}{R_1} \\ -\frac{1}{R_1} + 1 & 0 & -\frac{t}{R_1} & 0 \\ 0 & \frac{t}{R_2} & 0 & \frac{t}{R_2} - 1 \\ -\frac{t}{R_2} & 0 & -\frac{t}{R_2} + 1 & 0 \end{pmatrix}$$

$$A^1_{p_{-,-}} = \begin{pmatrix} 0 & -\frac{2t-1}{R_1} - 1 & 0 & \frac{t}{R_1} \\ \frac{2t-1}{R_1} + 1 & 0 & -\frac{t}{R_1} & 0 \\ 0 & -\frac{t}{R_2} & 0 & \frac{t}{R_2} - 1 \\ \frac{t}{R_2} & 0 & -\frac{t}{R_2} + 1 & 0 \end{pmatrix}$$

Observe that $A^1_{p_{+,+}}$ is equal to $A^0_{p_{+,+}}$ from Section 4.2.2. Then, for all values of $t$, $p_{+,+}$ is also a non-degenerate fixed point of elliptic-elliptic type in this system. Similarly, since $A^1_{p_{+,-}}$ is equal to $A^0_{p_{+,-}}$, the fixed point $p_{+,-}$ is non-degenerate and of elliptic-elliptic type if $t < t^-$ or $t > t^+$, of focus-focus type for $t^- < t < t^+$ and degenerate for $t \in \{t^-, t^+\}$, where

$$t^\pm = \frac{R_2}{2R_2 + R_1 \mp 2\sqrt{R_1 R_2}}.$$

On the other hand, by Corollary 4.10, since $p_{-,+}$ is symmetric to $p_{+,+}$, it is of the same type, so it is a non-degenerate fixed point of elliptic-elliptic type. Similarly, $p_{-,-}$ is symmetric to $p_{+,-}$, so it is non-degenerate and of elliptic-elliptic type if $t < t^-$ or $t > t^+$, of focus-focus type if $t^- < t < t^+$ and degenerate if $t \in \{t^-, t^+\}$. □

After classifying the four fixed points of System 1, we obtain their images by the moment map $F_t = (L, H_t)$:

- $F_t(p_{+,+}) = (R_2, 1)$,
- $F_t(p_{+,-}) = (-R_2, 1 - 2t)$,
- $F_t(p_{-,+}) = (R_2, -1)$,
- $F_t(p_{-,-}) = (-R_2, -1 + 2t)$.

Next, we identify and classify the singular points of rank 1 of System 1.

**Proposition 4.12.** *All the singular points of rank* 1 *of System 1 are:*

- *If* $t = 0$, *the union of*

$$\{(0, 0, \pm 1)\} \times \left(\mathbb{S}^2_2 \setminus \{(0, 0, \pm 1)\}\right)$$

*and*

$$\left(\mathbb{S}^2_1 \setminus \{(0, 0, \pm 1)\}\right) \times \{(0, 0, \pm 1)\}.$$

- *If* $t \neq 0$, *the union of* $\{(\theta_1, z_1, \theta_2, z_2) \in \mathbb{S}^2_1 \times \mathbb{S}^2_2\}$ *such that* $\theta_2 = \theta_1$ *and*

$$\frac{R_1}{R_2}\left(\frac{z_2}{\sqrt{1 - z_2^2}}\sqrt{1 - z_1^2} - z_1\right) = -\frac{1 - t}{t} z_1 + \frac{z_1^2}{\sqrt{1 - z_1^2}}\sqrt{1 - z_2^2} - z_1 z_2,$$

*and* $\{(\theta_1, z_1, \theta_2, z_2) \in \mathbb{S}^2_1 \times \mathbb{S}^2_2\}$ *such that* $\theta_2 = \theta_1 + \pi$ *and*

$$\frac{R_1}{R_2}\left(\frac{z_2}{\sqrt{1-z_2^2}}\sqrt{1-z_1^2} - z_1\right) = \frac{1-t}{t}z_1 + \frac{z_1^2}{\sqrt{1-z_1^2}}\sqrt{1-z_2^2} - z_1 z_2.$$

*All of them are of elliptic regular type.*

*Proof.* At the singular points of rank 1 the joint flow of the Hamiltonian $b$-vector fields $X_L$ and $X_{H_t}$ generates a 1-dimensional orbit. Then, at these points either only one of them vanishes or we have $\mu X_L = X_{H_t}$ for some constant $\mu \neq 0$.

In the proof of Proposition 4.11 we saw that first case only happens on the submanifold $\{(\theta_1, z_1, \theta_2, z_2) \in M^{0,0} | z_1 = 0, z_2 = 0, \theta_1 = \theta_2 + k\pi, k \in \{0, 1\}\}$, where $X_{H_t}$ vanishes but $X_L$ does not. Then, we just have to look for the points where the second case happens, that is, the points where we have $\mu X_L = X_{H_t}$ with $\mu \neq 0$.

Observe that $X_L$ generates a simultaneous rotation of the two components of $M = \mathbb{S}^2_1 \times \mathbb{S}^2_2$ around their respective vertical axis and at the same speed. Then, the points satisfying $\mu X_L = X_{H_t}$ correspond to points where $X_{H_t}$ generates the same kind of coupled rotation.

If $t = 0$, there is no solution of $\mu X_L = X_{H_t}$, with $\mu \neq 0$, in $M^{0,0}$ (see Equation (A.5)). However, for $\varepsilon_1, \varepsilon_2 \in \{+, -\}$, all the points of the form $(0, 0, \theta_2, z_2)$ satisfy $\mu X_L = X_{H_t}$ in $M^{\varepsilon_1,0}$ (see Equation (A.11)) and all the points of the form $(\theta_1, z_1, 0, 0)$ satisfy $\mu X_L = X_{H_t}$ in $M^{0,\varepsilon_2}$ (see Equation (A.13)). Then, for $t = 0$, the singular points of rank 1 are all the points in $\mathbb{S}^2_1 \times \mathbb{S}^2_2$ that project to a pole in only one of the two sphere components, which is just the union of $\{(0, 0, \pm 1)\} \times \left(\mathbb{S}^2_2 \setminus \{(0, 0, \pm 1)\}\right)$ and $\left(\mathbb{S}^2_1 \setminus \{(0, 0, \pm 1)\}\right) \times \{(0, 0, \pm 1)\}$.

If $t \neq 0$ we see that there are solutions of $\mu X_L = X_{H_t}$, with $\mu \neq 0$, in $M^{0,0}$. Indeed, in Equation (A.5) the condition $\mu X_L = X_{H_t}$ implies, in $M^{0,0}$ and in coordinates $\theta_1, z_1, \theta_2, z_2$, that $\sin(\theta_1 - \theta_2) = 0$. Then, either

- $\theta_1 = \theta_2$, or
- $\theta_1 = \theta_2 + \pi$.

If $\theta_1 = \theta_2$, the condition $\mu X_L = X_{H_t}$ on Equation (A.5) implies that

$$\frac{R_1}{R_2}\left(\frac{z_2}{\sqrt{1-z_2^2}}\sqrt{1-z_1^2} - z_1\right) = -\frac{1-t}{t}z_1 + \frac{z_1^2}{\sqrt{1-z_1^2}}\sqrt{1-z_2^2} - z_1 z_2 \tag{4.4}$$

If $\theta_1 = \theta_2 + \pi$, the condition $\mu X_L = X_{H_t}$ on Equation (A.5) implies that

$$\frac{R_1}{R_2}\left(\frac{z_2}{\sqrt{1-z_2^2}}\sqrt{1-z_1^2} - z_1\right) = \frac{1-t}{t}z_1 + \frac{z_1^2}{\sqrt{1-z_1^2}}\sqrt{1-z_2^2} - z_1 z_2 \tag{4.5}$$

Notice that the solutions of $\mu X_L = X_{H_t}$ with $\mu = 0$ are precisely the submanifold $\{(\theta_1, z_1, \theta_2, z_2) \in M^{0,0} | z_1 = 0, z_2 = 0, \theta_1 = \theta_2 + k\pi, k \in \{0, 1\}\}$ that we already identified as points of rank 1 where $X_{H_t}$ vanishes but $X_L$ does not.

Then, if $t \neq 0$, there are two 2-dimensional submanifolds of points of rank 1 in $M^{0,0}$. One of them is given by

$$\{(\theta_1, z_1, \theta_2, z_2) | \theta_2 = \theta_1, z_1 \text{ and } z_2 \text{ solve Equation } (4.4)\},$$

and the other one is given by

$$\{(\theta_1, z_1, \theta_2, z_2) | \theta_2 = \theta_1 + \pi, z_1 \text{ and } z_2 \text{ solve Equation } (4.5)\}.$$

From Equations (A.5), (A.11), (A.13), we see that, when $t \neq 0$, there are no other solutions of $\mu X_L = X_{H_t}$, with $\mu \neq 0$, in $M \setminus M^{0,0}$.

It is clear from the expression of the Hamiltonian $b$-vector fields, especially in the double cylindrical chart (see Equations (A.5), (A.7), (A.11) and (A.13)), that at the singular points of rank 1 of the system the Hamiltonian $b$-vector fields generate the $\mathbb{S}^1$ orbit corresponding to a coupled rotation around the vertical axis of the two sphere components of $M = \mathbb{S}^2_1 \times \mathbb{S}^2_2$. Then, all of them are of elliptic-regular type. □

Observe that the moment map $F_t = (L, H_t)$ depends only on $z_1$, $z_2$ and $\theta_1 - \theta_2$ on $M^{0,0}$ (see Equation (A.4)). Since $\theta_1 - \theta_2$ is constant in any connected component of the submanifold of singular points of rank 1, the images of these components by $(L, H_t)$ are parameterized by $z_1$ and $z_2$. At their turn, $z_1$ and $z_2$ are related either by Equation (4.4) or by Equation (4.5) in the submanifold of points of rank 1, making both $L$ and $H_t$ depend on only one parameter on this submanifold. Then, the images by $(L, H_t)$ of the submanifold of points of rank 1 of System 1 are 1-dimensional curves in $\mathbb{R}^2$.

After identifying the singular points of rank 0 and 1 of System 1 and their images by the moment map, we can describe the entire image of the moment map $F_t = (L, H_t)$ of the system. In Figure 4.6 we obtain the complete image of $F_t = (L, H_t)$ with a numerical approach. There, we use the parameters $R_1 = 1, R_2 = 2$ and different values of $t$ between 0 and 1.

In Figure 4.6, the image of the submanifold $\{z_1 > 0\} \times \mathbb{S}^2_2$ is depicted in sky blue and the image of the submanifold $\{z_1 < 0\} \times \mathbb{S}^2_2$ is depicted in yellow. The boundary of the sky blue region corresponds to the image of the singular points of rank 1 in $\{z_1 > 0\} \times \mathbb{S}^2_2$, while the boundary of the yellow region corresponds to the image of the singular points of rank 1 in $\{z_1 < 0\} \times \mathbb{S}^2_2$. The images of the four fixed points $p_{+,+}, p_{+,-}, p_{-,+}, p_{-,-}$ are depicted, respectively, in red, black, magenta and blue in Figure 4.6.

We proved in Proposition 4.11 that $p_{+,+}$ and $p_{-,+}$ are non-degenerate of elliptic-elliptic type for all values of $t$ and, therefore, lie in the vertex on the image of the moment map. Indeed, for every value of $t$, their images, depicted in red and magenta, correspond to a vertex of the image of the moment map.

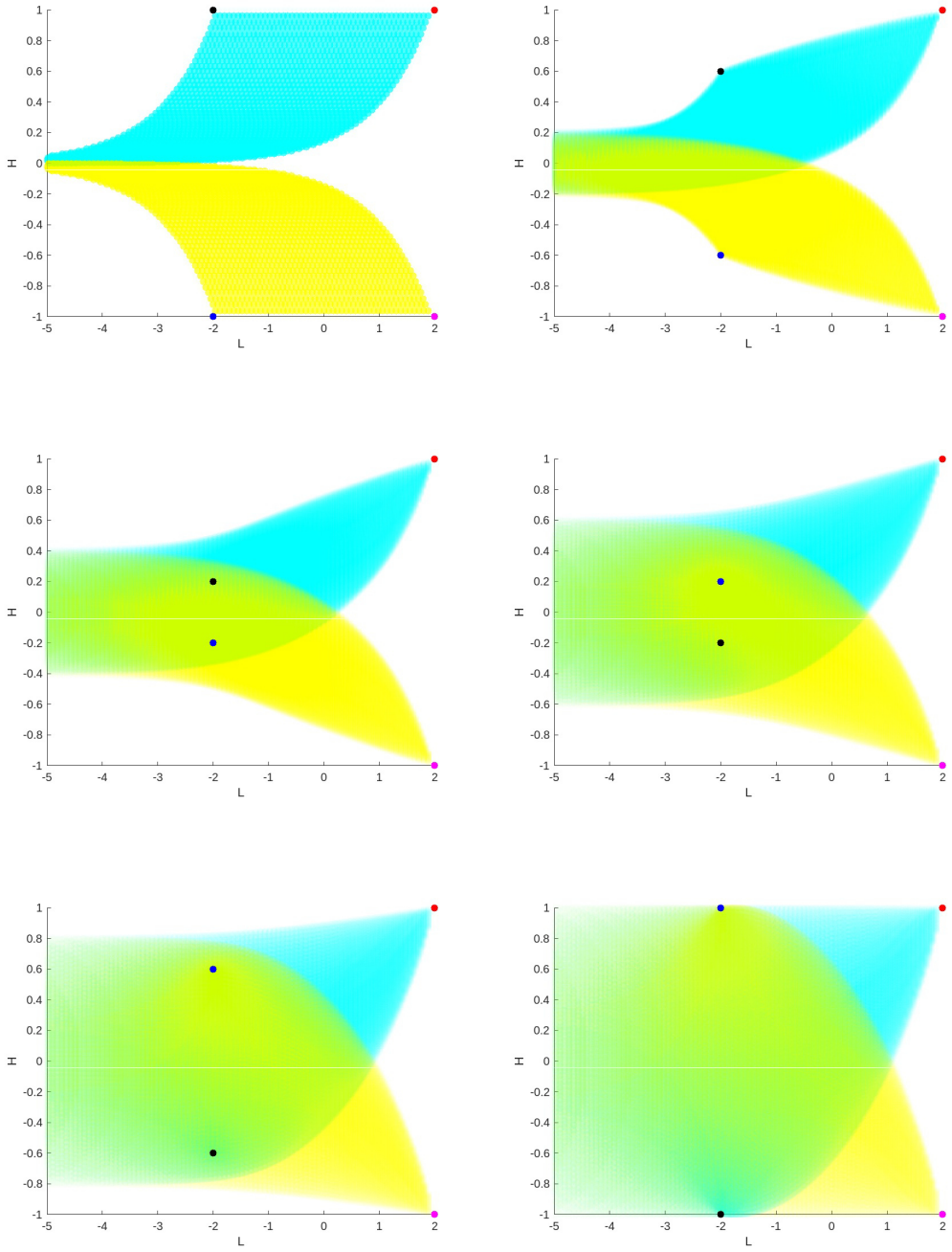


FIGURE 4.6: Image of the moment map $F_t = (L, H_t)$ of System 1 for $R_1 = 1, R_2 = 2$ and values of $t$ between 0 (top left) and 1 (bottom right) by intervals of 0.2. It has been obtained numerically, see the code in Section B.1.2 in Appendix B. In sky blue, the image of the submanifold $\{z_1 > 0\} \times \mathbb{S}^2_2$. In yellow, the image of the submanifold $\{z_1 < 0\} \times \mathbb{S}^2_2$. The images of the four fixed points $p_{+,+}, p_{+,-}, p_{-,+}, p_{-,-}$ are depicted, respectively, in red, black, magenta and blue.

On the other hand, in Proposition 4.11 we proved that $p_{+,-}$ and $p_{-,-}$ are non-degenerate and of elliptic-elliptic type if $t < t^-$ or $t > t^+$, non-degenerate and of

focus-focus type if $t^- < t < t^+$, and degenerate if $t \in \{t^-, t^+\}$, where

$$t^{\pm} = \frac{R_2}{2R_2 + R_1 \mp 2\sqrt{R_1 R_2}}.$$

For the particular case of $R_1 = 1, R_2 = 2$, we have

$$t^- \simeq 0.255479161794566, \qquad t^+ \simeq 0.920991426440728.$$

Indeed, for $t \in \{0, 0.2, 1\}$, the images of $p_{+,-}$ and $p_{-,-}$, depicted in black and blue, correspond to a vertex of the image of the moment map, while, for $t \in \subset \{0.4, 0.6, 0.8\}$, they correspond to interior points of the image of the moment map.

The study of the singular points of System 1 carried out in this section allows us to conclude that it is a *b*-semitoric family.

**Corollary 4.13** (Brugués-Hohloch-Mir-Miranda [Bru+23])**.** *System 1 is a b-semitoric family.*

*Proof.* By Lemma 4.8, for any value of $t$ System 1 is a 4-dimensional *b*-integrable system. We check that it also satisfies the requirements of a *b*-semitoric family (see Definitions 4.1 and 4.2).

First, the map $L : M \to \mathbb{R}$ is proper because $M = \mathbb{S}^2_1 \times \mathbb{S}^2_2$ is compact. Second, in $M^{0,0}$, the Hamiltonian *b*-vector field $X_L$ has the expression

$$X_L = -\frac{\partial}{\partial \theta_1} - \frac{\partial}{\partial \theta_2},$$

and, hence, its flow is $2\pi$-periodic almost everywhere in $M$. Finally, by Propositions 4.11 and 4.12, all singular points of $F_t = (L, H_t)$ are non-degenerate (except for the degenerate times $t^-, t^+$) and do not include components of hyperbolic type. □

Note that the image of the moment map of a *b*-semitoric system is not necessarily convex. This also true for semitoric systems, as it can be seen in the example of the Hirzeburg surface in the work of Le Floch and Palmer [LP18]).

### 4.2.4 Study of System 2

In this section we proceed to study System 2 with the same techniques. We prove that it is a *b*-integrable system for all values of $t$, classify its singular points and conclude that it is a *b*-semitoric family. Its complete definition is the following.

**Definition 4.14.** *Consider $M = \mathbb{S}^2_1 \times \mathbb{S}^2_2$ and take $Z = \{z_1 = 0\} \subset M$. Endow $(M, Z)$ with the b-symplectic form $\omega = -(R_1 \frac{1}{z_1} \omega_{\mathbb{S}^2_1} + R_2 \omega_{\mathbb{S}^2_2})$, where, for $i \in \{1, 2\}$, $\omega_{\mathbb{S}^2_i}$ is the standard symplectic form on $\mathbb{S}^2_i$ and $0 < R_1 < R_2$ are constants. For $i \in \{1, 2\}$, let $x_i, y_i, z_i$ be the Cartesian coordinates on the unit sphere $\mathbb{S}^2_i$ and introduce the parameter $t \in [0, 1]$.*

System 2 *is the family of* 4*-dimensional systems* $(M, Z, \omega, F_t = (L, H_t))$ *parameterized by* $t$ *and defined by*

$$\begin{cases} L(x_1, y_1, z_1, x_2, y_2, z_2) := R_1 \log|z_1| + R_2 z_2 \\ H_t(x_1, y_1, z_1, x_2, y_2, z_2) := (1-t)\log|z_1| + t(x_1x_2 + y_1y_2 + z_1z_2) \end{cases}. \tag{4.6}$$

With respect to the original coupled angular momenta system (see Definition 4.3), the changes introduced in System 2 are:

1. The choice of the hypersurface $Z = \{z_1 = 0\} \subset M$ where the $b$-symplectic form is singular.
2. The replacement of the $R_1 z_1$ term by the $R_1 \log|z_1|$ term in the $L$ component of the moment map.
3. The replacement of the $(1-t)z_1$ term by the $(1-t)\log|z_1|$ term in the $H_t$ component of the moment map.

With respect to System 1, the only change is replacement of the $(1-t)z_1$ term by the $(1-t)\log|z_1|$ term in the $H_t$ component of the moment map.

We first prove that System 2 is a $b$-integrable system.

**Lemma 4.15.** *System 2 is a b-integrable system.*

*Proof.* We prove that in System 2, as introduced in Definition 4.14, the differentials $dL$ and $dH_t$ are independent almost everywhere and $\{L, H_t\} = 0$ everywhere.

In the double cylindrical chart in $M^{0,0}$, the expressions of $dL$ and $dH_t$ are:

$$\begin{cases} dL(\theta_1, z_1, \theta_2, z_2) & = R_1 \frac{dz_1}{z_1} + R_2 dz_2 \\ dH_t(\theta_1, z_1, \theta_2, z_2) & = \left(1 - t + tz_1z_2 - t\frac{z_1^2}{\sqrt{1-z_1^2}}\sqrt{1-z_2^2}\cos(\theta_1-\theta_2)\right)\frac{dz_1}{z_1} \\ & \quad -t\sqrt{(1-z_1^2)(1-z_2^2)}\sin(\theta_1-\theta_2)d\theta_1 \\ & \quad +t\left(z_1 - \frac{z_2}{\sqrt{1-z_2^2}}\sqrt{1-z_1^2}\cos(\theta_1-\theta_2)\right)dz_2 \\ & \quad +t\sqrt{(1-z_1^2)(1-z_2^2)}\sin(\theta_1-\theta_2)d\theta_2 \end{cases}. \tag{4.7}$$

For any value of $t$, the set of points where $dL$ and $dH_t$ are not independent belongs to the union of two submanifolds of measure zero in $M$. These two submanifolds are the following:

1. $\{\theta_1 = \theta_2\} \cup \{\theta_1 = \theta_2 + \pi\} \subset M^{0,0}$, which is the 3-dimensional submanifold of $M$ where the solutions of $\mu dL + dH = 0$ in $M^{0,0}$ must belong to (see Equation (4.7)).
2. $M \setminus M^{0,0}$, which is the 2-dimensional submanifold of $M$ which is not covered by the double cylindrical chart in which $\mu dL + dH = 0$ is written in Equation (4.7).

Hence, $dL$ and $dH_t$ are independent almost everywhere in $M$.

Now, we compute $\{L, H_t\}$ on $M^{0,0}$ and we obtain:

$$\{L, H_t\} = X_L(H_t) =$$
$$\left(-\frac{\partial}{\partial\theta_1} - \frac{\partial}{\partial\theta_2}\right)\left((1-t)\log|z_1| + t\left(\sqrt{(1-z_1^2)(1-z_2^2)}\cos(\theta_1-\theta_2) + z_1z_2\right)\right) =$$
$$t\sqrt{(1-z_1^2)(1-z_2^2)}\sin(\theta_1-\theta_2) - t\sqrt{(1-z_1^2)(1-z_2^2)}\sin(\theta_1-\theta_2) = 0.$$

Since $M \setminus M^{0,0}$ is of measure 0 in $M$, we conclude that, for any value of $t$, $\{L, H_t\} = 0$ almost everywhere in $M$ and, by continuity of $\{L, H_t\}$ also in the entire $M$. □

Next, we identify and classify the fixed points of System 2.

**Proposition 4.16.** *System 2 has* 4 *fixed points. They are located at the double poles* $p_{\pm,\pm} = ((0,0,\pm1),(0,0,\pm1)) \in \mathbb{S}^2_1 \times \mathbb{S}^2_2$. *The fixed points* $p_{+,+}$, $p_{-,+}$ *and* $p_{-,-}$ *are non-degenerate of elliptic-elliptic type for all values of* $t$. *The fixed point* $p_{+,-}$ *is non-degenerate and of elliptic-elliptic type if* $t < t^-$ *or* $t > t^+$, *of focus-focus type if* $t^- < t < t^+$ *and degenerate if* $t \in \{t^-, t^+\}$, *where*

$$t^{\pm} = \frac{R_2}{2R_2 + R_1 \mp 2\sqrt{R_1R_2}}.$$

*Proof.* To find the fixed points of System 2, we look for the points where the Hamiltonian $b$-vector fields $X_L$ and $X_{H_t}$ vanish. Their expressions in the different charts (see equations (A.15), (A.17), (A.21), (A.23) in Section A.3 in Appendix A) show that:

- for any value of $t$, $X_L$ it does not vanish in $M^{0,0}$, $M^{\varepsilon_1,0}$ or $M^{0,\varepsilon_2}$, and only vanishes in $M^{\varepsilon_1,\varepsilon_2}$ at the four double poles $p_{\pm,\pm} = ((0,0,\pm1),(0,0,\pm1))$, and
- for $t = 0$, $X_{H_t}$ vanishes on $\{(0,0,\pm1)\} \times \mathbb{S}^2_2$, and for $t \neq 0$, $X_{H_t}$ vanishes only at the four double poles $p_{\pm,\pm}$.

Then, the Hamiltonian $b$-vector fields $X_L$ and $X_{H_t}$ only vanish simultaneously at the four double poles $p_{\pm,\pm} = ((0,0,\pm1),(0,0,\pm1)) \in \mathbb{S}^2_1 \times \mathbb{S}^2_2$, which are therefore the only fixed points of the system.

To classify the four fixed points $p_{\pm,\pm}$, we find the local expression of the operators $\Omega$, $d^2L$ and $d^2H_t$ there. Each point $p_{\varepsilon_1,\varepsilon_2}$ corresponds to the point $(0,0,0,0)$ in coordinates $x_1, y_1, x_2, y_2$ in the double Cartesian chart $(\varphi_1, U_1^{\varepsilon_1}) \times (\varphi_2, U_2^{\varepsilon_2})$ of $M^{\varepsilon_1,\varepsilon_2}$. Then, we find the expressions of $\Omega$, $d^2L$ and $d^2H_t$ for the four critical points simultaneously by using the combination of signs $\varepsilon_1, \varepsilon_2 \in \{+,-\}$ that corresponds to each of them, as we did in Section 4.2.2.

For $\varepsilon_1\varepsilon_2 \in \{+,-\}$, the $b$-symplectic form $\omega$ on $M^{\varepsilon_1,\varepsilon_2}$ writes as

$$\omega = -\frac{R_1}{1-x_1^2-y_1^2}dx_1 \wedge dy_1 - \varepsilon_2\frac{R_2}{\sqrt{1-x_2^2-y_2^2}}dx_2 \wedge dy_2.$$

Then, the operator $\Omega$ at the double pole $p_{\varepsilon_1,\varepsilon_2}$ writes as

$$\Omega = \begin{pmatrix} 0 & -R_1 & 0 & 0 \\ R_1 & 0 & 0 & 0 \\ 0 & 0 & 0 & -\varepsilon_2 R_2 \\ 0 & 0 & \varepsilon_2 R_2 & 0 \end{pmatrix}$$

At a fixed double pole $p_{\varepsilon_1,\varepsilon_2}$ we obtain the following expression for $d^2L$:

$$d^2L = \begin{pmatrix} -R_1 & 0 & 0 & 0 \\ 0 & -R_1 & 0 & 0 \\ 0 & 0 & -\varepsilon_2 R_2 & 0 \\ 0 & 0 & 0 & -\varepsilon_2 R_2 \end{pmatrix}$$

and the following expression for $d^2H_t$:

$$d^2H_t = \begin{pmatrix} -1+t-\varepsilon_1\varepsilon_2 t & 0 & t & 0 \\ 0 & -1+t-\varepsilon_1\varepsilon_2 t & 0 & t \\ t & 0 & -\varepsilon_1\varepsilon_2 t & 0 \\ 0 & t & 0 & -\varepsilon_1\varepsilon_2 t \end{pmatrix}$$

For details on the computations of $d^2L$ and $d^2H_t$ see Equations (A.18) and (A.19) in Section A.3 in Appendix A.

For any values of $t, \varepsilon_1, \varepsilon_2$, the matrices $d^2L$ and $d^2H_t$ are independent and give raise to the operators $A^2_L := \Omega^{-1}d^2L$ and $A^2_{H_t} := \Omega^{-1}d^2H_t$, which have the expression:

$$A^2_L = \begin{pmatrix} 0 & -1 & 0 & 0 \\ 1 & 0 & 0 & 0 \\ 0 & 0 & 0 & -1 \\ 0 & 0 & 1 & 0 \end{pmatrix}, \qquad A^2_{H_t} = \begin{pmatrix} 0 & \frac{-\varepsilon_1\varepsilon_2 t+t-1}{R_1} & 0 & \frac{t}{R_1} \\ -\frac{-\varepsilon_1\varepsilon_2 t+t-1}{R_1} & 0 & -\frac{t}{R_1} & 0 \\ 0 & \frac{t}{\varepsilon_2 R_2} & 0 & -\frac{\varepsilon_1 t}{R_2} \\ -\frac{t}{\varepsilon_2 R_2} & 0 & \frac{\varepsilon_1 t}{R_2} & 0 \end{pmatrix}.$$

At a double pole $p_{\varepsilon_1,\varepsilon_2}$, the linear combination $A^2 := A^2_L + A^2_{H_t}$ has the form

$$A^2 = \begin{pmatrix} 0 & \frac{-\varepsilon_1\varepsilon_2 t+t-1}{R_1} - 1 & 0 & \frac{t}{R_1} \\ -\frac{-\varepsilon_1\varepsilon_2 t+t-1}{R_1} + 1 & 0 & -\frac{t}{R_1} & 0 \\ 0 & \frac{t}{\varepsilon_2 R_2} & 0 & -\frac{\varepsilon_1 t}{R_2} - 1 \\ -\frac{t}{\varepsilon_2 R_2} & 0 & \frac{\varepsilon_1 t}{R_2} + 1 & 0 \end{pmatrix}.$$

And, at each of the four poles $\{p_{+,+}, p_{+,-}, p_{-,+}, p_{-,-}\}$, $A^2$ has the following expression:

$$A^2_{p_{+,+}} = \begin{pmatrix} 0 & -\frac{1}{R_1} - 1 & 0 & \frac{t}{R_1} \\ \frac{1}{R_1} + 1 & 0 & -\frac{t}{R_1} & 0 \\ 0 & \frac{t}{R_2} & 0 & -\frac{t}{R_2} - 1 \\ -\frac{t}{R_2} & 0 & \frac{t}{R_2} + 1 & 0 \end{pmatrix}$$

$$A^2_{p_{+,-}} = \begin{pmatrix} 0 & \frac{2t-1}{R_1} - 1 & 0 & \frac{t}{R_1} \\ -\frac{2t-1}{R_1} + 1 & 0 & -\frac{t}{R_1} & 0 \\ 0 & -\frac{t}{R_2} & 0 & -\frac{t}{R_2} - 1 \\ \frac{t}{R_2} & 0 & \frac{t}{R_2} + 1 & 0 \end{pmatrix}$$

$$A^2_{p_{-,+}} = \begin{pmatrix} 0 & \frac{2t-1}{R_1} - 1 & 0 & \frac{t}{R_1} \\ -\frac{2t-1}{R_1} + 1 & 0 & -\frac{t}{R_1} & 0 \\ 0 & \frac{t}{R_2} & 0 & \frac{t}{R_2} - 1 \\ -\frac{t}{R_2} & 0 & -\frac{t}{R_2} + 1 & 0 \end{pmatrix}$$

$$A^2_{p_{-,-}} = \begin{pmatrix} 0 & -\frac{1}{R_1} - 1 & 0 & \frac{t}{R_1} \\ \frac{1}{R_1} + 1 & 0 & -\frac{t}{R_1} & 0 \\ 0 & -\frac{t}{R_2} & 0 & \frac{t}{R_2} - 1 \\ \frac{t}{R_2} & 0 & -\frac{t}{R_2} + 1 & 0 \end{pmatrix}$$

Since $A^2_{p_{+,+}}$ is identical to $A^0_{p_{+,+}}$ from Section 4.2.2, $p_{+,+}$ is non-degenerate of elliptic-elliptic type for all values of $t$. Similarly, since $A^2_{p_{+,-}}$ is identical to $A^0_{p_{+,-}}$, $p_{+,-}$ is non-degenerate and of elliptic-elliptic type if $t < t^-$ or $t > t^+$, of focus-focus type if $t^- < t < t^+$ and degenerate if $t \in \{t^-, t^+\}$, where

$$t^{\pm} = \frac{R_2}{2R_2 + R_1 \mp 2\sqrt{R_1 R_2}}.$$

On the other hand, by direct computation one can see that the characteristic polynomial of $A^2_{p_{-,+}}$ coincides with $P^0_{-,-}(\lambda)$ defined in Section 4.2.2. Then, $p_{-,+}$ is a non-degenerate fixed point of elliptic-elliptic type for all values of $t$. Similarly, the characteristic polynomial of $A^2_{p_{-,-}}$ coincides with $P^0_{-,+}(\lambda)$ of Section 4.2.2, and then $p_{-,-}$ is also a non-degenerate fixed point of elliptic-elliptic type for all values of $t$. □

After classifying the four fixed points of System 2, we obtain their images by the moment map $F_t = (L, H_t)$:

- $F_t(p_{+,+}) = (R_2, t)$,
- $F_t(p_{+,-}) = (-R_2, -t)$,
- $F_t(p_{-,+}) = (R_2, -t)$,
- $F_t(p_{-,-}) = (-R_2, t)$.

Now, we identify the singular points of rank 1 of System 2.

**Proposition 4.17.** *All the singular points of rank* 1 *of System 2 are:*

- *If* $t = 0$, *the union of*

$$\{(0, 0, \pm 1)\} \times \left(\mathbb{S}^2_2 \setminus \{(0, 0, \pm 1)\}\right)$$

*and*

$$\left(\mathbb{S}^2_1 \setminus \{(0, 0, \pm 1)\}\right) \times \{(0, 0, \pm 1)\}.$$

- *If $t \neq 0$, the union of $\{(\theta_1, z_1, \theta_2, z_2) \in \mathbb{S}^2_1 \times \mathbb{S}^2_2\}$ such that $\theta_2 = \theta_1$ and*

$$-\frac{1-t}{t} + \frac{z_1^2}{\sqrt{1-z_1^2}}\sqrt{1-z_2^2} - z_1 z_2 = \frac{R_1}{R_2}\left(\frac{z_2}{\sqrt{1-z_2^2}}\sqrt{1-z_1^2} - z_1\right),$$

*and $\{(\theta_1, z_1, \theta_2, z_2) \in \mathbb{S}^2_1 \times \mathbb{S}^2_2\}$ such that $\theta_2 = \theta_1 + \pi$ and*

$$\frac{1-t}{t} + \frac{z_1^2}{\sqrt{1-z_1^2}}\sqrt{1-z_2^2} + z_1 z_2 = \frac{R_1}{R_2}\left(\frac{z_2}{\sqrt{1-z_2^2}}\sqrt{1-z_1^2} + z_1\right).$$

*All of them are of elliptic regular type.*

*Proof.* The singular points of rank 1 are those where the joint flow of the Hamiltonian $b$-vector fields $X_L$ and $X_{H_t}$ generates a 1-dimensional orbit. Then, at these points either only one of them vanishes or $\mu X_L = X_{H_t}$ with $\mu \neq 0$.

The first case only happens for $t = 0$ and on the submanifold $\{(0, 0, \pm 1)\} \times \left(\mathbb{S}^2_2 \setminus \{(0, 0, \pm 1)\}\right)$, where $X_{H_t}$ vanishes but $X_L$ does not (see the proof of Proposition 4.16). Then, we just have to look for the points where the second case happens, that is, the points where we have $\mu X_L = X_{H_t}$ with $\mu \neq 0$.

If $t = 0$ and for $\varepsilon_1 \in \{+, -\}$, the equation $\mu X_L = X_{H_t}$ has no solution with $\mu \neq 0$ in $M^{0,0}$ (see Equation (A.15)) or in $M^{\varepsilon_1,0}$ (see Equation (A.21)). However, for $\varepsilon_2 \in \{+, -\}$, all the points of the form $(\theta_1, z_1, 0, 0)$ in $M^{0,\varepsilon_2}$ satisfy $\mu X_L = X_{H_t}$ with $\mu \neq 0$ (see Equation (A.23)). Then, for $t = 0$, the singular points of rank 1 are all the points in $\mathbb{S}^2_1 \times \mathbb{S}^2_2$ that project to a pole in only one of the two sphere components, that is, the union of $\{(0, 0, \pm 1)\} \times \left(\mathbb{S}^2_2 \setminus \{(0, 0, \pm 1)\}\right)$ and $\left(\mathbb{S}^2_1 \setminus \{(0, 0, \pm 1)\}\right) \times \{(0, 0, \pm 1)\}$.

If $t \neq 0$, $\mu X_L = X_{H_t}$, with $\mu \neq 0$, can be solved in $M^{0,0}$. In Equation (A.15) the condition $\mu X_L = X_{H_t}$ implies, in $M^{0,0}$ and in coordinates $\theta_1, z_1, \theta_2, z_2$, that $\sin(\theta_1 - \theta_2) = 0$. Then, either $\theta_1 = \theta_2$ or $\theta_1 = \theta_2 + \pi$.

If $\theta_1 = \theta_2$, the condition $\mu X_L = X_{H_t}$ on Equation (A.15) implies that

$$-\frac{1-t}{t} + \frac{z_1^2}{\sqrt{1-z_1^2}}\sqrt{1-z_2^2} - z_1 z_2 = \frac{R_1}{R_2}\left(\frac{z_2}{\sqrt{1-z_2^2}}\sqrt{1-z_1^2} - z_1\right) \tag{4.8}$$

If $\theta_1 = \theta_2 + \pi$, the condition $\mu X_L = X_{H_t}$ on Equation (A.15) implies that

$$\frac{1-t}{t} + \frac{z_1^2}{\sqrt{1-z_1^2}}\sqrt{1-z_2^2} + z_1 z_2 = \frac{R_1}{R_2}\left(\frac{z_2}{\sqrt{1-z_2^2}}\sqrt{1-z_1^2} + z_1\right) \tag{4.9}$$

Then, when $t \neq 0$ there are two 2-dimensional submanifolds of points of rank 1 in $M^{0,0}$. One is given by

$$\{(\theta_1, z_1, \theta_2, z_2) | \theta_2 = \theta_1, z_1 \text{ and } z_2 \text{ solve Equation } (4.8)\},$$

and the other by

$$\{(\theta_1, z_1, \theta_2, z_2) | \theta_2 = \theta_1 + \pi, z_1 \text{ and } z_2 \text{ solve Equation } (4.9)\}.$$

Equations (A.15), (A.21), (A.23) reveal that, when $t \neq 0$, there are no other solutions of $\mu X_L = X_{H_t}$, with $\mu \neq 0$, in $M \setminus M^{0,0}$.

All the singular points of rank 1 are of elliptic-regular type, since at these points the Hamiltonian $b$-vector fields generate the periodic orbit corresponding to a simultaneous rotation around the vertical axis of the two sphere components of $M = \mathbb{S}^2_1 \times \mathbb{S}^2_2$ (see Equations (A.15), (A.17), (A.21) and (A.23)). □

As in the case of System 1, the moment map $F_t = (L, H_t)$ depends only on $z_1$, $z_2$ and $\theta_1 - \theta_2$ on $M^{0,0}$ (see Equation (A.14)). The value of $\theta_1 - \theta_2$ is constant in each connected component of the submanifold of singular points of rank 1. Then, $z_1$ and $z_2$ parameterize the images of these components by $(L, H_t)$. Moreover, since $z_1$ and $z_2$ are related either in the submanifold of points of rank 1 by Equation (4.8) or by Equation (4.9), $L$ and $H_t$ depend on only one parameter along each of the connected components of this submanifold. Then, the image by $(L, H_t)$ of the submanifold of points of rank 1 of System 2 is made by 1-dimensional curves in $\mathbb{R}^2$.

In Figure 4.7 we can see the complete image of the moment map $F_t = (L, H_t)$ of System 2 plotted numerically. There, we use the parameters $R_1 = 1, R_2 = 2$ and different values of $t$ between 0 and 1. The image of the submanifold $\{z_1 > 0\} \times \mathbb{S}^2_2$ is depicted in sky blue and the image of the submanifold $\{z_1 < 0\} \times \mathbb{S}^2_2$ is depicted in yellow. The boundary of the sky blue region corresponds to the image of the singular points of rank 1 in $\{z_1 > 0\} \times \mathbb{S}^2_2$, while the boundary of the yellow region corresponds to the image of the singular points of rank 1 in $\{z_1 < 0\} \times \mathbb{S}^2_2$. The images of the four fixed points $p_{+,+}, p_{+,-}, p_{-,+}, p_{-,-}$ are depicted, respectively, in red, black, magenta and blue in Figure 4.7.

We proved in Proposition 4.16 that $p_{+,+}$, $p_{-,+}$ and $p_{-,-}$ are non-degenerate of elliptic-elliptic type for all values of $t$. Hence, they lie in the vertex on the image of the moment map. And, indeed for every value of $t$, their images, depicted in red, magenta and blue, correspond to a vertex of the image of the moment map.

On the other hand, in Proposition 4.16 we also proved that $p_{+,-}$ is non-degenerate and of elliptic-elliptic type if $t < t^-$ or $t > t^+$, non-degenerate and of focus-focus type if $t^- < t < t^+$, and degenerate if $t \in \{t^-, t^+\}$, where

$$t^{\pm} = \frac{R_2}{2R_2 + R_1 \mp 2\sqrt{R_1 R_2}}.$$

In the case of $R_1 = 1, R_2 = 2$, which is the one plotted in Figure 4.7, these values are

$$t^- \simeq 0.255479161794566, \qquad t^+ \simeq 0.920991426440728.$$

And, indeed, for $t \in \{0, 0.2, 1\}$, the image of $p_{+,-}$, depicted in black, corresponds to a vertex of the image of the moment map, while, for $t \in\subset \{0.4, 0.6, 0.8\}$, it corresponds to an interior point of the sky blue image of the submanifold $\{z_1 > 0\} \times \mathbb{S}^2_2$ by the moment map.

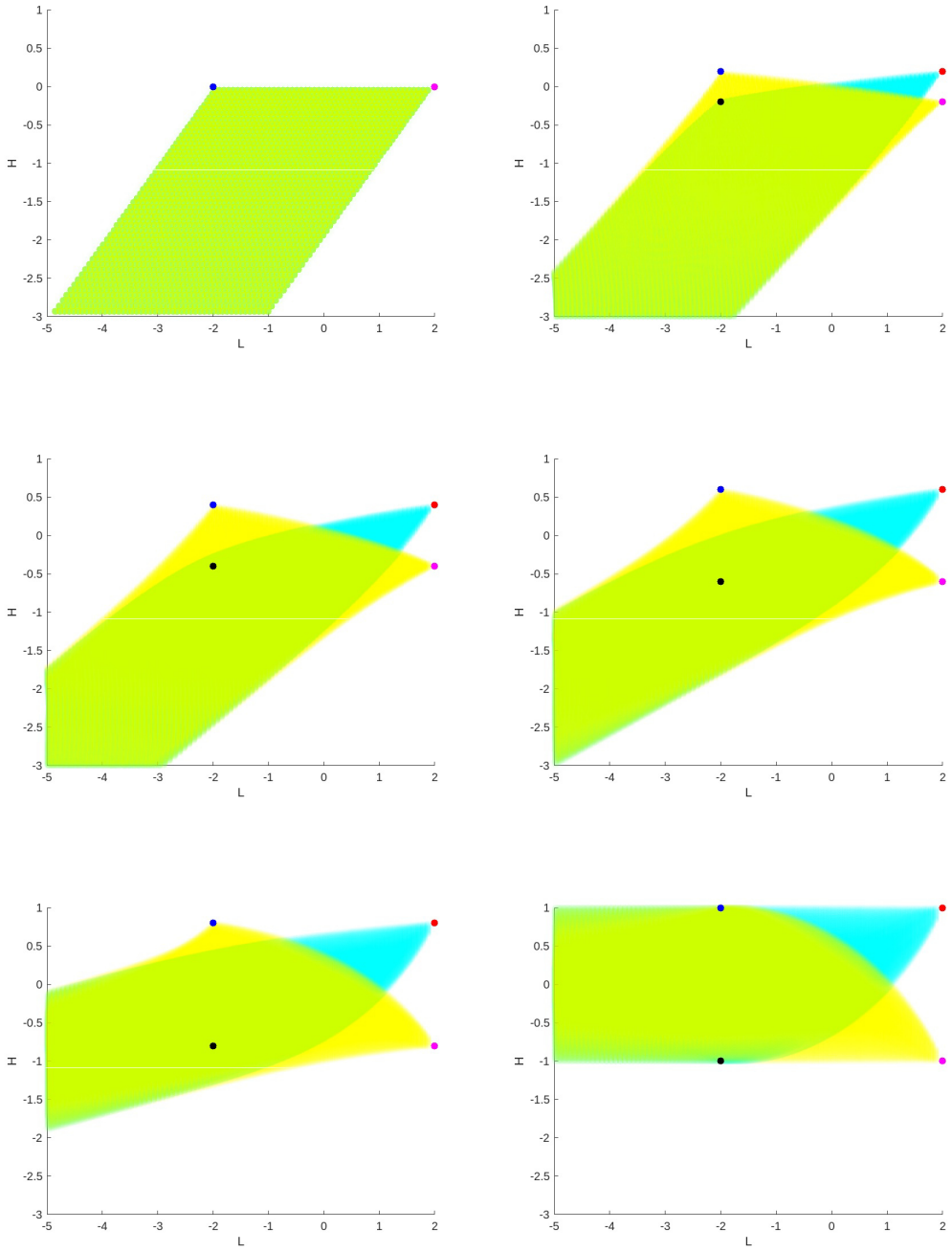


FIGURE 4.7: Image of the moment map of System 2 for values of $t$ between 0 (top left) and 1 (bottom right) by intervals of 0.2. It has been obtained numerically, see the code in Section B.1.3 in Appendix B. The image of the submanifold $\{z_1 > 0\} \times S^2_2$ is depicted in sky blue and the image of the submanifold $\{z_1 < 0\} \times S^2_2$ is depicted in yellow. The images of the four fixed points $p_{+,+}, p_{+,-}, p_{-,+}, p_{-,-}$ are depicted, respectively, in red, black, magenta and blue.

We are now ready to conclude that System 2 is a $b$-semitoric family.

**Corollary 4.18** (Brugués-Hohloch-Mir-Miranda [Bru+23])**.** *System 2 is a b-semitoric family.*

*Proof.* In Lemma 4.15 we proved that System 2 is a 4-dimensional $b$-integrable system for all values of $t$. It also satisfies the requirements of a $b$-semitoric family (see Definitions 4.1 and 4.2) because $M$ is compact and, hence, the map $L : M \to \mathbb{R}$ is proper, the Hamiltonian $b$-vector field $X_L$ generates a $2\pi$-periodic almost everywhere in $M$ (see Equation (A.15)) and, by Propositions 4.16 and 4.17, all singular points of $F_t = (L, H_t)$ are non-degenerate (except for the degenerate times $t^-, t^+$) and do not include components of hyperbolic type. □

### 4.2.5 Study of System 3

We end the study of the three $b$-symplectic modifications of the classical coupled angular momenta with the analysis of System 3. Again, we show that it is a $b$-integrable system for all values of $t$, we classify its singular points and finally we conclude that it is a $b$-semitoric family. The definition of System 3 is the following.

**Definition 4.19.** *Consider $M = \mathbb{S}^2_1 \times \mathbb{S}^2_2$ and take $Z = \{z_2 = 0\} \subset M$. Endow $(M, Z)$ with the b-symplectic form $\omega = -(R_1\omega_{\mathbb{S}^2_1} + R_2\frac{1}{z_2}\omega_{\mathbb{S}^2_2})$, where, for $i \in \{1,2\}$, $\omega_{\mathbb{S}^2_i}$ is the standard symplectic form on $\mathbb{S}^2_i$ and $0 < R_1 < R_2$ are constants. For $i \in \{1,2\}$, let $x_i, y_i, z_i$ be the Cartesian coordinates on the unit sphere $\mathbb{S}^2_i$ and introduce the parameter $t \in [0,1]$.*

System 3 *is the family of 4-dimensional systems $(M, Z, \omega, F_t = (L, H_t))$ parameterized by t and defined by*

$$\begin{cases} L(x_1, y_1, z_1, x_2, y_2, z_2) := R_1 z_1 + R_2 \log|z_2| \\ H_t(x_1, y_1, z_1, x_2, y_2, z_2) := (1-t)z_1 + t(x_1x_2 + y_1y_2 + z_1z_2) \end{cases}. \tag{4.10}$$

The changes introduced in System 3 with respect to the original coupled angular momenta system (see Definition 4.3) are:

1. The choice of the hypersurface $Z = \{z_2 = 0\} \subset M$ where the $b$-symplectic form is singular.
2. The replacement of the $R_2 z_2$ term by the $R_2 \log|z_2|$ term in the $L$ component of the moment map.

We first see that System 3 is $b$-integrable.

**Lemma 4.20.** *System 3 is a b-integrable system.*

*Proof.* We see that, in System 3 (see Definition 4.19), the differentials $dL$ and $dH_t$ are independent almost everywhere in $M$ and $\{L, H_t\} = 0$ everywhere in $M$.

In the double cylindrical chart in $M^{0,0}$, $dL$ and $dH_t$ write as:

$$\begin{cases} dL(\theta_1, z_1, \theta_2, z_2) & = R_1 z_1 + R_2 \frac{dz_2}{z_2} \\ dH_t(\theta_1, z_1, \theta_2, z_2) & = \left(1 - t + tz_2 - t\frac{z_1}{\sqrt{1-z_1^2}}\sqrt{1-z_2^2}\cos(\theta_1 - \theta_2)\right) dz_1 \\ & -t\sqrt{(1-z_1^2)(1-z_2^2)}\sin(\theta_1 - \theta_2)d\theta_1 \\ & +t\left(z_1 z_2 - \frac{z_2^2}{\sqrt{1-z_2^2}}\sqrt{1-z_1^2}\cos(\theta_1 - \theta_2)\right)\frac{dz_2}{z_2} \\ & +t\sqrt{(1-z_1^2)(1-z_2^2)}\sin(\theta_1 - \theta_2)d\theta_2 \end{cases} . \quad (4.11)$$

From Equation (4.11) we see that, for any value of $t$, the subset of points where $dL$ and $dH_t$ are not independent is contained in the union of the two following submanifolds of measure zero in $M$:

1. $\{\theta_1 = \theta_2\} \cup \{\theta_1 = \theta_2 + \pi\} \subset M^{0,0}$, which is a 3-dimensional submanifold of $M$.
2. $M \setminus M^{0,0}$, which is the 2-dimensional submanifold of $M$ which is not covered by the double cylindrical chart.

Then, $dL$ and $dH_t$ are independent almost everywhere in $M$.

Now we check that $\{L, H_t\} = 0$ everywhere in $M$. We compute $\{L, H_t\}$ on $M^{0,0}$, which yields:

$$\{L, H_t\} = X_L(H_t) =$$
$$\left(-\frac{\partial}{\partial\theta_1} - \frac{\partial}{\partial\theta_2}\right)\left((1-t)z_1 + t\left(\sqrt{(1-z_1^2)(1-z_2^2)}\cos(\theta_1 - \theta_2) + z_1 z_2\right)\right) =$$
$$t\sqrt{(1-z_1^2)(1-z_2^2)}\sin(\theta_1 - \theta_2) - t\sqrt{(1-z_1^2)(1-z_2^2)}\sin(\theta_1 - \theta_2) = 0.$$

Since $M \setminus M^{0,0}$ is of measure 0 in $M$ and $\{L, H_t\}$ is continuous in $M$, we conclude that, for every value of $t$, $\{L, H_t\}$ is equal to 0 on the entire manifold $M$. □

We proceed to identify and classify the fixed points of System 3.

**Proposition 4.21.** *System 3 has* 4 *fixed points. They are located at the double poles* $p_{\pm,\pm} = ((0,0,\pm 1),(0,0,\pm 1)) \in \mathbb{S}^2_1 \times \mathbb{S}^2_2$. *The fixed points* $p_{+,+}$, $p_{+,-}$ *and* $p_{-,+}$ *are non-degenerate of elliptic-elliptic type for all values of* $t$. *The fixed point* $p_{-,-}$ *is non-degenerate and of elliptic-elliptic type if* $t < t^-$ *or* $t > t^+$, *of focus-focus type if* $t^- < t < t^+$ *and degenerate if* $t \in \{t^-, t^+\}$, *where*

$$t^\pm = \frac{R_2}{2R_2 + R_1 \mp 2\sqrt{R_1 R_2}}.$$

*Proof.* The Hamiltonian $b$-vector fields $X_L$ and $X_{H_t}$ vanish simultaneously at the fixed points of the system. Their expressions in the different charts (see equations (A.25), (A.31), (A.33), (A.27) in Section A.4 in Appendix A) reveal that:

- for any value of $t$, $X_L$ vanishes only at the four double poles $p_{\pm,\pm} = ((0,0,\pm 1),(0,0,\pm 1))$, and
- for $t = 0$, $X_{H_t}$ vanishes on $\{(0,0,\pm 1)\} \times \mathbb{S}^2_2$, while for $t \neq 0$, it vanishes only at the four double poles $p_{\pm,\pm}$.

Then, the only fixed points of the system are the four double poles $p_{\pm,\pm} = ((0,0,\pm 1),(0,0,\pm 1)) \in \mathbb{S}^2_1 \times \mathbb{S}^2_2$.

We proceed to classify the four fixed points $p_{\pm,\pm}$ using the local expression of the operators $\Omega$, $d^2L$ and $d^2H_t$ there. Each point $p_{\varepsilon_1,\varepsilon_2}$ corresponds to the point $(0,0,0,0)$ in coordinates $x_1, y_1, x_2, y_2$ in the double Cartesian chart $(\varphi_1, U_1^{\varepsilon_1}) \times (\varphi_2, U_2^{\varepsilon_2})$ of $M^{\varepsilon_1,\varepsilon_2}$. Then, as we did in the previous sections, we find the expressions of $\Omega$, $d^2L$ and $d^2H_t$ for the four critical points simultaneously by using the combination of signs $\varepsilon_1, \varepsilon_2 \in \{+,-\}$ that corresponds to each of them.

For $\varepsilon_1\varepsilon_2 \in \{+,-\}$, the $b$-symplectic form $\omega$ on $M^{\varepsilon_1,\varepsilon_2}$ writes as

$$\omega = -\varepsilon_1 \frac{R_1}{\sqrt{1-x_1^2-y_1^2}} dx_1 \wedge dy_1 - \frac{R_2}{1-x_2^2-y_2^2} dx_2 \wedge dy_2.$$

Then, the operator $\Omega$ at the double pole $p_{\varepsilon_1,\varepsilon_2}$ writes as

$$\Omega = \begin{pmatrix} 0 & -\varepsilon_1 R_1 & 0 & 0 \\ \varepsilon_1 R_1 & 0 & 0 & 0 \\ 0 & 0 & 0 & -R_2 \\ 0 & 0 & R_2 & 0 \end{pmatrix}$$

At a fixed double pole $p_{\varepsilon_1,\varepsilon_2}$ the expression of $d^2L$ is:

$$d^2L = \begin{pmatrix} -\varepsilon_1 R_1 & 0 & 0 & 0 \\ 0 & -\varepsilon_1 R_1 & 0 & 0 \\ 0 & 0 & -R_2 & 0 \\ 0 & 0 & 0 & -R_2 \end{pmatrix}$$

and the expression of $d^2H_t$ is:

$$d^2H_t = \begin{pmatrix} \varepsilon_1(-1+t-\varepsilon_2 t) & 0 & t & 0 \\ 0 & \varepsilon_1(-1+t-\varepsilon_2 t) & 0 & t \\ t & 0 & -\varepsilon_1\varepsilon_2 t & 0 \\ 0 & t & 0 & -\varepsilon_1\varepsilon_2 t \end{pmatrix}.$$

In Section A.4 in Appendix A one can find the details on the computations of $d^2L$ and $d^2H_t$ (see Equations (A.28) and (A.29) there).

For all the values of $t, \varepsilon_1, \varepsilon_2$, the matrices $d^2L$ and $d^2H_t$ are independent and from them we construct the operators $A^3_L := \Omega^{-1} d^2L$ and $A^3_{H_t} := \Omega^{-1} d^2H_t$, which write as:

$$A^3_L = \begin{pmatrix} 0 & -1 & 0 & 0 \\ 1 & 0 & 0 & 0 \\ 0 & 0 & 0 & -1 \\ 0 & 0 & 1 & 0 \end{pmatrix}, \qquad A^3_{H_t} = \begin{pmatrix} 0 & \frac{-\varepsilon_2 t+t-1}{R_1} & 0 & \frac{t}{\varepsilon_1 R_1} \\ -\frac{-\varepsilon_2 t+t-1}{R_1} & 0 & -\frac{t}{\varepsilon_1 R_1} & 0 \\ 0 & \frac{t}{R_2} & 0 & -\frac{\varepsilon_1\varepsilon_2 t}{R_2} \\ -\frac{t}{R_2} & 0 & \frac{\varepsilon_1\varepsilon_2 t}{R_2} & 0 \end{pmatrix}.$$

At a double pole $p_{\varepsilon_1,\varepsilon_2}$, the linear combination $A^3 := A^3_L + A^3_{H_t}$ has the form

$$A^3 = \begin{pmatrix} 0 & \frac{-\varepsilon_2 t+t-1}{R_1} - 1 & 0 & \frac{t}{\varepsilon_1 R_1} \\ -\frac{-\varepsilon_2 t+t-1}{R_1} + 1 & 0 & -\frac{t}{\varepsilon_1 R_1} & 0 \\ 0 & \frac{t}{R_2} & 0 & -\frac{\varepsilon_1\varepsilon_2 t}{R_2} - 1 \\ -\frac{t}{R_2} & 0 & \frac{\varepsilon_1\varepsilon_2 t}{R_2} + 1 & 0 \end{pmatrix}.$$

And, at each of the four poles $\{p_{+,+}, p_{+,-}, p_{-,+}, p_{-,-}\}$, $A^3$ writes as:

$$A^3_{p_{+,+}} = \begin{pmatrix} 0 & -\frac{1}{R_1} - 1 & 0 & \frac{t}{R_1} \\ \frac{1}{R_1} + 1 & 0 & -\frac{t}{R_1} & 0 \\ 0 & \frac{t}{R_2} & 0 & -\frac{t}{R_2} - 1 \\ -\frac{t}{R_2} & 0 & \frac{t}{R_2} + 1 & 0 \end{pmatrix}$$

$$A^3_{p_{+,-}} = \begin{pmatrix} 0 & \frac{2t-1}{R_1} - 1 & 0 & \frac{t}{R_1} \\ -\frac{2t-1}{R_1} + 1 & 0 & -\frac{t}{R_1} & 0 \\ 0 & \frac{t}{R_2} & 0 & \frac{t}{R_2} - 1 \\ -\frac{t}{R_2} & 0 & -\frac{t}{R_2} + 1 & 0 \end{pmatrix}$$

$$A^3_{p_{-,+}} = \begin{pmatrix} 0 & -\frac{1}{R_1} - 1 & 0 & -\frac{t}{R_1} \\ \frac{1}{R_1} + 1 & 0 & \frac{t}{R_1} & 0 \\ 0 & \frac{t}{R_2} & 0 & \frac{t}{R_2} - 1 \\ -\frac{t}{R_2} & 0 & -\frac{t}{R_2} + 1 & 0 \end{pmatrix}$$

$$A^3_{p_{-,-}} = \begin{pmatrix} 0 & \frac{2t-1}{R_1} - 1 & 0 & -\frac{t}{R_1} \\ -\frac{2t-1}{R_1} + 1 & 0 & \frac{t}{R_1} & 0 \\ 0 & \frac{t}{R_2} & 0 & -\frac{t}{R_2} - 1 \\ -\frac{t}{R_2} & 0 & \frac{t}{R_2} + 1 & 0 \end{pmatrix}.$$

We see that $A^3_{p_{+,+}}$ is identical to $A^0_{p_{+,+}}$ from Section 4.2.2, which implies that, for all values of $t$, $p_{+,+}$ is non-degenerate of elliptic-elliptic type. Similarly, since $A^3_{p_{-,+}}$ is identical to $A^0_{p_{-,+}}$, for all values of $t$, $p_{-,+}$ is also non-degenerate of elliptic-elliptic type.

On the other hand, by direct computation one can see that the characteristic polynomial of $A^3_{p_{+,-}}$ coincides with the characteristic polynomial $P^0_{-,-}(\lambda)$ defined in Section 4.2.2. Then, for all values of $t$, $p_{+,-}$ is a non-degenerate fixed point of elliptic-elliptic type. Similarly, the characteristic polynomial of $A^3_{p_{-,-}}$ coincides with the characteristic polynomial $P^0_{+,-}(\lambda)$ of Section 4.2.2 and, then, $p_{-,-}$ is non-degenerate and of elliptic-elliptic type if $t < t^-$ or $t > t^+$, of focus-focus type if $t^- < t < t^+$ and degenerate if $t \in \{t^-, t^+\}$, where

$$t^{\pm} = \frac{R_2}{2R_2 + R_1 \mp 2\sqrt{R_1 R_2}}.$$

□

The images by the moment map $F_t = (L, H_t)$ of the four fixed points of System 3 are the following:

- $F_t(p_{+,+}) = (R_1, 1)$,
- $F_t(p_{+,-}) = (R_1, 1 - 2t)$,
- $F_t(p_{-,+}) = (-R_1, -1)$,
- $F_t(p_{-,-}) = (-R_1, -1 + 2t)$.

With the next proposition we identify and classify the singular points of rank 1 of System 3.

**Proposition 4.22.** *All the singular points of rank* 1 *of System 3 are:*

- *If* $t = 0$*, the union of*

$$\{(0, 0, \pm 1)\} \times \left(\mathbb{S}_2^2 \setminus \{(0, 0, \pm 1)\}\right)$$

*and*

$$\left(\mathbb{S}_1^2 \setminus \{(0, 0, \pm 1)\}\right) \times \{(0, 0, \pm 1)\}.$$

- *If* $t \neq 0$*, the union of* $\{(\theta_1, z_1, \theta_2, z_2) \in \mathbb{S}_1^2 \times \mathbb{S}_2^2\}$ *such that* $\theta_2 = \theta_1$ *and*

$$-\frac{1-t}{t} + \frac{z_1}{\sqrt{1-z_1^2}}\sqrt{1-z_2^2} - z_2 = \frac{R_1}{R_2}\left(\frac{z_2^2}{\sqrt{1-z_2^2}}\sqrt{1-z_1^2} - z_1 z_2\right),$$

*and* $\{(\theta_1, z_1, \theta_2, z_2) \in \mathbb{S}_1^2 \times \mathbb{S}_2^2\}$ *such that* $\theta_2 = \theta_1 + \pi$ *and*

$$\frac{1-t}{t} + \frac{z_1}{\sqrt{1-z_1^2}}\sqrt{1-z_2^2} + z_2 = \frac{R_1}{R_2}\left(\frac{z_2^2}{\sqrt{1-z_2^2}}\sqrt{1-z_1^2} + z_1 z_2\right).$$

*All of them are of elliptic regular type.*

*Proof.* The singular points of rank 1 are the points where the joint flow of the Hamiltonian $b$-vector fields $X_L$ and $X_{H_t}$ generates a 1-dimensional orbit. Then, at these points either only one of them vanishes or $\mu X_L = X_{H_t}$ with $\mu \neq 0$.

The points where just one of the Hamiltonian $b$-vector fields vanishes are the points in $\{(0, 0, \pm 1)\} \times \left(\mathbb{S}_2^2 \setminus \{(0, 0, \pm 1)\}\right)$, where $X_{H_t}$ vanishes but $X_L$ does not, and this is happens for $t = 0$ (see the proof of Proposition 4.21).

On the other hand, there are also points where none of the Hamiltonian $b$-vector fields vanishes but we have $\mu X_L = X_{H_t}$ with $\mu \neq 0$.

If $t = 0$ and for $\varepsilon_1 \in \{+, -\}$, $\mu X_L = X_{H_t}$, with $\mu \neq 0$, has no solution in $M^{0,0}$ (see Equation (A.25)) or in $M^{\varepsilon_1,0}$ (see Equation (A.31)). But, for $\varepsilon_2 \in \{+, -\}$, the points of the form $(\theta_1, z_1, 0, 0)$ in $M^{0,\varepsilon_2}$ satisfy $\mu X_L = X_{H_t}$ with $\mu \neq 0$ (see Equation (A.33)).

Then, for $t = 0$, the singular points of rank 1 are all the points in $\mathbb{S}^2_1 \times \mathbb{S}^2_2$ that get projected to a pole in only one of the two sphere components, that is, the union of $\{(0, 0, \pm 1)\} \times \left(\mathbb{S}^2_2 \setminus \{(0, 0, \pm 1)\}\right)$ and $\left(\mathbb{S}^2_1 \setminus \{(0, 0, \pm 1)\}\right) \times \{(0, 0, \pm 1)\}$.

Now, if $t \neq 0$, the equation $\mu X_L = X_{H_t}$, with $\mu \neq 0$, has solutions in $M^{0,0}$. Equation (A.25) together with the condition $\mu X_L = X_{H_t}$ implies, in $M^{0,0}$ and in coordinates $\theta_1, z_1, \theta_2, z_2$, that $\sin(\theta_1 - \theta_2) = 0$. Then, either $\theta_1 = \theta_2$ or $\theta_1 = \theta_2 + \pi$.

In the case $\theta_1 = \theta_2$, the condition $\mu X_L = X_{H_t}$ on Equation (A.25) is equivalent to

$$-\frac{1-t}{t} + \frac{z_1}{\sqrt{1-z_1^2}}\sqrt{1-z_2^2} - z_2 = \frac{R_1}{R_2}\left(\frac{z_2^2}{\sqrt{1-z_2^2}}\sqrt{1-z_1^2} - z_1 z_2\right) \tag{4.12}$$

In the case $\theta_1 = \theta_2 + \pi$, the condition $\mu X_L = X_{H_t}$ on Equation (A.25) is equivalent to

$$\frac{1-t}{t} + \frac{z_1}{\sqrt{1-z_1^2}}\sqrt{1-z_2^2} + z_2 = \frac{R_1}{R_2}\left(\frac{z_2^2}{\sqrt{1-z_2^2}}\sqrt{1-z_1^2} + z_1 z_2\right) \tag{4.13}$$

Then, when $t \neq 0$, there are two 2-dimensional submanifolds of points of rank 1 in $M^{0,0}$. One is given by

$$\{(\theta_1, z_1, \theta_2, z_2) | \theta_2 = \theta_1, z_1 \text{ and } z_2 \text{ solve Equation } (4.12)\},$$

and the other by

$$\{(\theta_1, z_1, \theta_2, z_2) | \theta_2 = \theta_1 + \pi, z_1 \text{ and } z_2 \text{ solve Equation } (4.13)\}.$$

From Equations (A.25), (A.31), (A.33) we obtain that, when $t \neq 0$, there are no other solutions of $\mu X_L = X_{H_t}$, with $\mu \neq 0$, in $M \setminus M^{0,0}$.

The singular points of rank 1 are all of elliptic-regular type because the Hamiltonian $b$-vector fields generate periodic orbits corresponding to rotations around the vertical axis of the two sphere components of $M = \mathbb{S}^2_1 \times \mathbb{S}^2_2$ (see equations (A.25), (A.27), (A.31) and (A.33)). □

Again, the moment map $F_t = (L, H_t)$ of System 3 depends only on $z_1$, $z_2$ and $\theta_1 - \theta_2$ on $M^{0,0}$ (see Equation (A.14)). Since the value of $\theta_1 - \theta_2$ is constant in each connected component of the submanifold of singular points of rank 1, the values of $z_1$ and $z_2$ parameterize the images of these components by $(L, H_t)$. Besides, since $z_1$ and $z_2$ are related in the submanifold of points of rank 1 by Equations (4.12) and (4.13), the functions $L$ and $H_t$ depend on just one parameter along each connected component of this submanifold. As consequence, the image by $(L, H_t)$ of the submanifold of points of rank 1 of System 3 is made by a set of curves in $\mathbb{R}^2$.

We can see in Figure 4.8 the complete image of the moment map $F_t = (L, H_t)$ of System 3 obtained numerically. We took the parameters $R_1 = 1, R_2 = 2$ and different

values of $t$ between 0 and 1. The image of the submanifold $\{z_2 > 0\} \times \mathbb{S}^2_2$ is depicted in sky blue and the image of the submanifold $\{z_2 < 0\} \times \mathbb{S}^2_2$ is depicted in yellow. The boundary of the sky blue region corresponds to the image of the singular points of rank 1 in $\{z_2 > 0\} \times \mathbb{S}^2_2$, while the boundary of the yellow region corresponds to the image of the singular points of rank 1 in $\{z_2 < 0\} \times \mathbb{S}^2_2$. The images of the four fixed points $p_{+,+}, p_{+,-}, p_{-,+}, p_{-,-}$ are depicted, respectively, in red, black, magenta and blue.

In Proposition 4.21 we proved that the fixed points $p_{+,+}$, $p_{+,-}$ and $p_{-,+}$ are non-degenerate and of elliptic-elliptic type for all values of $t$ and, hence, they lie in the vertex on the image of the moment map. Indeed in Figure 4.8 we can see that, for any value of $t$, their images, depicted in red, black and magenta, correspond to a vertex of the image of the moment map.

We also proved in Proposition 4.21 that $p_{-,-}$ is a non-degenerate fixed point of elliptic-elliptic type if $t < t^-$ or $t > t^+$, a non-degenerate fixed point of focus-focus type if $t^- < t < t^+$, and a degenerate fixed point if $t \in \{t^-, t^+\}$, where

$$t^{\pm} = \frac{R_2}{2R_2 + R_1 \mp 2\sqrt{R_1 R_2}}.$$

For $R_1 = 1$ and $R_2 = 2$, which corresponds to Figure 4.8, these values are

$$t^- \simeq 0.255479161794566, \qquad t^+ \simeq 0.920991426440728,$$

and, we can check that, for $t \in \{0, 0.2, 1\}$, the image of $p_{-,-}$, depicted in blue, corresponds to a vertex of the image of the moment map, while, for $t \in\subset \{0.4, 0.6, 0.8\}$, it corresponds to an interior point of the yellow image of the submanifold $\{z_2 < 0\} \times \mathbb{S}^2_2$ by the moment map.

After the study of the singular points of System 3, we conclude that it is a *b*-semitoric family.

**Corollary 4.23** (Brugués-Hohloch-Mir-Miranda [Bru+23])**.** *System 3 is a b-semitoric family.*

*Proof.* Lemma 4.20 proves that System 3 is a 4-dimensional *b*-integrable system for all values of $t$. Moreover, it is a *b*-semitoric family (see Definitions 4.1 and 4.2) because:

- the map $L : M \to \mathbb{R}$ is proper because $M = \mathbb{S}^2_1 \times \mathbb{S}^2_1$ is compact,
- in $M^{0,0}$, the Hamiltonian *b*-vector field $X_L$ generates a $2\pi$-periodic almost everywhere in $M$ (see Equation (A.25)) and
- by Propositions 4.21 and 4.22, all singular points of $F_t = (L, H_t)$ (except for the degenerate times $t^-, t^+$) are non-degenerate and do not include components of hyperbolic type.

□

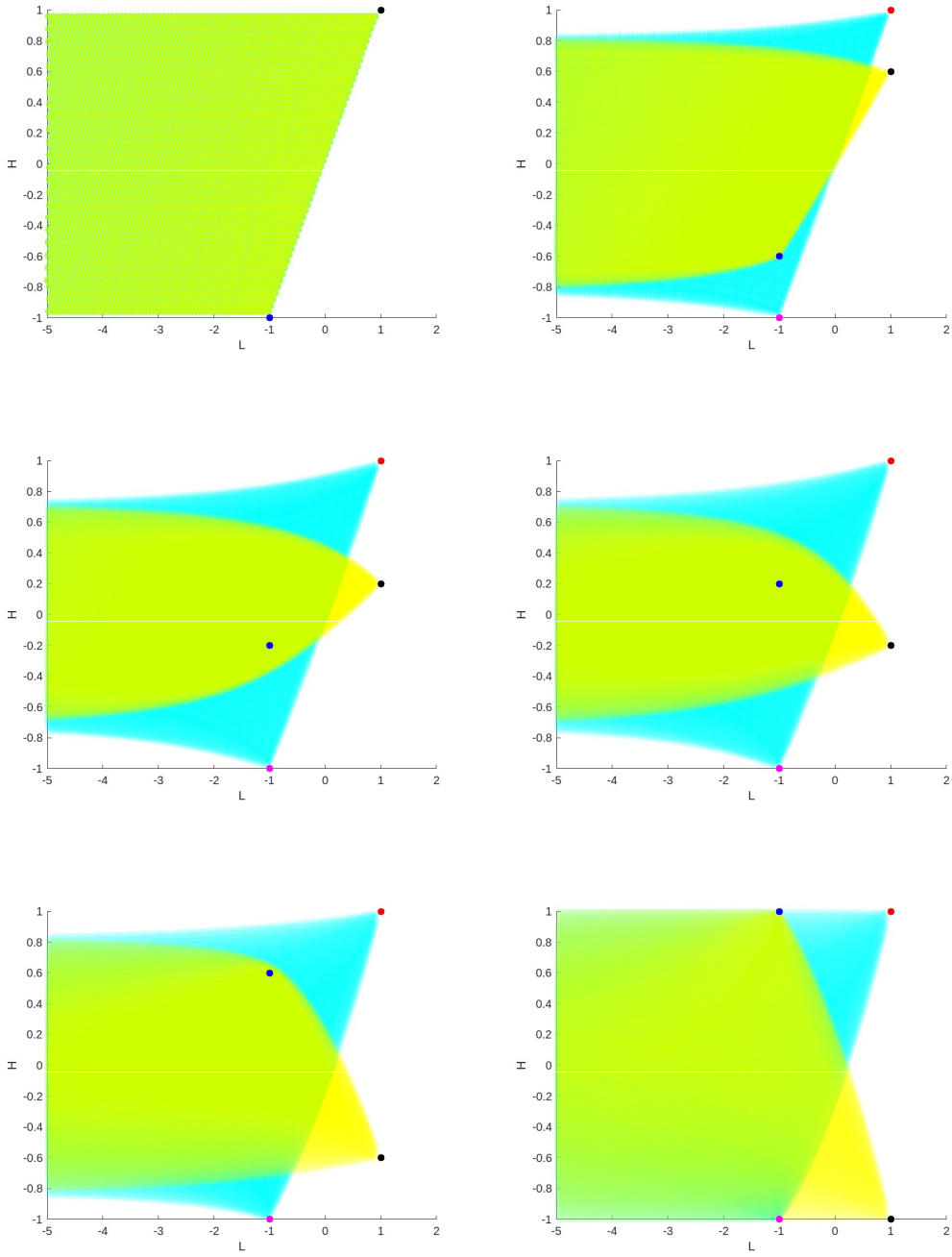


FIGURE 4.8: Image of the moment map of System 3 for values of $t$ between 0 (top left) and 1 (bottom right) by intervals of 0.2. It has been obtained numerically, see the code in Section B.1.4 in Appendix B. The image of the submanifold $\mathbb{S}^2_1 \times \{z_2 > 0\}$ is depicted in sky blue and the image of the submanifold $\mathbb{S}^2_1 \times \{z_2 < 0\}$ is depicted in yellow. The images of the four fixed points $p_{+,+}, p_{+,-}, p_{-,+}, p_{-,-}$ are depicted, respectively, in red, black, magenta and blue.

## 4.3 The focus-focus singular fibers on b-semitoric systems

The theory of semitoric systems (see Section 2.2.2 in Chapter 2) tells us that, in a semitoric system $(M, \omega, F = (L, H))$, the singular fiber corresponding to a focus-focus point is a 2-dimensional pinched torus like the one depicted in Figure 4.9. In particular, at any point on the singular focus-focus fiber except from the fixed point, the Hamiltonian $b$-vector field $X_L$ generates a periodic orbit and the Hamiltonian $b$-vector field $X_H$ generates a homoclinic orbit that starts and ends at the fixed point. Then, the 2-dimensional unstable manifold and the 2-dimensional stable manifold of a focus-focus fixed point are in fact the same manifold, which intersects itself transversally precisely at the pinch point.

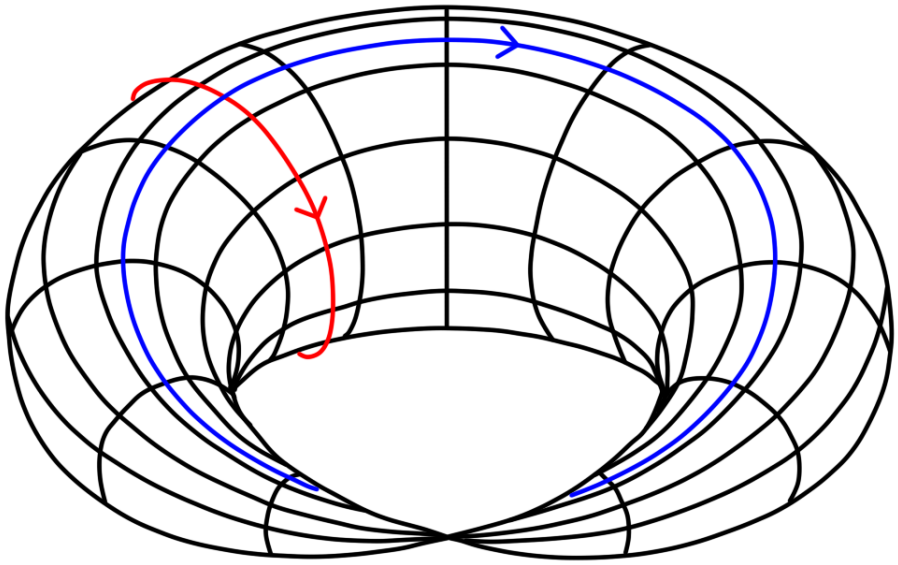

FIGURE 4.9: Representation of a focus-focus fiber in a semitoric system, which is topologically a pinched torus. The focus-focus fixed point is located at the pinch. In red, a periodic orbit generated by the flow of $X_L$. In blue, a homoclinic orbit generated by the flow of $X_H$.

In Section 4.1 we saw that, in $b$-integrable systems which only have non-degenerate singularities, the critical hypersurface $Z$ cannot contain fixed points of the system. It turns out that, besides, if $Z$ does not intersect the singular fiber of a non-degenerate fixed point of focus-focus type, then this singular fiber is precisely the pinched torus of Figure 4.9 as in the case of a focus-focus fiber in a semitoric system.

**Lemma 4.24.** *Let $(M^4, Z, \omega, F = (L, H))$ be a b-semitoric system. Suppose that $p \in M$ is a non-degenerate fixed point of focus-focus type and that the fiber $\Lambda_p := F^{-1}(F(p))$ containing $p$ is compact, connected, contains no other fixed points and does not intersect $Z$. Then, the fiber $\Lambda_p$ is topologically a pinched torus in which $X_L$ generates a periodic orbit and $X_H$ generates a homoclinic orbit at $p$.*

*Proof.* Since $p$ is a fixed point of the system, the rank of $F$ at $p$ is 0. Then, $p$ belongs to $M \setminus Z$ because the minimal rank of $F$ is 1 along $Z$ (see Section 4.1). Since the fiber $\Lambda_p = F^{-1}(F(p))$ containing $p$ is connected and does not intersect $Z$, it is entirely contained in a connected component $M_1$ of $M \setminus Z$.

On $M_1$, the $b$-semitoric system is just a semitoric system because the $b$-symplectic form is not singular and the components $L$ and $H$ of the moment map are smooth functions there. Then, we can use the semi-local classification of non-degenerate points for integrable systems (see Theorem 2.13) to conclude that the fiber $\Lambda_p$ is topologically and dynamically equivalent to a pinched torus. Moreover, since $\Lambda_p$ contains no fixed points other than $p$, it is a single pinched torus in which the Hamiltonian $b$-vector field $X_L$ generates a periodic orbit and the Hamiltonian $b$-vector field $X_H$ generates a homoclinic orbit that starts and ends at $p$ (see Figure 4.9). □

A consequence of Lemma 4.24 is that, in a $b$-semitoric system $(M^4, Z, \omega, F = (L, H))$, the singular fiber of a non-degenerate fixed point of focus-focus type is topologically and dynamically equivalent to a singular focus-focus fiber in a semitoric system. Moreover, the fiber is entirely contained in a single connected component of $M \setminus Z$.

In this section we compute numerically the singular fiber of a non-degenerate fixed point of focus-focus type on a $b$-semitoric system which does not intersect $Z$ and see that it is indeed a pinched torus. In particular, we study the fiber of the double pole $p_{+,-} = (0, 0, +1, 0, 0, -1)$ in System 1, which we review here.

System 1 (see Definition 4.7) is the $b$-semitoric family given by

$$(M = \mathbb{S}^2_1 \times \mathbb{S}^2_2, Z = \{z_1 = 0\} \subset M, \omega = -(R_1 \frac{1}{z_1} \omega_{\mathbb{S}^2_1} + R_2 \omega_{\mathbb{S}^2_2}), F_t = (L, H_t)),$$

where, for $i \in \{1, 2\}$, $\omega_{\mathbb{S}^2_i}$ is the standard symplectic form on $\mathbb{S}^2_i$ and

$$\begin{cases} L(x_1, y_1, z_1, x_2, y_2, z_2) := R_1 \log |z_1| + R_2 z_2 \\ H_t(x_1, y_1, z_1, x_2, y_2, z_2) := (1-t) z_1 + t(x_1 x_2 + y_1 y_2 + z_1 z_2) \end{cases},$$

with $x_i, y_i, z_i$ the Cartesian coordinates on the unit sphere $\mathbb{S}^2_i$, $0 < R_1 < R_2$ are constants and $t$ is a parameter between 0 and 1.

For the complete study of System 1, we refer to Section 4.2.3, where we proved that it is a $b$-semitoric family. In particular, we proved that the point $p_{+,-} = (0, 0, +1, 0, 0, -1)$ is a non-degenerate fixed point of focus-focus type if $t^- < t < t^+$, where

$$t^{\pm} = \frac{R_2}{2R_2 + R_1 \mp 2\sqrt{R_1 R_2}}.$$

We assume from now on that we are in this case, that is, that $t \in (t^-, t^+)$ and, hence, that $p_{+,-}$ is a fixed point of focus-focus type.

In the double cylindrical chart in $M^{0,0}$, the moment map $(L, H_t)$ of System 1 writes as

$$\begin{cases} L(\theta_1, z_1, \theta_2, z_2) = R_1 \log |z_1| + R_2 z_2 \\ H_t(\theta_1, z_1, \theta_2, z_2) = (1-t) z_1 + t \left( \sqrt{(1 - z_1^2)(1 - z_2^2)} \cos(\theta_1 - \theta_2) + z_1 z_2 \right) \end{cases}.$$

In Section 4.2.3 we saw that $F_t(p_{+,-}) = (L, H_t)(p_{+,-}) = (-R_2, 1-2t)$. Then, in $M^{0,0}$, the singular focus-focus fiber $\Lambda^t_{p_{+,-}} := F_t^{-1}(F_t(p_{+,-}))$ of $p_{+,-}$ is given by

$$\begin{cases} R_1 \log|z_1| + R_2 z_2 = -R_2, \\ (1-t)z_1 + t\left(\sqrt{(1-z_1^2)(1-z_2^2)}\cos(\theta_1-\theta_2) + z_1 z_2\right) = 1-2t \end{cases}$$

or, equivalently, by

$$\begin{cases} z_2 = -1 - \frac{R_1}{R_2}\log|z_1|, \\ \cos(\theta_1-\theta_2) = \frac{(1-z_1)(\frac{1}{t}-2) + z_1\frac{R_1}{R_2}\log|z_1|}{\sqrt{(1-z_1^2)\log|z_1|(-2\frac{R_1}{R_2} - \frac{R_1^2}{R_2^2}\log|z_1|))}} \end{cases}. \tag{4.14}$$

Observe that the height coordinate $z_2$ of a point in the fiber $\Lambda^t_{p_{+,-}}$ is uniquely determined by the height coordinate $z_1$ and that the angle difference $\theta_1 - \theta_2$ of a point in $\Lambda^t_{p_{+,-}}$ has, in general, two solutions for a given value of $z_1$. Observe also that we are under the hypotheses of Lemma 4.24 and, hence, $\Lambda^t_{p_{+,-}}$ is a pinched torus in which $X_L$ generates a periodic orbit and $X_{H_t}$ generates a homoclinic orbit at $p_{+,-}$.

The Hamiltonian $b$-vector fields $X_L$ and $X_{H_t}$ write in $M^{0,0}$ as:

$$\begin{cases} X_L = & -\frac{\partial}{\partial\theta_1} - \frac{\partial}{\partial\theta_2} \\ X_{H_t} = & \left[-\frac{z_1(1-t)}{R_1} + \frac{t}{R_1}\left(\frac{z_1^2}{\sqrt{1-z_1^2}}\sqrt{1-z_2^2}\cos(\theta_1-\theta_2) - z_1 z_2\right)\right]\frac{\partial}{\partial\theta_1} \\ & - \left[\frac{t}{R_1}\sqrt{(1-z_1^2)(1-z_2^2)}\sin(\theta_1-\theta_2)\right] z_1\frac{\partial}{\partial z_1} \\ & + \left[\frac{t}{R_2}\left(\frac{z_2}{\sqrt{1-z_2^2}}\sqrt{1-z_1^2}\cos(\theta_1-\theta_2) - z_1\right)\right]\frac{\partial}{\partial\theta_2} \\ & + \left[\frac{t}{R_2}\sqrt{(1-z_1^2)(1-z_2^2)}\sin(\theta_1-\theta_2)\right]\frac{\partial}{\partial z_2} \end{cases} \tag{4.15}$$

To illustrate the pinched torus corresponding to the focus-focus fiber of the fixed double pole $p_{+,-}$ we start setting the parameters of System 1. We take $R_1 = 1$, $R_2 = 2$ and $t = 0.5$, a choice of parameters that guarantees that $p_{+,-}$ is a non-degenerate fixed point of focus-focus type (see Proposition 4.11).

Next, we identify a regular point on the fiber $\Lambda^t_{p_{+,-}}$, that is, a point in $\mathbb{S}^2_1 \times \mathbb{S}^2_2$ with coordinates $\theta_1, z_1, \theta_2, z_2$ satisfying Equation (4.14). Then, on the one hand, we compute its flow along $X_L$, we project it to the two sphere components of $\mathbb{S}^2_1 \times \mathbb{S}^2_2$ and we plot it. On the other hand, we compute its flow along $X_{H_t}$ forward and backward in time, we project it to the two sphere components of $\mathbb{S}^2_1 \times \mathbb{S}^2_2$ and we also plot it. In Figure 4.10 we can see the resulting plot, which can be compared to the pinched torus of Figure 4.9.

The flow $\varphi_L$ generated by $X_L$ at any regular point on the fiber $\Lambda^t_{p_{+,-}}$ is simple to describe since the trajectory of regular point under $X_L$ is just the coupled rotation around the vertical axis of both sphere components of $\mathbb{S}^2_1 \times \mathbb{S}^2_2$. That is, along an orbit of $X_L$, the height coordinates $z_1$ and $z_2$ remain constant while the angles $\theta_1$ and $\theta_2$ change at the same speed. Then, an orbit of $X_L$ gets projected to a circle in both

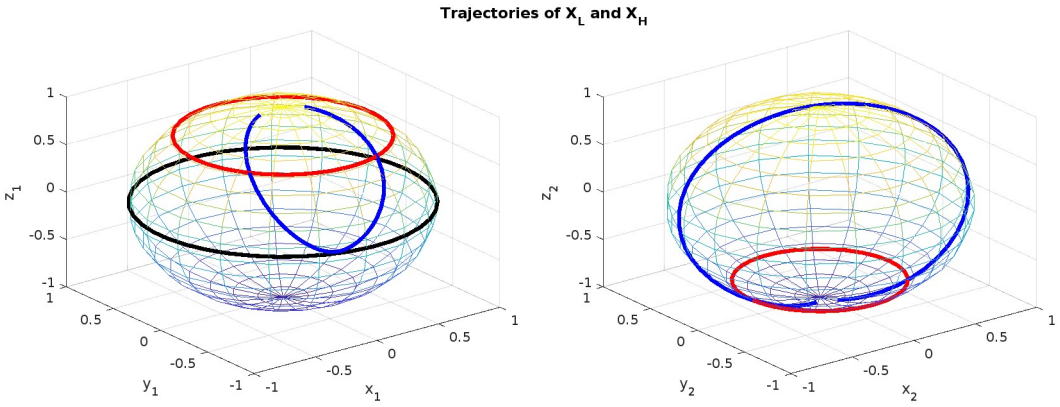


FIGURE 4.10: Plot of the trajectories of a point in the fiber $\Lambda^t_{p_{+,-}}$ of System 1 under the joint flow of $F_t = (L, H_t)$ projected to both components of $\mathbb{S}^2_1 \times \mathbb{S}^2_2$. In red, the trajectory under $X_L$. In blue, the trajectory under $X_{H_t}$. In black, the equator $\{z_1 = 0\}$ where the $b$-symplectic form is singular. See Section B.2 in Appendix B for the code generating the plot.

components of $\mathbb{S}^2_1 \times \mathbb{S}^2_2$ (see the red trajectory in Figure 4.10).

The evolution of the trajectories generated by the flow of $X_{H_t}$ (see Equation (4.15)) is more intricate. In Figure 4.10 and depicted in blue we see the projection of an orbit of $X_{H_t}$ to the two sphere components of $\mathbb{S}^2_1 \times \mathbb{S}^2_2$. Since it is a homoclinic orbit which starts and ends at the focus focus point $p_{+,-} = (0, 0, 1, 0, 0, -1)$, we see that it gets projected to a homoclinic orbit at the North Pole $(0, 0, 1)$ on $\mathbb{S}^2_1$ and it gets projected to a homoclinic orbit at the South Pole $(0, 0, -1)$ on $\mathbb{S}^2_2$.

We also see in Figure 4.10 that the trajectory of $X_{H_t}$ depicted in blue gets close to the singular hypersurface $Z = \{z_1 = 0\}$ depicted in black but does not intersect it. In Figure 4.11 we can analyze in detail how the coordinates $\theta_1, z_1, \theta_2, z_2$ of the trajectory depicted in blue in Figure 4.10 evolve in time.

We obtain an evidence of the fact that the computed orbit of $X_{H_t}$ is a homoclinic orbit at $p_{+,-} = (0, 0, 1, 0, 0, -1)$, since it tends to $p_{+,-}$ both forward and backward in time. We also observe that the value of the coordinate $z_1$ gets close to 0 but never reaches it, which is consistent with the fact that $Z$ is invariant by the flows of Hamiltonian $b$-vector fields (see Section 2.3 in Chapter 2) and, hence, the orbit of any point in $M \setminus Z$ and the orbit of any point in $Z$ are disjoint.

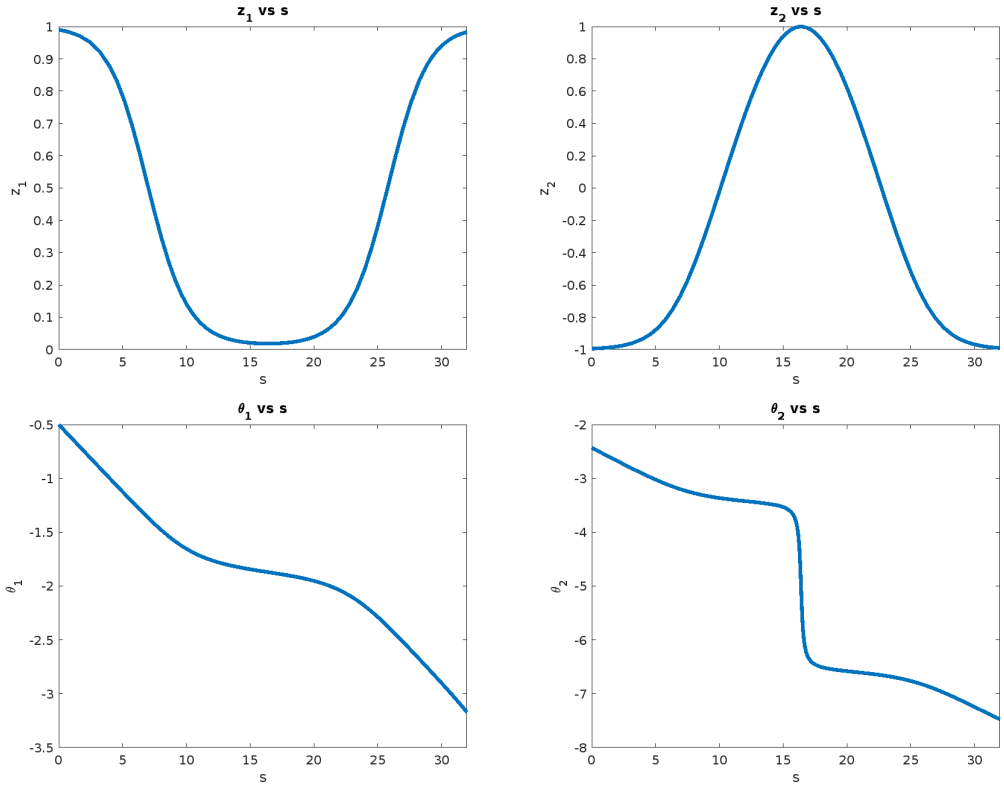


FIGURE 4.11: Evolution over the time variable $s$ of the four coordinates $\theta_1, z_1, \theta_2, z_2$ of a point in the fiber $\Lambda^t_{p_{+,-}}$ of System 1 under the flow of $X_{H_t}$. See Section B.2 in Appendix B for the code generating the plots.

# Chapter 5

# Bohr-Sommerfeld quantization of b-symplectic toric manifolds

In this chapter we revisit the Bohr-Sommerfeld quantization of symplectic toric manifolds and the result of Guillemin and Sternberg which relates it to the integer points in its Delzant polytope [GS83]. Then, we define a *Bohr-Sommerfeld quantization with sign* for $b$-symplectic toric manifolds that also allows us to read the quantization from its $b$-Delzant polytope and which is finite whenever the manifold is compact.

Next, we prove our main result, which states that, for any quantizable $b$-symplectic toric manifold, the Bohr-Sommerfeld quantization with sign agrees with the formal geometric quantization of [GMW18b].

With respect to the published papers [MMW22] and [MM21], this chapter includes the essential new results of both. We kept the same proofs of the paper except for the proof of Proposition 5.2, which was rewritten in order to clarify it. The basic but not-so-short introduction to geometric quantization that we required in the published papers and that we consider good to have at the readers' disposal is included in Chapter 2.

This chapter is organized as follows: In Section 5.1 we prove that the Bohr-Sommerfeld leaves of a quantizable $b$-symplectic toric manifold can be obtained from the image of the moment map of the torus action. In Section 5.2 we introduce the Bohr-Sommerfeld quantization with sign via $\mathbb{T}$-modules. In Section 5.3 we prove the equivalence between Bohr-Sommerfeld quantization and formal geometric quantization both for quantizable symplectic and quantizable $b$-symplectic toric manifolds. In Section 5.4 we propose a model, redefining the previous quantizations, for non.degenerate singularities with elliptic and hyperbolic components. Throughout all this chapter, we use $\mu$ instead of $F$ to denote the moment map of an integrable system, as it is done in the literature on geometric quantization, and we also take the usual convention of setting $\hbar$ equal to 1.

## 5.1 Bohr-Sommerfeld leaves via the moment map

In this section we revisit the proof of the fact that, for a quantizable symplectic toric manifold, the set of Bohr-Sommerfeld leaves, which we call the *Bohr-Sommerfeld set*,

is in one-to-one correspondence with the set of integer points in the image of the moment map of the torus action. That is why we refer to the set of images of the Bohr-Sommerfeld leaves by the moment map also as the *Bohr-Sommerfeld set*. Then, we adapt the proof to show that the same result also holds for quantizable $b$-symplectic toric manifolds.

First, let us recall a result from Guillemin and Sternberg [GS83] that identifies the Bohr-Sommerfeld leaves in a symplectic manifold using the moment map of an integrable system. In particular, it proves that the count of Bohr-Sommerfeld leaves of a quantizable symplectic manifold equals the count of the integer points in the image of the moment map. This result has also been used to identify Bohr-Sommerfeld leaves in moduli spaces by Jeffrey and Weitsman [JW92].

**Theorem 5.1** (Guillemin-Sternberg, Theorem 2.4 in [GS83])**.** *Let $(M^{2n}, \omega)$ be a quantizable symplectic manifold endowed with an integrable system with moment map $\mu : M \to B$. Let $p$ and $q$ be two distinct points of $B$ contained in an open simply connected subset $B_0$ of $B$. Then:*

- *There exists a globally defined system of action coordinates $f_1, \dots, f_n$ on $B_0$ such that $f_1(p) = \cdots = f_n(p) = 0$, and*
- *if $p \in B$ is in the Bohr-Sommerfeld set, that is, if $\pi^{-1}(p)$ is a Bohr-Sommerfeld leaf, then $q \in B$ is in the Bohr-Sommerfeld set if and only if $f_1(q), \dots, f_n(q)$ are integers.*

In Theorem 5.1, the correspondence between the Bohr-Sommerfeld leaves and the integer points of the moment map is established after the election of a globally defined system of action coordinates. After a Bohr-Sommerfeld leaf is identified at a point $p \in B$, the origin of all the action coordinates $f_1, \dots, f_n$ is set at $p$ and the rest of integer points in these coordinates correspond to the rest of Bohr-Sommerfeld leaves.

As a consequence, the integer condition that the Bohr-Sommerfeld leaves have to satisfy can be shifted by an additive constant as long as it is the same constant for all the leaves, since the essential implication of Theorem 5.1 is that the difference between the action variables at any two Bohr-Sommerfeld leaves is an integer. In view of this, the value of the moment map has to be fixed at some point of $M$ or, equivalently, at some leaf of $M$. This can always be done by resetting the constant in the moment map $\mu : M \to B$ or, equivalently, by selecting an appropriate connection 1-form $\theta$ which is a *symplectic potential* for $M$, that is, which satisfies $d\theta = \omega$. with curvature $\omega$.

A symplectic toric manifold $(M^{2n}, \omega, \mu)$ is an integrable system with moment map $\mu : M \to \mathbb{R}^n$ in which Theorem 5.1 can be applied directly. It allows to identify the Bohr-Sommerfeld leaves of $M$ with the integer points in the image of the moment map. We want to extend this correspondence to $b$-symplectic toric manifolds and, to do so, we first revisit the proof of Theorem 5.1 for the particular case of symplectic toric manifolds in Proposition 5.2. Then, we prove the same result for $b$-symplectic toric manifolds in Corollary 5.3, which is a consequence of Proposition 5.2.

**Proposition 5.2.** *Let $(M, \omega, \mu)$ be a quantizable symplectic toric manifold. There is a one-to-one correspondence between the Bohr-Sommerfeld set and the set of integer points in the image of $\mu$.*

*Proof.* Suppose $(M^{2n}, \omega, \mu)$ is a quantizable symplectic toric manifold with Hermitian line bundle $\pi : \mathbb{L} \to M$ with connection $\nabla$ of curvature $\omega$. We will compute the Bohr-Sommerfeld leaves of $M$ with respect to the real polarization $P$ given by $\mu$ and see that each one of them is mapped to an integer point of $\mu(M)$.

We construct the action and angle coordinates on $M$ of Theorem 2.10 in the following way. We take a basis $(\xi_1, \dots, \xi_1)$ of $\mathbb{R}^n$ such that the orbits of the action of $\exp t\xi_i$ on $M$ are periodic with minimal period $2\pi$. Then, the functions $\mu_i = \langle \mu, \xi_i \rangle$ are the action coordinates and the parameters along the orbits of $\exp t\xi_i$, which we denote by $\phi_i$, are the angle coordinates. In these coordinates, the symplectic form on $M$ has the expression

$$\omega = d\theta = d\left(\sum_{i=1}^{n} \mu_i d\phi_i\right) = \sum_{i=1}^{n} d\mu_i \wedge d\phi_i.$$

The Hermitian line bundle $\pi : \mathbb{L} \to M$ is just $M \times \mathbb{C}$ because $\omega = d\theta$ is exact and, hence, we can take $s_0 : M \to \mathbb{L} : p \mapsto (p, 1)$ as a trivializing section of $\mathbb{L}$.

Notice that the real polarization $P$ induced by $\mu$ is the Lagrangian involutive distribution whose integral manifolds are the tori generated by the action of the torus group $\mathbb{T}^n$ on $(M, \omega)$ with moment map $\mu$, which are parametrized by $\phi_1, \dots, \phi_n$. The Bohr-Sommerfeld leaves of the polarization $P$ are the ones supporting polarized sections, that is, sections $s$ of $\mathbb{L}$ satisfying $\nabla_X(s) = 0$ for any vector field $X$ tangent to $P$. Then, the Bohr-Sommerfeld leaves are those admitting sections $s = fs_0$ of $L$ which are polarized with respect $P$, that is, sections satisfying, for all $j = 1, \dots, n$, $\nabla_{\frac{\partial}{\partial \phi_j}}(fs_0) = 0$.

This equivalent to

$$\nabla_{\frac{\partial}{\partial \phi_j}}(fs_0) = \frac{\partial f}{\partial \phi_j} s_0 + if\langle \theta, \frac{\partial}{\partial \phi_j} \rangle s_0 = \left(\frac{\partial f}{\partial \phi_j} + if\mu_j\right) s_0 = 0,$$

and, therefore, $s = fs_0$ is polarized with respect to $P$ if, for all $j = 1, \dots, n$,

$$\frac{\partial f}{\partial \phi_j} = -if\mu_j.$$

If $f \neq 0$ at a point $p \in M$, then $f$ does not vanish on the whole orbit of the torus action through $p$ and we have

$$\frac{df}{f} = -i\mu_j(p)d\phi_j. \tag{5.1}$$

Integrating Equation (5.1) from 0 to $2\pi$ along any $\mathbb{S}^1$-orbit of $\exp t\xi_i$, we obtain

$$\ln(f)|_{\phi_j=0}^{\phi_j=2\pi} = -i\int_0^{2\pi} \mu_j(p)d\phi_j. \tag{5.2}$$

Now, on the one hand, the value of $\mu_j$ is constant along any leaf of $P$ and, hence, it does not depend on $\phi_j$ and Equation (5.2) is equivalent to

$$\ln(f)|_{\phi_j=2\pi} - \ln(f)|_{\phi_j=0} = -i2\pi\mu_j(p). \tag{5.3}$$

On the other hand, the value of $f$ at $\phi_j = 0$ has to coincide with the value of $f$ at $\phi_j = 2\pi$ in order to be a well-defined section. Then,

$$1 = \frac{f|_{\phi_j=2\pi}}{f|_{\phi_j=0}} = \frac{e^{\ln f|_{\phi_j=2\pi}}}{e^{\ln f|_{\phi_j=0}}} = e^{\ln f|_{\phi_j=2\pi} - \ln f|_{\phi_j=0}},$$

which implies that

$$\ln f|_{\phi_j=2\pi} - \ln f|_{\phi_j=0} = 2\pi i k_j,$$

with $k_j \in \mathbb{Z}$.

Hence, Equation 5.2 can be rewritten as

$$2\pi i k_j = -i2\pi\mu_j(p), \tag{5.4}$$

and it leads to the following condition on the moment map components $\mu_j$ at the points $p$ in $M$ where $f(p) \neq 0$: for all $j = 1, \ldots, n$, $\mu_j(p)$ is an integer number $k_j$. As a consequence, from Equation 5.1 we deduce that

$$f = f_0 e^{i(k_1\phi_1 + \cdots + k_n\phi_n)},$$

with $f_0$ a constant.

Then, we just proved that there exist polarized sections that are supported on some particular leaves of $P$: the ones in which it is fulfilled that, for all $j = 1, \ldots, n$, the value of the moment map component $\mu_j(p)$ is an integer number $k_j$. These leaves, which are tori and make up the Bohr-Sommerfeld set, are therefore in one-to-one correspondence with the set of integer points in the image of $\mu$. □

**Corollary 5.3.** *Let $(M^{2n}, Z, \omega, \mu)$ be a quantizable b-symplectic toric manifold. Suppose that each connected component $Z_i$ of the critical hypersurface $Z \subset M$ has a nonzero modular weight. Then, there is a one-to-one correspondence between the Bohr-Sommerfeld set and the set of integer points in the image of $\mu$.*

*Proof.* By Proposition 2.35, in a neighborhood $L \times \mathbb{S}^1 \times (-\varepsilon, \varepsilon) \cong U \subseteq M$ of any connected component $Z_i$ of $Z$, where $L$ is a leaf of the symplectic foliation of $Z_i$, the moment map of the $b$-toric integrable system is

$$\mu_{U\setminus Z_i} : L \times \mathbb{S}^1 \times ((-\varepsilon, \varepsilon) \setminus \{0\}) \to \mathbb{R}^{n-1} \times \mathbb{R} : (\ell, \theta, t) \mapsto (\mu_L(\ell), c \log|t|),$$

where $c$ is the modular weight of $Z_i$, which is non-zero, and $\mu_L : L \to \mathbb{R}^{n-1}$ is a moment map for the $b$-toric integrable system restricted to $L$.

As $M \setminus Z$ is a quantizable symplectic toric manifold, we can apply Proposition 5.2 on $M \setminus Z$. Then, Bohr-Sommerfeld leaves of $M \setminus Z$ correspond to the points $(\mu_L(\ell), c \log |t|)$ such that $\mu_L(\ell) \in \mathbb{Z}^{n-1}$ and $c \log |t| \in \mathbb{Z}$. □

We will use Corollary 5.3 in the following section to identify the Bohr-Sommerfeld leaves of a $b$-symplectic toric manifold via its moment map. From now on, in order to apply Corollary 5.3, we assume that the modular weights of all the $b$-symplectic toric manifolds we consider are non-zero.

## 5.2 Bohr-Sommerfeld quantization with sign for b-symplectic toric manifolds

In this section we introduce the notion of counting Bohr-Sommerfeld leaves to find the quantization virtual vector spaces and we redefine the standard Bohr-Sommerfeld quantization in order to have it defined as a sum of $\mathbb{T}$-modules, which will allow us to quantize $b$-symplectic toric manifolds. First, we do it for the case of symplectic toric manifolds, in which the quantization is finite. Then, using the orientation of the manifold, we define a quantization with sign that allows us to construct the quantization as a $\mathbb{T}$-module. We illustrate these concepts with the quantization of the 2-sphere.

### 5.2.1 Bohr-Sommerfeld quantization via T-modules

We start revisiting the Bohr-Sommerfeld quantization for symplectic toric manifolds. Assume that $(M, \omega, \mu)$ is a symplectic toric manifold, that $\pi : \mathbb{L} \to M$ is a Hermitian line bundle with connection $\nabla$ of curvature $\omega$, and suppose that $B_{BS}$ is the Bohr-Sommerfeld set of the polarization given by the moment map $\mu$, that is,

$$B_{BS} = \{b \in \mathrm{Im}(\mu) \colon \mu^{-1}(b) \text{ is a Bohr-Sommerfeld leaf}\},$$

and $s_b$ is the corresponding polarized section of $\mathbb{L}|_{\mu^{-1}(b)}$.

To each $b \in B_{BS}$ which is a regular value of $\mu$ or, equivalently, which is in the interior of the image of the moment map $\Delta = \mu(M)$, we can associate a representation $\mathbb{C}(b)$ of $\mathbb{T}^n$, where $b$ is the weight obtained by taking the quotient with the lifted action given by $\mu$. By the following Proposition, this representation $\mathbb{C}(b)$ is equal to the representation $\mathbb{C}\langle s_b \rangle$ that appears in Equation (2.9).

**Proposition 5.4.** *For any $b = \mu(x) \in B_{BS}$ in the interior of $\Delta = \mu(M)$, $\mathbb{C}\langle s_b \rangle = \mathbb{C}(b)$.*

*Proof.* Suppose $b = \mu(x) \in B_{BS}$. Then, $s_b$ is a section of the Hermitian line bundle $\mathbb{L}$ over $M$ that satisfies the polarization condition $\nabla_X(s_b) = 0$. If $b$ is in the interior of $\Delta = \mu(M)$, it has a neighborhood $U$ in which all points are regular values of $\mu$. Equivalently, it has a neighborhood $U$ such that the torus action has no singularities in its pre-image $\mu^{-1}(U)$. Then, on the pre-image of $\mu^{-1}(b)$, which is a torus $\mathbb{T}^n$, the line bundle $\mathbb{L}$ restricts to a line bundle $\mathbb{L} \to \mu^{-1}(b)$. The connection on this line bundle $\mathbb{L} \to \mu^{-1}(b)$, since $\mu(x)$ is integer, is given by the line $\mathbb{C}(\mu(x))$, where

$\mathbb{C}(\mu(x))$ is the quotient $\mathbb{L}_{\mu^{-1}(\mu(x))}/\mathbb{T}^n$ [Kos70]. Hence, the representation $\mathbb{C}\langle s_b\rangle$ is $\mathbb{C}(\mu(x)) = \mathbb{C}(b)$. □

In the case of a point $b$ in the boundary of $\Delta$, the identification in Proposition 5.4 does not hold. Instead, the quantization for such point $b$ is directly defined as the representation $\mathbb{C}(b)$. This way, either if $b \in B_{BS}$ is in the interior or in the boundary of the $\Delta$, there is a representation $\mathbb{C}(b)$ associated to it, and the Bohr-Sommerfeld quantization is defined as follows.

**Definition 5.5.** *The Bohr-Sommerfeld quantization of a quantizable symplectic toric manifold is*

$$Q(M) = \bigoplus_{b\in B_{BS}} \mathbb{C}(b). \tag{5.5}$$

Notice that the infinite sum $\bigoplus_{b\in B_{BS}} \mathbb{C}(b)$ is well defined because the group action of $\mathbb{T}^n$ on $M$ is acting with weights with finite multiplicity. Also, observe that the quantization $Q(M)$ can also be defined directly as $Q(M) = \bigoplus_{b\in\Delta\cap Z^n} \mathbb{C}(b)$, since the Bohr-Sommerfeld set $B_{BS}$ is precisely composed of the integer points in the image of the moment map.

The quantization $Q(M)$ may be an infinite-dimensional module since the sum $\bigoplus_{b\in B_{BS}} \mathbb{C}(b)$ may have infinitely many terms if $M$ is a non-compact toric manifold, because $\Delta$ may be unbounded. In particular, if try to quantize a $b$-symplectic toric manifold, which is a compact manifold, using Definition 5.5, we obtain an infinite-dimensional quantization space. But the quantization of a compact manifold is expected to be finite, and that is why we introduce in the following sections a *Bohr-Sommerfeld quantization with sign* for $b$-symplectic toric manifolds, which we define again as a $\mathbb{T}$-module.

### 5.2.2 The motivating example, the Bohr-Sommerfeld quantization of the canonical b-sphere

The simplest example of a $b$-symplectic toric manifold is the *$b$-2-sphere* $(\mathbb{S}^2, Z, \omega)$ of Example 2.28 endowed with the action of $\mathbb{S}^1$ that makes it rotate around its vertical axis. We are going to see that its standard Bohr-Sommerfeld quantization gives an infinite-dimensional space and that, on the other hand, its Bohr-Sommerfeld quantization *with sign* gives a finite-dimensional space. Later, in Section 5.3 we will prove that the latter quantization coincides with the formal geometric quantization in the general case.

Consider the $b$-symplectic sphere $(\mathbb{S}^2, Z, \omega)$, that is, the unit sphere $\mathbb{S}^2 \subset \mathbb{R}^3$ with the critical hypersurface $Z$ in the equator $\{z = 0\}$ and with a $b$-symplectic form $\omega$ that coincides with the standard symplectic form of $\mathbb{S}^2$ in the North and South poles and has the expression $\omega = d\theta \wedge \frac{dz}{z}$ away from the poles in the cylindrical coordinates $\{(z,\theta)\colon -1 < z < 1, 0 \leq \theta < 2\pi\}$.

Make $(\mathbb{S}^2, Z, \omega)$ into a $b$-symplectic toric manifold by equipping it with the rotation action of $\mathbb{S}^1$ around the vertical axis, which has as moment map the $b$-function $\mu = -\log|z|$ and as Hamiltonian $b$-vector field $X_\mu = \frac{\partial}{\partial\theta}$.

Let $\mathbb{L}$ be a Hermitian line bundle on $\mathbb{S}^2$ with connection $\nabla$ of curvature $\omega$ defined on $\mathbb{S}^2 \setminus Z$ by

$$\nabla_X(s) = X(s) - i \log|z|\, d\theta(X)s,$$

and consider the real polarization $P$ of $\mathbb{S}^2 \setminus Z$ induced by the moment map $\mu = -\log|z|$. The polarization is made of infinitely many circles of the form $\{z_0\} \times \mathbb{S}^1$, with $z_0 \in (-1,0) \cup (0,1)$, and the two poles, which are the only two non-regular leaves.

The polarized sections of $P$, which satisfy $\nabla_X(s) = 0$ for any $X$ tangent to the polarization $P$, are of the form

$$s(z,\theta) = a(z)e^{i \log|z|\theta}, \tag{5.6}$$

with $a(z) \in \mathbb{C}$ (see the proof of Proposition 5.2 for the explicit computation of the polarized sections of a real polarization). And the Bohr-Sommerfeld leaves are precisely the leaves of $P$ that admit a non-trivial polarized section $s$, that is, the leaves of $P$ that admit sections of the form $s = a(z)e^{i \log|z|\theta}$ with $a(z)$ not identically zero.

Along each leaf $\{z_0\} \times \mathbb{S}^1$ of the polarization $P$ of $\mathbb{S}^2 \setminus Z$, the coordinate $z$ is fixed and the angular coordinate $\theta$ takes values from 0 to $2\pi$. Then, a leaf $\{z_0\} \times \mathbb{S}^1$ is a Bohr-Sommerfeld leaf if it admits a section $s(z_0,\theta)$ such that

$$s(z_0,\theta) = s(z_0,\theta + 2\pi).$$

Therefore, $\{z_0\} \times \mathbb{S}^1$ is a Bohr-Sommerfeld leaf if $1 = e^{2\pi i \log|z_0|}$ or, equivalently, if $\log|z_0| \in \mathbb{Z}$. This is exactly what Corollary 5.3 gives if we use it directly on $(\mathbb{S}^2, Z = \{z = 0\}, \omega = d\theta \wedge \frac{dz}{z}, \mu = -\log|z|)$. Hence, the set of all Bohr-Sommerfeld leaves of $P$ is

$$B_{BS} = \{\{e^{-m}\} \times \mathbb{S}^1 \subset \mathbb{S}^2 \setminus Z \colon m \in \mathbb{N}\} \bigcup \{\{-e^{-m}\} \times \mathbb{S}^1 \subset \mathbb{S}^2 \setminus Z \colon m \in \mathbb{N}\}.$$

The Bohr-Sommerfeld quantization of $(\mathbb{S}^2, Z, \omega, \mu)$ is, by Definition 5.5, the following

$$Q(\mathbb{S}^2) = \bigoplus_{b \in B_{BS}} \mathbb{C}(b) = \bigoplus_{b \in \mathbb{N}} \mathbb{C}(b) \oplus \mathbb{C}(b),$$

which is an infinite-dimensional space.

Observe also that the quantization is infinite-dimensional because there is an infinite number of Bohr-Sommerfeld leaves arbitrarily close to $Z$ both in the upper and the lower hemisphere (see Figure 5.1). Explicitly, for any $a > 0$, there is an infinite number of values of $z \in (0,a)$ and also of $z \in (-a,0)$ satisfying the condition $\log|z| \in \mathbb{Z}$.

### 5.2.3 Bohr-Sommerfeld quantization with sign for the b-symplectic toric sphere

Consider now a more general version of the $b$-symplectic sphere in which the critical hypersurface is any circle $\{z_0\} \times \mathbb{S}^1$ parallel to the equator and the $b$-symplectic

form is $\omega = d\theta \wedge \frac{dz}{z-z_0}$. To make it into a $b$-symplectic toric sphere endow it with the moment map $\mu = -\log|z - z_0|$, which induces the Hamiltonian $b$-vector field $X_\mu = \frac{\partial}{\partial\theta}$ and a rotation action of $\mathbb{S}^1$ around the vertical axis. In order to obtain a finite-dimensional quantization of $(\mathbb{S}^2, Z = \{z_0\} \times \mathbb{S}^1, \omega, \mu)$ we will define a *Bohr-Sommerfeld quantization with sign*. That is, we will define a signed sum of the quantization spaces corresponding to the Bohr-Sommerfeld leaves of $\mathbb{S}^2$ that takes into account the orientation of the connected component of $\mathbb{S}^2 \setminus Z$ in which each Bohr-Sommerfeld leaf lies. Morally, we will define the quantization space by "adding" the virtual vector spaces of Bohr-Sommerfeld leaves lying in one component and "subtracting" the virtual vector spaces of Bohr-Sommerfeld leaves lying in the other component. This way, the final quantization space will be a finite-dimensional virtual vector space.

Endow $(\mathbb{S}^2, Z = \{z_0\} \times \mathbb{S}^1, \omega, \mu)$ with a Hermitian line bundle $\mathbb{L}$ with connection $\nabla$ of curvature $\omega$, consider the real polarization $P$ of $\mathbb{S}^2 \setminus Z$ induced by $\mu$ and identify the Bohr-Sommerfeld leaves of $P$ applying Corollary 5.3, that is, as the leaves that are mapped to an integer point by the moment map $\mu$. To each Bohr-Sommerfeld leaf of $P$, one can associate a sign $+$ or $-$ depending on the component of $\mathbb{S}^2 \setminus Z$ to which it belongs, which is either $\mathbb{S}^2_+ := (z_0, 1) \times \mathbb{S}^1 \subset \mathbb{S}^2 \setminus Z$ or $\mathbb{S}^2_- := (-1, z_0) \times \mathbb{S}^1 \subset \mathbb{S}^2 \setminus Z$.

**Definition 5.6.** *Let $B_{BS}$ be the Bohr-Sommerfeld set of $(\mathbb{S}^2, Z = \{z_0\} \times \mathbb{S}^1, \omega, \mu)$. For each $b \in B_{BS}$, define $\epsilon(b)$ as $\epsilon(b) = +1$ if $\mu^{-1}(b)$ is a Bohr-Sommerfeld leaf in $\mathbb{S}^2_+$ and $\epsilon(b) = -1$ if $\mu^{-1}(b)$ is a Bohr-Sommerfeld leaf in $\mathbb{S}^2_-$. We call $\epsilon(b)$ the* sign of the Bohr-Sommerfeld leaf corresponding to $b$.

Formally, we define the *Bohr-Sommerfeld quantization with sign* of the $b$-symplectic toric sphere $(\mathbb{S}^2, Z = \{z_0\} \times \mathbb{S}^1, \omega, \mu)$ as the direct difference of the sum of the virtual vector spaces $\mathbb{C}(b)$ associated to the Bohr-Sommerfeld leaves in $\mathbb{S}^2_+ = (z_0, 1) \times \mathbb{S}^1 \subset \mathbb{S}^2 \setminus Z$ and the sum of the virtual vector spaces $\mathbb{C}(b)$ associated to the Bohr-Sommerfeld leaves in $\mathbb{S}^2_- = (-1, z_0) \times \mathbb{S}^1 \subset \mathbb{S}^2 \setminus Z$.

**Definition 5.7** (Bohr-Sommerfeld quantization with sign of a $b$-2-sphere)**.** *Let $B_{BS}$ be the Bohr-Sommerfeld set of $(\mathbb{S}^2, Z = \{z_0\} \times \mathbb{S}^1, \omega, \mu)$. The* quantization with sign of $(\mathbb{S}^2, Z = \{z_0\} \times \mathbb{S}^1, \omega, \mu)$ *is*

$$\tilde{Q}(\mathbb{S}^2) = \bigoplus_{b \in B_{BS}} \epsilon(b)\mathbb{C}(b).$$

**Lemma 5.8.** *The quantization $\tilde{Q}(\mathbb{S}^2)$ is a finite-dimensional vector space.*

*Proof.* First, observe that $\bigoplus_{b \in B_{BS}} \epsilon(b)\mathbb{C}(b)$ is an infinite-dimensional module but it is well-defined because its multiplicities, which may be negative, are finite.

For any $\delta > 0$ small enough, and for each Bohr-Sommerfeld leaf of the form $\{z_0 + \delta\} \times \mathbb{S}^1$ in $\mathbb{S}^2_+$, there is a Bohr-Sommerfeld leaf of the form $\{z_0 - \delta\} \times \mathbb{S}^1$ in $\mathbb{S}^2_-$. Then, at any symmetric neighborhood $U$ of $Z = \{z_0\} \times \mathbb{S}^1$ in $\mathbb{S}^2 \setminus Z$, the virtual module $\bigoplus_{b \in B_{BS} \cap \mu(U)} \epsilon(b)\mathbb{C}(b)$ is exactly 0.

On the other hand, there are only finitely many Bohr-Sommerfeld leaves in $\mathbb{S}^2 \setminus U$ and, therefore, $\bigoplus_{b \in B_{BS} \cap \mu(\mathbb{S}^2 \setminus U)} \epsilon(b)\mathbb{C}(b)$ is finite-dimensional. Hence, $\tilde{Q}(\mathbb{S}^2)$ is a finite-dimensional vector space. □

Observe that, in the particular case that the critical hypersurface $Z$ is the equator $\{0\} \times \mathbb{S}^1$, the Bohr-Sommerfeld quantization with sign of the $b$-symplectic toric sphere $(\mathbb{S}^2, Z, \omega, \mu)$, is the zero-dimensional vector space due to the symmetry in the set of Bohr-Sommerfeld leaves (see Figure 5.1).

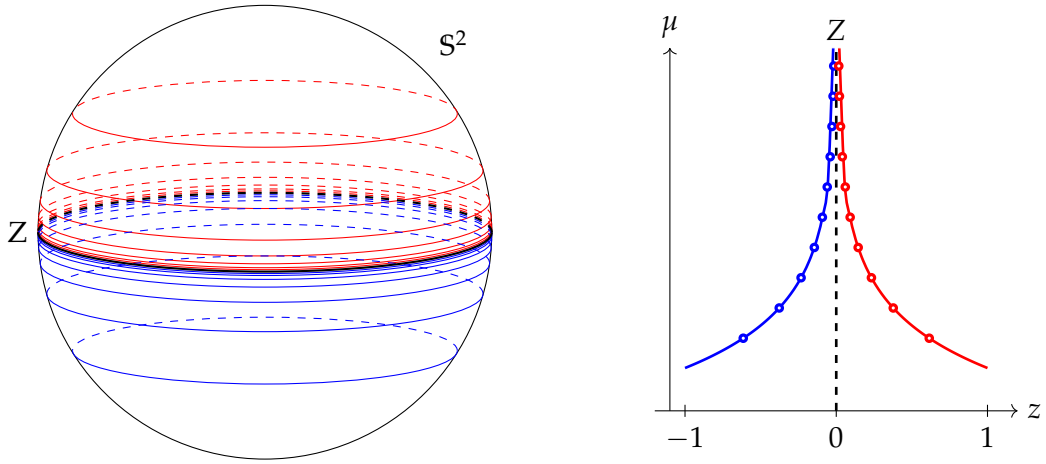


FIGURE 5.1: On the left, Bohr-Sommerfeld leaves on the northern hemisphere (in red) and the southern hemisphere (in blue) of the real polarization of $(\mathbb{S}^2, Z = \{z = 0\} \times \mathbb{S}^1, \omega, \mu)$ induced by $\mu$. On the right, the moment map $\mu = -\log|z|$ with the dots indicating Bohr-Sommerfeld leaves.

### 5.2.4 Bohr-Sommerfeld quantization with sign for a b-symplectic toric surface

We can naturally generalize the definition of Bohr-Sommerfeld quantization with sign of the $b$-symplectic toric sphere $(\mathbb{S}^2, Z = \{z_0\} \times \mathbb{S}^1, \omega, \mu)$ to any $b$-symplectic toric surface $(M^2, Z, \omega, \mu)$. Suppose that $(M^2, Z, \omega, \mu)$ is a quantizable system endowed with a Hermitian line bundle $\mathbb{L}$ with connection $\nabla$ of curvature $\omega$, consider the real polarization $P$ of $\mathbb{S}^2 \setminus Z$ induced by $\mu$ and identify the Bohr-Sommerfeld leaves of $P$ applying Corollary 5.3, that is, as the leaves that are mapped to an integer point by the moment map $\mu$.

By Theorem 2.34, the $b$-symplectic toric surface $(M^2, Z, \omega, \mu)$ is diffeomorphic either to the $b$-symplectic toric sphere $(\mathbb{S}^2, Z, \omega, \mu)$ studied in the last section or to the $b$-symplectic torus $(\mathbb{T}^2, Z, \omega)$. In all cases, the $b$-symplectic form defines an orientation in each connected component of $M^2 \setminus Z$, and we can associate a sign $+$ or $-$ to each Bohr-Sommerfeld leaf of $P$ depending on whether the orientation of the component to which it belongs agrees with the orientation of $M$.

**Definition 5.9.** *Let $B_{BS}$ be the Bohr-Sommerfeld set of $(M^2, Z, \omega, \mu)$. For each $b \in B_{BS}$, define $\epsilon(b)$ as $\epsilon(b) = +1$ if $\mu^{-1}(b)$ belongs to a component whose orientation agrees with that given by the b-symplectic form and as $\epsilon(b) = -1$ if $\mu^{-1}(b)$ belongs to a component*

*whose orientation is the opposite of that given by the b-symplectic form. We call* $\epsilon(b)$ *the* sign of the Bohr-Sommerfeld leaf corresponding to $b$.

Again, we define the *Bohr-Sommerfeld quantization with sign* of the $b$-symplectic toric manifold $(M^2, Z, \omega, \mu)$ as the direct sum of the virtual vector spaces $\mathbb{C}(b)$ associated to each Bohr-Sommerfeld $\mu^{-1}(b)$ and taking into account their sign $\epsilon(b)$.

**Definition 5.10** (Bohr-Sommerfeld quantization with sign of a $b$-symplectic toric surface)**.** *Let* $B_{BS}$ *be the Bohr-Sommerfeld set of* $(M^2, Z, \omega, \mu)$. *The* quantization with sign of $(M^2, Z, \omega, \mu)$ *is*

$$\tilde{Q}(M^2) = \bigoplus_{b \in B_{BS}} \epsilon(b)\mathbb{C}(b).$$

**Lemma 5.11.** *The quantization* $\tilde{Q}(M^2)$ *is a finite-dimensional vector space.*

*Proof.* Take a symmetric neighborhood $U \subset M^2 \setminus Z$ of $Z$. Such a neighborhood exists by Proposition 2.35. By the argument in the proof of Lemma 5.8, the contribution of leaves in $U \setminus Z$ to the sum $\bigoplus_{b \in B_{BS}} \epsilon(b)\mathbb{C}(b)$ is 0, and the contribution of leaves in $M^2 \setminus U$ is a finite-dimensional vector space. Hence, $\tilde{Q}(M^2)$ is finite-dimensional. □

In the upper part of Figure 5.2 we depicted the Bohr-Sommerfeld leaves of a $b$-symplectic toric sphere with a critical hypersurface $Z$ made of 5 components. In the lower part of the figure, we depicted the image of the moment map one of the same system, marking the integer values with which one can identify the Bohr-Sommerfeld leaves. This example illustrates how a $b$-symplectic toric manifold still yields a finite-dimensional quantization despite having an infinite number of Bohr-Sommerfeld leaves.

### 5.2.5 Bohr-Sommerfeld quantization with sign for a b-symplectic toric manifold

A consequence of Theorem 2.34 is that any $b$-symplectic toric manifold $(M^{2n}, Z, \omega, \mu)$ decomposes either into the product of a $b$-symplectic torus $(\mathbb{T}^2, Z, \omega, \mu)$ with a symplectic toric manifold, or else can be obtained from the product of a $b$-symplectic toric sphere $(\mathbb{S}^2, Z, \omega, \mu)$ with a symplectic toric manifold. This makes it straightforward to define a Bohr-Sommerfeld quantization with sign for $b$-symplectic toric manifolds in the same way that it was done in the previous section, that is, using the orientation given by the $b$-symplectic form on the connected components of $M$.

Suppose that $(M^{2n}, Z, \omega, \mu)$ is a quantizable $b$-symplectic toric manifold endowed with a Hermitian line bundle $\mathbb{L}$ with connection $\nabla$ of curvature $\omega$, consider the real polarization $P$ of $M \setminus Z$ induced by $\mu$ and identify the Bohr-Sommerfeld leaves of $P$ applying again Corollary 5.3, that is, as the leaves that are mapped to an integer point by the moment map $\mu$.

By Theorem 2.34, the $b$-symplectic toric surface $(M^2, Z, \omega, \mu)$ is diffeomorphic either to the $b$-symplectic toric sphere $(\mathbb{S}^2, Z, \omega, \mu)$ studied in the last section or to the $b$-symplectic torus $(\mathbb{T}^2, Z, \omega)$. In all cases, the $b$-symplectic form defines an orientation in each connected component of $M^2 \setminus Z$, and we can associate a sign $+$ or

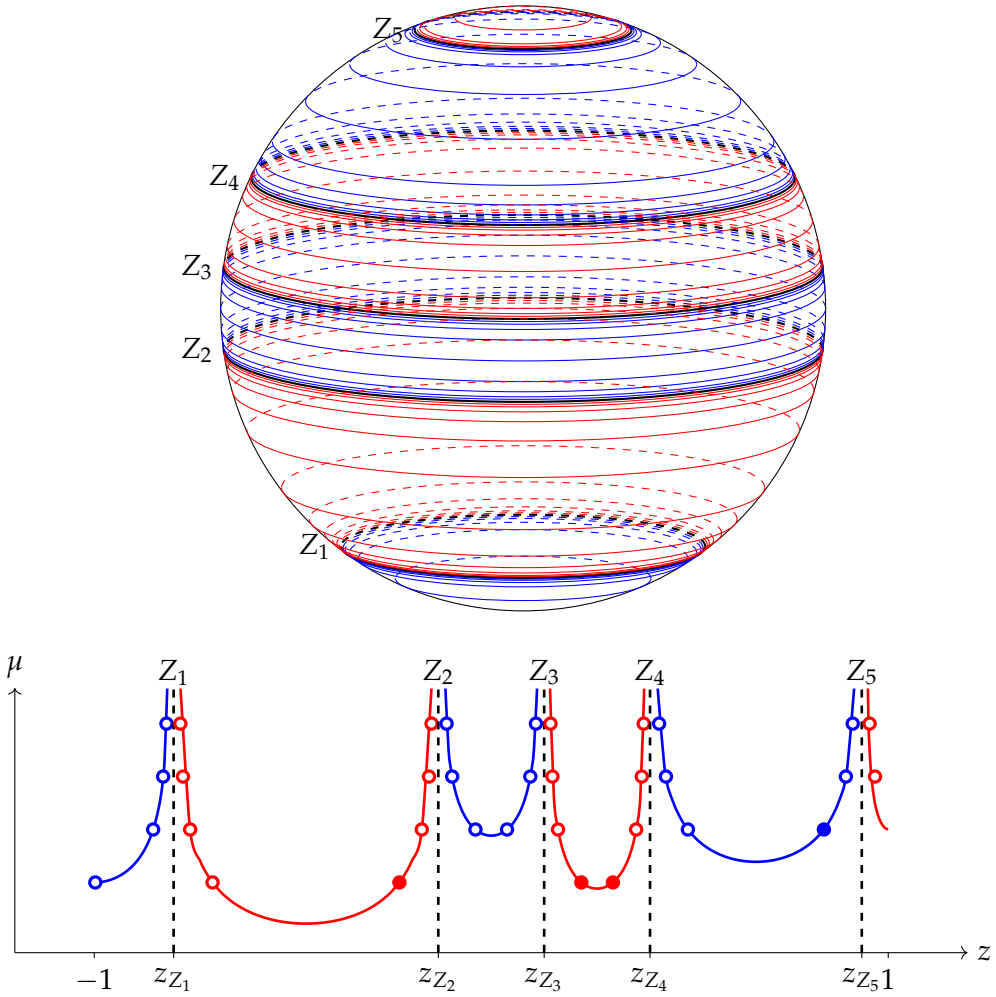


FIGURE 5.2: Above, an example of a $b$-symplectic toric sphere with $Z$ consisting of 5 latitude circles. The blue and red circles correspond to Bohr-Sommerfeld leaves. Below, the moment map of the same system. The blue dots correspond to the Bohr-Sommerfeld leaves in positively oriented components of $\mathbb{S}^2 \setminus Z$. The red dots correspond to the Bohr-Sommerfeld leaves in negatively oriented components of $\mathbb{S}^2 \setminus Z$. White-filled dots represent Bohr-Sommerfeld leaves in the neighborhood of each $Z_i$ whose contributions to the quantization $Q(M)$ cancel.

$-$ to each Bohr-Sommerfeld leaf of $P$ depending on whether the orientation of the component to which it belongs agrees with the orientation of $M$.

**Definition 5.12.** *Let $B_{BS}$ be the Bohr-Sommerfeld set of $(M^{2n}, Z, \omega, \mu)$. For each $b \in B_{BS}$, define $\epsilon(b)$ by $\epsilon(b) = +1$ if $\pi\left(\mu^{-1}(b)\right)$ belongs to a component of $M \setminus Z$ where the orientation of $M$ agrees with the orientation given by $\omega$, and by $\epsilon(b) = -1$ otherwise. We call $\epsilon(b)$ the* sign of the Bohr-Sommerfeld leaf corresponding to $b$.

The *Bohr-Sommerfeld quantization with sign* of the $b$-symplectic toric manifold $(M^{2n}, Z, \omega, \mu)$ is defined as the direct sum of the virtual vector spaces $\mathbb{C}(b)$ associated to each Bohr-Sommerfeld $\mu^{-1}(b)$ and taking into account their sign $\epsilon(b)$.

**Definition 5.13** (Bohr-Sommerfeld quantization with sign of a $b$-symplectic toric manifold)**.** *Let $B_{BS}$ be the Bohr-Sommerfeld set of $(M^{2n}, Z, \omega, \mu)$. The* quantization with

sign of $(M^{2n}, Z, \omega, \mu)$ *is*

$$\tilde{Q}(M^{2n}) = \bigoplus_{b \in B_{BS}} \epsilon(b)\mathbb{C}(b).$$

**Lemma 5.14.** *The quantization $\tilde{Q}(M^{2n})$ is a finite-dimensional vector space.*

*Proof.* Take a symmetric neighborhood $U \subset M^{2n} \setminus Z$. Such a neighborhood always exists by Proposition 2.35.The same argument used in the proof of Lemmas 5.8 and 5.11 shows that $\tilde{Q}(M^{2n})$ is finite-dimensional. □

Notice that, again, in the definition of the Bohr-Sommerfeld quantization with sign and, in particular, in the sum $\bigoplus_{b \in B_{BS}} \epsilon(b)\mathbb{C}(b)$, we are using the fact that we have a group $\mathbb{T}$ acting with weights with finite multiplicity. Thus, the infinite sum $\bigoplus_{b \in B_{BS}} \epsilon(b)\mathbb{C}(b)$ is well-defined.

## 5.3 The final count. Bohr-Sommerfeld quantization equals formal geometric quantization

In this section we compare the Bohr-Sommerfeld quantization with the formal geometric quantization. We show that both of them are given by the integer points in the image of the moment map and that they coincide. We do it first in the symplectic case in Theorem 5.15 and then in the *b*-symplectic case in Theorem 5.16. In the latter case, the Bohr-Sommerfeld quantization we consider is the Bohr-Sommerfeld quantization with sign of Definition 5.13.

**Theorem 5.15** (Mir-Miranda-Weitsman [MMW22])**.** *Let $(M^{2n}, \omega, \mu)$ be a symplectic toric manifold. Then, the formal geometric quantization of M coincides with the Bohr-Sommerfeld quantization.*

*Proof.* We compute the formal geometric quantization of a symplectic toric manifold and then we compute its Bohr-Sommerfeld quantization by counting the Bohr-Sommerfeld leaves. We see that they are the same and, in particular, they coincide with the count of the integer points in the image of the moment map of the torus action.

In view of Theorem 2.46 (Quantization commutes with reduction), the formal geometric quantization of a symplectic toric manifold $(M^{2n}, \omega, \mu)$ is given by

$$Q(M) = \bigoplus_{\alpha \in \mathbb{Z}^n} Q(M/\!/_\alpha \mathbb{T})\alpha. \tag{5.7}$$

Notice that the sum is taken over all weights $\alpha$ of $\mathbb{T}$.

Suppose $\mu : M \to \mathfrak{t}$ is the moment map of the torus action. Then, the reduced spaces $M/\!/_\alpha \mathbb{T}$ are either empty if $\alpha$ is not in $\mu(M)$ or a point if it is. Since the quantization of a point is given by $\mathbb{C}$, we have that

$$Q(M) = \bigoplus_{\alpha \in \mathbb{Z}^n \cap \mu(M)} \mathbb{C}(\alpha). \tag{5.8}$$

Thus, the formal geometric quantization of $M$ is given by as many copies of $\mathbb{C}$ as there are integer points in the image of the moment map.

On the other hand, by Proposition 5.2, the Bohr-Sommerfeld quantization is given by the count of Bohr-Sommerfeld leaves of $M$, which are in one-to-one correspondence with the integer points in the image of the moment map. □

In the $b$-symplectic case we have the analogous result if we consider the Bohr-Sommerfeld quantization with sign.

**Theorem 5.16** (Mir-Miranda-Weitsman [MMW22])**.** *Let $(M^{2n}, Z, \omega, \mu)$ be a b-symplectic toric manifold. Then, the formal geometric quantization of $M$ coincides with the Bohr-Sommerfeld quantization with sign.*

*Proof.* For any $b$-symplectic toric manifold $(M, Z, \omega, \mu)$, the quantization space $Q(M)$ is defined as the vector space such that the following equality holds

$$(Q(M) \otimes Q(N))^{\mathbb{T}} = \varepsilon(\alpha) Q((M \times N)//_0 \mathbb{T}) \tag{5.9}$$

for any compact symplectic manifold $N$ and any weight $\alpha$ of $\mathbb{T}$, where $\mathbb{T}$ is the torus generating the action with moment map $\mu$ [GMW18a].

Alternatively, we have

$$Q(M) = \bigoplus_{\alpha \in \mathbb{Z}^n \cap \mu(M)} \varepsilon(\alpha) \mathbb{C}(\alpha), \tag{5.10}$$

where $\varepsilon(\alpha)$ are the signs given in Equation (2.14).

On the other hand, by Corollary 5.3, the Bohr-Sommerfeld set of $M$ coincides with the lattice of integer points in the image of $\mu$. Therefore, by Definition 5.13, the Bohr-Sommerfeld quantization with sign of $M$ is

$$\tilde{Q}(M) = \bigoplus_{b \in B_{BS}} \epsilon(b) \mathbb{C}(b) = \bigoplus_{b \in \mathbb{Z}^n \cap \mu(M)} \epsilon(b) \mathbb{C}(b). \tag{5.11}$$

Finally, for any point $p$ in the Bohr-Sommerfeld set $B_{BS}$, the sign $\epsilon(p)$ coincides with the sign $\varepsilon(p)$ since, by definition, both of them are $+1$ if the orientation given by the symplectic form on the component of $M \setminus Z$ containing $\mu^{-1}(p)$ and the overall orientation of $M$ agree and $-1$ otherwise. Hence, $Q(M) = \tilde{Q}(M)$. □

## 5.4 Geometric quantization for non-degenerate singularities

In [Ham10], Mark Hamilton obtained the Bohr-Sommerfeld quantization of a quantizable symplectic toric manifold via sheaf surgery (see Theorem 2.57). The dimension of this quantization is equal to the number of integer lattice points in the *interior* of the moment polytope because the count excludes the singular leaves, which are made of non-degenerate singular points with elliptic components. Following his idea, we give a quantization model for integrable systems which admit non-degenerate singular points with elliptic and hyperbolic components. In this model,

the singular leaves also do not contribute to the quantization, differently from the results of [HM10] and [MPS20].

Let $(M, \omega, F)$ be a quantizable symplectic manifold equipped with an integrable system. Let $\pi : \mathbb{L} \to M$ be a Hermitian line bundle with connection $\nabla$ of curvature $\omega$. In [HM10], Hamilton and Miranda proved that in a semi-local neighborhood $U$ of a non-degenerate singular point $p$ of $F$ with only hyperbolic components, if $s : U \to \mathbb{L}$ is a smooth polarized section, then it is Taylor flat at $p$. That is, for all $j, k$,

$$\left.\frac{\partial^{j+k} s}{\partial^j x \, \partial^k y}\right|_{(0,0)} = 0.$$

As a consequence, the only polarized analytic section in a semi-local neighborhood of a singularity with only hyperbolic components is the zero section.

Now, we construct a new sheaf of polarized sections by modifying the sheaf of smooth polarized sections in a neighborhood of a singularity with only hyperbolic components.

**Lemma 5.17.** *Let $(M^2, \omega, F)$ be a quantizable symplectic manifold endowed with an integrable system. Suppose that it is equipped with a Hermitian line bundle $\mathbb{L}$ and a connection $\nabla$ whose curvature is $\omega$. Let $p \in M$ be a non-degenerate singular point of $F$ whose single component is of hyperbolic type. Then, the sheaf of polarized smooth sections is still a sheaf when smooth sections are required to be analytic in a neighborhood of $p$. We denote this sheaf by $\mathcal{J}_h$.*

*Proof.* First, observe that analytic sections are a subclass of smooth sections. Thanks to the local normal form of a non-degenerate singularity of an integrable system (see Theorem 2.13 and, in particular, the version by Eliasson in [Eli90b]), the polarized sections equation $\nabla_X(s) = 0$ is formed by analytic data around a non-degenerate singular point with only hyperbolic components. That is, the moment map component around such a point is $f = xy$, the associated Hamiltonian vector field is $X_f = -x\frac{\partial}{\partial x} + y\frac{\partial}{\partial y}$ in dimension 2 and the sections that solve $\nabla_{X_f}(s) = 0$ are analytic. Requiring smooth sections to be analytic, which is a local property, in a small neighborhood does not change the fact that the intersection condition in the definition of the sheaf $\mathcal{J}_h$ of polarized sections works well, because we are extending sections which are required to be analytic and, hence, zero in the neighborhood of the singularity. □

We propose a new model for geometric quantization which has which is convenient for non-degenerate singularities of both elliptic and hyperbolic type of certain characteristics. First, we introduce, the simple version for manifolds of dimension 2 and later we generalize it to bigger dimensions. In dimension 2, our model can be stated as follows.

**Theorem 5.18** (Geometric quantization of non-degenerate singularities in dimension 2, Mir-Miranda [MM21])**.** *Let $(M^2, \omega)$ be a quantizable symplectic manifold and suppose it is equipped with an integrable system $F$ with non-degenerate singularities of only elliptic and hyperbolic components. Let $\mathbb{L}$ be a Hermitian line bundle over $M$ with connection $\nabla$ of*

*curvature $\omega$. Let $\mathcal{J}_h$ be the sheaf of polarized sections of $\mathbb{L}$ defined in Lemma 5.17. Then, the cohomology groups $H^k(M;\mathcal{J}_h)$ are zero for all $k \neq 1$, and*

$$H^1(M;\mathcal{J}_h) \cong \bigoplus_{b\in BS} \mathbb{C},$$

*where the sum is taken over all non-singular Bohr-Sommerfeld leaves. Hence,*

$$\dim \mathcal{Q}(M) = \dim H^1(M;\mathcal{J}_h) = \#(\mathrm{Int}F(M) \cap \mathbb{Z}).$$

*Proof.* At the neighborhood of a regular leaf, the sheaf $\mathcal{J}_h$ coincides with the usual sheaf of smooth polarized sections. At the neighborhood of a singular leaf, if it is of elliptic type it also coincides with the usual sheaf and if it is of hyperbolic type it is required to be made of analytic polarized sections. Consider the corresponding sheaf cohomology, which is the same as the sheaf cohomology in the toric case of Theorem 2.57 because the sections over leaves of hyperbolic type are zero and do not contribute. Then, the quantization is computed as the sum of the cohomology groups, which are 0 for $k \neq n$ and $H^n(M;\mathcal{J}) \cong \bigoplus_{b\in BS} \mathbb{C}$ where the sum is taken over all non-singular Bohr-Sommerfeld leaves. Hence,

$$\dim \mathcal{Q}(M) = \dim H^n(M;\mathcal{J}) = \#(\mathrm{Int}\Delta \cap \mathbb{Z}^n).$$

□

For systems in higher-dimensional manifolds, we can still quantize non-degenerate singular points with components of both elliptic and hyperbolic type. Nevertheless, we need that there is at most 1 component of hyperbolic type at each singularity. We also have to require compactness of the manifold to apply a Künneth Formula for the product sheaf.

**Theorem 5.19** (Geometric quantization of non-degenerate singularities, Mir-Miranda [MM21])**.** *Let $(M^{2n},\omega)$ be a compact symplectic manifold and suppose it is equipped with an integrable system $F$ with non-degenerate singularities of only elliptic components and at most 1 hyperbolic component. Let $\mathbb{L}$ be a Hermitian line bundle over $M$ with connection $\nabla$ of curvature $\omega$, and let $\mathcal{J}_h$ be the product sheaf of polarized sections of $\mathbb{L}$ defined in Lemma 5.17. Then, the cohomology groups $H^k(M;\mathcal{J})$ are zero for all $k \neq n$, and*

$$H^n(M;\mathcal{J}) \cong \bigoplus_{b\in BS} \mathbb{C},$$

*where the sum is taken over all non-singular Bohr-Sommerfeld leaves. Hence,*

$$\dim \mathcal{Q}(M) = \dim H^n(M;\mathcal{J}_h) = \#(\mathrm{Int}F(M) \cap \mathbb{Z}^n).$$

*Proof.* Suppose that a non-degenerate singularity has only components of elliptic type. Then, the result of quantization for toric systems (see Theorem 2.57) applies and the quantization is given by $H^n(M;\mathcal{J}) \cong \bigoplus_{b\in BS} \mathbb{C}$.

Otherwise, that a non-degenerate singularity has 1 component of hyperbolic type and any number of components of elliptic type. Because $M$ is compact, at the neighborhood of the singular leaf containing the singularity, the sheaf $\mathcal{J}_h$ of polarized sections is the product of the following sheaves:

- the usual sheaves of smooth polarized sections in the regular components,
- also usual sheaves of smooth polarized sections in the elliptic components, as modeled in [Ham10], and
- the sheaf of polarized sections required to be analytic as described in Lemma 5.17 in the hyperbolic component, which are extensions of the zero section in a neighborhood of the singularity.

Constructing the corresponding sheaf cohomology and applying a Künneth formula for geometric quantization (see for instance Theorem 3.4 in [MP15]), we obtain that the total cohomology is the sum of the cohomology of each component, and it coincides with the quantization of the toric case because the hyperbolic component does not add any contribution. Then, the quantization is computed as the sum of the cohomology groups, which are 0 for $k \neq n$ and

$$H^n(M;\mathcal{J}) \cong \bigoplus_{b\in BS} \mathbb{C},$$

where the sum is taken over all non-singular Bohr-Sommerfeld leaves. □

In cases where the multiplicity of the hyperbolic component of the singularity is bigger than 1, the situation is not that clear because the sheaf can not always be realized as a product [BI19].

# Appendix A

# Details of the computations of b-semitoric systems

This Appendix includes the details of the computations of the vector fields and Hessians used in the analysis of the different systems carried out in Chapter 4. For completeness and in order to make it easier for the reader to reconstruct the details of the proofs of Section 4.2, we include all the expressions in the different coordinate charts. For the precise definition of all the coordinate charts see Definitions 4.4, 4.5 and 4.6 in Section 4.2.1.

## A.1 Classical coupled angular momenta

The following expressions correspond to the classical coupled angular momenta (see Definition 4.3). For $\varepsilon_1, \varepsilon_2 \in \{+, -\}$, all of them are written in coordinates $(x_1, y_1, x_2, y_2)$ in the double Cartesian chart $(\varphi_1, U_1^{\varepsilon_1}) \times (\varphi_2, U_2^{\varepsilon_2})$ of $M^{\varepsilon_1,\varepsilon_2}$.

Moment map component $L$:

$$L(x_1, y_1, x_2, y_2) = \varepsilon_1 R_1 \sqrt{1 - x_1^2 - y_1^2} + \varepsilon_2 R_2 \sqrt{1 - x_2^2 - y_2^2} \tag{A.1}$$

Second partial derivatives of $L$:

$$\begin{cases} \frac{\partial^2 L}{\partial x_1^2}(x_1, y_1, x_2, y_2) = -\varepsilon_1 R_1 \frac{1-y_1^2}{(1-x_1^2-y_1^2)^{3/2}} \\ \frac{\partial^2 L}{\partial y_1^2}(x_1, y_1, x_2, y_2) = -\varepsilon_1 R_1 \frac{1-x_1^2}{(1-x_1^2-y_1^2)^{3/2}} \\ \frac{\partial^2 L}{\partial x_1 \partial y_1}(x_1, y_1, x_2, y_2) = -\varepsilon_1 R_1 \frac{x_1 y_1}{(1-x_1^2-y_1^2)^{3/2}} \\ \frac{\partial^2 L}{\partial x_2^2}(x_1, y_1, x_2, y_2) = -\varepsilon_2 R_2 \frac{1-y_2^2}{(1-x_2^2-y_2^2)^{3/2}} \\ \frac{\partial^2 L}{\partial y_2^2}(x_1, y_1, x_2, y_2) = -\varepsilon_2 R_2 \frac{1-x_2^2}{(1-x_2^2-y_2^2)^{3/2}} \\ \frac{\partial^2 L}{\partial x_2 \partial y_2}(x_1, y_1, x_2, y_2) = -\varepsilon_2 R_2 \frac{x_2 y_2}{(1-x_2^2-y_2^2)^{3/2}} \\ \frac{\partial^2 L}{\partial x_1 \partial x_2} = \frac{\partial^2 L}{\partial x_1 \partial y_2} = \frac{\partial^2 L}{\partial y_1 \partial x_2} = \frac{\partial^2 L}{\partial y_1 \partial y_2} = 0 \end{cases} \tag{A.2}$$

Expression of the matrix operator $d^2L$ at $p_{\varepsilon_1,\varepsilon_2}$, which corresponds to $(0,0,0,0) \in M^{\varepsilon_1,\varepsilon_2}$:

$$d^2L = \begin{pmatrix} -\varepsilon_1 R_1 & 0 & 0 & 0 \\ 0 & -\varepsilon_1 R_1 & 0 & 0 \\ 0 & 0 & -\varepsilon_2 R_2 & 0 \\ 0 & 0 & 0 & -\varepsilon_2 R_2 \end{pmatrix}$$

Moment map component $H_t$:

$$\begin{aligned} H_t(x_1,y_1,x_2,y_2) =& \varepsilon_1(1-t)\sqrt{1-x_1^2-y_1^2}+ \\ & t\left(x_1x_2+y_1y_2+\varepsilon_1\varepsilon_2\sqrt{(1-x_1^2-y_1^2)(1-x_2^2-y_2^2)}\right) \end{aligned}$$

Second partial derivatives of $H_t$:

$$\begin{cases} \frac{\partial^2 H}{\partial x_1^2}(x_1,y_1,x_2,y_2) = -\varepsilon_1\left(1-t+\varepsilon_2 t\sqrt{1-x_2^2-y_2^2}\right)\frac{1-y_1^2}{(1-x_1^2-y_1^2)^{3/2}} \\ \frac{\partial^2 H}{\partial y_1^2}(x_1,y_1,x_2,y_2) = -\varepsilon_1\left(1-t+\varepsilon_2 t\sqrt{1-x_2^2-y_2^2}\right)\frac{1-x_1^2}{(1-x_1^2-y_1^2)^{3/2}} \\ \frac{\partial^2 H}{\partial x_1\partial y_1}(x_1,y_1,x_2,y_2) = -\varepsilon_1\left(1-t+\varepsilon_2 t\sqrt{1-x_2^2-y_2^2}\right)\frac{x_1y_1}{(1-x_1^2-y_1^2)^{3/2}} \\ \frac{\partial^2 H}{\partial x_1\partial x_2}(x_1,y_1,x_2,y_2) = t\left(1+\varepsilon_1\varepsilon_2\frac{x_1x_2}{\sqrt{1-x_1^2-y_1^2}\sqrt{1-x_2^2-y_2^2}}\right) \\ \frac{\partial^2 H}{\partial x_1\partial y_2}(x_1,y_1,x_2,y_2) = \varepsilon_1\varepsilon_2 t\frac{x_1y_2}{\sqrt{1-x_1^2-y_1^2}\sqrt{1-x_2^2-y_2^2}} \\ \frac{\partial^2 H}{\partial y_1\partial x_2}(x_1,y_1,x_2,y_2) = \varepsilon_1\varepsilon_2 t\frac{y_1x_2}{\sqrt{1-x_1^2-y_1^2}\sqrt{1-x_2^2-y_2^2}} \\ \frac{\partial^2 H}{\partial y_1\partial y_2}(x_1,y_1,x_2,y_2) = t\left(1+\varepsilon_1\varepsilon_2\frac{y_1y_2}{\sqrt{1-x_1^2-y_1^2}\sqrt{1-x_2^2-y_2^2}}\right) \\ \frac{\partial^2 H}{\partial x_2^2}(x_1,y_1,x_2,y_2) = -\varepsilon_1\varepsilon_2 t\sqrt{1-x_1^2-y_1^2}\frac{1-y_2^2}{(1-x_2^2-y_2^2)^{3/2}} \\ \frac{\partial^2 H}{\partial y_2^2}(x_1,y_1,x_2,y_2) = -\varepsilon_1\varepsilon_2 t\sqrt{1-x_1^2-y_1^2}\frac{1-x_2^2}{(1-x_2^2-y_2^2)^{3/2}} \\ \frac{\partial^2 H}{\partial x_2\partial y_2}(x_1,y_1,x_2,y_2) = -\varepsilon_1\varepsilon_2 t\sqrt{1-x_1^2-y_1^2}\frac{x_2y_2}{(1-x_2^2-y_2^2)^{3/2}} \end{cases} \tag{A.3}$$

Expression of the matrix operator $d^2H_t$ at $p_{\varepsilon_1,\varepsilon_2}$, which corresponds to $(0,0,0,0) \in M^{\varepsilon_1,\varepsilon_2}$:

$$d^2H = \begin{pmatrix} \varepsilon_1(-1+t-\varepsilon_2 t) & 0 & t & 0 \\ 0 & \varepsilon_1(-1+t-\varepsilon_2 t) & 0 & t \\ t & 0 & -\varepsilon_1\varepsilon_2 t & 0 \\ 0 & t & 0 & -\varepsilon_1\varepsilon_2 t \end{pmatrix}$$

## A.2 System 1

The following expressions correspond to System 1 (see Definition 4.7 in Chapter 4).

**Expressions in the double cylindrical chart**

Complete expressions of $\omega$, $L$, $H_t$, $X_L$, $X_{H_t}$ in the double cylindrical coordinates $(\theta_1, z_1, \theta_2, z_2)$ in $M^{0,0}$.

The $b$-symplectic form:

$$\omega = R_1 d\theta_1 \wedge \frac{dz_1}{z_1} + R_2 d\theta_2 \wedge dz_2$$

The components of the moment map:

$$\begin{cases} L(\theta_1, z_1, \theta_2, z_2) = R_1 \log|z_1| + R_2 z_2 \\ H_t(\theta_1, z_1, \theta_2, z_2) = (1-t)z_1 + t\left(\sqrt{(1-z_1^2)(1-z_2^2)}\cos(\theta_1-\theta_2) + z_1 z_2\right) \end{cases} \tag{A.4}$$

The Hamiltonian $b$-vector fields:

$$\begin{cases} X_L = & -\frac{\partial}{\partial\theta_1} - \frac{\partial}{\partial\theta_2} \\ X_{H_t} = & \left[-\frac{z_1(1-t)}{R_1} + \frac{t}{R_1}\left(\frac{z_1^2}{\sqrt{1-z_1^2}}\sqrt{1-z_2^2}\cos(\theta_1-\theta_2) - z_1 z_2\right)\right]\frac{\partial}{\partial\theta_1} \\ & -\left[\frac{t}{R_1}\sqrt{(1-z_1^2)(1-z_2^2)}\sin(\theta_1-\theta_2)\right] z_1\frac{\partial}{\partial z_1} \\ & +\left[\frac{t}{R_2}\left(\frac{z_2}{\sqrt{1-z_2^2}}\sqrt{1-z_1^2}\cos(\theta_1-\theta_2) - z_1\right)\right]\frac{\partial}{\partial\theta_2} \\ & +\left[\frac{t}{R_2}\sqrt{(1-z_1^2)(1-z_2^2)}\sin(\theta_1-\theta_2)\right]\frac{\partial}{\partial z_2} \end{cases} \tag{A.5}$$

**Expressions in the double Cartesian chart**

For $\varepsilon_1, \varepsilon_2 \in \{+,-\}$, expressions of $\omega$, $L$, $H_t$, $X_L$, $X_{H_t}$, $\partial^2 L$, $\partial^2 H_t$ in the double Cartesian coordinates $(x_1, y_1, x_2, y_2)$ in $M^{\varepsilon_1,\varepsilon_2}$.

The $b$-symplectic form:

$$\omega = -\frac{R_1}{1-x_1^2-y_1^2}dx_1\wedge dy_1 - \varepsilon_2\frac{R_2}{\sqrt{1-x_2^2-y_2^2}}dx_2\wedge dy_2$$

The components of the moment map:

$$\begin{cases} L(x_1,y_1,x_2,y_2) = & \frac{1}{2}R_1\log|1-x_1^2-y_1^2| + \varepsilon_2 R_2\sqrt{1-x_2^2-y_2^2} \\ H_t(x_1,y_1,x_2,y_2) = & \varepsilon_1(1-t)\sqrt{1-x_1^2-y_1^2} + \\ & t\left(x_1x_2 + y_1y_2 + \varepsilon_1\varepsilon_2\sqrt{(1-x_1^2-y_1^2)(1-x_2^2-y_2^2)}\right) \end{cases} \tag{A.6}$$

The Hamiltonian $b$-vector fields:

$$\begin{cases} X_L = & -y_1\frac{\partial}{\partial x_1} + x_1\frac{\partial}{\partial y_1} - y_2\frac{\partial}{\partial x_2} + x_2\frac{\partial}{\partial y_2} \\ X_{H_t} = & \frac{1}{R_1}\Big[ty_2(1-x_1^2-y_1^2) - \\ & \varepsilon_1 y_1\sqrt{1-x_1^2-y_1^2}(1+t(\varepsilon_2\sqrt{1-x_2^2-y_2^2}-1))\Big]\frac{\partial}{\partial x_1} \\ & -\frac{1}{R_1}\Big[tx_2(1-x_1^2-y_1^2) - \\ & \varepsilon_1 x_1\sqrt{1-x_1^2-y_1^2}(1+t(\varepsilon_2\sqrt{1-x_2^2-y_2^2}-1))\Big]\frac{\partial}{\partial y_1} \\ & +\frac{1}{R_2}\left[\varepsilon_2 ty_1\sqrt{1-x_2^2-y_2^2} - \varepsilon_1 ty_2\sqrt{1-x_1^2-y_1^2}\right]\frac{\partial}{\partial x_2} \\ & -\frac{1}{R_2}\left[\varepsilon_2 tx_1\sqrt{1-x_2^2-y_2^2} - \varepsilon_1 tx_2\sqrt{1-x_1^2-y_1^2}\right]\frac{\partial}{\partial y_2} \end{cases} \tag{A.7}$$

Second partial derivatives of $L$:

$$\begin{cases} \frac{\partial^2 L}{\partial x_1^2}(x_1,y_1,x_2,y_2) = -R_1 \frac{1+x_1^2-y_1^2}{(1-x_1^2-y_1^2)^2} \\ \frac{\partial^2 L}{\partial y_1^2}(x_1,y_1,x_2,y_2) = -R_1 \frac{1-x_1^2+y_1^2}{(1-x_1^2-y_1^2)^2} \\ \frac{\partial^2 L}{\partial x_1 \partial y_1}(x_1,y_1,x_2,y_2) = -2R_1 \frac{x_1 y_1}{(1-x_1^2-y_1^2)^2} \\ \frac{\partial^2 L}{\partial x_2^2}(x_1,y_1,x_2,y_2) = -\varepsilon_2 R_2 \frac{1-y_2^2}{(1-x_2^2-y_2^2)^{3/2}} \\ \frac{\partial^2 L}{\partial y_2^2}(x_1,y_1,x_2,y_2) = -\varepsilon_2 R_2 \frac{1-x_2^2}{(1-x_2^2-y_2^2)^{3/2}} \\ \frac{\partial^2 L}{\partial x_2 \partial y_2}(x_1,y_1,x_2,y_2) = -\varepsilon_2 R_2 \frac{x_2 y_2}{(1-x_2^2-y_2^2)^{3/2}} \\ \frac{\partial^2 L}{\partial x_1 \partial x_2} = \frac{\partial^2 L}{\partial x_1 \partial y_2} = \frac{\partial^2 L}{\partial y_1 \partial x_2} = \frac{\partial^2 L}{\partial y_1 \partial y_2} = 0 \end{cases} \tag{A.8}$$

Second partial derivatives of $H_t$:

$$\begin{cases} \frac{\partial^2 H}{\partial x_1^2}(x_1,y_1,x_2,y_2) = -\varepsilon_1 \left(1 - t + \varepsilon_2 t \sqrt{1-x_2^2-y_2^2}\right) \frac{1-y_1^2}{(1-x_1^2-y_1^2)^{3/2}} \\ \frac{\partial^2 H}{\partial y_1^2}(x_1,y_1,x_2,y_2) = -\varepsilon_1 \left(1 - t + \varepsilon_2 t \sqrt{1-x_2^2-y_2^2}\right) \frac{1-x_1^2}{(1-x_1^2-y_1^2)^{3/2}} \\ \frac{\partial^2 H}{\partial x_1 \partial y_1}(x_1,y_1,x_2,y_2) = -\varepsilon_1 \left(1 - t + \varepsilon_2 t \sqrt{1-x_2^2-y_2^2}\right) \frac{x_1 y_1}{(1-x_1^2-y_1^2)^{3/2}} \\ \frac{\partial^2 H}{\partial x_1 \partial x_2}(x_1,y_1,x_2,y_2) = t \left(1 + \varepsilon_1 \varepsilon_2 \frac{x_1 x_2}{\sqrt{1-x_1^2-y_1^2}\sqrt{1-x_2^2-y_2^2}}\right) \\ \frac{\partial^2 H}{\partial x_1 \partial y_2}(x_1,y_1,x_2,y_2) = \varepsilon_1 \varepsilon_2 t \frac{x_1 y_2}{\sqrt{1-x_1^2-y_1^2}\sqrt{1-x_2^2-y_2^2}} \\ \frac{\partial^2 H}{\partial y_1 \partial x_2}(x_1,y_1,x_2,y_2) = \varepsilon_1 \varepsilon_2 t \frac{y_1 x_2}{\sqrt{1-x_1^2-y_1^2}\sqrt{1-x_2^2-y_2^2}} \\ \frac{\partial^2 H}{\partial y_1 \partial y_2}(x_1,y_1,x_2,y_2) = t \left(1 + \varepsilon_1 \varepsilon_2 \frac{y_1 y_2}{\sqrt{1-x_1^2-y_1^2}\sqrt{1-x_2^2-y_2^2}}\right) \\ \frac{\partial^2 H}{\partial x_2^2}(x_1,y_1,x_2,y_2) = -\varepsilon_1 \varepsilon_2 t \sqrt{1-x_1^2-y_1^2} \frac{1-y_2^2}{(1-x_2^2-y_2^2)^{3/2}} \\ \frac{\partial^2 H}{\partial y_2^2}(x_1,y_1,x_2,y_2) = -\varepsilon_1 \varepsilon_2 t \sqrt{1-x_1^2-y_1^2} \frac{1-x_2^2}{(1-x_2^2-y_2^2)^{3/2}} \\ \frac{\partial^2 H}{\partial x_2 \partial y_2}(x_1,y_1,x_2,y_2) = -\varepsilon_1 \varepsilon_2 t \sqrt{1-x_1^2-y_1^2} \frac{x_2 y_2}{(1-x_2^2-y_2^2)^{3/2}} \end{cases} \tag{A.9}$$

**Expressions in the Cartesian-cylindrical chart**

For $\varepsilon_1 \in \{+,-\}$, expressions of $\omega$, $L$, $H_t$, $X_L$, $X_{H_t}$ in the Cartesian-cylindrical coordinates $(x_1, y_1, \theta_2, z_2)$ in $M^{\varepsilon_1,0}$:

The $b$-symplectic form:

$$\omega = -\frac{R_1}{1-x_1^2-y_1^2} dx_1 \wedge dy_1 + R_2 d\theta_2 \wedge dz_2$$

The components of the moment map:

$$\begin{cases} L(x_1,y_1,\theta_2,z_2) = & \frac{1}{2} R_1 \log\left|1-x_1^2-y_1^2\right| + R_2 z_2 \\ H_t(x_1,y_1,\theta_2,z_2) = & \varepsilon_1 (1-t)\sqrt{1-x_1^2-y_1^2} + \\ & t\left(x_1\sqrt{1-z_2^2}\cos\theta_2 + y_1\sqrt{1-z_2^2}\sin\theta_2 + \varepsilon_1\sqrt{1-x_1^2-y_1^2}z_2\right) \end{cases} \tag{A.10}$$

The Hamiltonian $b$-vector fields:

$$\begin{cases} X_L = & -y_1\frac{\partial}{\partial x_1} + x_1\frac{\partial}{\partial y_1} - \frac{\partial}{\partial \theta_2} \\ X_{H_t} = & \frac{1}{R_1}\left[t\sqrt{1-z_2^2}\sin\theta_2(1-x_1^2-y_1^2) - \varepsilon_1 y_1\sqrt{1-x_1^2-y_1^2}(1+t(z_2-1))\right]\frac{\partial}{\partial x_1} \\ & -\frac{1}{R_1}\left[t\sqrt{1-z_2^2}\cos\theta_2(1-x_1^2-y_1^2) - \varepsilon_1 x_1\sqrt{1-x_1^2-y_1^2}(1+t(z_2-1))\right]\frac{\partial}{\partial y_1} \\ & +\left[\frac{t}{R_2}\left(\frac{z_2}{\sqrt{1-z_2^2}}(x_1\cos\theta_2 + y_1\sin\theta_2) - \varepsilon_1\sqrt{1-x_1^2-y_1^2}\right)\right]\frac{\partial}{\partial \theta_2} \\ & +\left[\frac{t}{R_2}\sqrt{1-z_2^2}(y_1\cos\theta_2 - x_1\sin\theta_2)\right]\frac{\partial}{\partial z_2} \end{cases} \tag{A.11}$$

**Expressions in the cylindrical-Cartesian chart**

For $\varepsilon_2 \in \{+,-\}$, expressions of $\omega$, $L$, $H_t$, $X_L$, $X_{H_t}$ in the cylindrical-Cartesian coordinates $(\theta_1, z_1, x_2, y_2)$ in $M^{0,\varepsilon_2}$.

The $b$-symplectic form:

$$\omega = R_1 d\theta_1 \wedge \frac{dz_1}{z_1} - \varepsilon_2 \frac{R_2}{\sqrt{1-x_2^2-y_2^2}} dx_2 \wedge dy_2$$

The components of the moment map:

$$\begin{cases} L(\theta_1, z_1, x_2, y_2) = & R_1\log|z_1| + \varepsilon_2 R_2\sqrt{1-x_2^2-y_2^2} \\ H_t(\theta_1, z_1, x_2, y_2) = & (1-t)z_1 + \\ & t\left(x_2\sqrt{1-z_1^2}\cos\theta_1 + y_2\sqrt{1-z_1^2}\sin\theta_1 + \varepsilon_2\sqrt{1-x_2^2-y_2^2}z_1\right) \end{cases} \tag{A.12}$$

The Hamiltonian $b$-vector fields:

$$\begin{cases} X_L = & -\frac{\partial}{\partial \theta_1} - y_2\frac{\partial}{\partial x_2} + x_2\frac{\partial}{\partial y_2} \\ X_{H_t} = & \left[-\frac{z_1(1-t)}{R_1} + \frac{t}{R_1}\left(\frac{z_1^2}{\sqrt{1-z_1^2}}(x_2\cos\theta_1 + y_2\sin\theta_1) - z_1\varepsilon_2\sqrt{1-x_2^2-y_2^2}\right)\right]\frac{\partial}{\partial \theta_1} \\ & -\left[\frac{t}{R_1}\sqrt{1-z_1^2}(x_2\sin\theta_1 - y_2\cos\theta_1)\right]z_1\frac{\partial}{\partial z_1} \\ & +\frac{1}{R_2}\left[\varepsilon_2 t\sqrt{1-z_1^2}\sin\theta_1\sqrt{1-x_2^2-y_2^2} - t y_2 z_1\right]\frac{\partial}{\partial x_2} \\ & -\frac{1}{R_2}\left[\varepsilon_2 t\sqrt{1-z_1^2}\cos\theta_1\sqrt{1-x_2^2-y_2^2} - t x_2 z_1\right]\frac{\partial}{\partial y_2} \end{cases} \tag{A.13}$$

## A.3 System 2

The following expressions correspond to System 2 (see Definition 4.14 in Chapter 4).

**Expressions in the double cylindrical chart**

Complete expressions of $\omega$, $L$, $H_t$, $X_L$, $X_{H_t}$ in the double cylindrical coordinates $(\theta_1, z_1, \theta_2, z_2)$ in $M^{0,0}$.

The $b$-symplectic form:

$$\omega = R_1 d\theta_1 \wedge \frac{dz_1}{z_1} + R_2 d\theta_2 \wedge dz_2$$

The components of the moment map:

$$\begin{cases} L(\theta_1, z_1, \theta_2, z_2) = & R_1 \log|z_1| + R_2 z_2 \\ H_t(\theta_1, z_1, \theta_2, z_2) = & (1-t)\log|z_1| + \\ & t\left(\sqrt{(1-z_1^2)(1-z_2^2)}\cos(\theta_1-\theta_2) + z_1 z_2\right) \end{cases} \tag{A.14}$$

The Hamiltonian $b$-vector fields:

$$\begin{cases} X_L = & -\frac{\partial}{\partial\theta_1} - \frac{\partial}{\partial\theta_2} \\ X_{H_t} = & \left[-\frac{1-t}{R_1} + \frac{t}{R_1}\left(\frac{z_1^2}{\sqrt{1-z_1^2}}\sqrt{1-z_2^2}\cos(\theta_1-\theta_2) - z_1 z_2\right)\right]\frac{\partial}{\partial\theta_1} \\ & -\left[\frac{t}{R_1}\sqrt{(1-z_1^2)(1-z_2^2)}\sin(\theta_1-\theta_2)\right] z_1 \frac{\partial}{\partial z_1} \\ & +\left[\frac{t}{R_2}\left(\frac{z_2}{\sqrt{1-z_2^2}}\sqrt{1-z_1^2}\cos(\theta_1-\theta_2) - z_1\right)\right]\frac{\partial}{\partial\theta_2} \\ & +\left[\frac{t}{R_2}\sqrt{(1-z_1^2)(1-z_2^2)}\sin(\theta_1-\theta_2)\right]\frac{\partial}{\partial z_2} \end{cases} \tag{A.15}$$

**Expressions in the double Cartesian chart**

For $\varepsilon_1, \varepsilon_2 \in \{+,-\}$, expressions of $\omega$, $L$, $H_t$, $X_L$, $X_{H_t}$, $\partial^2 L$, $\partial^2 H_t$ in the double Cartesian coordinates $(x_1, y_1, x_2, y_2)$ in $M^{\varepsilon_1,\varepsilon_2}$.

The $b$-symplectic form:

$$\omega = -\frac{R_1}{1-x_1^2-y_1^2} dx_1 \wedge dy_1 - \varepsilon_2 \frac{R_2}{\sqrt{1-x_2^2-y_2^2}} dx_2 \wedge dy_2$$

The components of the moment map:

$$\begin{cases} L(x_1, y_1, x_2, y_2) = & \frac{1}{2}R_1 \log\left|1-x_1^2-y_1^2\right| + \varepsilon_2 R_2\sqrt{1-x_2^2-y_2^2} \\ H_t(x_1, y_1, x_2, y_2) = & \frac{1}{2}(1-t)\log\left|1-x_1^2-y_1^2\right| + \\ & t\left(x_1 x_2 + y_1 y_2 + \varepsilon_1\varepsilon_2\sqrt{(1-x_1^2-y_1^2)(1-x_2^2-y_2^2)}\right) \end{cases} \tag{A.16}$$

The Hamiltonian $b$-vector fields:

$$\begin{cases} X_L = & -y_1\frac{\partial}{\partial x_1} + x_1\frac{\partial}{\partial y_1} - y_2\frac{\partial}{\partial x_2} + x_2\frac{\partial}{\partial y_2} \\ X_{H_t} = & \frac{1}{R_1}\Big[ty_2(1-x_1^2-y_1^2)- \\ & y_1(1+t(\varepsilon_1\varepsilon_2\sqrt{1-x_1^2-y_1^2}\sqrt{1-x_2^2-y_2^2}-1))\Big]\frac{\partial}{\partial x_1} \\ & -\frac{1}{R_1}\Big[tx_2(1-x_1^2-y_1^2)- \\ & x_1(1+t(\varepsilon_1\varepsilon_2\sqrt{1-x_1^2-y_1^2}\sqrt{1-x_2^2-y_2^2}-1))\Big]\frac{\partial}{\partial y_1} \\ & +\frac{1}{R_2}\left[\varepsilon_2 ty_1\sqrt{1-x_2^2-y_2^2}-\varepsilon_1 ty_2\sqrt{1-x_1^2-y_1^2}\right]\frac{\partial}{\partial x_2} \\ & -\frac{1}{R_2}\left[\varepsilon_2 tx_1\sqrt{1-x_2^2-y_2^2}-\varepsilon_1 tx_2\sqrt{1-x_1^2-y_1^2}\right]\frac{\partial}{\partial y_2} \end{cases} \tag{A.17}$$

Second partial derivatives of $L$:

$$\begin{cases} \frac{\partial^2 L}{\partial x_1^2}(x_1,y_1,x_2,y_2) = -R_1\frac{1+x_1^2-y_1^2}{(1-x_1^2-y_1^2)^2} \\ \frac{\partial^2 L}{\partial y_1^2}(x_1,y_1,x_2,y_2) = -R_1\frac{1-x_1^2+y_1^2}{(1-x_1^2-y_1^2)^2} \\ \frac{\partial^2 L}{\partial x_1\partial y_1}(x_1,y_1,x_2,y_2) = -2R_1\frac{x_1y_1}{(1-x_1^2-y_1^2)^2} \\ \frac{\partial^2 L}{\partial x_2^2}(x_1,y_1,x_2,y_2) = -\varepsilon_2 R_2\frac{1-y_2^2}{(1-x_2^2-y_2^2)^{3/2}} \\ \frac{\partial^2 L}{\partial y_2^2}(x_1,y_1,x_2,y_2) = -\varepsilon_2 R_2\frac{1-x_2^2}{(1-x_2^2-y_2^2)^{3/2}} \\ \frac{\partial^2 L}{\partial x_2\partial y_2}(x_1,y_1,x_2,y_2) = -\varepsilon_2 R_2\frac{x_2y_2}{(1-x_2^2-y_2^2)^{3/2}} \\ \frac{\partial^2 L}{\partial x_1\partial x_2} = \frac{\partial^2 L}{\partial x_1\partial y_2} = \frac{\partial^2 L}{\partial y_1\partial x_2} = \frac{\partial^2 L}{\partial y_1\partial y_2} = 0 \end{cases} \tag{A.18}$$

Second partial derivatives of $H_t$:

$$\begin{cases} \frac{\partial^2 H}{\partial x_1^2}(x_1,y_1,x_2,y_2) = -(1-t)\frac{1+x_1^2-y_1^2}{(1-x_1^2-y_1^2)^2} - \varepsilon_1\varepsilon_2 t\frac{1-y_1^2}{(1-x_1^2-y_1^2)^{3/2}}\sqrt{1-x_2^2-y_2^2} \\ \frac{\partial^2 H}{\partial y_1^2}(x_1,y_1,x_2,y_2) = -(1-t)\frac{1-x_1^2+y_1^2}{(1-x_1^2-y_1^2)^2} - \varepsilon_1\varepsilon_2 t\frac{1-x_1^2}{(1-x_1^2-y_1^2)^{3/2}}\sqrt{1-x_2^2-y_2^2} \\ \frac{\partial^2 H}{\partial x_1\partial y_1}(x_1,y_1,x_2,y_2) = -(1-t)\frac{2x_1y_1}{(1-x_1^2-y_1^2)^2} - \varepsilon_1\varepsilon_2 t\frac{x_1y_1}{(1-x_1^2-y_1^2)^{3/2}}\sqrt{1-x_2^2-y_2^2} \\ \frac{\partial^2 H}{\partial x_1\partial x_2}(x_1,y_1,x_2,y_2) = t\left(1+\varepsilon_1\varepsilon_2\frac{x_1x_2}{\sqrt{1-x_1^2-y_1^2}\sqrt{1-x_2^2-y_2^2}}\right) \\ \frac{\partial^2 H}{\partial x_1\partial y_2}(x_1,y_1,x_2,y_2) = \varepsilon_1\varepsilon_2 t\frac{x_1y_2}{\sqrt{1-x_1^2-y_1^2}\sqrt{1-x_2^2-y_2^2}} \\ \frac{\partial^2 H}{\partial y_1\partial x_2}(x_1,y_1,x_2,y_2) = \varepsilon_1\varepsilon_2 t\frac{y_1x_2}{\sqrt{1-x_1^2-y_1^2}\sqrt{1-x_2^2-y_2^2}} \\ \frac{\partial^2 H}{\partial y_1\partial y_2}(x_1,y_1,x_2,y_2) = t\left(1+\varepsilon_1\varepsilon_2\frac{y_1y_2}{\sqrt{1-x_1^2-y_1^2}\sqrt{1-x_2^2-y_2^2}}\right) \\ \frac{\partial^2 H}{\partial x_2^2}(x_1,y_1,x_2,y_2) = -\varepsilon_1\varepsilon_2 t\sqrt{1-x_1^2-y_1^2}\frac{1-y_2^2}{(1-x_2^2-y_2^2)^{3/2}} \\ \frac{\partial^2 H}{\partial y_2^2}(x_1,y_1,x_2,y_2) = -\varepsilon_1\varepsilon_2 t\sqrt{1-x_1^2-y_1^2}\frac{1-x_2^2}{(1-x_2^2-y_2^2)^{3/2}} \\ \frac{\partial^2 H}{\partial x_2\partial y_2}(x_1,y_1,x_2,y_2) = -\varepsilon_1\varepsilon_2 t\sqrt{1-x_1^2-y_1^2}\frac{x_2y_2}{(1-x_2^2-y_2^2)^{3/2}} \end{cases} \tag{A.19}$$

**Expressions in the Cartesian-cylindrical chart**

For $\varepsilon_1 \in \{+,-\}$, expressions of $\omega$, $L$, $H_t$, $X_L$, $X_{H_t}$ in the Cartesian-cylindrical coordinates $(x_1, y_1, \theta_2, z_2)$ in $M^{\varepsilon_1,0}$:

The $b$-symplectic form:

$$\omega = -\frac{R_1}{1-x_1^2-y_1^2} dx_1 \wedge dy_1 + R_2 d\theta_2 \wedge dz_2$$

The components of the moment map:

$$\begin{cases} L(x_1, y_1, \theta_2, z_2) = & \frac{1}{2} R_1 \log\left|1 - x_1^2 - y_1^2\right| + R_2 z_2 \\ H_t(x_1, y_1, \theta_2, z_2) = & \frac{1}{2}(1-t)\log\left|1 - x_1^2 - y_1^2\right| + \\ & t\left(x_1\sqrt{1-z_2^2}\cos\theta_2 + y_1\sqrt{1-z_2^2}\sin\theta_2 + \varepsilon_1\sqrt{1-x_1^2-y_1^2}z_2\right) \end{cases} \tag{A.20}$$

The Hamiltonian $b$-vector fields:

$$\begin{cases} X_L = & -y_1\frac{\partial}{\partial x_1} + x_1\frac{\partial}{\partial y_1} - \frac{\partial}{\partial \theta_2} \\ X_{H_t} = & \frac{1}{R_1}\left[t\sqrt{1-z_2^2}\sin\theta_2(1-x_1^2-y_1^2) - y_1(1+t(\varepsilon_1 z_2\sqrt{1-x_1^2-y_1^2}-1))\right]\frac{\partial}{\partial x_1} \\ & -\frac{1}{R_1}\left[t\sqrt{1-z_2^2}\cos\theta_2(1-x_1^2-y_1^2) - x_1(1+t(\varepsilon_1 z_2\sqrt{1-x_1^2-y_1^2}-1))\right]\frac{\partial}{\partial y_1} \\ & +\left[\frac{t}{R_2}\left(\frac{z_2}{\sqrt{1-z_2^2}}(x_1\cos\theta_2 + y_1\sin\theta_2) - \varepsilon_1\sqrt{1-x_1^2-y_1^2}\right)\right]\frac{\partial}{\partial \theta_2} \\ & +\left[\frac{t}{R_2}\sqrt{1-z_2^2}(y_1\cos\theta_2 - x_1\sin\theta_2)\right]\frac{\partial}{\partial z_2} \end{cases} \tag{A.21}$$

**Expressions in the cylindrical-Cartesian chart**

For $\varepsilon_2 \in \{+,-\}$, expressions of $\omega$, $L$, $H_t$, $X_L$, $X_{H_t}$ in the cylindrical-Cartesian coordinates $(\theta_1, z_1, x_2, y_2)$ in $M^{0,\varepsilon_2}$.

The $b$-symplectic form:

$$\omega = R_1 d\theta_1 \wedge \frac{dz_1}{z_1} - \varepsilon_2 \frac{R_2}{\sqrt{1-x_2^2-y_2^2}} dx_2 \wedge dy_2$$

The components of the moment map:

$$\begin{cases} L(\theta_1, z_1, x_2, y_2) = & R_1 \log|z_1| + \varepsilon_2 R_2\sqrt{1-x_2^2-y_2^2} \\ H_t(\theta_1, z_1, x_2, y_2) = & (1-t)\log|z_1| + \\ & t\left(x_2\sqrt{1-z_1^2}\cos\theta_1 + y_2\sqrt{1-z_1^2}\sin\theta_1 + \varepsilon_2\sqrt{1-x_2^2-y_2^2}z_1\right) \end{cases} \tag{A.22}$$

The Hamiltonian $b$-vector fields:

$$\begin{cases} X_L = & -\frac{\partial}{\partial \theta_1} - y_2\frac{\partial}{\partial x_2} + x_2\frac{\partial}{\partial y_2} \\ X_{H_t} = & \left[-\frac{(1-t)}{R_1} + \frac{t}{R_1}\left(\frac{z_1^2}{\sqrt{1-z_1^2}}(x_2\cos\theta_1 + y_2\sin\theta_1) - z_1\varepsilon_2\sqrt{1-x_2^2-y_2^2}\right)\right]\frac{\partial}{\partial \theta_1} \\ & -\left[\frac{t}{R_1}\sqrt{1-z_1^2}(x_2\sin\theta_1 - y_2\cos\theta_1)\right]z_1\frac{\partial}{\partial z_1} \\ & +\frac{1}{R_2}\left[\varepsilon_2 t\sqrt{1-z_1^2}\sin\theta_1\sqrt{1-x_2^2-y_2^2} - t y_2 z_1\right]\frac{\partial}{\partial x_2} \\ & -\frac{1}{R_2}\left[\varepsilon_2 t\sqrt{1-z_1^2}\cos\theta_1\sqrt{1-x_2^2-y_2^2} - t x_2 z_1\right]\frac{\partial}{\partial y_2} \end{cases} \tag{A.23}$$

## A.4 System 3

The following expressions correspond to System 3 (see Definition 4.19 in Chapter 4).

**Expressions in the double cylindrical chart**

Complete expressions of $\omega$, $L$, $H_t$, $X_L$, $X_{H_t}$ in the double cylindrical coordinates $(\theta_1, z_1, \theta_2, z_2)$ in $M^{0,0}$.

The $b$-symplectic form:

$$\omega = R_1 d\theta_1 \wedge dz_1 + R_2 d\theta_2 \wedge \frac{dz_2}{z_2}$$

The components of the moment map:

$$\begin{cases} L(\theta_1, z_1, \theta_2, z_2) = & R_1 z_1 + R_2 \log |z_2| \\ H_t(\theta_1, z_1, \theta_2, z_2) = & (1-t) z_1 + \\ & t\left(\sqrt{(1-z_1^2)(1-z_2^2)}\cos(\theta_1 - \theta_2) + z_1 z_2\right) \end{cases} \tag{A.24}$$

The Hamiltonian $b$-vector fields:

$$\begin{cases} X_L = & -\frac{\partial}{\partial\theta_1} - \frac{\partial}{\partial\theta_2} \\ X_{H_t} = & \left[-\frac{1-t}{R_1} + \frac{t}{R_1}\left(\frac{z_1}{\sqrt{1-z_1^2}}\sqrt{1-z_2^2}\cos(\theta_1-\theta_2) - z_2\right)\right]\frac{\partial}{\partial\theta_1} \\ & -\left[\frac{t}{R_1}\sqrt{(1-z_1^2)(1-z_2^2)}\sin(\theta_1-\theta_2)\right]\frac{\partial}{\partial z_1} \\ & +\left[\frac{t}{R_2}\left(\frac{z_2^2}{\sqrt{1-z_2^2}}\sqrt{1-z_1^2}\cos(\theta_1-\theta_2) - z_1 z_2\right)\right]\frac{\partial}{\partial\theta_2} \\ & +\left[\frac{t}{R_2}\sqrt{(1-z_1^2)(1-z_2^2)}\sin(\theta_1-\theta_2)\right] z_2\frac{\partial}{\partial z_2} \end{cases} \tag{A.25}$$

**Expressions in the double Cartesian chart**

For $\varepsilon_1, \varepsilon_2 \in \{+, -\}$, expressions of $\omega$, $L$, $H_t$, $X_L$, $X_{H_t}$, $\partial^2 L$, $\partial^2 H_t$ in the double Cartesian coordinates $(x_1, y_1, x_2, y_2)$ in $M^{\varepsilon_1,\varepsilon_2}$.

The $b$-symplectic form:

$$\omega = -\varepsilon_1 \frac{R_1}{\sqrt{1-x_1^2-y_1^2}} dx_1 \wedge dy_1 - \frac{R_2}{1-x_2^2-y_2^2} dx_2 \wedge dy_2$$

The components of the moment map:

$$\begin{cases} L(x_1, y_1, x_2, y_2) = & \varepsilon_1 R_1\sqrt{1-x_1^2-y_1^2} + \frac{1}{2}R_2 \log\left|1-x_2^2-y_2^2\right| \\ H_t(x_1, y_1, x_2, y_2) = & \varepsilon_1(1-t)\sqrt{1-x_1^2-y_1^2} + \\ & t\left(x_1 x_2 + y_1 y_2 + \varepsilon_1\varepsilon_2\sqrt{(1-x_1^2-y_1^2)(1-x_2^2-y_2^2)}\right) \end{cases} \tag{A.26}$$

The Hamiltonian $b$-vector fields:

$$\begin{cases} X_L = & -y_1\frac{\partial}{\partial x_1} + x_1\frac{\partial}{\partial y_1} - y_2\frac{\partial}{\partial x_2} + x_2\frac{\partial}{\partial y_2} \\ X_{H_t} = & \frac{1}{R_1}\left[\varepsilon_1 t y_2\sqrt{1-x_1^2-y_1^2} - y_1(1+t(\varepsilon_2\sqrt{1-x_2^2-y_2^2}-1))\right]\frac{\partial}{\partial x_1} \\ & -\frac{1}{R_1}\left[\varepsilon_1 t x_2\sqrt{1-x_1^2-y_1^2} - x_1(1+t(\varepsilon_2\sqrt{1-x_2^2-y_2^2}-1))\right]\frac{\partial}{\partial y_1} \\ & +\frac{1}{R_2}\left[t y_1(1-x_2^2-y_2^2) - \varepsilon_1\varepsilon_2 t y_2\sqrt{1-x_1^2-y_1^2}\sqrt{1-x_2^2-y_2^2}\right]\frac{\partial}{\partial x_2} \\ & -\frac{1}{R_2}\left[t x_1(1-x_2^2-y_2^2) - \varepsilon_1\varepsilon_2 t x_2\sqrt{1-x_1^2-y_1^2}\sqrt{1-x_2^2-y_2^2}\right]\frac{\partial}{\partial y_2} \end{cases} \tag{A.27}$$

Second partial derivatives of $L$:

$$\begin{cases} \frac{\partial^2 L}{\partial x_1^2}(x_1,y_1,x_2,y_2) = -\varepsilon_1 R_1\frac{1-y_1^2}{(1-x_1^2-y_1^2)^{3/2}} \\ \frac{\partial^2 L}{\partial y_1^2}(x_1,y_1,x_2,y_2) = -\varepsilon_1 R_1\frac{1-x_1^2}{(1-x_1^2-y_1^2)^{3/2}} \\ \frac{\partial^2 L}{\partial x_1\partial y_1}(x_1,y_1,x_2,y_2) = -2\varepsilon_1 R_1\frac{x_1 y_1}{(1-x_1^2-y_1^2)^{3/2}} \\ \frac{\partial^2 L}{\partial x_2^2}(x_1,y_1,x_2,y_2) = -R_2\frac{1+x_2^2-y_2^2}{(1-x_2^2-y_2^2)^2} \\ \frac{\partial^2 L}{\partial y_2^2}(x_1,y_1,x_2,y_2) = -R_2\frac{1-x_2^2+y_2^2}{(1-x_2^2-y_2^2)^2} \\ \frac{\partial^2 L}{\partial x_2\partial y_2}(x_1,y_1,x_2,y_2) = -2R_2\frac{x_2 y_2}{(1-x_2^2-y_2^2)^2} \\ \frac{\partial^2 L}{\partial x_1\partial x_2} = \frac{\partial^2 L}{\partial x_1\partial y_2} = \frac{\partial^2 L}{\partial y_1\partial x_2} = \frac{\partial^2 L}{\partial y_1\partial y_2} = 0 \end{cases} \tag{A.28}$$

Second partial derivatives of $H_t$:

$$\begin{cases} \frac{\partial^2 H}{\partial x_1^2}(x_1,y_1,x_2,y_2) = -\varepsilon_1\left(1-t+\varepsilon_2 t\sqrt{1-x_2^2-y_2^2}\right)\frac{1-y_1^2}{(1-x_1^2-y_1^2)^{3/2}} \\ \frac{\partial^2 H}{\partial y_1^2}(x_1,y_1,x_2,y_2) = -\varepsilon_1\left(1-t+\varepsilon_2 t\sqrt{1-x_2^2-y_2^2}\right)\frac{1-x_1^2}{(1-x_1^2-y_1^2)^{3/2}} \\ \frac{\partial^2 H}{\partial x_1\partial y_1}(x_1,y_1,x_2,y_2) = -\varepsilon_1\left(1-t+\varepsilon_2 t\sqrt{1-x_2^2-y_2^2}\right)\frac{x_1 y_1}{(1-x_1^2-y_1^2)^{3/2}} \\ \frac{\partial^2 H}{\partial x_1\partial x_2}(x_1,y_1,x_2,y_2) = t\left(1+\varepsilon_1\varepsilon_2\frac{x_1 x_2}{\sqrt{1-x_1^2-y_1^2}\sqrt{1-x_2^2-y_2^2}}\right) \\ \frac{\partial^2 H}{\partial x_1\partial y_2}(x_1,y_1,x_2,y_2) = \varepsilon_1\varepsilon_2 t\frac{x_1 y_2}{\sqrt{1-x_1^2-y_1^2}\sqrt{1-x_2^2-y_2^2}} \\ \frac{\partial^2 H}{\partial y_1\partial x_2}(x_1,y_1,x_2,y_2) = \varepsilon_1\varepsilon_2 t\frac{y_1 x_2}{\sqrt{1-x_1^2-y_1^2}\sqrt{1-x_2^2-y_2^2}} \\ \frac{\partial^2 H}{\partial y_1\partial y_2}(x_1,y_1,x_2,y_2) = t\left(1+\varepsilon_1\varepsilon_2\frac{y_1 y_2}{\sqrt{1-x_1^2-y_1^2}\sqrt{1-x_2^2-y_2^2}}\right) \\ \frac{\partial^2 H}{\partial x_2^2}(x_1,y_1,x_2,y_2) = -\varepsilon_1\varepsilon_2 t\sqrt{1-x_1^2-y_1^2}\frac{1-y_2^2}{(1-x_2^2-y_2^2)^{3/2}} \\ \frac{\partial^2 H}{\partial y_2^2}(x_1,y_1,x_2,y_2) = -\varepsilon_1\varepsilon_2 t\sqrt{1-x_1^2-y_1^2}\frac{1-x_2^2}{(1-x_2^2-y_2^2)^{3/2}} \\ \frac{\partial^2 H}{\partial x_2\partial y_2}(x_1,y_1,x_2,y_2) = -\varepsilon_1\varepsilon_2 t\sqrt{1-x_1^2-y_1^2}\frac{x_2 y_2}{(1-x_2^2-y_2^2)^{3/2}} \end{cases} \tag{A.29}$$

**Expressions in the Cartesian-cylindrical chart**

For $\varepsilon_1 \in \{+,-\}$, expressions of $\omega$, $L$, $H_t$, $X_L$, $X_{H_t}$ in the Cartesian-cylindrical coordinates $(x_1, y_1, \theta_2, z_2)$ in $M^{\varepsilon_1,0}$:

The $b$-symplectic form:

$$\omega = -\varepsilon_1 \frac{R_1}{\sqrt{1-x_1^2-y_1^2}} dx_1 \wedge dy_1 + R_2 d\theta_2 \wedge \frac{dz_2}{z_2}$$

The components of the moment map:

$$\begin{cases} L(x_1, y_1, \theta_2, z_2) = & \varepsilon_1 R_1 \sqrt{1-x_1^2-y_1^2} + R_2 \log|z_2| \\ H_t(x_1, y_1, \theta_2, z_2) = & \varepsilon_1 (1-t)\sqrt{1-x_1^2-y_1^2} + \\ & t\left(x_1\sqrt{1-z_2^2}\cos\theta_2 + y_1\sqrt{1-z_2^2}\sin\theta_2 + \varepsilon_1\sqrt{1-x_1^2-y_1^2}z_2\right) \end{cases} \tag{A.30}$$

The Hamiltonian $b$-vector fields:

$$\begin{cases} X_L = & -y_1\frac{\partial}{\partial x_1} + x_1\frac{\partial}{\partial y_1} - \frac{\partial}{\partial \theta_2} \\ X_{H_t} = & \frac{1}{R_1}\left[\varepsilon_1 t\sqrt{1-z_2^2}\sin\theta_2\sqrt{1-x_1^2-y_1^2} - y_1(1+t(z_2-1))\right]\frac{\partial}{\partial x_1} \\ & -\frac{1}{R_1}\left[\varepsilon_1 t\sqrt{1-z_2^2}\cos\theta_2\sqrt{1-x_1^2-y_1^2} - x_1(1+t(z_2-1))\right]\frac{\partial}{\partial y_1} \\ & +\left[\frac{t}{R_2}\left(\frac{z_2^2}{\sqrt{1-z_2^2}}(x_1\cos\theta_2 + y_1\sin\theta_2) - z_2\varepsilon_1\sqrt{1-x_1^2-y_1^2}\right)\right]\frac{\partial}{\partial \theta_2} \\ & +\left[\frac{t}{R_2}\sqrt{1-z_2^2}(y_1\cos\theta_2 - x_1\sin\theta_2)\right] z_2\frac{\partial}{\partial z_2} \end{cases} \tag{A.31}$$

**Expressions in the cylindrical-Cartesian chart**

For $\varepsilon_2 \in \{+,-\}$, expressions of $\omega$, $L$, $H_t$, $X_L$, $X_{H_t}$ in the cylindrical-Cartesian coordinates $(\theta_1, z_1, x_2, y_2)$ in $M^{0,\varepsilon_2}$.

The $b$-symplectic form:

$$\omega = R_1 d\theta_1 \wedge dz_1 - \frac{R_2}{1-x_2^2-y_2^2} dx_2 \wedge dy_2$$

The components of the moment map:

$$\begin{cases} L(\theta_1, z_1, x_2, y_2) = & R_1 z_1 + \frac{1}{2}R_2 \log\left|1-x_2^2-y_2^2\right| \\ H_t(\theta_1, z_1, x_2, y_2) = & (1-t)z_1 + \\ & t\left(x_2\sqrt{1-z_1^2}\cos\theta_1 + y_2\sqrt{1-z_1^2}\sin\theta_1 + \varepsilon_2\sqrt{1-x_2^2-y_2^2}z_1\right) \end{cases} \tag{A.32}$$

The Hamiltonian $b$-vector fields:

$$\begin{cases} X_L = & -\frac{\partial}{\partial \theta_1} - y_2\frac{\partial}{\partial x_2} + x_2\frac{\partial}{\partial y_2} \\ X_{H_t} = & \left[-\frac{1-t}{R_1} + \frac{t}{R_1}\left(\frac{z_1}{\sqrt{1-z_1^2}}(x_2\cos\theta_1 + y_2\sin\theta_1) - \varepsilon_2\sqrt{1-x_2^2-y_2^2}\right)\right]\frac{\partial}{\partial \theta_1} \\ & -\left[\frac{t}{R_1}\sqrt{1-z_1^2}(x_2\sin\theta_1 - y_2\cos\theta_1)\right]\frac{\partial}{\partial z_1} \\ & +\frac{1}{R_2}\left[t\sqrt{1-z_1^2}\sin\theta_1(1-x_2^2-y_2^2) - \varepsilon_2 t y_2\sqrt{1-x_2^2-y_2^2}z_1\right]\frac{\partial}{\partial x_2} \\ & -\frac{1}{R_2}\left[t\sqrt{1-z_1^2}\cos\theta_1(1-x_2^2-y_2^2) - \varepsilon_2 t x_2\sqrt{1-x_2^2-y_2^2}z_1\right]\frac{\partial}{\partial y_2} \end{cases} \tag{A.33}$$

# Appendix B

# Matlab codes for b-semitoric systems

This Appendix includes the Matlab codes used to create the plots of Chapter 4. A reader that wants to explore the systems studied in that chapter by changing the value of their parameters will find them useful.

## B.1 Computation and plot of the image of the moment map

In this section we include the Matlab codes used to generate the image by the moment map of the systems studied in Section 4.2.

### B.1.1 Coupled angular momenta

The following code has been used to generate the pictures in Figure 2.2, corresponding to the classical coupled angular momenta.

```
%Set parameters
R1=1;R2=2;
%Set mesh size
J=50;K=50;M=50;
%Create point set
cosdiftheta=linspace(-1,1,K);
z1=linspace(-1,1,J);
z2=linspace(-1,1,M);
%Set transparency
transp=0.02;
%Set values of t and start loop
for t = 0:0.2:1
%Create LH matrix to store values of L and H
LH=zeros(0,2);
%Loops that cover the point set
for j = 1:J
for k = 1:K
for m = 1:M
%Computation of L and H at each point
```

```
LH=[LH;L(z1(j),z2(m),R1,R2),H(t,cosdiftheta(k),z1(j),z2(m))
   ];
end
end
end
%Delete repeated rows
LH = unique(LH,'rows');
%Plot all points
scatter(LH(:,1),LH(:,2),'green','filled','MarkerFaceAlpha',
   transp,'MarkerEdgeAlpha',transp);
hold on
%Plot fixed points
scatter(L(1,1,R1,R2),H(t,0,1,1),'red','filled');
scatter(L(1,-1,R1,R2),H(t,0,1,-1),'black','filled');
scatter(L(-1,1,R1,R2),H(t,0,-1,1),'magenta','filled');
a=scatter(L(-1,-1,R1,R2),H(t,0,-1,-1),'blue','filled');
hold off
%Set environment
xlim([-3 3]);ylim([-1 1]);xlabel('L');ylabel('H');
%Export figure to existing document
exportgraphics(gca,'cam0f.pdf','Append',true)
end
%L and H functions of the classical coupled angular momenta
function l = L(z1,z2,R1,R2)
l = R1*z1 + R2*z2;
end
function h = H(t,cosdiftheta,z1,z2)
h = (1-t)*(z1)+t*(sqrt((1-(z1)^2)*(1-(z2)^2))*cosdiftheta+(
   z1)*(z2));
end
```

### B.1.2 System 1

The following code has been used to generate the pictures in Figure 4.6, corresponding to System 1.

```
%Set parameters
R1=1;R2=2;
%Set mesh size
J=50;K=50;M=50;
%Create point set
cosdiftheta=linspace(-1,1,K);
z1=linspace(0,1,J).^2;
z2=linspace(-1,1,M);
%Set transparency
transp=0.02;
```

```
%Set values of t and start loop
for t = 0:0.2:1
%Create LH matrix to store values of L and H for S_1^2+ x
   S_2^2
LH=zeros(0,2);
%Loops that cover the point set
for j = 1:J
for k = 1:K
for m = 1:M
%Computation of L and H at each point of S_1^2+ x S_2^2
LH=[LH;L(z1(j),z2(m),R1,R2),H(t,cosdiftheta(k),z1(j),z2(m))
   ];
end
end
end
%Delete repeated rows
LH = unique(LH,'rows');
%Plot image of S_1^2+ x S_2^2
scatter(LH(:,1),LH(:,2),'cyan','filled','MarkerFaceAlpha',
   transp,'MarkerEdgeAlpha',transp);
hold on
%Create LH matrix to store values of L and H for S_1^2- x
   S_2^2
LH=zeros(0,2);
%Loops that cover the point set
for j = 1:J
for k = 1:K
for m = 1:M
%Computation of L and H at each point of S_1^2- x S_2^2
LH=[LH;L(-z1(j),z2(m),R1,R2),H(t,cosdiftheta(k),-z1(j),z2(m
   ))];
end
end
end
%Delete repeated rows
LH = unique(LH,'rows');
%Plot image of S_1^2- x S_2^2
scatter(LH(:,1),LH(:,2),'yellow','filled','MarkerFaceAlpha'
   ,transp,'MarkerEdgeAlpha',transp);
%Plot fixed points
scatter(L(1,1,R1,R2),H(t,0,1,1),'red','filled');
scatter(L(1,-1,R1,R2),H(t,0,1,-1),'black','filled');
scatter(L(-1,1,R1,R2),H(t,0,-1,1),'magenta','filled');
a=scatter(L(-1,-1,R1,R2),H(t,0,-1,-1),'blue','filled');
hold off
%Set environment
```

```
xlim([-5 2]);ylim([-1 1]);xlabel('L');ylabel('H');
%Export figure to existing document
exportgraphics(gca,'cam1f.pdf','Append',true)
end
%L and H functions of System 1
function l = L(z1,z2,R1,R2)
l = R1*log(abs(z1)) + R2*z2;
end
function h = H(t,cosdiftheta,z1,z2)
h = (1-t)*(z1)+t*(sqrt((1-(z1)^2)*(1-(z2)^2))*cosdiftheta+(
    z1)*(z2));
end
```

### B.1.3 System 2

The following code has been used to generate the pictures in Figure 4.7, corresponding to System 2.

```
%Set parameters
R1=1;R2=2;
%Set mesh size
J=150;K=50;M=50;
%Create point set
cosdiftheta=linspace(-1,1,K);
z1=linspace(0,1,J).^7;
z2=linspace(-1,1,M);
%Set transparency
transp=0.02;
%Set values of t and start loop
for t = 0:0.2:1
%Create LH matrix to store values of L and H for S_1^2+ x
    S_2^2
LH=zeros(0,2);
%Loops that cover the point set
for j = 1:J
for k = 1:K
for m = 1:M
%Computation of L and H at each point of S_1^2+ x S_2^2
LH=[LH;L(z1(j),z2(m),R1,R2),H(t,cosdiftheta(k),z1(j),z2(m))
    ];
end
end
end
%Delete repeated rows
LH = unique(LH,'rows');
%Plot image of S_1^2+ x S_2^2
```

```
scatter(LH(:,1),LH(:,2),'cyan','filled','MarkerFaceAlpha',
    transp,'MarkerEdgeAlpha',transp);
hold on
%Create LH matrix to store values of L and H for S_1^2- x
    S_2^2
LH=zeros(0,2);
%Loops that cover the point set
for j = 1:J
for k = 1:K
for m = 1:M
%Computation of L and H at each point of S_1^2- x S_2^2
LH=[LH;L(-z1(j),z2(m),R1,R2),H(t,cosdiftheta(k),-z1(j),z2(m
    ))];
end
end
end
%Delete repeated rows
LH = unique(LH,'rows');
%Plot image of S_1^2- x S_2^2
scatter(LH(:,1),LH(:,2),'yellow','filled','MarkerFaceAlpha'
    ,transp,'MarkerEdgeAlpha',transp);
%Plot fixed points
scatter(L(1,1,R1,R2),H(t,0,1,1),'red','filled');
scatter(L(1,-1,R1,R2),H(t,0,1,-1),'black','filled');
scatter(L(-1,1,R1,R2),H(t,0,-1,1),'magenta','filled');
a=scatter(L(-1,-1,R1,R2),H(t,0,-1,-1),'blue','filled');
hold off
%Set environment
xlim([-5 2]);ylim([-3 1]);xlabel('L');ylabel('H');
%Export figure to existing document
exportgraphics(gca,'cam2f.pdf','Append',true)
end
%L and H functions of System 2
function l = L(z1,z2,R1,R2)
l = R1*log(abs(z1)) + R2*z2;
end
function h = H(t,cosdiftheta,z1,z2)
h = (1-t)*log(abs(z1))+t*(sqrt((1-(z1)^2)*(1-(z2)^2))*
    cosdiftheta+(z1)*(z2));
end
```

### B.1.4 System 3

The following code has been used to generate the pictures in Figure 4.8, corresponding to System 3.

```
%Set parameters
R1=1;R2=2;
%Set mesh size
J=50;K=50;M=200;
%Create point set
cosdiftheta=linspace(-1,1,K);
z1=linspace(-1,1,J);
z2=linspace(0.2,1,M).^7;
%Set transparency
transp=0.02;
%Set values of t and start loop
for t = 0:0.2:1
%Create LH matrix to store values of L and H for S_1^2 x
   S_2^2+
LH=zeros(0,2);
%Loops that cover the point set
for j = 1:J
for k = 1:K
for m = 1:M
%Computation of L and H at each point of S_1^2 x S_2^2+
LH=[LH;L(z1(j),z2(m),R1,R2),H(t,cosdiftheta(k),z1(j),z2(m))
   ];
end
end
end
%Delete repeated rows
LH = unique(LH,'rows');
%Plot image of S_1^2 x S_2^2+
scatter(LH(:,1),LH(:,2),'cyan','filled','MarkerFaceAlpha',
   transp,'MarkerEdgeAlpha',transp);
hold on
%Create LH matrix to store values of L and H for S_1^2 x
   S_2^2-
LH=zeros(0,2);
%Loops that cover the point set
for j = 1:J
for k = 1:K
for m = 1:M
%Computation of L and H at each point of S_1^2 x S_2^2-
LH=[LH;L(z1(j),-z2(m),R1,R2),H(t,cosdiftheta(k),z1(j),-z2(m
   ))];
end
end
end
%Delete repeated rows
LH = unique(LH,'rows');
```

```
%Plot image of S_1^2 x S_2^2-
scatter(LH(:,1),LH(:,2),'yellow','filled','MarkerFaceAlpha'
   ,transp,'MarkerEdgeAlpha',transp);
%Plot fixed points
scatter(L(1,1,R1,R2),H(t,0,1,1),'red','filled');
scatter(L(1,-1,R1,R2),H(t,0,1,-1),'black','filled');
scatter(L(-1,1,R1,R2),H(t,0,-1,1),'magenta','filled');
a=scatter(L(-1,-1,R1,R2),H(t,0,-1,-1),'blue','filled');
hold off
%Set environment
xlim([-5 2]);ylim([-1 1]);xlabel('L');ylabel('H');
%Export figure to existing document
exportgraphics(gca,'cam3f.pdf','Append',true)
end
%L and H functions of System 3
function l = L(z1,z2,R1,R2)
l = R1*z1 + R2*log(abs(z2));
end
function h = H(t,cosdiftheta,z1,z2)
h = (1-t)*(z1)+t*(sqrt((1-(z1)^2)*(1-(z2)^2))*cosdiftheta+(
   z1)*(z2));
end
```

## B.2 Computation and plot of the orbits

In this section we include the Matlab code used to generate the plots of Section 4.3. In particular the following code has been used to generate the pictures in Figures 4.10 and 4.11.

```
%set format
format long
%Set parameters
R1=1;R2=2;
t=1/2;

%Integration of X_L
%Set initial conditions for z1 and theta1
z1L=0.7;theta1L=0.;
%Compute initial z2 and theta2
z2L=-1-R1/R2*log(abs(z1L))
cosdifthetaL=((1-z1L)*(1/t-2)+z1L*R1/R2*log(abs(z1L)))/(
   sqrt((1-z1L^2)*log(abs(z1L))*(-2*R1/R2-R1^2/R2^2*log(abs
   (z1L)))))
theta2L=theta1L-acos(cosdifthetaL);
%The Hamiltonian b-vector field X_L
fL = @(sL,xL) [0;-1;0;-1];
```

```
%Vector of initial conditions
x0L = [z1L;theta1L;z2L;theta2L];
%Set time range
sspanL = [0 8];
%Numerical solution of trajectory
[sL,xL] = ode45(fL, sspanL, x0L);
nL=size(xL,1);
vL=zeros(nL,2);
%Control check of L and H
for i = 1:nL
vL(i,1)=R1*log(abs(xL(i,1)))+R2*xL(i,3)+R2;
vL(i,2)=(1-t)*xL(i,1)+t*(sqrt((1-xL(i,1)^2)*(1-xL(i,3)^2))*
   cos(xL(i,2)-xL(i,4))+xL(i,1)*xL(i,3))-1+2*t;
end
%Cartesian coordinates of trajectory
for i = 1:nL
wL(i,1)=sqrt(1-xL(i,1)^2)*cos(xL(i,2));
wL(i,2)=sqrt(1-xL(i,1)^2)*sin(xL(i,2));
wL(i,3)=sqrt(1-xL(i,3)^2)*cos(xL(i,4));
wL(i,4)=sqrt(1-xL(i,3)^2)*sin(xL(i,4));
end
%Save full trajectory of XL in Cartesian coordinates
flowL=[wL(:,1),wL(:,2),xL(:,1),wL(:,3),wL(:,4),xL(:,3)]

%Integration of X_H
%Set initial conditions for z1 and theta1
z1H=0.99;theta1H=-0.5;
%Compute initial z2 and theta2
z2H=-1-R1/R2*log(abs(z1H))
cosdifthetaH=((1-z1H)*(1/t-2)+z1H*R1/R2*log(abs(z1H)))/(
   sqrt((1-z1H^2)*log(abs(z1H))*(-2*R1/R2-R1^2/R2^2*log(abs
   (z1H)))))
theta2H=theta1H-acos(cosdifthetaH);
%The Hamiltonian b-vector field X_H
fH = @(sH,xH) [-t/R1*xH(1)*sqrt((1-xH(1)^2)*(1-xH(3)^2))*
   sin(xH(2)-xH(4));-(1-t)/R1*xH(1)+t/R1*(xH(1)^2/sqrt(1-xH
   (1)^2)*sqrt(1-xH(3)^2)*cos(xH(2)-xH(4))-xH(1)*xH(3));t/
   R2*sqrt((1-xH(1)^2)*(1-xH(3)^2))*sin(xH(2)-xH(4));t/R2*(
   xH(3)/sqrt(1-xH(3)^2)*sqrt(1-xH(1)^2)*cos(xH(2)-xH(4))-
   xH(1))]
%Vector of initial conditions
x0H = [z1H;theta1H;z2H;theta2H];
%Set time range
sspanH = [0 32];
%Numerical solution of trajectory
[sH,xH] = ode45(fH, sspanH, x0H);
```

```
nH=size(xH,1);
vH=zeros(nH,2);
%Control check of L and H
for i = 1:nH
vH(i,1)=R1*log(abs(xH(i,1)))+R2*xH(i,3)+R2;
vH(i,2)=(1-t)*xH(i,1)+t*(sqrt((1-xH(i,1)^2)*(1-xH(i,3)^2))*
   cos(xH(i,2)-xH(i,4))+xH(i,1)*xH(i,3))-1+2*t;
end
%Cartesian coordinates of trajectory
for i = 1:nH
wH(i,1)=sqrt(1-xH(i,1)^2)*cos(xH(i,2));
wH(i,2)=sqrt(1-xH(i,1)^2)*sin(xH(i,2));
wH(i,3)=sqrt(1-xH(i,3)^2)*cos(xH(i,4));
wH(i,4)=sqrt(1-xH(i,3)^2)*sin(xH(i,4));
end
%Save full trajectory in Cartesian coordinates
flowH=[wH(:,1),wH(:,2),xH(:,1),wH(:,3),wH(:,4),xH(:,3)]

%Plots of cylindrical coordinates z1, theta1, z2, theta2 vs
    s of X_H
plot(sH, xH(:,1),'linewidth',3);xlim([0 32]);
xlabel('s');ylabel('z_1');title('z_1 vs s');
plot(sH, xH(:,2),'linewidth',3);xlim([0 32]);
xlabel('s');ylabel('\theta_1');title('\theta_1 vs s');
plot(sH, xH(:,3),'linewidth',3);xlim([0 32]);
xlabel('s');ylabel('z_2');title('z_2 vs s');
plot(sH, xH(:,4),'linewidth',3);xlim([0 32]);
xlabel('s');ylabel('\theta_2');title('\theta_2 vs s');

%Plots of trajectories of X_L and X_H
%Create sphere mesh
alpha=linspace(0,2*pi,20);
phi=linspace(0,pi,20);
[alpha,phi]=meshgrid(alpha,phi);
rho=1;
xx=rho*sin(phi).*cos(alpha);
yy=rho*sin(phi).*sin(alpha);
zz=rho*cos(phi);
%Plot first sphere component
p1 = mesh(xx,yy,zz);
hold on;
set(p1,'FaceAlpha',0);
%Plot projection of trajectory of XL on first sphere
plot3(flowL(:,1),flowL(:,2),flowL(:,3),'red','linewidth',3)
%Plot projection of trajectory of XH on first sphere
```

```
plot3(flowH(:,1),flowH(:,2),flowH(:,3),'blue','linewidth'
    ,3)
%Plot singular hypersurface Z on first sphere
eq=linspace(0,2*pi,40);
e=[cos(eq)',sin(eq)',zeros(40,1)]
plot3(e(:,1),e(:,2),e(:,3),'black','linewidth',3)
hold off
%First sphere labels
xlabel('x_1');ylabel('y_1');zlabel('z_1');title('
   Trajectories of X_L and X_H');
%Plot second sphere component
p1 = mesh(xx,yy,zz);
hold on;
set(p1,'FaceAlpha',0);
%Plot projection of trajectory of XL on second sphere
plot3(flowL(:,4),flowL(:,5),flowL(:,6),'red','linewidth',3)
%Plot projection of trajectory of XH on second sphere
plot3(flowH(:,4),flowH(:,5),flowH(:,6),'blue','linewidth'
    ,3)
hold off
%Second sphere labels
xlabel('x_2');ylabel('y_2');zlabel('z_2');title('
   Trajectories of X_L and X_H');
```

# Bibliography


[ADH19] Jaume Alonso, Holger R. Dullin, and Sonja Hohloch. "Taylor series and twisting-index invariants of coupled spin-oscillators". In: *J. Geom. Phys.* 140 (2019), pp. 131–151. ISSN: 0393-0440. DOI: 10.1016/j.geomphys.2018.09.022. URL: https://doi.org/10.1016/j.geomphys.2018.09.022.

[ADH20] Jaume Alonso, Holger R. Dullin, and Sonja Hohloch. "Symplectic classification of coupled angular momenta". In: *Nonlinearity* 33.1 (2020), pp. 417–468. ISSN: 0951-7715. DOI: 10.1088/1361-6544/ab4e05. URL: https://doi.org/10.1088/1361-6544/ab4e05.

[AH19] Jaume Alonso and Sonja Hohloch. "Survey on recent developments in semitoric systems". In: *Conference Proceedings of RIMS Kokyuroku 2019 (Research Institute for Mathematical Sciences, Kyoto University, Japan)* 2137 (2019). ISSN: 1880-2818. eprint: 1901.10433 (math.DS).

[Arn78] V. I. Arnold. *Mathematical methods of classical mechanics*. Vol. 60. Graduate Texts in Mathematics. Translated from the Russian by K. Vogtmann and A. Weinstein. Springer-Verlag, New York-Heidelberg, 1978, pp. x+462. ISBN: 0-387-90314-3.

[Ati82] M. F. Atiyah. "Convexity and commuting Hamiltonians". In: *Bull. London Math. Soc.* 14.1 (1982), pp. 1–15. ISSN: 0024-6093. DOI: 10.1112/blms/14.1.1. URL: https://doi.org/10.1112/blms/14.1.1.

[BCD09] O. Babelon, L. Cantini, and B. Douçot. "A semi-classical study of the Jaynes-Cummings model". In: *J. Stat. Mech. Theory Exp.* (2009), P07011, 45. DOI: 10.1088/1742-5468/2009/07/p07011. URL: https://doi.org/10.1088/1742-5468/2009/07/p07011.

[BF04] A. V. Bolsinov and A. T. Fomenko. *Integrable Hamiltonian systems*. Geometry, topology, classification, Translated from the 1999 Russian original. Chapman & Hall/CRC, Boca Raton, FL, 2004, pp. xvi+730. ISBN: 0-415-29805-9. DOI: 10.1201/9780203643426. URL: https://doi.org/10.1201/9780203643426.

[BI19] Alexey Bolsinov and Anton Izosimov. "Smooth invariants of focus-focus singularities and obstructions to product decomposition". In: *J. Symplectic Geom.* 17.6 (2019), pp. 1613–1648. ISSN: 1527-5256. DOI: 10.4310/JSG.2019.v17.n6.a2. URL: https://doi.org/10.4310/JSG.2019.v17.n6.a2.

[Bla73] Robert J. Blattner. "Quantization and representation theory". In: *Harmonic analysis on homogeneous spaces (Proc. Sympos. Pure Math., Vol. XXVI, Williams Coll., Williamstown, Mass., 1972)*. Vol. Vol. XXVI. Proc. Sympos. Pure Math. Amer. Math. Soc., Providence, RI, 1973, pp. 147–165.

[BLS21] Maxim Braverman, Yiannis Loizides, and Yanli Song. "Geometric quantization of b -symplectic manifolds". In: *J. Symplectic Geom.* 19.1 (2021), pp. 1–36. DOI: 10.4310/JSG.2021.v19.n1.a1. URL: https://dx.doi.org/10.4310/JSG.2021.v19.n1.a1.

[Bru+23] Joaquim Brugués et al. "Constructions of $b$-semitoric systems". In: *J. Math. Phys.* 64.7 (2023), Paper No. 072703, 30. ISSN: 0022-2488,1089-7658. DOI: 10.1063/5.0152551. URL: https://doi.org/10.1063/5.0152551.

[Can01] Ana Cannas da Silva. *Lectures on symplectic geometry*. Vol. 1764. Lecture Notes in Mathematics. Springer-Verlag, Berlin, 2001, pp. xii+217. ISBN: 3-540-42195-5. DOI: 10.1007/978-3-540-45330-7. URL: https://doi.org/10.1007/978-3-540-45330-7.

[Cha13] Marc Chaperon. "Normalisation of the smooth focus-focus: a simple proof". In: *Acta Math. Vietnam.* 38.1 (2013), pp. 3–9. ISSN: 0251-4184. DOI: 10.1007/s40306-012-0003-y. URL: https://doi.org/10.1007/s40306-012-0003-y.

[CHP19] Dan Cristofaro-Gardiner, Michael Hutchings, and Daniel Pomerleano. "Torsion contact forms in three dimensions have two or infinitely many Reeb orbits". In: *Geom. Topol.* 23.7 (2019), pp. 3601–3645. ISSN: 1465-3060. DOI: 10.2140/gt.2019.23.3601. URL: https://doi.org/10.2140/gt.2019.23.3601.

[CMM23] Baptiste Coquinot, Pau Mir, and Eva Miranda. "Singular cotangent models in fluids with dissipation". In: *Phys. D* 446 (2023), Paper No. 133655, 11. ISSN: 0167-2789,1872-8022. DOI: 10.1016/j.physd.2023.133655. URL: https://doi.org/10.1016/j.physd.2023.133655.

[CV79] Y. Colin de Verdière and J. Vey. "Le lemme de Morse isochore". In: *Topology* 18.4 (1979), pp. 283–293. ISSN: 0040-9383. DOI: 10.1016/0040-9383(79)90019-3. URL: https://doi.org/10.1016/0040-9383(79)90019-3.

[Del88] Thomas Delzant. "Hamiltoniens périodiques et images convexes de l'application moment". In: *Bull. Soc. Math. France* 116.3 (1988), pp. 315–339. ISSN: 0037-9484. URL: http://www.numdam.org/item?id=BSMF_1988__116_3_315_0.

[DM88] J.-P. Dufour and P. Molino. "Compactification d'actions de $\mathbf{R}^n$ et variables action-angle avec singularités". In: *Travaux du Séminaire Sud-Rhodanien de Géométrie, I*. Vol. 88. Publ. Dép. Math. Nouvelle Sér. B. Univ. Claude-Bernard, Lyon, 1988, pp. 161–183.

[Dui80] J. J. Duistermaat. "On global action-angle coordinates". In: *Comm. Pure Appl. Math.* 33.6 (1980), pp. 687–706. ISSN: 0010-3640. DOI: 10.1002/cpa.3160330602. URL: https://doi.org/10.1002/cpa.3160330602.

[Eli90a] L. H. Eliasson. "Hamiltonian systems with Poisson commuting integrals". In: *Stockholm University* PhD Thesis (1990).

[Eli90b] L. H. Eliasson. "Normal forms for Hamiltonian systems with Poisson commuting integrals—elliptic case". In: *Comment. Math. Helv.* 65.1 (1990), pp. 4–35. ISSN: 0010-2571. DOI: 10.1007/BF02566590. URL: https://doi.org/10.1007/BF02566590.

[FL85] Marc R. Feix and H. Ralph Lewis. "Invariants for dissipative nonlinear systems by using rescaling". en. In: *Journal of Mathematical Physics* 26.1 (Jan. 1985), pp. 68–73. ISSN: 0022-2488, 1089-7658. DOI: 10.1063/1.526750. URL: http://aip.scitation.org/doi/10.1063/1.526750 (visited on 10/27/2022).

[GGK02] Victor Guillemin, Viktor Ginzburg, and Yael Karshon. *Moment maps, cobordisms, and Hamiltonian group actions*. Vol. 98. Mathematical Surveys and Monographs. Appendix J by Maxim Braverman. American Mathematical Society, Providence, RI, 2002, pp. viii+350. ISBN: 0-8218-0502-9. DOI: 10.1090/surv/098. URL: https://doi.org/10.1090/surv/098.

[GH22] Yannick Gullentops and Sonja Hohloch. "Creating hyperbolic-regular singularities in the presence of an $\mathbb{S}^1$-symmetry". In: *arXiv:2209.15631* (2022). arXiv: 2209.15631 [math.DS].

[GH23] Yannick Gullentops and Sonja Hohloch. *Recent examples of hypersemitoric systems and first steps towards a classification: a brief survey*. 2023. arXiv: 2308.16346 [math.DS].

[GM13] S. R. De Groot and P. Mazur. *Non-Equilibrium Thermodynamics*. en. Google-Books-ID: mfFyG9jfaMYC. Courier Corporation, Jan. 2013. ISBN: 978-0-486-15350-6.

[GMP11] Victor Guillemin, Eva Miranda, and Ana Rita Pires. "Codimension one symplectic foliations and regular Poisson structures". In: *Bull. Braz. Math. Soc. (N.S.)* 42.4 (2011), pp. 607–623. ISSN: 1678-7544. DOI: 10.1007/s00574-011-0031-6. URL: https://doi.org/10.1007/s00574-011-0031-6.

[GMP14] Victor Guillemin, Eva Miranda, and Ana Rita Pires. "Symplectic and Poisson geometry on $b$-manifolds". In: *Adv. Math.* 264 (2014), pp. 864–896. ISSN: 0001-8708. DOI: 10.1016/j.aim.2014.07.032. URL: https://doi.org/10.1016/j.aim.2014.07.032.

[GMW18a] Victor W. Guillemin, Eva Miranda, and Jonathan Weitsman. "Convexity of the moment map image for torus actions on $b^m$-symplectic manifolds". In: *Philos. Trans. Roy. Soc. A* 376.2131 (2018), pp. 20170420, 6. ISSN: 1364-503X. DOI: 10.1098/rsta.2017.0420. URL: https://doi.org/10.1098/rsta.2017.0420.

[GMW18b] Victor W. Guillemin, Eva Miranda, and Jonathan Weitsman. "On geometric quantization of $b$-symplectic manifolds". In: *Adv. Math.* 331 (2018), pp. 941–951. ISSN: 0001-8708. DOI: 10.1016/j.aim.2018.04.003. URL: https://doi.org/10.1016/j.aim.2018.04.003.

[GMW21] Victor W. Guillemin, Eva Miranda, and Jonathan Weitsman. "On geometric quantization of $b^m$-symplectic manifolds". In: *Math. Z.* 298.1-2 (2021), pp. 281–288. ISSN: 0025-5874. DOI: 10.1007/s00209-020-02590-w. URL: https://doi.org/10.1007/s00209-020-02590-w.

[GP71] P. Glansdorff and Ilya Prigogine. *Thermodynamic Theory of Structure, Stability and Fluctuations*. en. Google-Books-ID: vf9QAAAAMAAJ. Wiley-Interscience, 1971. ISBN: 978-0-471-30280-3.

[GS82a] V. Guillemin and S. Sternberg. "Convexity properties of the moment mapping". In: *Invent. Math.* 67.3 (1982), pp. 491–513. ISSN: 0020-9910. DOI: 10.1007/BF01398933. URL: https://doi.org/10.1007/BF01398933.

[GS82b] V. Guillemin and S. Sternberg. "Geometric quantization and multiplicities of group representations". In: *Invent. Math.* 67.3 (1982), pp. 515–538. ISSN: 0020-9910. DOI: 10.1007/BF01398934. URL: https://doi.org/10.1007/BF01398934.

[GS83] V. Guillemin and S. Sternberg. "The Gelfand-Cetlin system and quantization of the complex flag manifolds". In: *J. Funct. Anal.* 52.1 (1983), pp. 106–128. ISSN: 0022-1236. DOI: 10.1016/0022-1236(83)90092-7. URL: https://doi.org/10.1016/0022-1236(83)90092-7.

[GS84] Victor Guillemin and Shlomo Sternberg. *Symplectic techniques in physics*. Cambridge University Press, Cambridge, 1984, pp. xi+468. ISBN: 0-521-24866-3.

[Gua+17] Marco Gualtieri et al. "The tropical momentum map: a classification of toric log symplectic manifolds". In: *Mathematische Annalen* 367 (2017), pp. 1217–1258. DOI: 10.1007/s00208-016-1427-9.

[Gui+15] Victor Guillemin et al. "Toric actions on $b$-symplectic manifolds". In: *Int. Math. Res. Not. IMRN* 2015.14 (2015), pp. 5818–5848. ISSN: 1073-7928. DOI: 10.1093/imrn/rnu108. URL: https://doi.org/10.1093/imrn/rnu108.

[Hal13] Brian C. Hall. *Quantum Theory for Mathematicians*. Springer New York, NY, 2013. ISBN: 978-1-4614-7115-8. DOI: doi:10.1007/978-1-4614-7116-5. URL: https://link.springer.com/book/10.1007/978-1-4614-7116-5.

[Ham10] Mark D. Hamilton. "Locally toric manifolds and singular Bohr-Sommerfeld leaves". In: *Mem. Amer. Math. Soc.* 207.971 (2010), pp. vi+60. ISSN: 0065-9266. DOI: 10.1090/S0065-9266-10-00583-1. URL: https://doi.org/10.1090/S0065-9266-10-00583-1.

[HM10] Mark D. Hamilton and Eva Miranda. "Geometric quantization of integrable systems with hyperbolic singularities". In: *Ann. Inst. Fourier (Grenoble)* 60.1 (2010), pp. 51–85. ISSN: 0373-0956. URL: http://aif.cedram.org/item?id=AIF_2010__60_1_51_0.

[HM16] Peter Hochs and Varghese Mathai. "Formal geometric quantisation for proper actions". In: *J. Homotopy Relat. Struct.* 11.3 (2016), pp. 409–424. ISSN: 2193-8407. DOI: 10.1007/s40062-015-0109-8. URL: https://doi.org/10.1007/s40062-015-0109-8.

[HP21] Sonja Hohloch and Joseph Palmer. "Extending compact Hamiltonian $S^1$-spaces to integrable systems with mild degeneracies in dimension four". In: *arXiv:2105.00523* (2021). arXiv: 2105.00523 [math.SG].

[HWZ98] H. Hofer, K. Wysocki, and E. Zehnder. "The dynamics on three-dimensional strictly convex energy surfaces". In: *Ann. of Math. (2)* 148.1 (1998), pp. 197–289. ISSN: 0003-486X. DOI: 10.2307/120994. URL: https://doi.org/10.2307/120994.

[JC63] E. T. Jaynes and F. W. Cummings. "Comparison of quantum and semiclassical radiation theories with application to the beam maser". In: *IEEE Proc.* 51 (1963), pp. 89–109. DOI: 10.1109/PROC.1963.1664.

[JW92] Lisa C. Jeffrey and Jonathan Weitsman. "Bohr-Sommerfeld orbits in the moduli space of flat connections and the Verlinde dimension formula". In: *Comm. Math. Phys.* 150.3 (1992), pp. 593–630. ISSN: 0010-3616,1432-0916. URL: http://projecteuclid.org/euclid.cmp/1104251961.

[KM17] Anna Kiesenhofer and Eva Miranda. "Cotangent models for integrable systems". In: *Comm. Math. Phys.* 350.3 (2017), pp. 1123–1145. ISSN: 0010-3616. DOI: 10.1007/s00220-016-2720-x. URL: https://doi.org/10.1007/s00220-016-2720-x.

[KMS16] Anna Kiesenhofer, Eva Miranda, and Geoffrey Scott. "Action-angle variables and a KAM theorem for *b*-Poisson manifolds". In: *J. Math. Pures Appl. (9)* 105.1 (2016), pp. 66–85. ISSN: 0021-7824. DOI: 10.1016/j.matpur.2015.09.006. URL: https://doi.org/10.1016/j.matpur.2015.09.006.

[Kos70] Bertram Kostant. "Quantization and unitary representations. I. Prequantization". In: *Lectures in modern analysis and applications, III*. Springer-Verlag, Berlin, 1970, 87–208. Lecture Notes in Math., Vol. 170.

[Ler95] Eugene Lerman. "Symplectic cuts". In: *Math. Res. Lett.* 2.3 (1995), pp. 247–258. ISSN: 1073-2780. DOI: 10.4310/MRL.1995.v2.n3.a2. URL: https://doi.org/10.4310/MRL.1995.v2.n3.a2.

[Lin+22] Yi Lin et al. "Log symplectic manifolds and $[Q, R] = 0$". In: *Int. Math. Res. Not. IMRN* 18 (2022), pp. 14034–14066. ISSN: 1073-7928,1687-0247. DOI: 10.1093/imrn/rnab140. URL: https://doi.org/10.1093/imrn/rnab140.

[LP18] Yohann Le Floch and Joseph Palmer. "Semitoric families". In: *arXiv: 1810.06915* (2018). To appear in Mem. Amer. Math. Soc. arXiv: 1810.06915 [math.SG]. URL: https://arxiv.org/abs/1810.06915.

[LP19] Yohann Le Floch and Álvaro Pelayo. "Symplectic geometry and spectral properties of classical and quantum coupled angular momenta". In: *J. Nonlinear Sci.* 29.2 (2019), pp. 655–708. ISSN: 0938-8974. DOI: 10.1007/s00332-018-9501-y. URL: https://doi.org/10.1007/s00332-018-9501-y.

[LP23] Yohann Le Floch and Joseph Palmer. "Families of four-dimensional integrable systems with $S^1$-symmetries". In: *arXiv:2307.10670* (2023). arXiv: 2307.10670 [math.SG]. URL: https://arxiv.org/abs/2307.10670.

[LS10] Naichung Conan Leung and Margaret Symington. "Almost toric symplectic four-manifolds". In: *J. Symplectic Geom.* 8.2 (2010), pp. 143–187. ISSN: 1527-5256. URL: http://projecteuclid.org/euclid.jsg/1279199213.

[Mei96] Eckhard Meinrenken. "On Riemann-Roch formulas for multiplicities". In: *J. Amer. Math. Soc.* 9.2 (1996), pp. 373–389. ISSN: 0894-0347. DOI: 10.1090/S0894-0347-96-00197-X. URL: https://doi.org/10.1090/S0894-0347-96-00197-X.

[Mel93] Richard Melrose. *The Atiyah-Patodi-Singer index theorem*. CRC press, 1993.

[Min36] Henri Mineur. "Reduction des systèmes mecaniques à n degrées de liberte admettant n intégrales premieres uniformes en involution aux système à variable separe". In: *J. Math Pure Appl* IX (1936), pp. 385–389.

[Mir03] Eva Miranda. "On symplectic linearization of singular Lagrangian foliations". PhD thesis. Universitat de Barcelona, June 2003. ISBN: 9788469412374. URL: http://diposit.ub.edu/dspace/handle/2445/35155.

[Mir14] Eva Miranda. "Integrable systems and group actions". In: *Cent. Eur. J. Math.* 12.2 (2014), pp. 240–270. ISSN: 1895-1074. DOI: 10.2478/s11533-013-0333-6. URL: https://doi.org/10.2478/s11533-013-0333-6.

[MM21] Pau Mir and Eva Miranda. "Geometric quantization via cotangent models". In: *Anal. Math. Phys.* 11.3 (2021), Paper No. 118. ISSN: 1664-2368. DOI: 10.1007/s13324-021-00559-4. URL: https://doi.org/10.1007/s13324-021-00559-4.

[MMW22] Pau Mir, Eva Miranda, and Jonathan Weitsman. *Bohr-Sommerfeld quantization of b-symplectic toric manifolds*. 2022. arXiv: 2203.03340. URL: https://arxiv.org/abs/2203.03340.

[MO21] Eva Miranda and Cédric Oms. "The singular Weinstein conjecture". In: *Adv. Math.* 389 (2021), Paper No. 107925, 41. ISSN: 0001-8708. DOI: 10.1016/j.aim.2021.107925. URL: https://doi.org/10.1016/j.aim.2021.107925.

[MOP22] Eva Miranda, Cédric Oms, and Daniel Peralta-Salas. "On the singular Weinstein conjecture and the existence of escape orbits for $b$-Beltrami fields". In: *Commun. Contemp. Math.* 24.7 (2022), Paper No. 2150076, 25. ISSN: 0219-1997. DOI: 10.1142/S0219199721500760. URL: https://doi.org/10.1142/S0219199721500760.

[Mor86] Philip J. Morrison. "A paradigm for joined Hamiltonian and dissipative systems". In: *Phys. D* 18.1-3 (1986). Solitons and coherent structures (Santa Barbara, Calif., 1985), pp. 410–419. ISSN: 0167-2789. DOI: 10.1016/0167-2789(86)90209-5. URL: https://doi.org/10.1016/0167-2789(86)90209-5.

[MP15] Eva Miranda and Francisco Presas. "Geometric quantization of real polarizations via sheaves". In: *J. Symplectic Geom.* 13.2 (2015), pp. 421–462. ISSN: 1527-5256. DOI: 10.4310/JSG.2015.v13.n2.a6. URL: https://doi.org/10.4310/JSG.2015.v13.n2.a6.

[MPS20] Eva Miranda, Francisco Presas, and Romero Solha. "Geometric quantization of almost toric manifolds". In: *J. Symplectic Geom.* 18.4 (2020), pp. 1147–1168. ISSN: 1527-5256.

[MR99] Jerrold E. Marsden and Tudor S. Ratiu. *Introduction to mechanics and symmetry*. Second. Vol. 17. Texts in Applied Mathematics. A basic exposition of classical mechanical systems. Springer-Verlag, New York, 1999, pp. xviii+582. ISBN: 0-387-98643-X. DOI: 10.1007/978-0-387-21792-5. URL: https://doi.org/10.1007/978-0-387-21792-5.

[MV05] Eva Miranda and San Vũ Ngoc. "A singular Poincaré lemma". In: *Int. Math. Res. Not.* (2005), pp. 27–45. ISSN: 1073-7928. DOI: 10.1155/IMRN.2005.27. eprint: https://academic.oup.com/imrn/article-pdf/2005/1/27/1845847/2005-1-27.pdf. URL: https://doi.org/10.1155/IMRN.2005.27.

[MZ04] Eva Miranda and Nguyen Tien Zung. "Equivariant normal form for nondegenerate singular orbits of integrable Hamiltonian systems". In: *Ann. Sci. École Norm. Sup. (4)* 37.6 (2004), pp. 819–839. ISSN: 0012-9593. DOI: 10.1016/j.ansens.2004.10.001. URL: https://doi.org/10.1016/j.ansens.2004.10.001.

[Par09] Paul-Émile Paradan. "Formal geometric quantization". In: *Ann. Inst. Fourier (Grenoble)* 59.1 (2009), pp. 199–238. ISSN: 0373-0956. URL: http://aif.cedram.org/item?id=AIF_2009__59_1_199_0.

[Pel21] Álvaro Pelayo. "Symplectic invariants of semitoric systems and the inverse problem for quantum systems". In: *Indag. Math. (N.S.)* 32.1 (2021), pp. 246–274. ISSN: 0019-3577,1872-6100. DOI: 10.1016/j.indag.2020.04.005. URL: https://doi.org/10.1016/j.indag.2020.04.005.

[PPT19] Joseph Palmer, Álvaro Pelayo, and Xiudi Tang. "Semitoric systems of non-simple type". In: *arXiv:1909.03501* (2019). arXiv: 1909.03501 [math.SG].

[PV09] Alvaro Pelayo and San Vũ Ngoc. "Semitoric integrable systems on symplectic 4-manifolds". In: *Invent. Math.* 177.3 (2009), pp. 571–597. ISSN: 0020-9910. DOI: 10.1007/s00222-009-0190-x. URL: https://doi.org/10.1007/s00222-009-0190-x.

[PV11] Álvaro Pelayo and San Vũ Ngoc. "Constructing integrable systems of semitoric type". In: *Acta Math.* 206.1 (2011), pp. 93–125. ISSN: 0001-5962. DOI: 10.1007/s11511-011-0060-4. URL: https://doi.org/10.1007/s11511-011-0060-4.

[PV12] Álvaro Pelayo and San Vũ Ngoc. "Hamiltonian dynamics and spectral theory for spin-oscillators". In: *Comm. Math. Phys.* 309.1 (2012), pp. 123–154. ISSN: 0010-3616. DOI: 10.1007/s00220-011-1360-4. URL: https://doi.org/10.1007/s00220-011-1360-4.

[Rad02] Olga Radko. "A classification of topologically stable Poisson structures on a compact oriented surface". In: *J. Symplectic Geom.* 1.3 (2002), pp. 523–542. ISSN: 1527-5256,1540-2347. URL: http://projecteuclid.org/euclid.jsg/1092403031.

[Rüs64] Helmut Rüssmann. "Über das Verhalten analytischer Hamiltonscher Differentialgleichungen in der Nähe einer Gleichgewichtslösung". In: *Math. Ann.* 154 (1964), pp. 285–300. ISSN: 0025-5831. DOI: 10.1007/BF01362565. URL: https://doi.org/10.1007/BF01362565.

[Sja96] Reyer Sjamaar. "Symplectic reduction and Riemann-Roch formulas for multiplicities". In: *Bull. Amer. Math. Soc. (N.S.)* 33.3 (1996), pp. 327–338. ISSN: 0273-0979,1088-9485. DOI: 10.1090/S0273-0979-96-00661-1. URL: https://doi.org/10.1090/S0273-0979-96-00661-1.

[Śni77] Jedrzej Śniatycki. "On cohomology groups appearing in geometric quantization". In: *Differential geometrical methods in mathematical physics (Proc. Sympos., Univ. Bonn, Bonn, 1975)*. 1977, 46–66. Lecture Notes in Math., Vol. 570.

[Sou66] J.-M. Souriau. "Quantification géométrique". In: *Comm. Math. Phys.* 1 (1966), pp. 374–398. URL: http://projecteuclid.org/euclid.cmp/1103758996.

[Sym03] Margaret Symington. "Four dimensions from two in symplectic topology". In: Proc. Sympos. Pure Math. 71 (2003), pp. 153–208. DOI: 10.1090/pspum/071/2024634. URL: https://doi.org/10.1090/pspum/071/2024634.

[SZ99] D. A. Sadovskiĭ and B. I. Zhilinskiĭ. "Monodromy, diabolic points, and angular momentum coupling". In: *Phys. Lett. A* 256.4 (1999), pp. 235–244. ISSN: 0375-9601. DOI: 10.1016/S0375-9601(99)00229-7. URL: https://doi.org/10.1016/S0375-9601(99)00229-7.

[SZM96] D. A. Sadovskiĭ, B. I. Zhilinskiĭ, and L. Michel. "Collapse of the Zeeman structure of the hydrogen atom in an external electric field". In: *Phys. Rev. A* 53 (6 June 1996), pp. 4064–4067. DOI: 10.1103/PhysRevA.53.4064. URL: https://link.aps.org/doi/10.1103/PhysRevA.53.4064.

[TN96] Boris Tsygan and Ryszard Nest. "Formal deformations of symplectic manifolds with boundary". In: *J. Reine Angew. Math* 481 (1996), pp. 27–54.

[Vey78] J. Vey. "Sur certains systèmes dynamiques séparables". In: *Amer. J. Math.* 100.3 (1978), pp. 591–614. ISSN: 0002-9327. DOI: 10.2307/2373841. URL: https://doi.org/10.2307/2373841.

[Vũ 03] San Vũ Ngoc. "On semi-global invariants for focus-focus singularities". In: *Topology* 42.2 (2003), pp. 365–380. ISSN: 0040-9383. DOI: 10.1016/S0040-9383(01)00026-X. URL: https://doi.org/10.1016/S0040-9383(01)00026-X.

[Vũ 07] San Vũ Ngoc. "Moment polytopes for symplectic manifolds with monodromy". In: *Advances in Mathematics* 208.2 (2007), pp. 909–934.

[VW13] San Vũ Ngoc and Christophe Wacheux. "Smooth normal forms for integrable Hamiltonian systems near a focus-focus singularity". In: *Acta Math. Vietnam.* 38.1 (2013), pp. 107–122. ISSN: 0251-4184. DOI: 10.1007/s40306-013-0012-5. URL: https://doi.org/10.1007/s40306-013-0012-5.

[Wei01] Jonathan Weitsman. "Non-abelian symplectic cuts and the geometric quantization of noncompact manifolds". In: *Lett. Math. Phys.* 56.1 (2001). EuroConférence Moshé Flato 2000, Part I (Dijon), pp. 31–40. ISSN: 0377-9017. DOI: 10.1023/A:1010907708197. URL: https://doi.org/10.1023/A:1010907708197.

[Wil36] John Williamson. "On the Algebraic Problem Concerning the Normal Forms of Linear Dynamical Systems". In: *Amer. J. Math.* 58.1 (1936), pp. 141–163. ISSN: 0002-9327. DOI: 10.2307/2371062. URL: https://doi.org/10.2307/2371062.

[Woo92] N. M. J. Woodhouse. *Geometric quantization*. Second. Oxford Mathematical Monographs. Oxford Science Publications. The Clarendon Press, Oxford University Press, New York, 1992, pp. xii+307. ISBN: 0-19-853673-9.

[Zun03] Nguyen Tien Zung. "Symplectic topology of integrable Hamiltonian systems. II. Topological classification". In: *Compositio Math.* 138.2 (2003), pp. 125–156. ISSN: 0010-437X. DOI: 10.1023/A:1026133814607. URL: https://doi.org/10.1023/A:1026133814607.

[Zun96] Nguyen Tien Zung. "Symplectic topology of integrable Hamiltonian systems. I. Arnold-Liouville with singularities". In: *Compositio Math.* 101.2 (1996), pp. 179–215. ISSN: 0010-437X. URL: http://www.numdam.org/item?id=CM_1996__101_2_179_0.